1981

A Computer Study of the Correlation Between Aquifer Hydraulic and Aquifer Electric Properties

Paul Frederick Reiter
University of Rhode Island

A COMPUTER STUDY OF THE CORRELATION BETWEEN AQUIFER HYDRAULIC AND AQUIFER ELECTRIC PROPERTIES

BY

PAUL FREDERICK REITER

A THESIS SUBMITTED IN PARTIAL FULFILLMENT OF THE REQUIREMENTS FOR THE DEGREE OF

MASTER OF SCIENCE

IN

CIVIL & ENVIRONMENTAL ENGINEERING

UNIVERSITY OF RHODE ISLAND

1981

ABSTRACT

Correlations between aquifer resistivity and aquifer permeability are examined as an improved method for freshwater aquifer exploration. Layered aquifer models were developed where permeabilities for each layer were obtained from a random distribution between reasonable limits. The permeabilities of the layers were then converted to resistivity layers by using a previously developed semi-empirical relationship between permeability and resistivity at the small sample level. Hence, the hydraulic model with layered permeabilities was converted to an electrical model with layered resistivities. Resistivities and permeabilities for the entire aquifer model were then calculated with analytical equations for linear flow parallel and perpendicular to layering. Trends were plotted from three hundred models for the four possible combinations of these properties with respect to flow paths. Results showed that the best predictor of horizontal aquifer permeability in a horizontally layered aquifer, is the vertical or transverse aquifer resistivity. Horizontal or longitudinal aquifer resistivity can be used effectively to predict horizontal aquifer permeability only if the electric or hydraulic anisotropy is known.

To compute aquifer properties for the spacially mixed case, where permeabilities were distributed as monomodal

probability density functions, a finite difference computer program was developed. Trends of aquifer resistivity versus aquifer permeability were developed for the uniform, exponential and lognormal permeability distributions. Flow geometry was approximately linear (quasi-linear).

To relate the results of linear flow aquifer property trends more to the field situation, where pump tests determine aquifer permeabilities based on radial flow, and the current from an electric sounding moves from point source to point sink, radial and point to point flow geometries were used to compute aquifer properties where the aquifer was considered to be isolated from surrounding strata. Results showed that flow geometry does not make a significant difference in computing aquifer properties in spacially mixed isolated aquifers, yet may be very important for the layered case.

For non-isolated aquifers, where current is refracted by surrounding strata, methods of obtaining linear flow aquifer resistivities by interpreting sounding curves for various formation resistivity stratifications are discussed. Results indicate that good correlations between aquifer resistivity and aquifer permeability are possible when formation stratifications are such that the aquifer resistivity and its directional sense can be found through sounding curve interpretations.

ACKNOWLEDGEMENTS

I welcome this opportunity to thank those associated with this study and its development throughout my graduate years. The research was supported by a grant (ENG 7819408) from the National Science Foundation.

I am particularly grateful to Dr. William E. Kelly for obtaining funds for the research, giving freely of his time and providing valuable guidance and suggestions during the study. His avid pursuit of developments in groundwater hydrology has provided an invaluable example.

Appreciation is given to Dr. Daniel W. Urish for detailed explanations of his dissertation and to Professor Francis H. Lavelle and Roger K. Greenall for providing computer programing assistance. All computer work was done at the University of Rhode Island Academic Computer Center.

I am indebted to the Rhode Island Water Resources Board for assisting in the funding of my graduate studies.

Special thanks is extended to Mr. Herbert E. Johnston of the United States Geological Survey for providing valuble data and explanations of hydrogeologic processes;

The assistance of my fellow graduate students is greatly appreciated throughout these years, especially Bill Beckman, Jerry Baird, Scott Bamford, Bob McMonagle, Mark Brickell, Bill Gordon and Melih Ozbilgin.

My sincere thanks to Clarice Coleman and Donna

Brightman for assisting in the typing.

Finally, I must thank my parents and grandmother for their support and understanding throughout this undertaking.

TABLE OF CONTENTS

LIST OF TABLES

LIST OF FIGURES

FIGURE TITLE

SECTION I

INTRODUCTION

As groundwater is increasingly used as a source of water supply, the need to plan and manage aquifer systems becomes more important to insure that these resources will remain pollution free and hydraulically sound. Accurate estimates of aquifer properties are essential for engineers, geologists and hydrologists to predict water levels due to pumpage, drought, change in stream stage or infiltration (Walton, 1970).

Over the past decade, geophysical methods have played a more significant role in aquifer exploration programs (Urish, 1978). Surface electrical resistivity is an attractive exploration technique because: (1) of the relative low cost; (2) it relates to the large aquifer volumes that control well yields rather than to the local conditions sampled with test borings; and (3) because of the analogous physical relationship between electrical conductivity and hydraulic conductivity. An electric current flows through saturated intergranular spaces in porous media in essentially the same channels as hydraulic flow, with both depending on porosity and tortuosity (Bear, 1972). Field investigations, where hydraulic properties were determined by pump tests, and electrical properties were obtained through surficial electrical resistivity methods, have shown a large spread of values with differences not only in the regression slope, but in sign as well (Ungemach, 1969; Kelly, 1977; Heigold et al., 1979).

These differences need to be resolved in order to determine the effectiveness of electrical techniques. As an initial step toward solving this problem, this study will attempt to relate average "aquifer permeability" to average "aquifer resistivity" using idealized models with the assumption that the soil has an exact relationship between permeability and resistivity at the small sample scale. The term permeability as used in this study includes the effects of the grain matrix and the pore fluid.

These average "aquifer" quantities are dependent upon the transport properties of the region being studied, as well as the flow geometry (Warren and Price, 1961). Primarily the effects of the integration of transport properties will be examined. Flow geometries will be kept close to linear (quasi-linear) by driving flow through a confined aquifer section, where constant potentials prevail at the vertical boundaries. Cases will be examined where the aquifer is composed of definite layers (each layer with a different deterministic value of permeability) and where permeabilities are spacially mixed, following a given probability distribution. To relate results to field methods, where flow for the hydraulic case is usually radial and current in the electrical case moves from point to point, the effect of flow geometry on aquifer properties will be shown.

MATERIAL RELATIONSHIP DEVELOPMENT

An aquifer's hydraulic properties may be examined at various levels, but only two are of interest in this study. The first is called the material level, where a small sample of soil is tested and its properties are assumed to be constant in space and direction. Sample sizes are generally small, from 50 cm^3 for fine sands to 400 cm^3 for gravels. The second level refers to the aquifer scale and is called macroscopic. This broad scoped macroscopic level is made up of many material level parts.

The term "aquifer permeability" refers to an average permeability at the macroscopic level. Computation of this term is based on hydraulic potential theory. Likewise, "aquifer resistivity" will refer to a macroscopic average apparent resistivity based on electrical potential theory. Exact equations and methods used to obtain these averages under various spacial configurations of transport properties will be presented.

Researchers have shown with empirical and theoretical studies, that good relationships may exist at the material level between hydraulic and electric transport properties, with the best correlation suitable for determining permeability of a fresh water saturated unconsolidated sand being a direct relationship between apparent formation factor (F_a) and permeability (k) (see appendix A). The general empirical relationship may be expressed as

$$k = A\ F_a^m \qquad (1)$$

where A and m are positive constants

The effectiveness of this relationship may be due to the mutual dependence both quantities have for surface area of the soil matrix.

Apparent formation factor is defined as

$$F = \rho_a / \rho_w \qquad (2)$$

where ρ_a = apparent resistivity

ρ_w = pore water resistivity

Since laboratory data in the literature for F_a versus k material relationships is either for constant porosity (Jones and Buford, 1951; Kelly, 1976) or argillaceous sandstones (Worthington and Barker, 1972), a theoretical relationship was chosen which was close to the "probable average" curve developed by Urish (1978). A literature review of the F_a vs. k relationship, including the Urish model, is provided in appendix A.

Fig. 1 shows the F_a vs. k Urish model, which is based

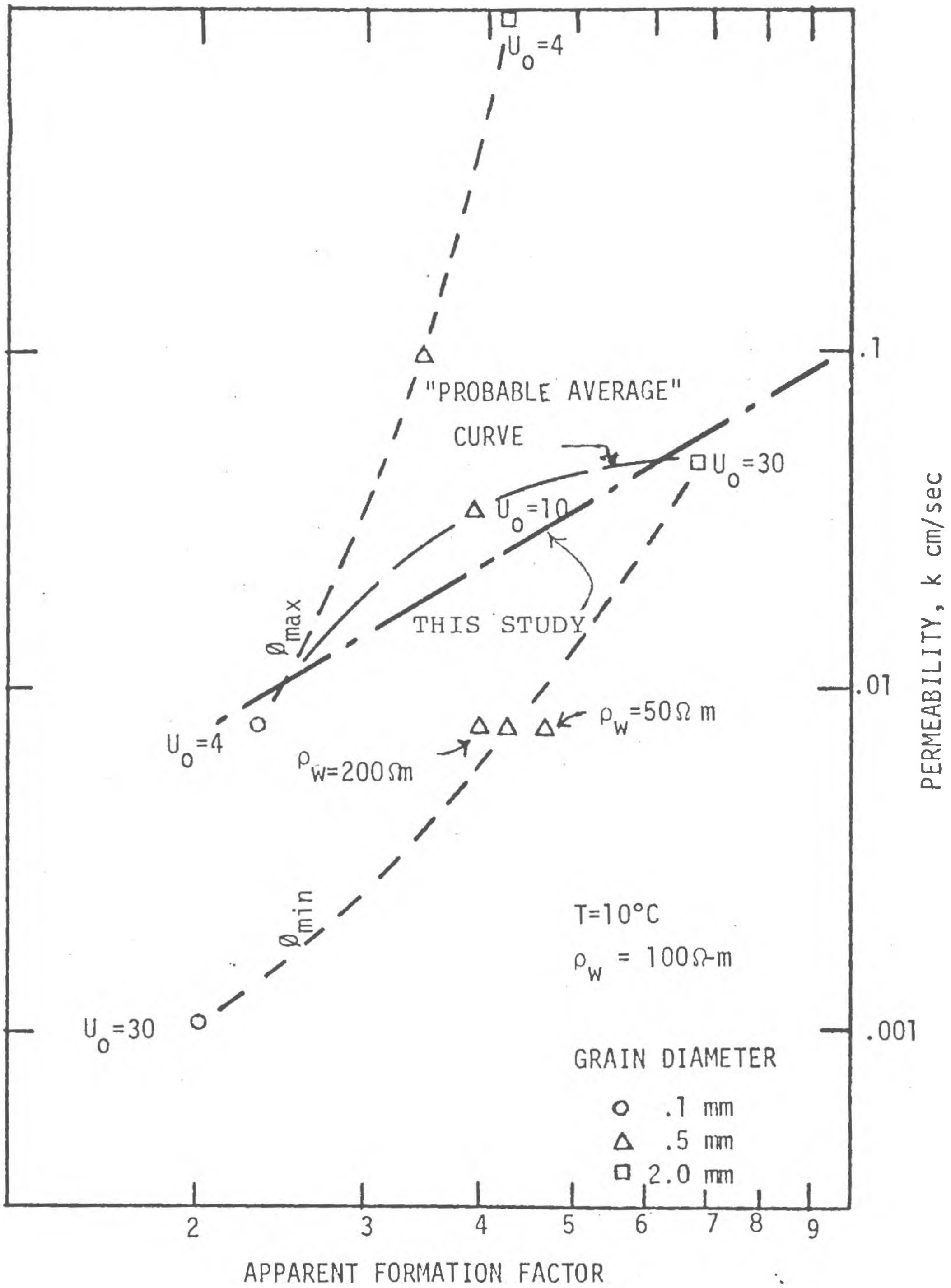

Fig. 1. Range limits for variation of apparent formation factor versus permeability under in-situ condition (from Urish, 1978)

on porosities obtained by wet packing tests for both the loosest (ϕ_{MAX}) and the densest (ϕ_{MIN}) states. Independent variables included the median grain size (D_{50}), uniformity coefficient ($U_c = D_{40}/D_{10}$), and pore water resistivity (shown for one group of points with D_{50} =.5 and U_o=30). The porosity states (ϕ_{MAX} and ϕ_{MIN}) are actually determined by regression equations where average grain size (D_{50}) and uniformity coefficient were independent variables. Inherent in the plot of Fig. 1 is an assumed inverse trend between porosity and uniformity coefficient. The "probable average" curve (Fig. 1) is believed to approximate the insitu case, where it is assumed fine grained material is more uniform and tends to pack at higher porosities than coarse grained material. This trend implies an in-situ inverse relationship between porosity and permeability, which many researchers have demonstrated on a sample to sample basis (Graton and Fraser, 1935; Kelly, 1980). A simplified version of the probable average curve, shown in Figs. 1 and 2, was used in this study.

This study will further simplify the material F_a vs. k relationship by assuming pore water resistivity is constant within an aquifer. The material level relationship of Fig. 2 was converted to a ρ_a vs. k relationship by using a value of 100 Ω-m. This material level ρ_a vs. k line is shown plotted in Fig. 2a, which represents the equation

$$k = 5.13\times10^{-6}\ \rho_a^{\,1.43} \qquad (3)$$

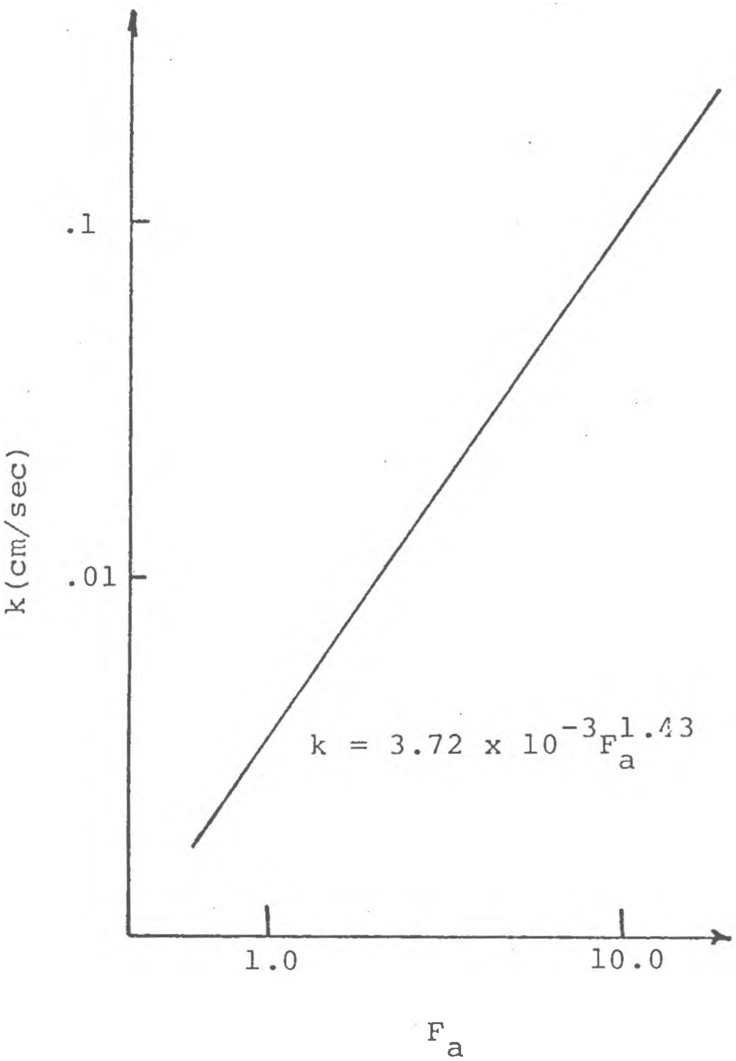

Figure 2. Apparent Formation Factor (F_a) vs. permeability (k) used in this study.

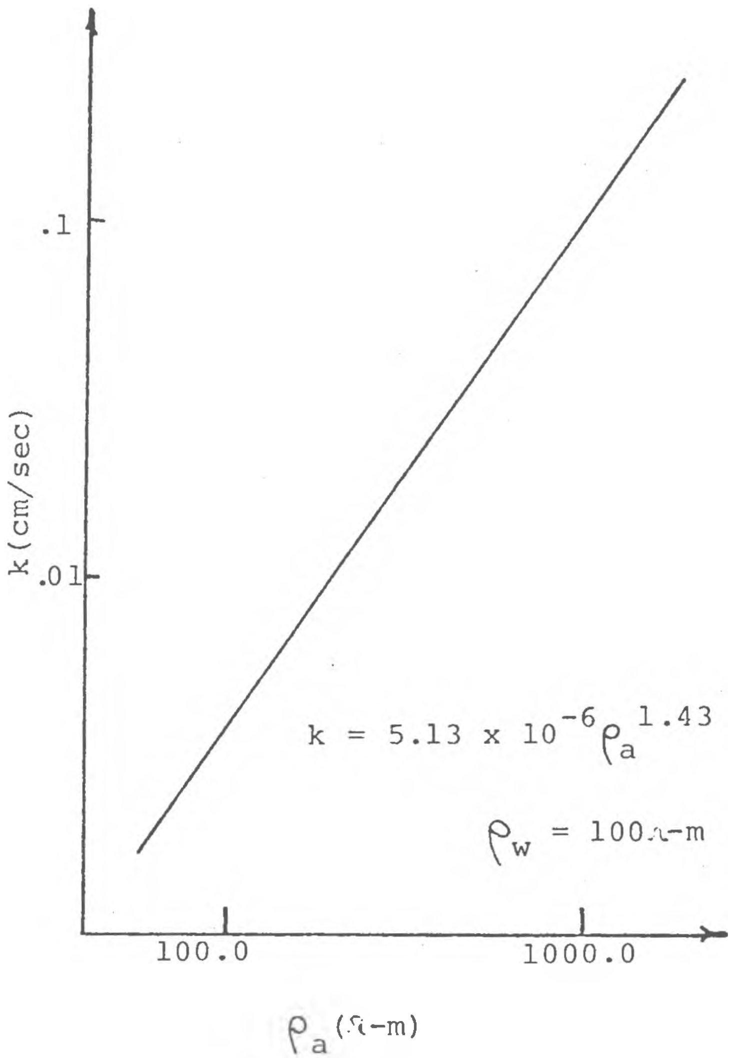

Figure 2a. Apparent resistivity (ρ_a) vs. permeability (k) used in this study.

where k = permeability (cm/sec)

ρ_a = apparent resistivity (Ω-m)

Equation 3 is the basic material relationship used in this study. It should be noted that this equation is for material that is isotropic and of constant permeability and resistivity throughout. The basis of this relationship is not considered since the aim of the study is to examine macroscopic transport relationships when the material relation of ρ_a to k is exactly known. In the real situation this relation is probably not exactly known; however, it was felt the material level uncertainty should not be included in this study.

Layered Model Development

Estimates of permeabilities from pump tests and apparent resistivities from surficial electrical measurements represent average quantities. Field relationships between aquifer hydraulic and electric properties differ not only from laboratory relationships but from one another as well. Kelly (1977) found a direct relationship between F_a and k, while Heigold and others (1979) found an inverse relationship. In France, Ungemach, Mostaghimi and Duprat (1969) showed a direct relationship between aquifer transverse resistance and transmissivity.

Laboratory tests conducted by Kelly (1976) generally followed the trend found by Jones and Buford (1951), which showed a much larger positive slope than the Kelly (1977) field correlation for F_a (absissa) vs. k (ordinate). Both researchers used graded samples and reported results for a constant porosity.

One possible reason for the differences between laboratory and field relationships of F_a vs. k is the effect of layering (Urish, 1978). Aquifer permeability and aquifer resistivity can be computed for layered cases where flow is either parallel or perpendicular to the layering and moves through constant cross sectional area (linear flow). Aquifer permeability and aquifer resistivity can be calculated for the desired directions and type of layering from the following equations:

$$k_{hh} = k_{vv} = \frac{\sum_{i=1}^{n} k_i h_i}{\sum_{i=1}^{n} h_i} \quad \text{(Perloff and Baron, 1976)} \quad (4)$$

$$\rho_{hh} = \rho_{vv} = \frac{\sum_{i=1}^{n} h_i}{\sum_{i=1}^{n} \frac{h_i}{\rho_i}} \quad \text{(Zohdy et al., 1974)} \quad (5)$$

for flow parallel to the beds, and

$$k_{hv} = k_{vh} = \frac{\sum_{i=1}^{n} h_i}{\sum_{i=1}^{n} \frac{h_i}{k_i}} \quad \text{(Perloff and Baron, 1976)} \quad (6)$$

$$\rho_{vh} = \rho_{hv} = \frac{\sum_{i=1}^{n} h_i \rho_i}{\sum_{i=1}^{n} h_i} \qquad \text{(Zohdy et al., 1974)} \quad (7)$$

for flow perpendicular to the beds.

where

k_{xy} = aquifer permeability in the $\begin{bmatrix} x=h=\text{horizontal} \\ x=v=\text{vertical} \end{bmatrix}$ direction with $\begin{bmatrix} y=h=\text{horizontal} \\ y=v=\text{vertical} \end{bmatrix}$ layering

ρ_{xy} = aquifer resistivity, where x and y are the same as in k

h_i = thickness of the i'th layer

n = number of layers

Urish (1978) used equations 4 and 5 to demonstrate how the material F_a (abscissa) versus k (ordinate) relationship would flatten at the macroscopic level under conditions of horizontal flow, horizontal layering, and constant pore water resistivity.

The testing done by Urish (1978) was extended in this study, where both the horizontal and vertical layered cases are considered. A computer program was written which would perform the following steps;

1) Pick one value of permeability for each of five layers where each layer is isotropic and has equal thickness. Permeability values are randomly selected between limits of 10 and 600

ft/d.

2) Compute the associated resistivity for each layer based on equation 3.

3) Compute the aquifer permeability and aquifer resistivity based on equations 4 and 5, for the case of horizontal flow with horizontal layering (k_{hh} and ρ_{hh}) or vertical flow with vertical layering (k_{hh} and ρ_{vv}). Compute aquifer properties with equations 6 and 7, for the case of horizontal flow with vertical layering (k_{hv} and ρ_{hv}) or vertical flow with horizontal layering (k_{vh} and ρ_{vh}).

Limiting permeability values in the range of 10 to 600 ft/d are reasonable for aquifer material in southern Rhode Island (Gonthier et al., 1974). The random number generator used in step one was the GGUBFS routine in International Mathematical and Statistical Libraries (IMSL, Inc; 1979).

RESULTS: LAYERED MODEL

Correlations were first attempted where the hydraulic and electrical cases both have the same flow path. The procedure outlined in the previous section was repeated three hundred times.

Data for the case of flow parallel to the layering is shown in figure 3, where each point represents one of 300 simulated horizontally layered models (ρ_{hh} versus k_{hh}) or one of 300 simulated vertically layered models (ρ_{vv} versus k_{vv}). The line for the material level relationship, which represents an isotropic aquifer of constant permeability and apparent resistivity, is also shown in Fig. 3 . When the values in of Fig. 3 are separated according to their hydraulic anisotropy, the points tend to form lines parallel to the material relationship or isotropic line.

Hydraulic anisotropy is defined as the aquifer permeability for horizontal flow divided by the aquifer permeability for vertical flow. Thus, the value is equal to k_{hh}/k_{vh} for the horizontally layered case and is always greater than one. Likewise, electrical anisotropy will be defined as the aquifer resistivity for vertical flow divided by the aquifer resistivity for horizontal flow. For the horizontally layered case the value is ρ_{vh}/ρ_{hh}, which is also always greater than one. It should be noted that this is not the conventional definition of electrical anisotropy as defined by Keller and Frischknecht, which would be $\sqrt{\rho_{vh}/\rho_{hh}}$.

The results in Fig. 3 representing horizontal layering (ρ_{hh} vs. k_{hh}) were sorted according to hydraulic anisotropy ranges of 1.0 to 1.1 (Fig. 4), 2.0 to 2.5 (Fig. 5) and 3.5 to 7.0 (Fig. 6).

Results for the case of flow moving perpendicular to

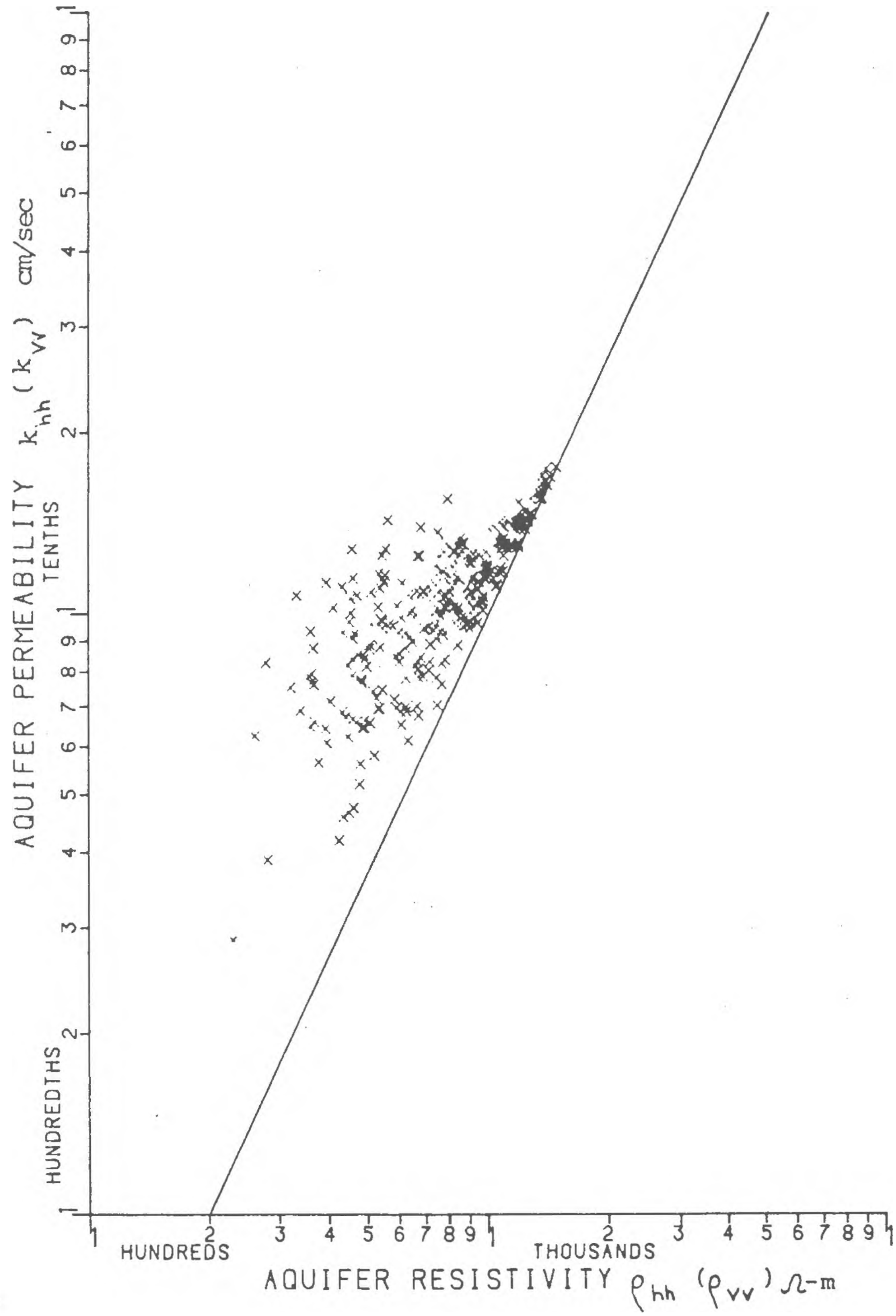

Figure 3. Aquifer resistivity vs. aquifer permeability points for 300 layered aquifer models, where flow parallels layering. Line is equation 3.

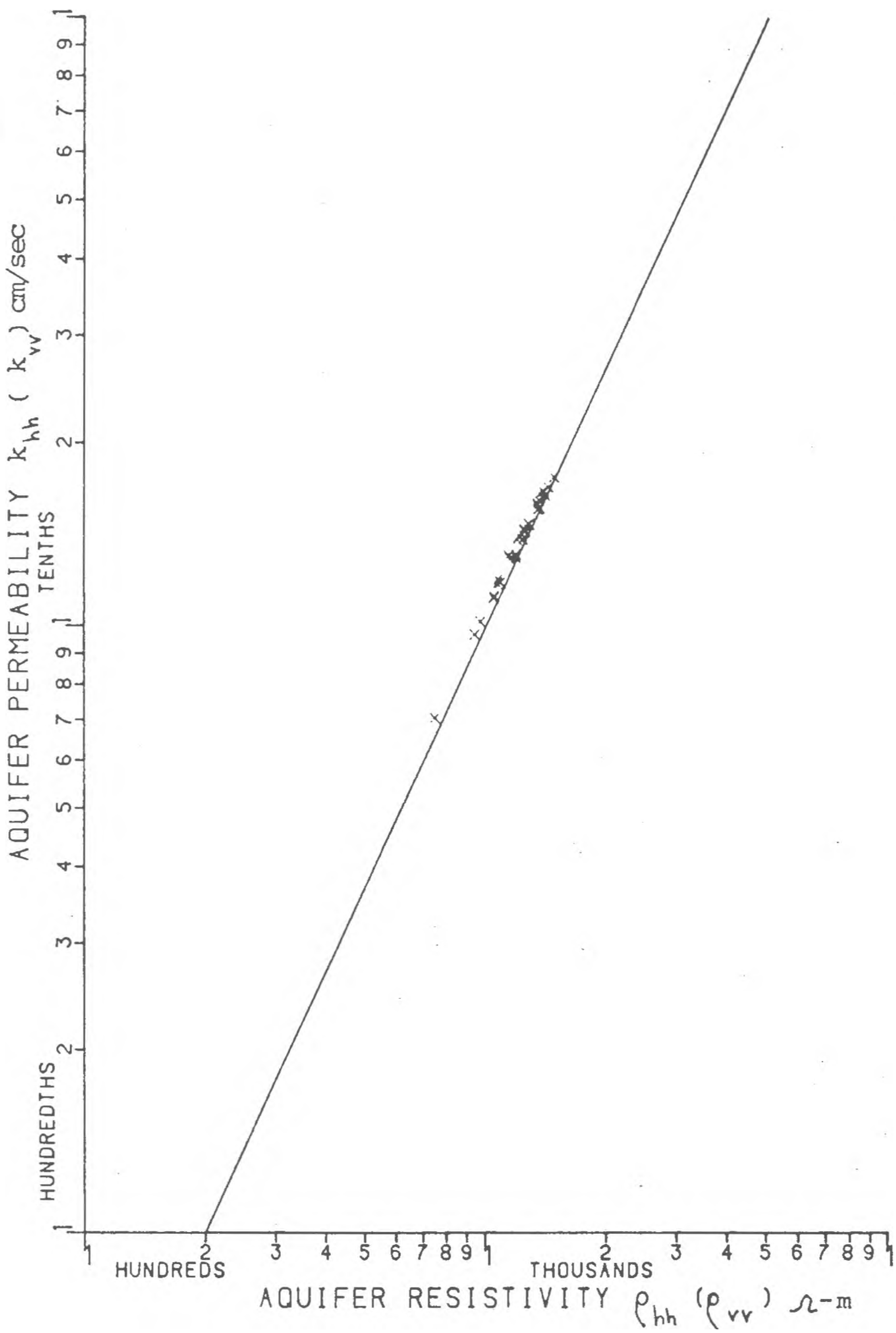

Figure 4. Aquifer resistivity vs. aquifer permeability for points from Fig. 3 with hydraulic anisotropies (horizontally layered) ranging from 1.0 to 1.1 (34 points).

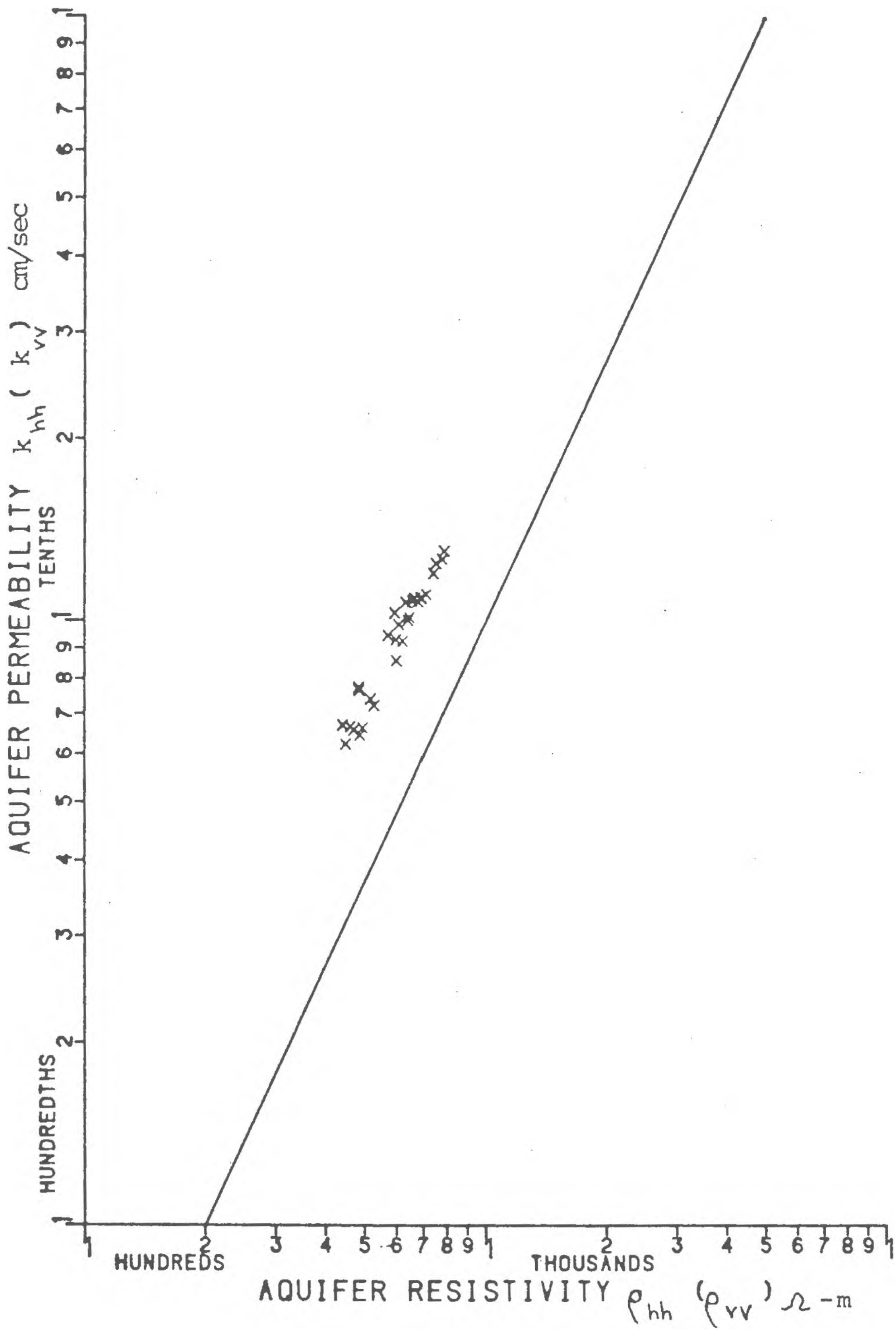

Figure 5. Aquifer resistivity vs. aquifer permeability for points from Figure 3 with hydraulic anisotropies (horizontally layered) ranging from 2.0 to 2.5 (29 points).

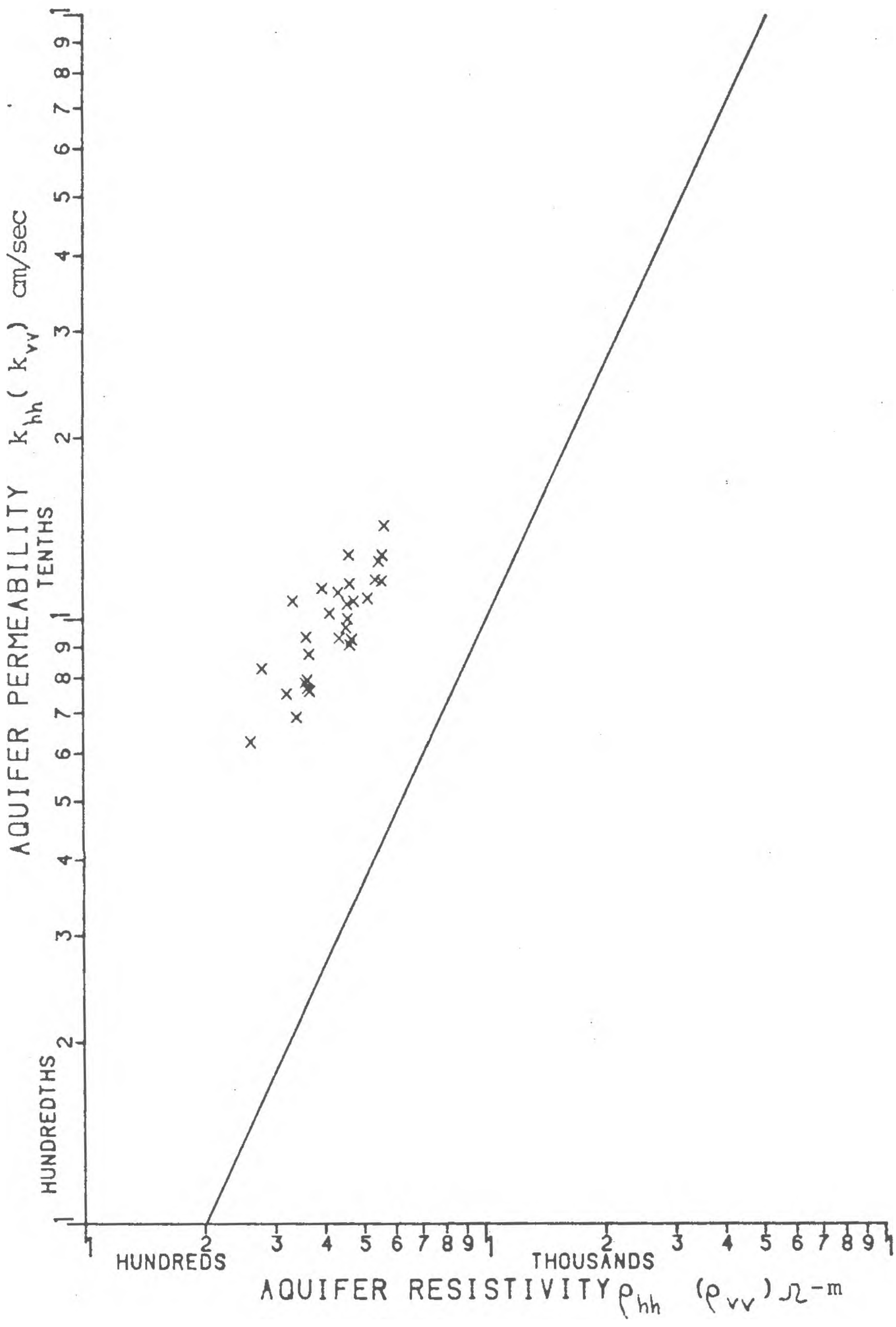

Figure 6. Aquifer resistivity vs. aquifer permeability for points from Figure 3 with hydraulic anisotropies (horizontally layered) ranging from 3.5 to 7.0 (29 points).

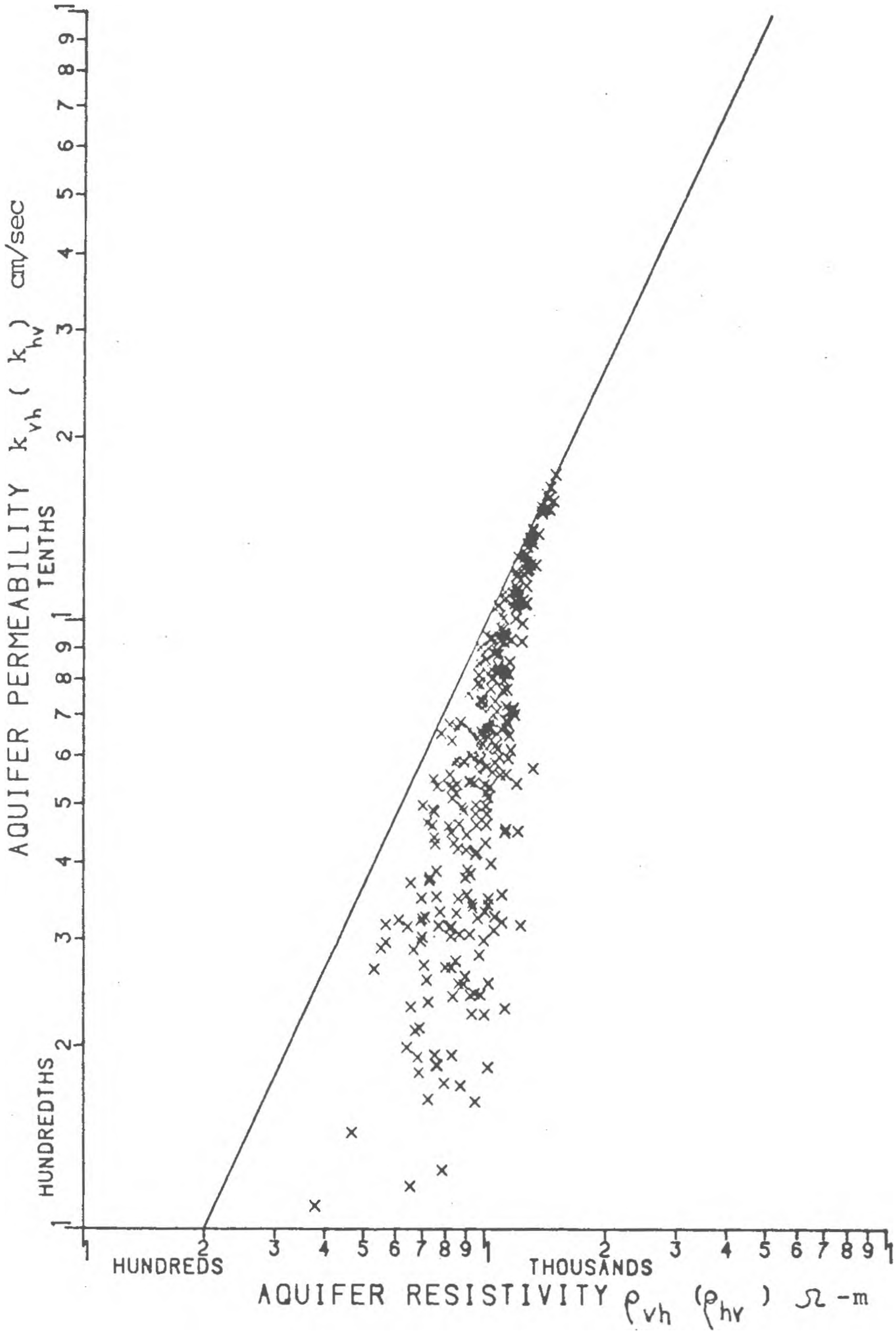

Figure 7. Aquifer resistivity vs. aquifer permeability points for 300 layered aquifer models, where flow is perpendicular to layering. Line is equation 3.

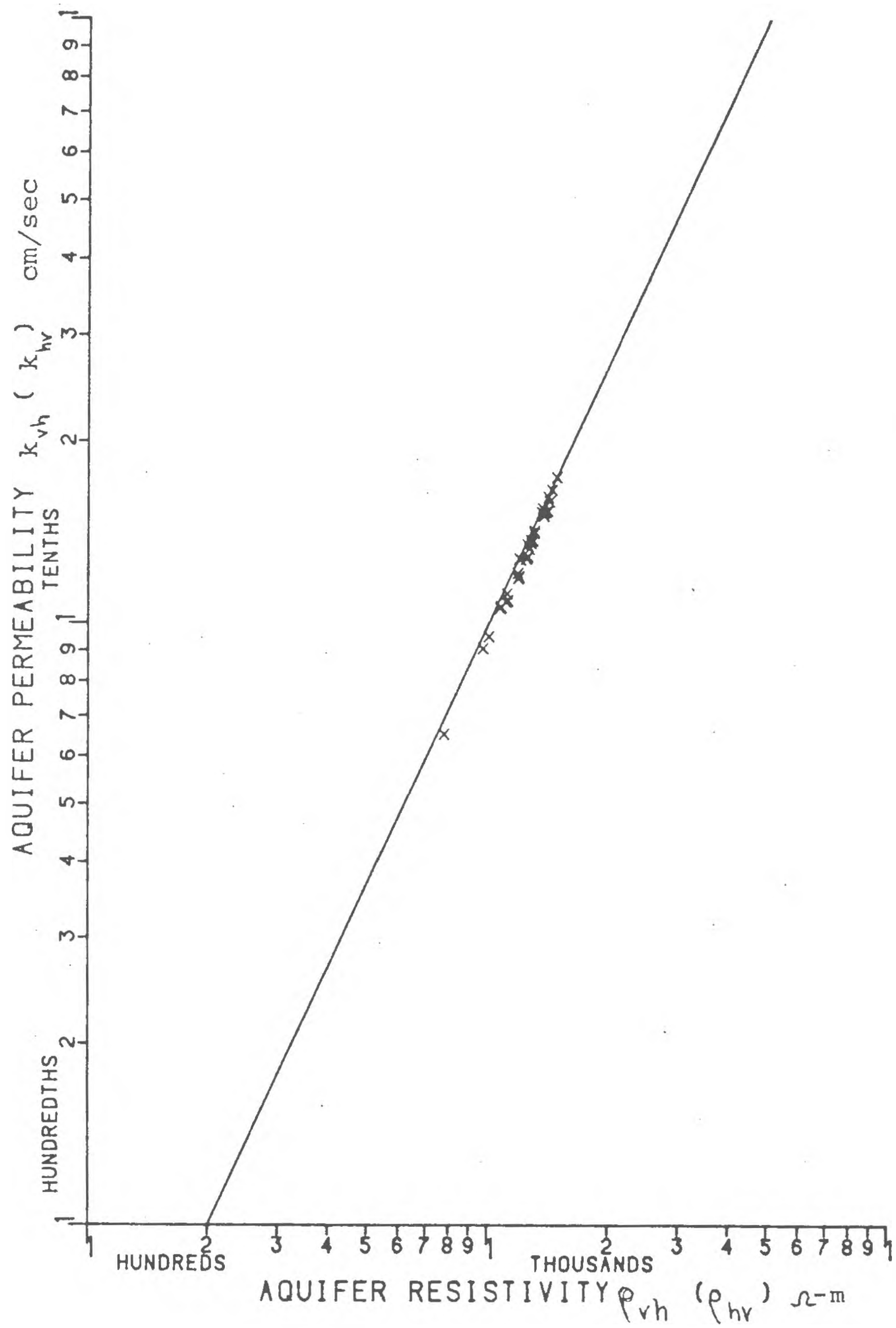

Figure 8. Aquifer resistivity vs. aquifer permeability for points from Figure 7 with hydraulic anisotropies (vertically layered) ranging from 1.0 to .91 (34 points).

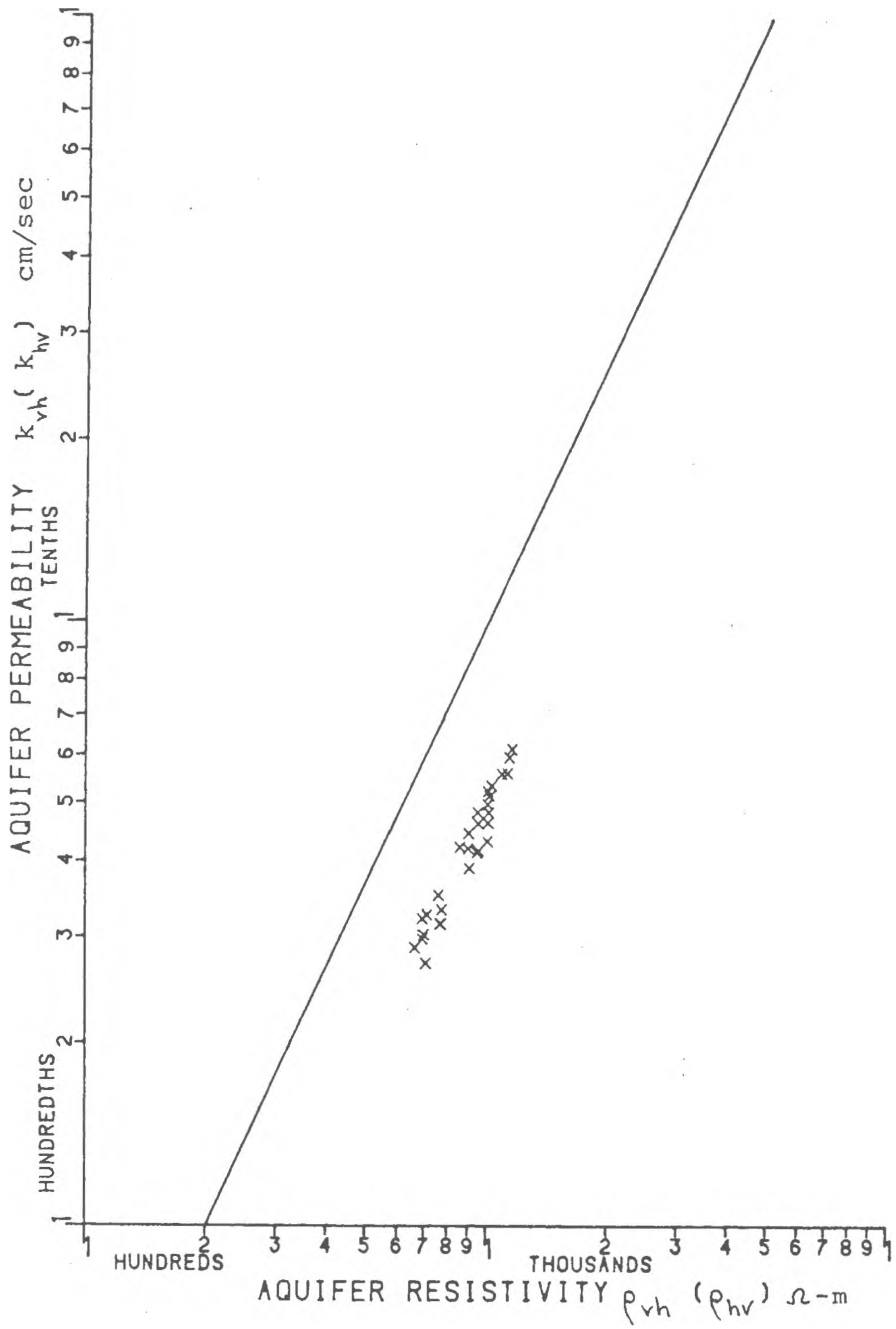

Figure 9. Aquifer resistivity vs. aquifer permeability for points from Figure 7 with hydraulic anisotropies (vertically layered) ranging from .5 to .4 (29 points).

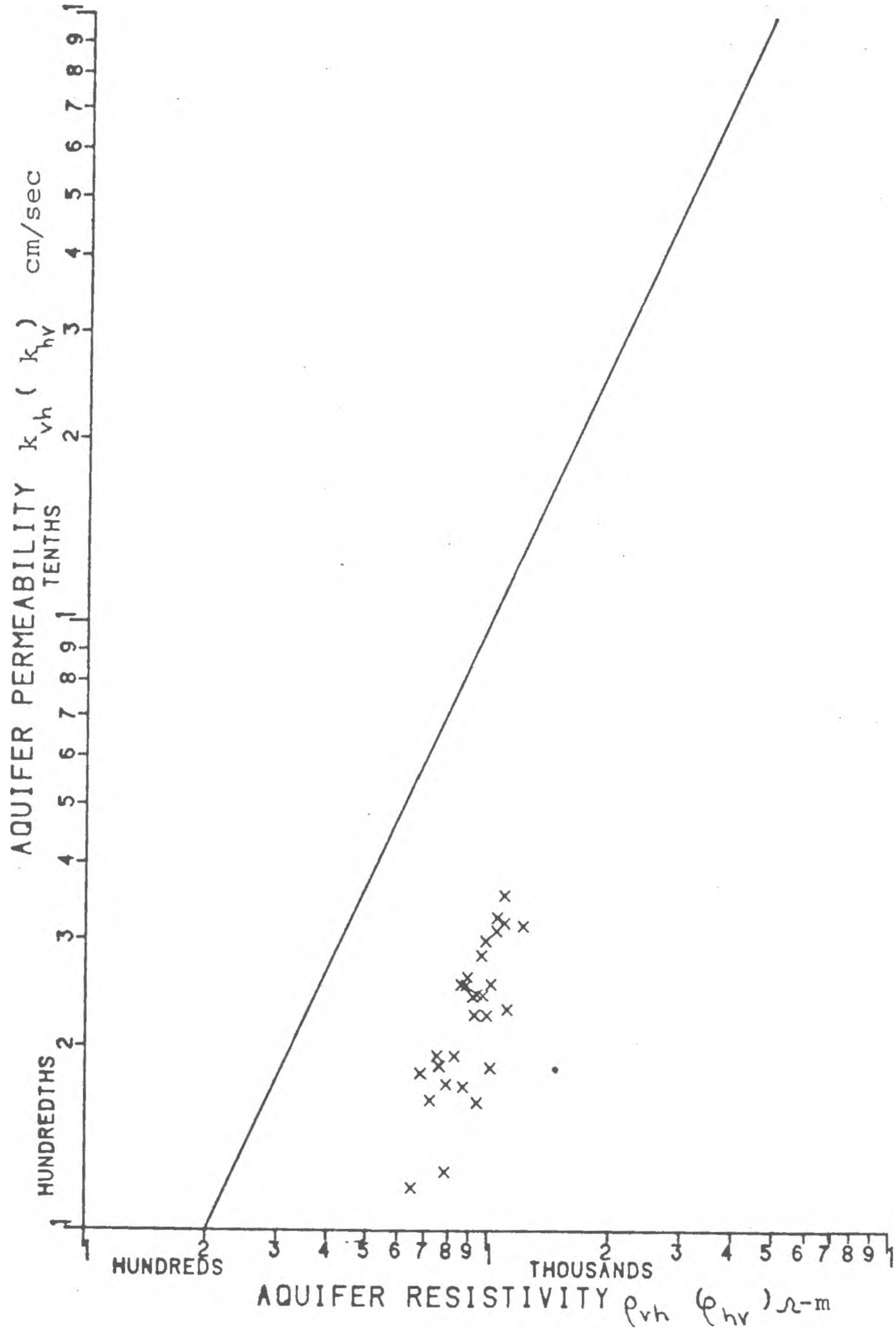

Figure 10. Aquifer resistivity vs. aquifer permeability for points from Figure 7 with hydrualic anisotropies (vertically layered) ranging from .29 to .14 (29 points).

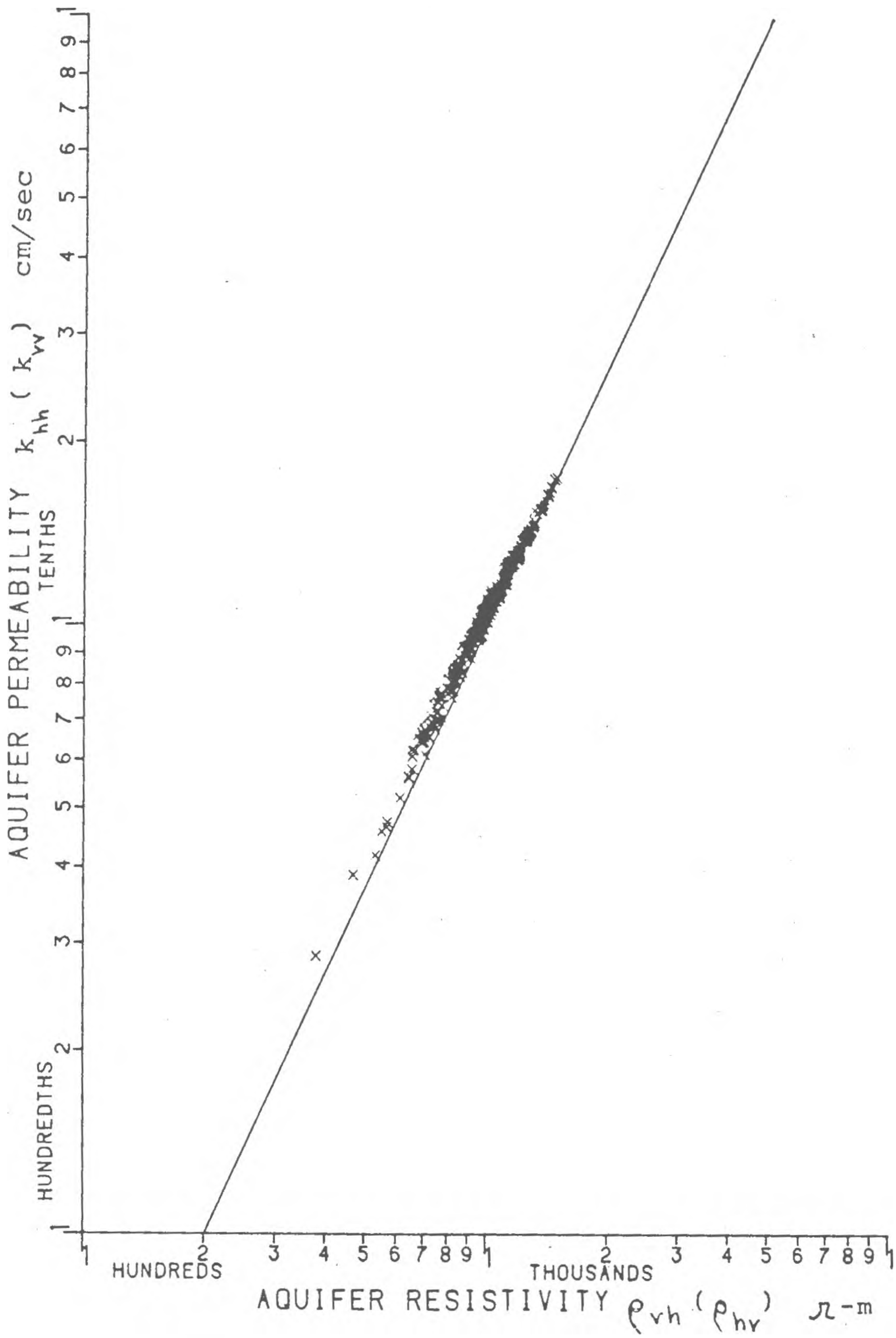

Figure 11. Aquifer resistivity vs. aquifer permeability for points for 300 layered aquifer models, where electric current flows perpendicular and hydraulic flow moves parallel to the layering.

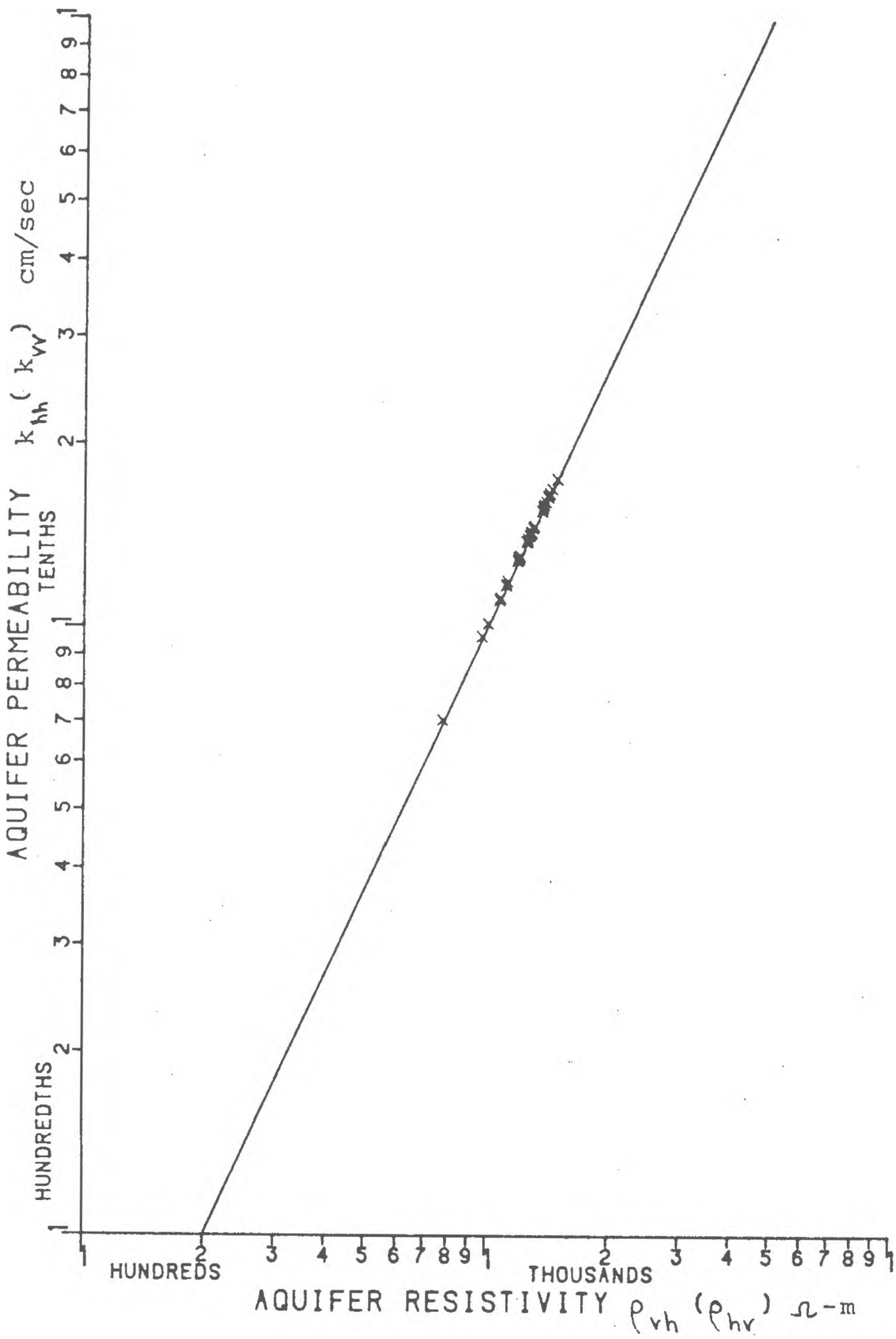

Figure 12. Aquifer resistivity vs. aquifer permeability for points from Figure 11 with hydraulic anisotropies (horizontally layered) ranging from 1.0 to 1.1 (34 points).

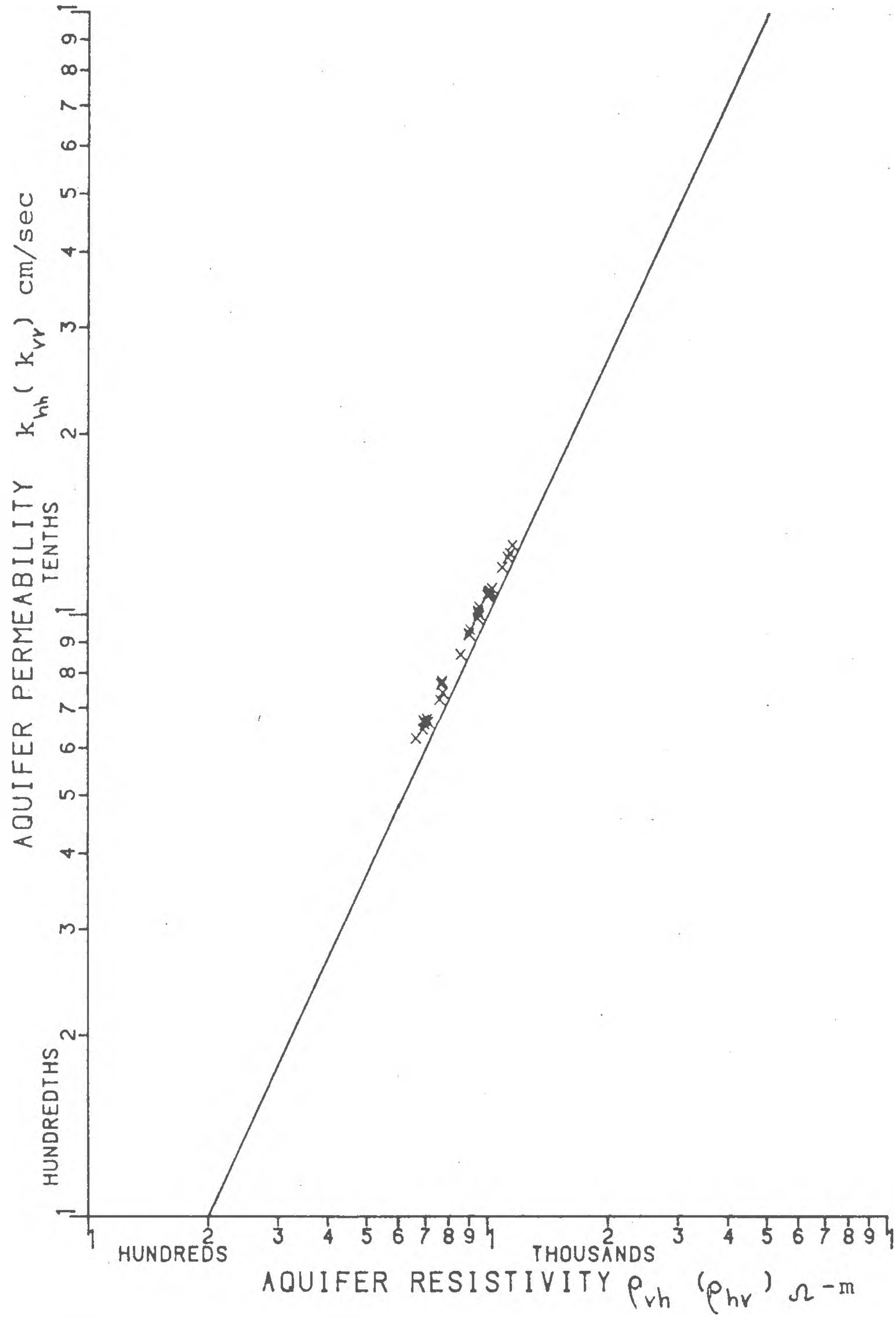

Figure 13. Aquifer resistivity vs. aquifer permeability for points from Figure 11 with hydraulic anisotropies (horizontally layered) ranging from 2.0 to 2.5 (29 points).

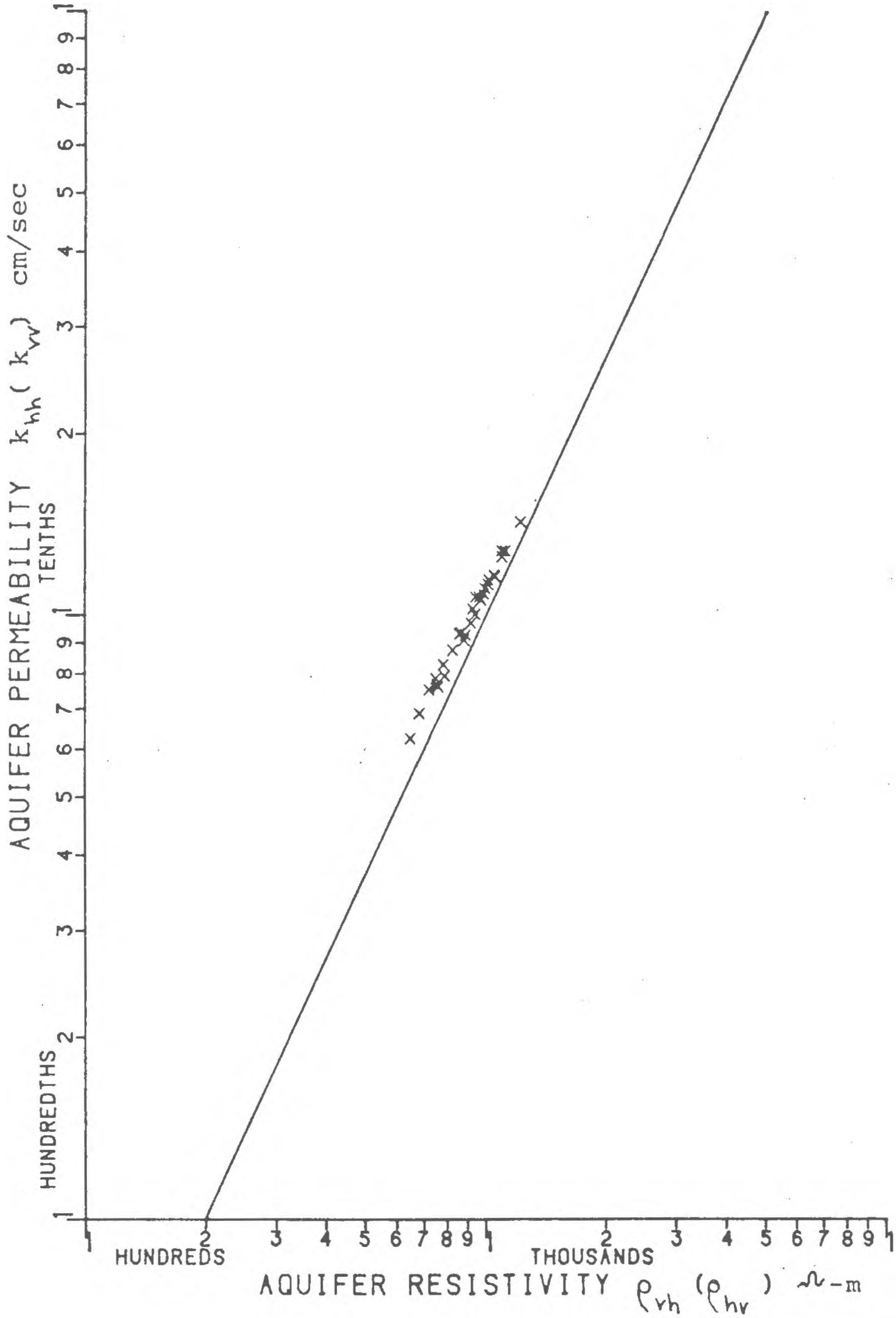

Figure 14. Aquifer resistivity vs. aquifer permeability for points from Figure 11 with hydraulic anisotropies (horizontally layered) ranging from 3.5 to 7.0 (29 points).

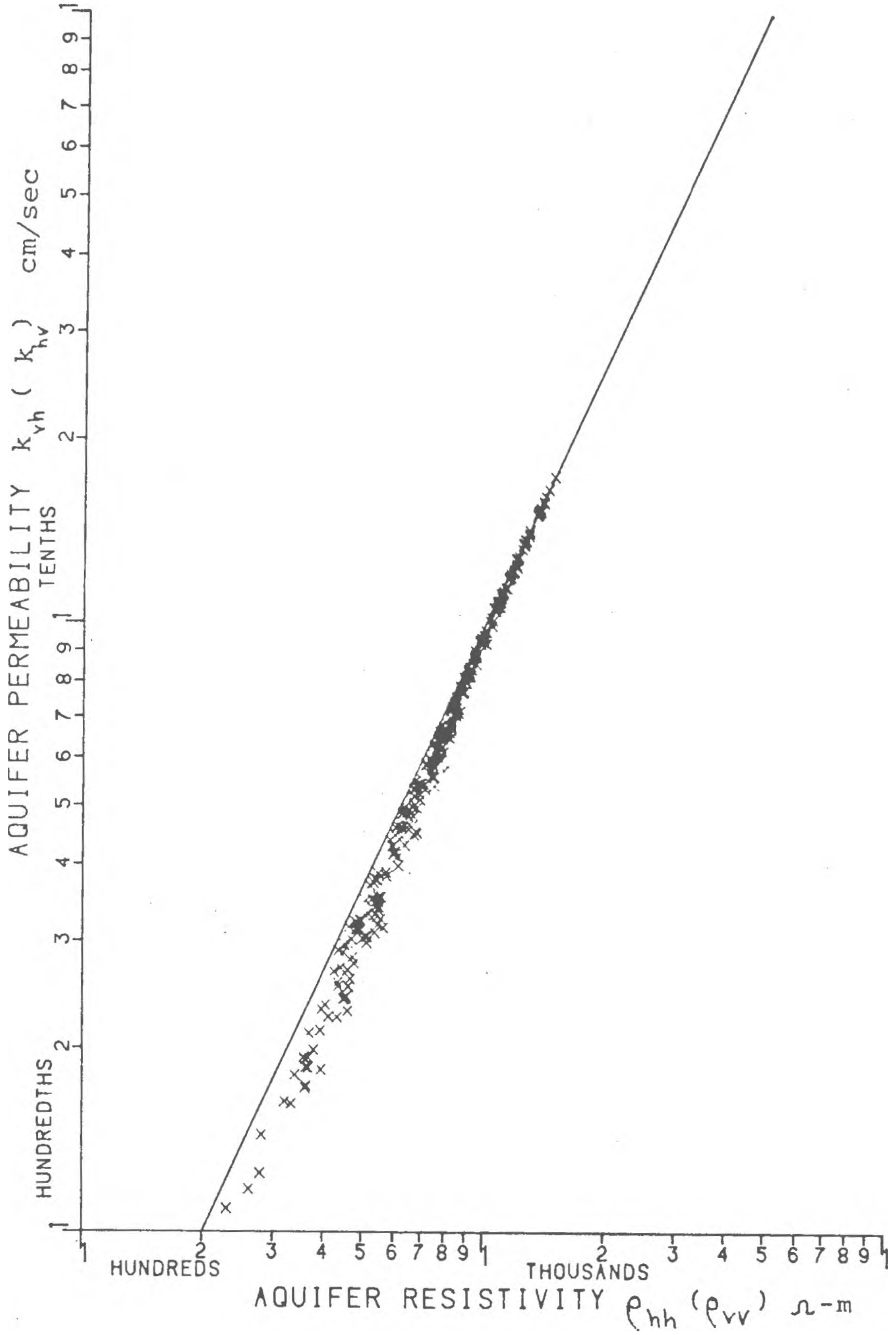

Figure 15. Aquifer resistivity vs. aquifer permeability points for 300 layered aquifer models, where electric current flows parallel and hydraulic flow moves perpendicular to the layering.

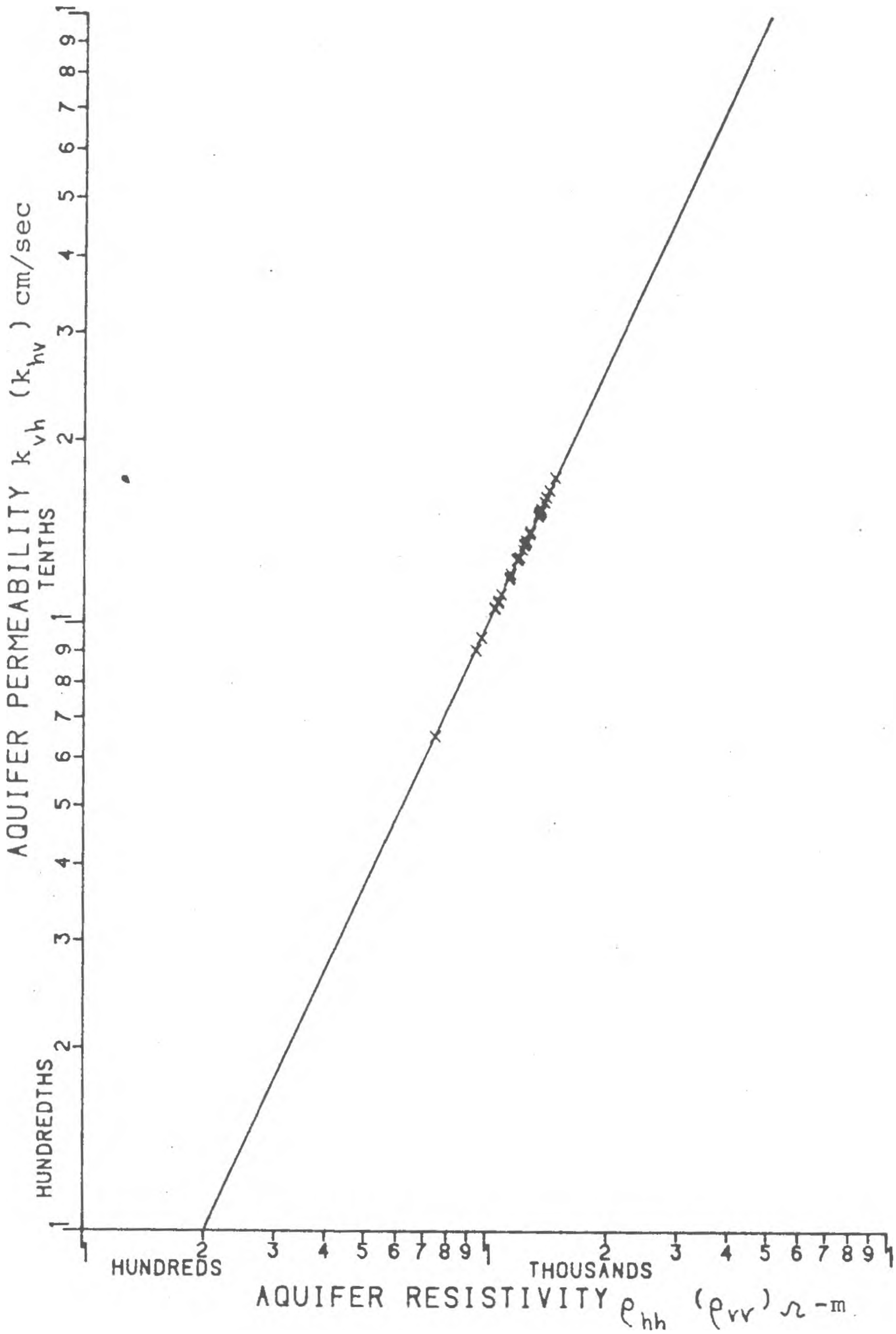

Figure 16. Aquifer resistivity vs. aquifer permeability for points from Figure 15 with hydraulic anisotropies (horizontally layered) ranging from 1.0 to 1.1 (34 points).

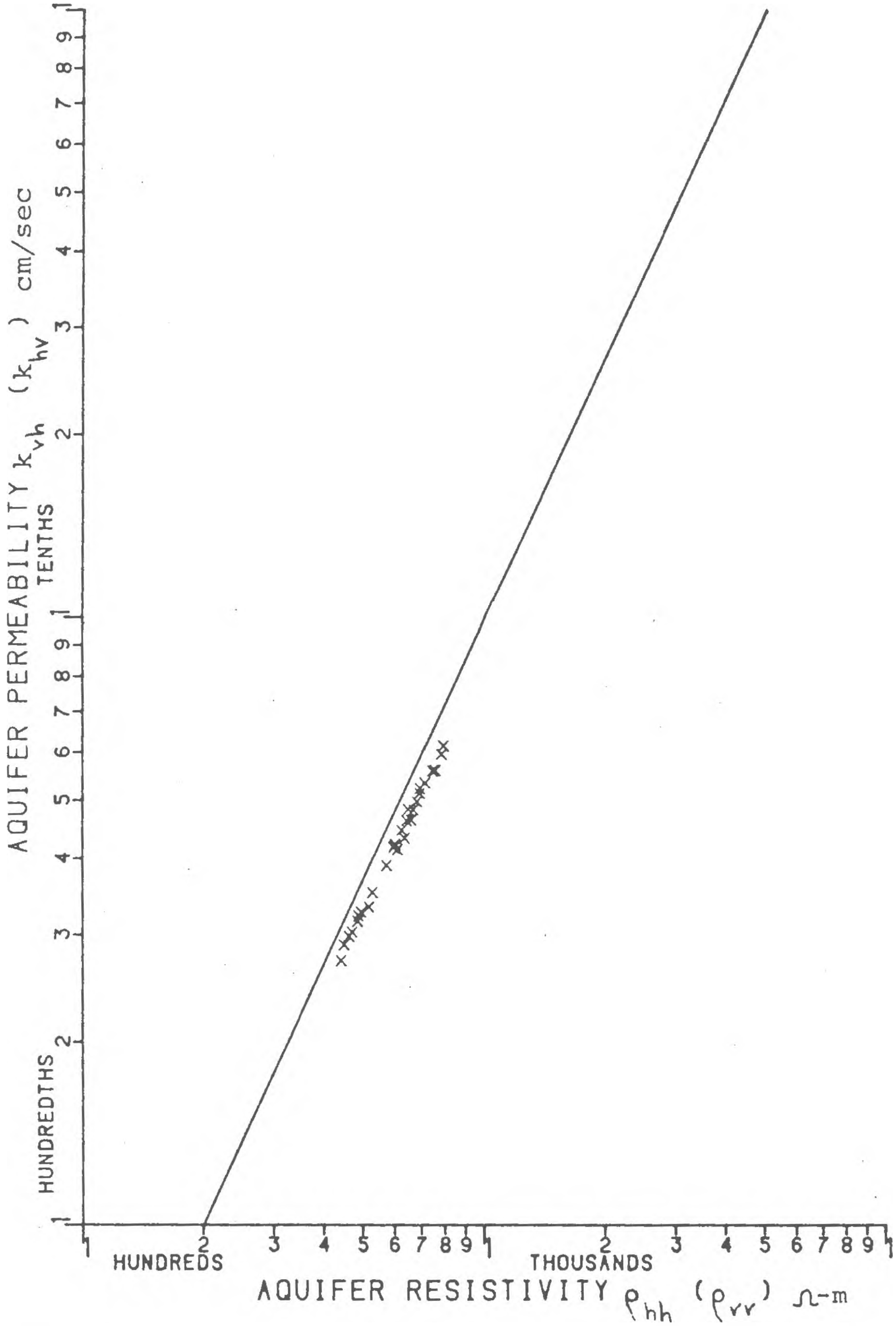

Figure 17. Aquifer resistivity vs. aquifer permeability for points from Figure 15 with hydraulic anisotropies (horizontally layered) ranging from 2.0 to 2.5 (29 points).

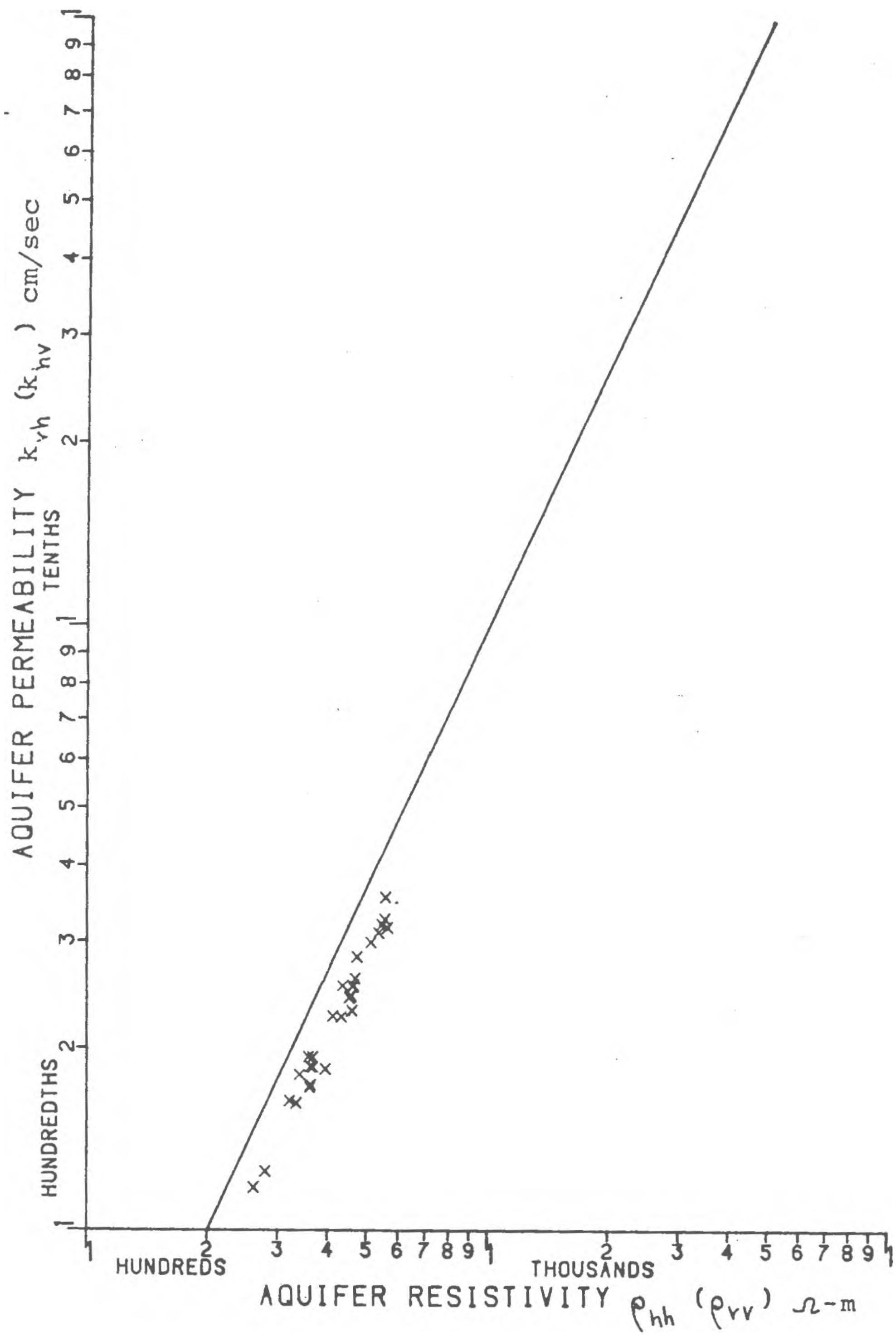

Figure 18. Aquifer resisitivity vs. aquifer permeability for points from Figure 15 with hydraulic anisotropies (horizontally layered) ranging from 3.5 to 7.0 (29 points).

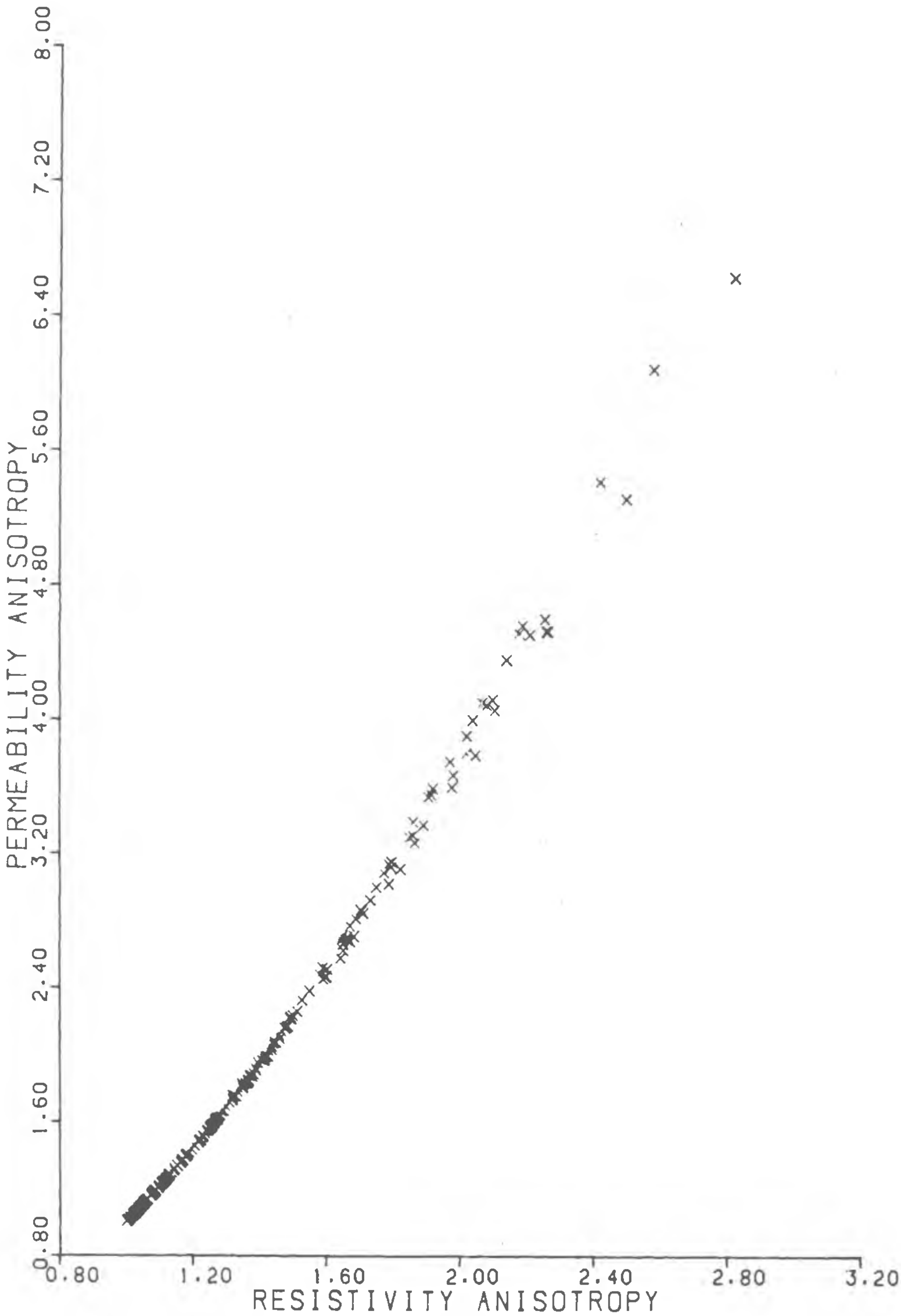

Figure 19. Resistivity anisotropy vs. hydraulic anisotropy points for horizontally layered models.

the layering are shown in Fig. 7, where each point represents one of 300 simulated vertical layered models (ρ_{hv} versus k_{hv}) or horizontally layered models (ρ_{vh} versus k_{vh}). The points in Fig. 7 representing vertical layering (ρ_{hv} versus k_{hv}) were then sorted according to hydraulic anisotropy ranges of 1.0 to .91 (Fig. 8), .5 to .4 (Fig. 9), and .29 to .14 (Fig. 10).

Correlations were then attempted where the hydraulic and electrical cases had opposite flow paths. This correlation may be expected to be good, since an examination of equations 4 and 7 reveals both quantities are computed as the weighted (layer thickness) arithmetic mean. Likewise, equations 5 and 6 are similar in that both are weighted harmonic mean values.

Conditions where the electrical current flows perpendicular to the layering and the hydraulic flow moves parallel will be examined first. If the horizontal layered case is considered, then Fig. 11 is a plot of ρ_{vh} versus k_{hh} for the 300 aquifer models. Fig. 11 also represents ρ_{hv} versus k_{vv} for the vertically layered case. The points in Fig. 11 representing the horizontally layered case (ρ_{vh} versus k_{hh}) were then sorted according to hydraulic anisotropy ranges of 1.0 to 1.1 (Fig. 12), 2.0 to 2.5 (Fig. 13) and 3.5 to 7.0 (Fig. 14).

Conditions where the electrical current moves parallel to the layering and the hydraulic flow moves perpendicular are shown in Fig. 15, where ρ_{hh} versus k_{vh}

or ρ_{vv} versus k_{hv} are shown. The points in Fig. 15 representing the horizontally layered case (ρ_{hh} versus k_{vh}) were then sorted according to hydraulic anisotropy ranges of 1.0 to 1.1 (Fig. 16), 2.0 to 2.5 (Fig. 17) and 3.5 to 7.0 (Fig. 18).

Fig. 19 shows the correlation between electrical anisotropy (ρ_{vh} / ρ_{hh})and hydraulic anisotropy (k_{hh} / k_{vh}).

OBSERVATIONS: LAYERED MODEL

The following observations are made for the layered case, where flow is linear, permeabilities within a layer range between reasonable limits and these permeabilities obey a material relationship similar to that of equation 3 (approximately equal in slope).

1. There is a good correlation between hydraulic and electric anisotropy.

2. If the hydraulic flow and electric current both move parallel to the layering, the aquifer values of ρ_{hh} vs. k_{hh} (or ρ_{vv} vs. k_{vv}) will always fall on or to the left of the material level ρ_a vs. k line (Fig. 3), with the distance from the line being proportional to the hydraulic or electric anisotropy (Figs. 4,5,6 and 19).

3. If the hydraulic flow and electric current both move perpendicular to the layering, the aquifer values of ρ_{hv} vs. k_{hv} (or ρ_{vh} vs. k_{vh}) will always fall on or to the right of the material level line (Fig. 7), with the distance from the line being proportional to the hydraulic or electric anisotropy (Figs. 8,9,10 and 19). Furthermore, each range of anisotropy comes close to producing a unique projection against the ρ or k axis (Figs. 8,9 and 10).

4. If hydraulic flow is parallel and electric current perpendicular to the layering, aquifer values of ρ_{vh} vs. k_{hh} (or ρ_{hv} vs. k_{vv}) will always fall on or to the left of the material ρ_a vs. k line (Fig. 11), with much less spread than was exhibited for the results of ρ_{hh} vs. k_{hh} (or ρ_{vv} vs. k_{vv}) in Fig. 3. Distances of plotted values from the material line appear to be proportional to the hydraulic or electric anisotropy (Figs. 12,13,14 and 19).

5. If the hydraulic flow moves perpendicular and the electric current moves parallel to the layering, the aquifer values of ρ_{hh} vs. k_{vh} (or ρ_{vv} vs. k_{hv}) will always fall on or to the right of the material level line (Fig. 15), with much less spread than was exhibited for the results of ρ_{hv} vs. k_{hv} (or ρ_{vh} vs.

k_{vh}) in Fig. 7. Distances of plotted values from the material line appear to be proportional to the hydraulic or electric anisotropy (Figs. 16,17,18 and 19), and each range of anisotropy comes closer to producing a unique projection against the ρ or k axis than occurs in Figs. 8,9 and 10.

6. The values of hydraulic anisotropy due to layering were found to range from 1.0 to about 7.0, with the majority of the values being between 1.0 and 4.0. These values may seen low, however, their value is a multiplication factor to an aquifer with anisotropy at the material level (micro-anisotropy).

CONVENTIONAL and STOCHASTIC DESCRIPTORS

Permeability values usually show variations in space within a geologic formation. By conventional definitions, if permeability is independent of position within a geologic formation, the formation is homogeneous. If permeability is dependent upon position within a geologic formation, the formation is heterogeneous (Freeze and Cherry, 1979).

Greenkorn and Kessler (1969) recognized that soil descriptors such as homogeneous and heterogeneous need to be defined stochastically. Their notation, which will be used in this study, is explained in the following excerpt from Freeze (1975).

> In general the probability density function for permeability (for example) is a function of location and orientation. This function can be described with five independent variables: three rectangular coordinaates for location and two angular coordinates for orientation. If the probability density function is independent of orientation, the media is isotropic; if it is dependent of orientation, the media is anisotropic. If the distribution is expressible by a finite linear combination of delta functions, the media is uniform; if not, it is nonuniform. When the distribution is monomodal, the media is homogeneous; if it is multimodal, it is heterogeneous.

Fig. 20 shows example frequency distributions of permeability for the four possible combinations of uniformity and homogeneity in isotropic media. Furthermore, any heterogeneous or nonuniform distribution will be considered spacially mixed (figs. 20b, c, and d).

If numerical modeling is used, an aquifer containing permeabilities which are spacially mixed will ultimately be resolved into an assemblage of pieces, where each piece may be micro-isotropic or micro-anisotropic. Thus the terms micro-isotropic and micro-anisotropic will be used in this study to describe material (or nodal) properties. The terms isotropic and anisotropic will be reserved for describing the entire modeled region (aquifer). Note that these specifications do not destroy the Greenkorn and Kessler definitions. Thus, an aquifer will be considered

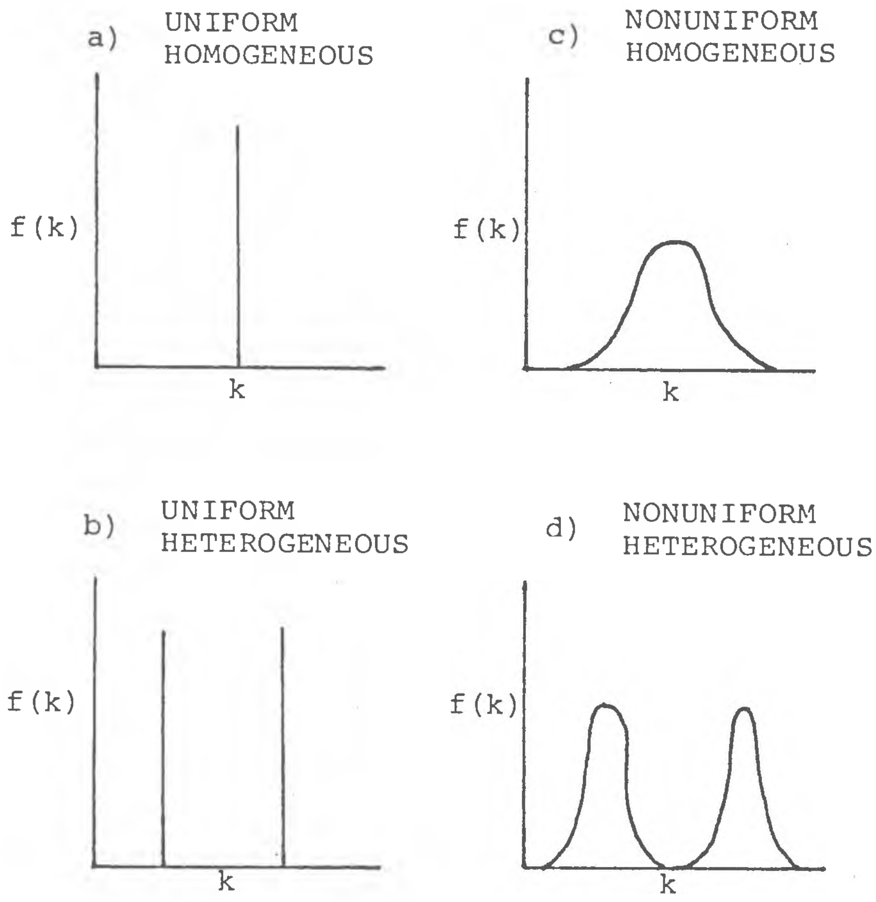

Fig. 20. Frequency distribution for permeability (k), illustrating Greenkorn and Kessler's (1969) definition of uniformity, homogeneity and heterogeneity

isotropic only if the assemblage of component pieces are micro-isotropic and have a uniform homogeneous distribution.

Clarke (1972), provides a comprehensiive list of terms and definitions to classify hydraulic models. His definition of a deterministic model will be used for cases where the permeabilities do not have some spacial distribution, that is, when the permeability values are exactly known.

PREVIOUS WORK: STOCHASTIC MODELS

When an aquifer is composed of a mixture of stratified drift materials, very often the distribution of permeabilities can be approximated by a probability density function (Freeze, 1975). Many researchers have used stochastic models in groundwater hydrology, although none are known to have been applied to resistiviity modeling.

The first researchers to stochastically model aquifer permeabilities were Warren and Price (1961). They found that the most probable behavior of a nonuniform homogeneous (see Fig. 20) or a uniform heterogeneous system approaches that of a uniform system with an aquifer permeability equal to the geometric mean of the nodal permeabilities. Distributions tested included uniform, exponential, and lognormal. They utilized a three dimensional finite difference model with single phase flow forced by boundary conditions to move predominately in one direction (quasi-linear). After steady state total heads were obtained, total flow was calculated through a plane near a constant head boundary and used to compute aquifer permeability.

Warren and Price also analyzed the effects of flow geometry, anisotropy, and partial penetration on computed aquifer permeabilities. In a comparison betweeen quasi-linear and quasi-radial flow, they found that the expected or mean aquifer permeability is essentially independent of flow geometry. However, differences in quasi-radial and quasi-linear flow geometries were found to influence the standard deviation of the aquifer permeabilities computed for different arrangements of a distribution. Standard deviation was used as a measure of what Warren and Price call the scale of heterogeneity. They also showed this scale of heterogeneity to be a function of the number of model elements and the number of elements in each class of permeability values on a discretized frequency diagram (histogram). Limits are zero for the conventionally defined homogeneously heterogeneous case, and one for completely heterogeneous conditions. The scale of heterogeneity was used as a measure of the redundancy or entropy of the permeability distribution in space. Anisotropy was shown to cause a finite but not a particularly significant effect, and the apparent increase in aquifer permeability with increasing micro-anisotropy, was attributed to crossflow. Partial penetration of half the full depth was shown to cause a reduction in the expected aquifer permeability by about fifteen percent of the fully penetrating value.

McMillan (1966) found that the standard deviation of the hydraulic potential was a function of the mean and standard deviation of the permeability, the mean of the gradient and the nodal spacing. He used lognormal permeability distributions in the range of .5 to .8, which several studies indicated to exist in the field. Bouwer (1969), using a two dimensional electric analog model, found the aquifer permeability to be closest to the geometric mean of nodal permeabilities, when permeabilitieswere selected from a uniform distribution. Freeze (1975) thoroughly examined the effect of uncertainties in soil properties, boundary condition, and initial conditions on the hydraulic heads with one-dimensional steady state and transient flow. For steady state conditions, he concluded the best possible prediction that can be provided for the hydraulic head at any point is a description of the probability density function of hydraulic head at that point. Freeze also demonstrated the difficulties (and perhaps the impossibility) of defining an equivalent uniform media for transient flow in nonuniform homogeneous geologic formations. In his analysis he used multivariate relations between permeability, porosity, and soil compressibility.

COMPUTER MODEL DEVELOPMENT (CARTESIAN COORDINATES)

There are no equations for computing average macroscopic transport properties when the material level components are spacially mixed. However, if the steady state potentials are known under conditions where the flow is macroscopically linear (quasi-linear), a technique may be employed to solve for the "aquifer permeability" (Warren and Price, 1961). Since there are no analytical solutions for potential quantities in these spacially mixed problems, numerical methods will be used to solve a two-dimensional confined aquifer cross sectional model, where left and right side vertical boundaries are constant potentials (2-D, quasi-linear).

Numerical methods are widely used today and many good computer codes are available for groundwater models (Trescott et al., 1976; Prickett and Lonniquist, 1971). Resistivity modeling is not as developed, particularly for spacially mixed problems. Shortcomings are apparent in methods used to compute connection conductivity values (see appendix D).

In order to facilitate program alterations for various tests and to use a minimum of computer core requirements, a computer model was developed. The model procedure is as follows:

1. Input permeability values, which can be any of the

following:

A: Deterministic

1. all equal
2. horizontally layered
3. vertically layered

B: Stochastic

1. a uniform distribution over the entire model
2. different uniform distributions within each layer
3. an exponential distribution over the entire model
4. a lognormal distribution over the entire model

2. Calculate the connection value permeabilities.

3. Compute the steady state total heads.

4. Compute the aquifer permeability.

This procedure would then be repeated for the related electrical model.

1. Input the exact same permeabilities at the same locations but convert these to electrical conductivities (σ) according to the following equation:

$$\sigma_a = \frac{1}{\rho_a} = \frac{1}{\left(\frac{k}{5.13 \times 10^{-6}}\right)^{.7}} \tag{8}$$

which is a rearrangement of equation 3.

2. Calculate the connection value electrical conductivities .

3. Compute the steady state scalar electrical potentials.

4. Compute the aquifer resistivity.

The computed (aquifer resistivity, aquifer permeability) points were plotted and compared to the material level line (equation 3).

Numerical modeling is based upon the discretization of a differential equation which results in a set of simultaneous equations which are then solved for the unknown potentials at discrete locations (nodes). In the hydraulic case, each node has an asssociated permeability value, or nodal permeability. Invariably, the connection permeability between adjacent nodes must be computed. In most state-of-the-art hydraulic models (Trescott, 1975; Trescott et al., 1976), this connection permeability is computed as the weighted harmonic mean of two adjacent nodal permeabilities, where the weight factor is the nodal thickness orthogonal to flow. The validity of this approach is easily shown, since this weighted harmonic mean can be shown to be the average permeability for flow perpendicular to the layering (eq. 6). Connection permeabilities are computed as the two layer case of equation 6.

Since electrical conductivity is the reciprocal of electrical resistivity,

$$\sigma = \frac{1}{\rho} \tag{9}$$

equation 7 may be rewritten as

$$\sigma_{vh} = \sigma_{hv} = \frac{\sum_{i=1}^{n} h_i}{\sum_{i=1}^{n} \frac{h_i}{\sigma_i}} \tag{10}$$

Connection conductivities in the electrical model were computed as the two layer case of equation 10, which is a weighted harmonic mean of the nodal conductivities.

In solving for the steady state hydraulic potentials, the iterative alternating direction implicit procedure (IADI) was used to solve the finite difference form of the following equation:

$$\frac{\partial\left(k_x \frac{\partial h}{\partial x}\right)}{\partial x} + \frac{\partial\left(k_y \frac{\partial h}{\partial y}\right)}{\partial y} = 0 \tag{11}$$

where h = total hydraulic head

k_x = permeability in the x-direction

k_y = permeability in the y-direction

Likewise, the IADI procedure was used to solve for scalar electrical potentials in the following equation:

$$\frac{\partial\left(\sigma_x \frac{\partial v}{\partial x}\right)}{\partial x} + \frac{\partial\left(\sigma_y \frac{\partial v}{\partial y}\right)}{\partial y} = 0 \qquad (12)$$

where v = scalar electrical potential

σ_x = conductivity in the x-direction

σ_y = conductivity in the y-direction

Comparison of equations 11 and 12, reveals they are completely analogous. This is discussed further in appendix F, where equations 11 and 12 are derived and discretized.

The IADI method requires the solution of a set of simultaneous equations, which when in matrix form yield a tridiagonal coefficient matrix. These equations are then solved using the Thomas algorithm, which is described in appendix G.

The IADI procedure was used for the following reasons:

1. The algorithm is relatively straight forward and could easily be adjusted to suit model boundary conditions should the need arise.

2. According to Roach (1972), ADI methods are very effective for problems with regular boundary conditions.
3. The Thomas algorithm is extremely stable with respect to roundoff errors (Remsen, Hornberger and Moltz, 1973)
4. The IADI procedure was used in other well documented digital groundwater modeling programs (Trescott et al., 1976; Prickett and Lonnquist, 1971).

Computation of the aquifer permeability followed the method used by Warren and Price for quasi-linear flow. They computed aquifer permeability in a 3-D model by calculating the flow between two steady state potential surfaces and dividing by a shape factor equal to the change in potential through the entire model times the total cross sectional area divided by the total model length.

In this study, quasi-linear horizontal flow is achieved by setting constant hydraulic head boundaries at the left and right boundaries of the confined (top and bottom boundaries have no flow across them) aquifer cross section model. Horizontal flow is then computed by summing the result of Darcy's law for steady state total heads at each discrete point over an entire column. Expressed numerically, the aquifer permeability for quasi-linear horizontal flow is;

$$k_h = \left[\sum_{i=1}^{R} \bar{k}_{i,j+1} \frac{\Delta h_{i,j}}{\Delta l} \right] \frac{\Delta L}{\Delta H A} \tag{13}$$

Fig. 21 shows parameters in this equation,

where R = number of model rows

$\bar{k}_{i,j+1}$ = connection value of permeability between $h_{i,j}$ and $h_{i,j+1}$, where i, j indicate row and column respectively

$$= \frac{\Delta x_j + \Delta x_{j+1}}{\frac{\Delta x_j}{k_{i,j}} + \frac{\Delta x_{j+1}}{k_{j+1}}} \tag{13a}$$

$\Delta h_{i,j}$ = change in steady state total hydraulic head across Δl

$= h_{i,j} - h_{i,j+1}$

Δl = length between $h_{i,j}$ and $h_{i,j+1}$

a = nodal cross sectional area (normal to flow)

ΔL = total length over which ΔH is dissipated

ΔH = total dissipated head through the model

A = total model cross sectional area (normal to flow)

Equation 13 was applied between columns 2 and 3, since no numerical error exists at the constant head nodes in column 2. The value for k_V is computed in similar fashion, where flow moves vertically.

Since the electrical potential flow problem is completely analogous to the hydraulic case, the aquifer resistivity for quasi-linear horizontal current flow was

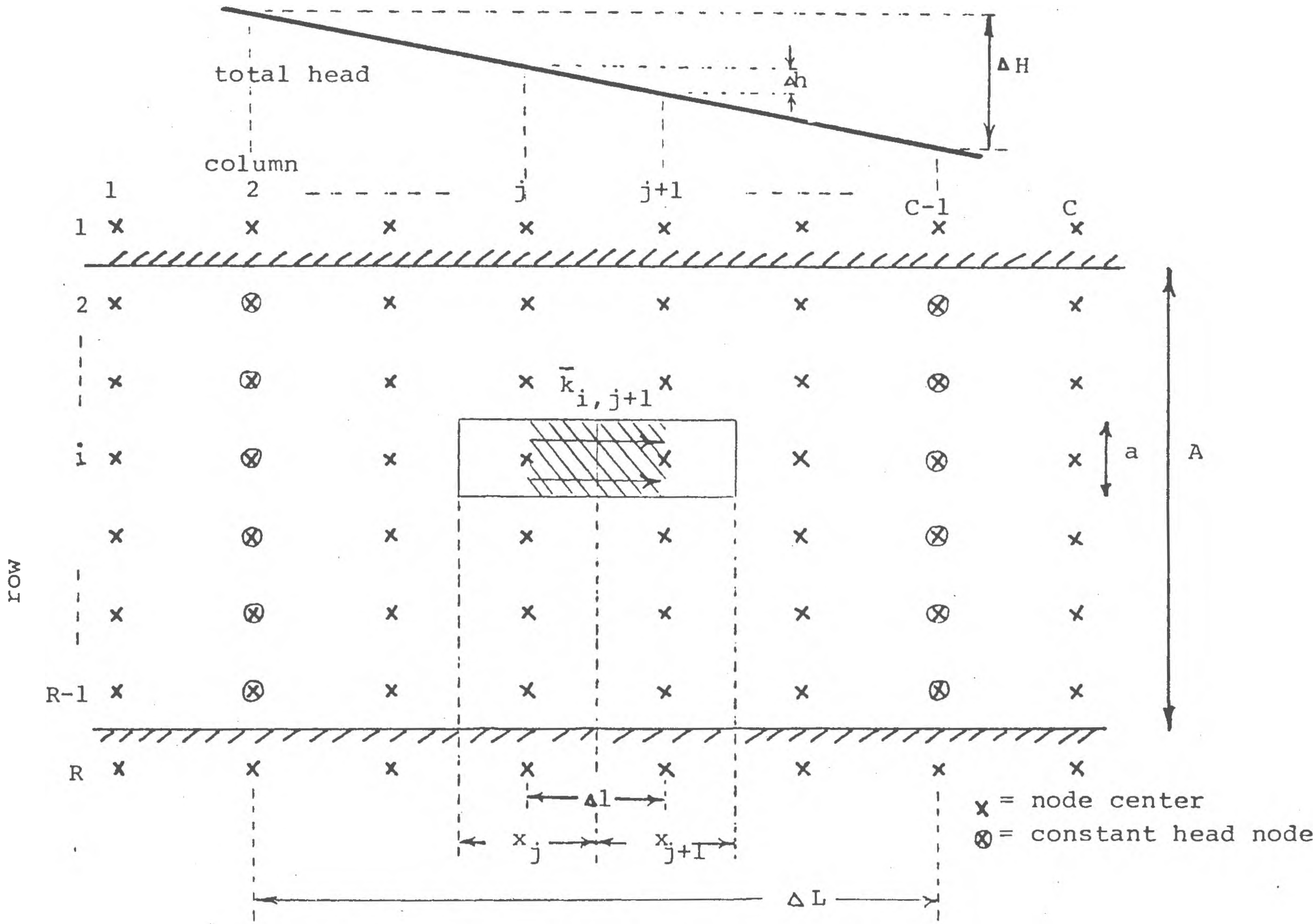

Figure 21. Sketch of 2-D Section with Horizontal Flow

computed as

$$\rho_h = \frac{1}{\sigma_h} = \frac{1}{\sum_{i=1}^{R} \bar{\sigma}_{i,j} \frac{\Delta V_{i,j}}{\Delta l} \frac{\Delta L}{\Delta VA}} \qquad (14)$$

where σ_h = aquifer conductivity for horizontal quasi-linear flow.

$\bar{\sigma}_{i,j}$ = connection value of conductivity between $v_{i,j}$ and $v_{i,j+1}$

$\Delta v_{i,j}$ = change in steady state electrical potential across 1

ΔV = total change in steady state electrical potential through the model

Other quantities are previously defined.

The value for ρ_v is computed in similar fashion, where current flows vertically.

PROGRAM VALIDATION AND TESTING

The program was first checked against the program developed by Trescott (1976). For the isotropic uniform case, results were identical to five significant figures with differences representing less than .005% of the total dissipated head. A model having three vertical layers was then tested and the aquifer permeability computed from the numerical results using equation 13 (k_h) was within .009% of the theoretical value calculated by equation 6 (k_{hv}).

In both of these tests five iteration parameters were used with an error criteria for closure (ECC) of .001 . Iteration paramerers are used to aid convergence in the IADI procedure. Their use is discussed in appendix H and by Trescott (1976). The ECC value is the maximum difference in potential at any discrete point between successive iterations, as required to achieve the steady state.

When ECC values of 1.0, .1, and .01 were used for the vertically layered model, differences in hydraulic head, from the case of ECC equal to .001, were noted. These differences are shown in table 1 and represent the maximum difference in hydraulic head at any point through the middle row of the model. A single row was felt to be representative, since the difference in head within any column is small when horizontal flow occurs.

Error Criteria for Closure at Steady State (ECC)	ECC / Total Dissipated Head	Maximum % Difference in Hydraulic Heads from ECC=.001 Hydraulic Heads*
1	10%	8.4%
.1	1%	.6%
.01	.1%	.05%
.001	.01%	0%

Table 1 : Effect of the error criteria for closure on steady state potentials. * computed at the middle row of the model.

Table 1 shows the ratio of ECC to the total dissipated head to be close to the error in the potential quantities. To be conservative, an ECC value of .001 was used in subsequent program runs.

When a uniform distribution of permeabilities (with limits of 10 to 600 ft/d) was input to the model with a total dissipated head of 20 ft. and five iteration parameters, convergence was not achieved. Since the optimum minimum iteration parameter (w_{min}) is computed by the program only for simple problems (Trescott et al., 1976), other values were tested by trial and error. First, the total dissipated head was raised to 100 and the limits of the uniform distribution were restricted to the range of 40 to 600 ft/d. The fastest convergence occurred when w_{min} equaled .005.

The other factor that may be critical with the IADI procedure is the number of iteration parameters, which should be increased if the difference between the maximum and minimum parameters are greater than three orders of magnitude (Trescott et al., 1976). When nine iteration parameters were used with the computed w_{min}, satisfactory convergence was achieved. Since convergence was not as good (required more iterations) when w_{min} equaled .005 with nine iteration parameters, subsequent runs utilized the calculated value of w_{min} and nine iteration parameters.

RESULTS: QUASI-LINEAR STOCHASTIC MODEL

The model was first run with nodal permeabilities selected at random from a uniform distribution. This distribution fits Greenkorn and Kessler's general category of nonuniform and homogeneous (Fig. 20). Figure 21a shows the flow net for a typical run with horizontal quasi-linear flow (a detailed explanation of the techniques used to draw the flow net using computer graphics is provided in appendix K). The uniform distribution was selected because of its simplicity; it is not known to occur in the field. Appendix H shows how the distribution is simulated with the IMSL routine GGUBFS. Table 2 shows the limits and the mean or expected value for the distributions tested. These limits were selected to keep the range evenly balanced about some point on a log k scale; reasons will become apparent later.

# of models tested	A (lower limit) (ft/d)	μ (mean) (ft/d)	B (upper limit) (ft/d)
1	62	80	98
2	39	97	155
3	25	135	245
4	15	202	389
5	10	305	600

Table 2 : Uniform distribution limits and means

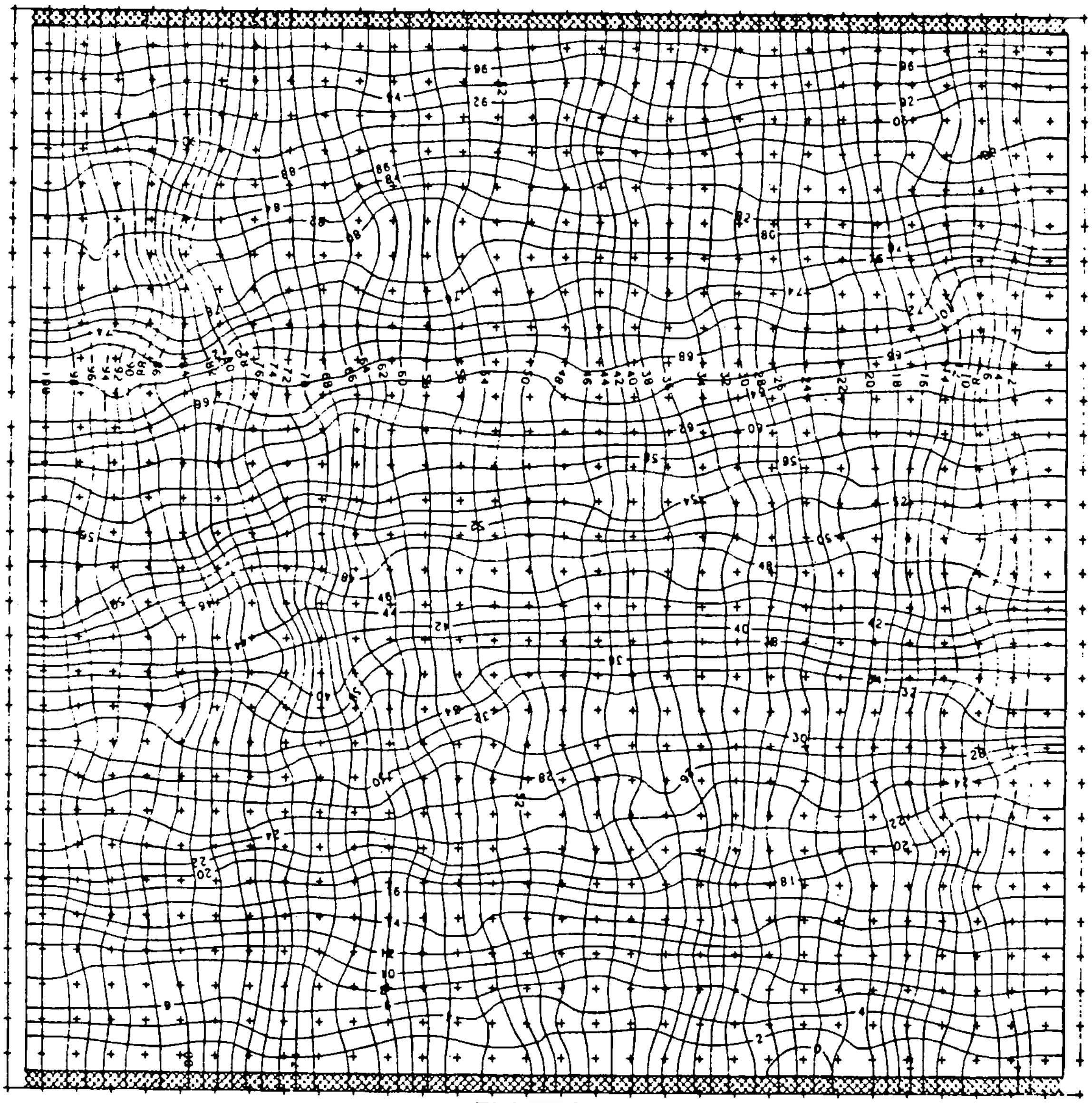

FLOW NET

Figure 21a. Flow net showing horizontal quasi-linear flow through an aquifer model, where nodal permeabilities are uniformly distributed between 10 ft/d and 600 ft/d.

The model contained 32 rows and 32 columns. For quasi-linear horizontal flow, k_h and ρ_v were determined from two separate program runs. Likewise, k_v and ρ_v were obtained for the quasi-linear vertical flow regime. Anisotropies k_h/k_v and ρ_v/ρ_h were then computed. Table 3 shows all the data, and the horizontal aquifer resistivity (ρ_h) is plotted versus the horizontal aquifer permeability (k_h) in Fig. 22. It was observed that wider ranges gave greater deviations in ρ_h, k_h points; hence, more points were plotted for these ranges.

The effect of the number of model nodes was examined when models of 64 (8 x 8) and 3844 (62x62) nodes were compared. The ρ_h, k_h points are shown for the 8x8 case in Fig. 23, and Fig. 24 shows the 62x62 model results.

In an attempt to link the layered deterministic case with the spacially mixed, a test was conducted where a deterministic layered model was gradually changed to a model with a uniform distribution. Table 4 shows the distribution limits within each layer for each step. Values of ρ_h, k_h are plotted for each step in Fig. 25. Paths from starting points of ρ_{hh}, k_{hh} and ρ_{hv}, k_{hv} are both shown.

#	Range of k ft/d	k_h ft/d cm/s	k_v ft/d cm/s	$\frac{k_h}{k_v}$	ρ_h Ω-m	ρ_v Ω-m	$\frac{\rho_v}{\rho_h}$
1	10-600	225.92 .079700	222.05 .078300	1.017	947.95	957.35	1.010
2	"	209.25 .073824	212.57 .074995	.9844	929.96	935.72	1.006
3	"	229.02 .080798	228.07 .080464	1.004	968.66	967.07	.998
4	"	223.61 .078751	219.99 .077612	1.015	939.53	948.96	1.010
5	"	224.61 .079242	227.49 .080260	.9873	959.03	954.86	.996
6	15-389	148.45 .052374	147.74 .052121	1.005	704.58	702.86	.998
7	"	164.53 .058045	160.54 .056639	1.025	741.54	745.56	1.005
8	"	145.60 .051369	150.35 .053043	.968	708.88	703.44	.992
9	"	153.41 .054122	151.78 .053547	1.011	719.12	719.86	1.001
10	25-245	111.60 .039372	110.23 .038888	1.012	555.13		
11	"	113.90 .040182	114.77 .040492	.992	566.6		
12	"	114.32 .040334	112.65 .039743	1.015	560.53		
13	39-155	89.970 .031741	89.894 .031715	1.001	462.78	464.44	1.004
14	"	88.645 .031274	88.524 .031231	1.001	459.77	460.28	1.001
15	62-98	78.510	78.480	1.000	411.45	411.22	.999

Table 3: Aquifer permeability and aquifer resistivity values for the UNIFORM distribution

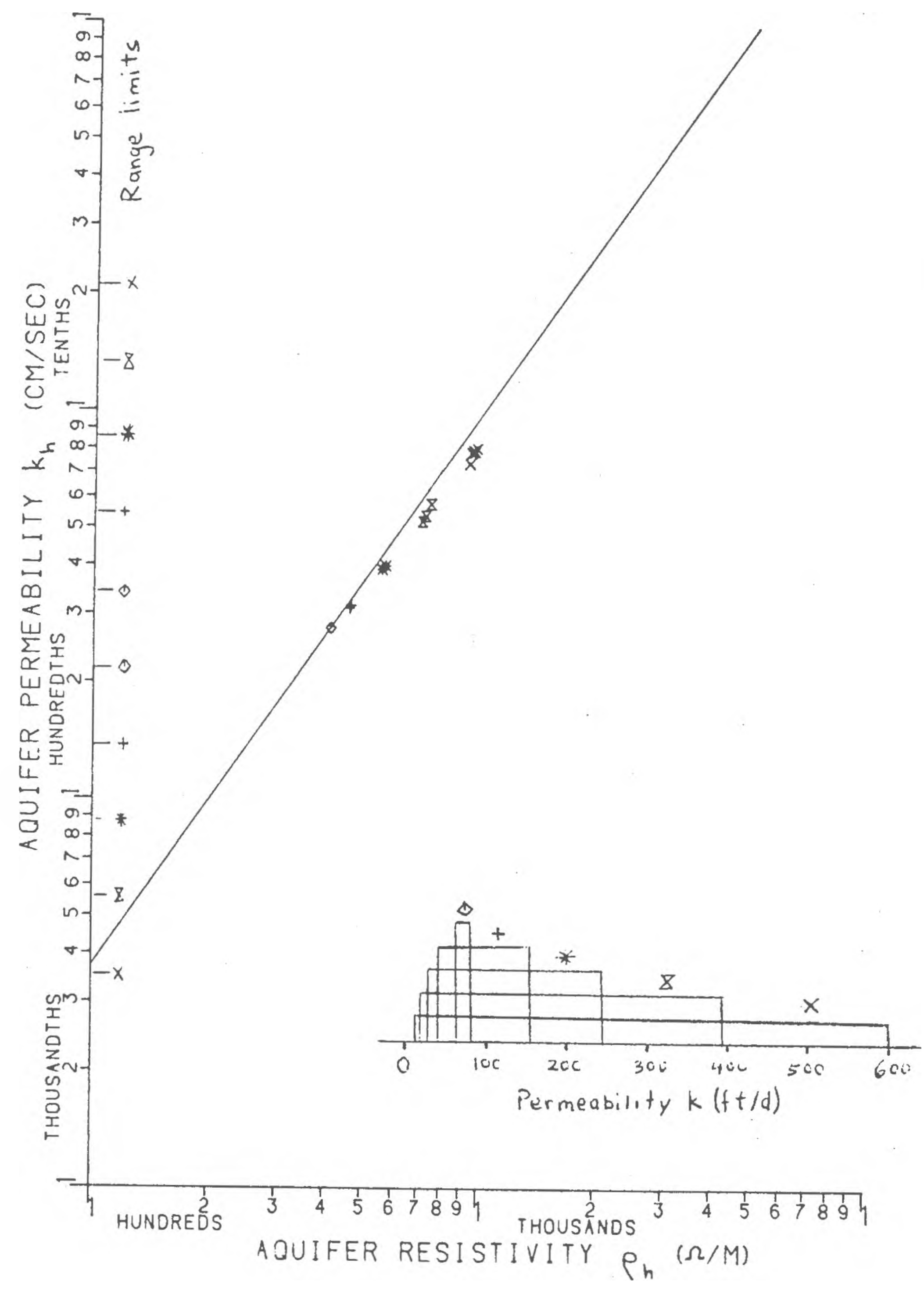

Figure 22. Aquifer permeability vs. aquifer resistivity points for the UNIFORM permeability distribution, with indicated ranges. Model grid was 32 x 32. Line is equation 3.

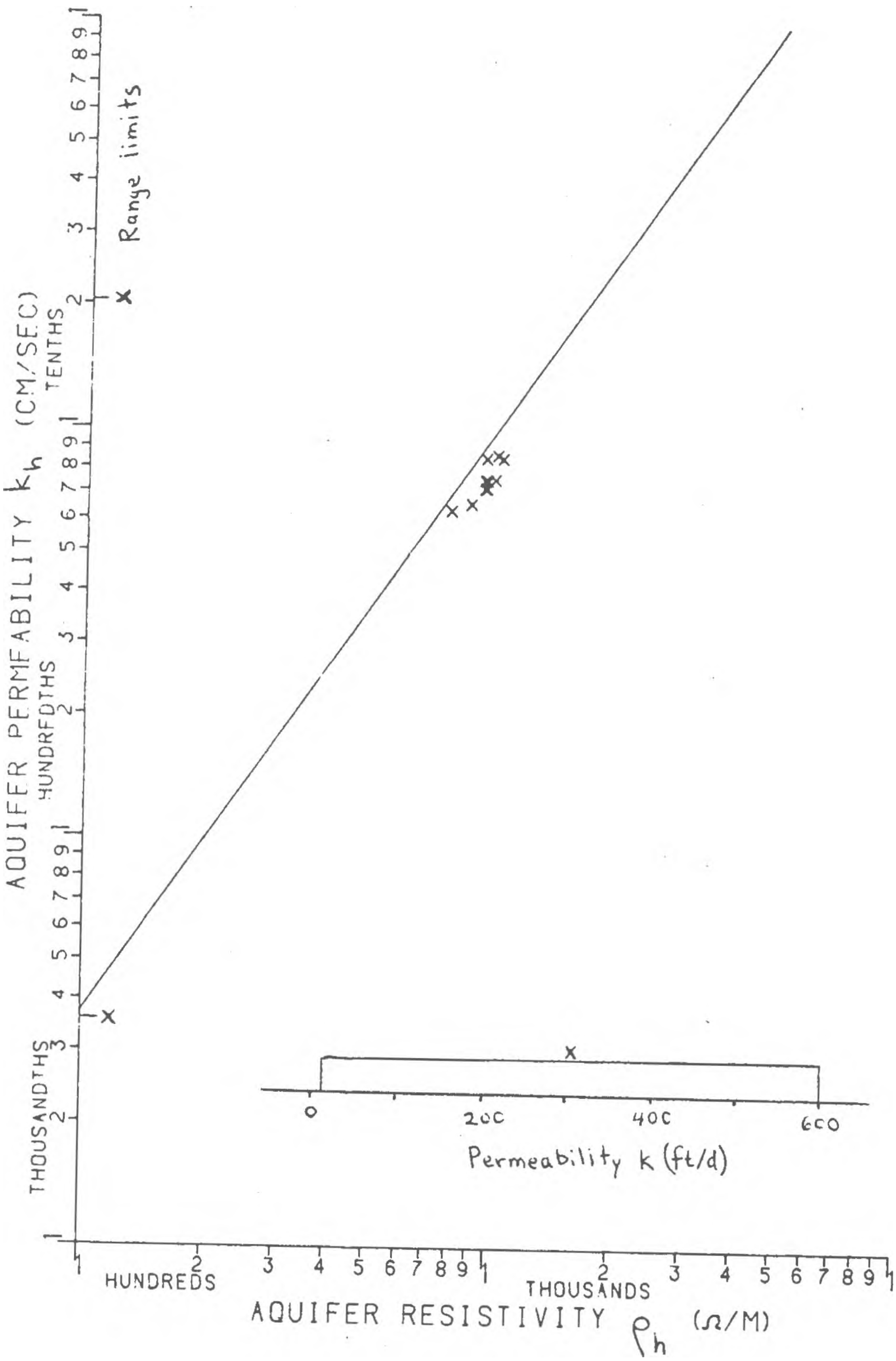

Figure 23. Aquifer permeability vs. aquifer resistivity points for the 8 x 8 model grid with a UNIFORM permeability distribution from 10 to 600 ft/d. Line is equation 3.

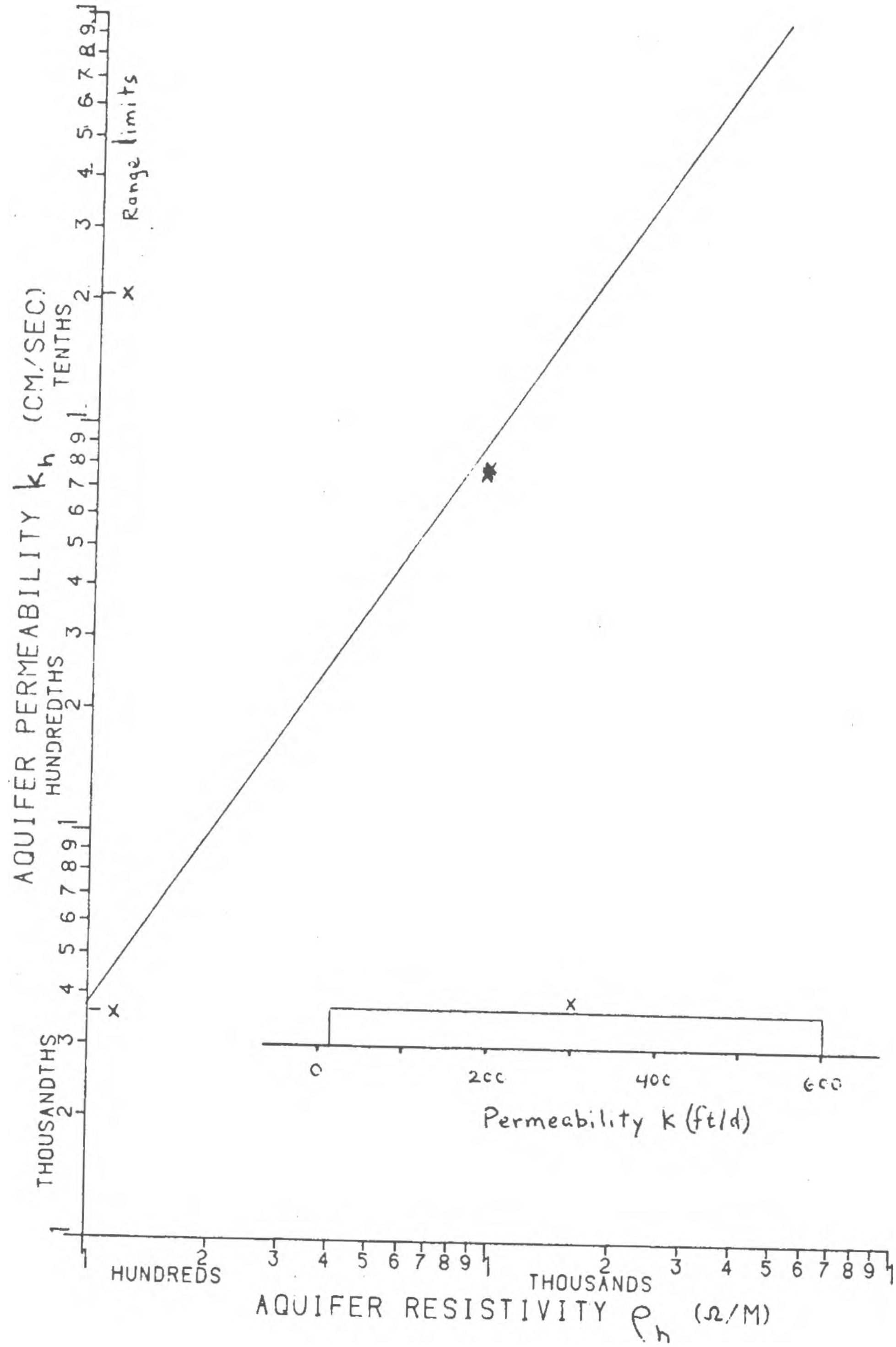

Figure 24. Aquifer permeability vs. aquifer resistivity points for the 62 x 62 model grid with a UNIFORM permeability distribution from 10 to 600 ft/d. Line is equation 3.

Layer	Deterministic 1	2	Steps → 3	4	5	Uniform 6
1	500	400-600	300-600	250-600	150-600	10-600
2	20	10-30	10-100	10-250	10-350	10-600
3	500	400-600	300-600	250-600	150-600	10-600
4	20	10-30	10-100	10-250	10-350	10-600
5	500	400-600	300-600	250-600	150-600	10-600

Table 4 : Range of permeability (ft/d) uniform distribution in each of five layers as the model is transformed from a layered deterministic case (step 1) to a uniform stochastic distribution (step 6).

An exponential (log-uniform) distribution of nodal permeabilities was then tested. Although no basis for this distribution has been hypothesized, its existance has been frequently observed (Warren and Price, 1961). Appendix G shows how this distribution was simulated. The mean or expected value of log k (k in ft/d) was held constant at 1.89. Ranges for log k tested were; 1.79 to 1.99, 1.59 to 2.19, 1.39 to 2.39, 1.19 to 2.59 and 1.0 to 2.78. Fig. 26 shows these tested distributions, which have the same limiting values of k as the uniform distribution. Table 5 shows results for the exponential distributions and Fig. 27 is a plot of these results. Points move downward (away

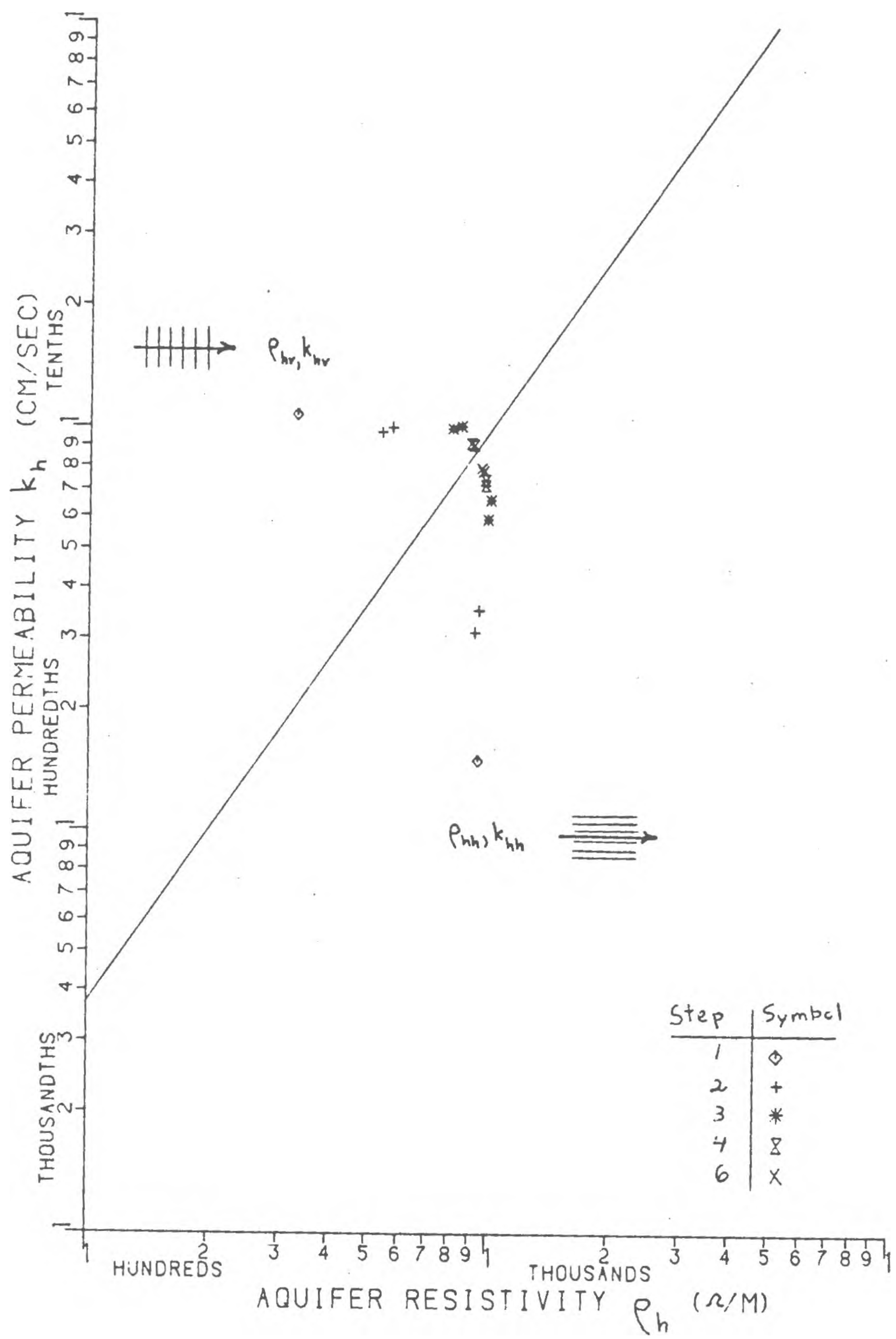

Figure 25. Aquifer permeability vs. aquifer resistivity points as the section is transformed from layered deterministic permeabilities to a uniform distribution. Table 4 shows the layer distributions at each step. The line is equation 3.

from the isotropic line) because of the increased weight given to low values in the log k range as opposed to the uniform range.

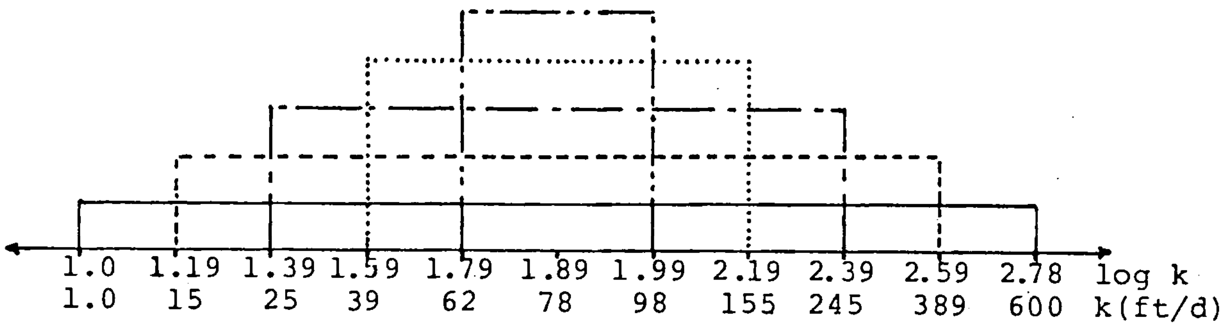

Fig. 26. Sketch of the EXPONENTIAL distributions tested.

The lognormal distribution of permeability has been found in many field situations (Law, 1944; Warren, 1961; McMillan, 1966; Freeze, 1975). This distribution was tested at two different means (μ =1.5 and 2.2) using standard deviations (σ) of .1, .3, .5, and .8 . Appendix L shows how the lognormal distribution was simulated. Table 6 and Fig. 28 display the results.

#	Range of log k ft/d	k_h ft/d cm/s	k_v ft/d cm/s	$\frac{k_h}{k_v}$	ρ_h Ω-m	ρ_v Ω-m	$\frac{\rho_v}{\rho_h}$
1	1.0-2.78	63.621 .022318	64.677 .022818	.978	443.46	446.53	1.007
2	"	61.488 .021693	61.125 .021565	1.006	442.12	445.91	1.008
3	"	63.889 .02254	61.891 .021835	1.03	451.54	452.80	1.003
4	"	55.155 .019459	55.374 .019536	.996	412.82	416.88	1.010
5	"	62.782 .022150	65.584 .023138	.957	464.95	454.83	.980
6	1.19-2.59	67.174 .023699	67.306 .023745	.998	433.20	431.65	.996
7	"	72.913 .025724	72.776 .025675	1.002	462.29	461.93	.9992
8	"	67.338 .023757	67.033 .023649	1.005	435.12	434.86	.9994
9	"	67.395 .023777	66.003 .023286	1.021	428.52	434.75	1.014
10	1.39-2.39	70.305 .024804	70.124	1.003	415.36	415.07	.9993
11	"	73.627 .025976	72.377 .025534	1.017	419.81	421.46	1.004
12	"	71.481 .025219	70.049 .024713	1.02	416.56	421.61	1.012
13	1.59-2.19	75.283 .026560	74.425 .026257	1.01	408.78	411.11	1.006
14	"	74.048 .026124	74.102 .026143	.999	407.05	406.53	.999
15	1.79-1.99	76.563 .027011	76.586 .027019	1.0	404.22	404.66	1.001

Table 5: Aquifer permeability and aquifer resistivity values for the EXPONENTIAL distribution

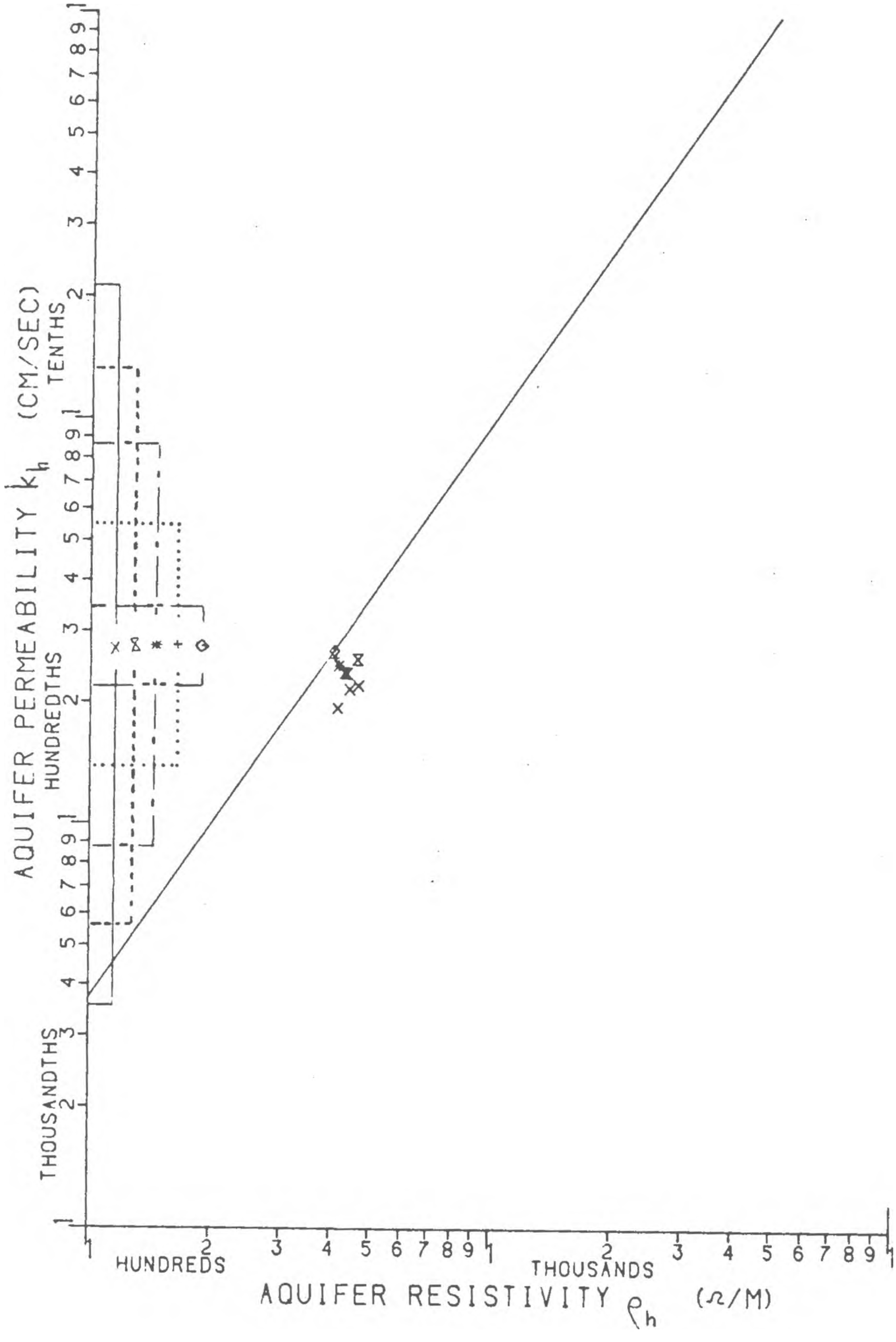

Figure 27. Aquifer permeability vs. aquifer resistivity points for the EXPONENTIAL permeability (ft/d) distribution, with indicated ranges. Model grid was 32 x 32 and the line is equation 3.

#	S.Dev. (σ)	k_h ft/d cm/s	k_v ft/d cm/s	$\frac{k_h}{k_v}$	ρ_h Ω-m	ρ_v Ω-m	$\frac{\rho_v}{\rho_h}$
1	.1	156.39 .055175	156.09 .055070	1.002	671.11	670.31	.999
2	"	155.34 .054806	156.23 .055116	.9943	669.63	669.72	1.000
3	"	158.11 .055782	157.75 .055654	1.002	676.19	674.62	.998
4	.3	147.07 .051885	146.34 .051630	1.005	687.63	696.33	1.013
5	"	150.01 .052923	150.54 .053110	.9965	710.82	707.17	.995
6	"	145.95	146.73	.9947	689.52	690.06	1.001
7	.5	131.29 .046319	137.08 .048362	.9578	738.66	722.04	.978
8	"	130.40 .046005	123.94 .043725	1.052	683.75	705.96	1.033
9	"	139.45 .049199	140.14 .049440	.9951	741.74	738.18	.995
10	.8	105.45 .037204	120.81 .042623	.8729	765.53	769.88	1.006
11	"	118.64 .041856	102.46 .036148	1.158	793.89	865.05	1.09
12	"	120.26 .042427	121.74 .042950	.9878	837.60	805.64	.962

Table 6: Aquifer permeability and aquifer resistivity values for the LOGNORMAL distribution (γ =2.2)

#	S.Dev. (σ)	k_h ft/d cm/s	k_v ft/d cm/s	$\frac{k_h}{k_v}$	ρ_h Ω-m	ρ_v Ω-m	$\frac{\rho_v}{\rho_h}$
1	.1	31.37 .011068	31.42 .011085	.9984	218.40	218.11	.999
2	.3	30.09 .010614	30.82 .010872	.9763	232.83	230.21	.989
3	.5	27.26 .009617	27.79 .009805	.9809	243.07	240.36	.989
4	"	26.34 .009292	25.60 .009030	1.029	233.54	232.76	.997
5	.8	22.018 .007768	23.622 .008334	.9321	261.24	252.72	.967
6	"	21.389 .007546	20.826 .007347	1.027	256.24	253.40	.989
7	"	21.397 .007549	18.031 .006361	1.187	223.76	247.32	1.105

Table 6a: Aquifer permeability and aquifer resistivity values for the LOGNORMAL distribution (μ=1.5)

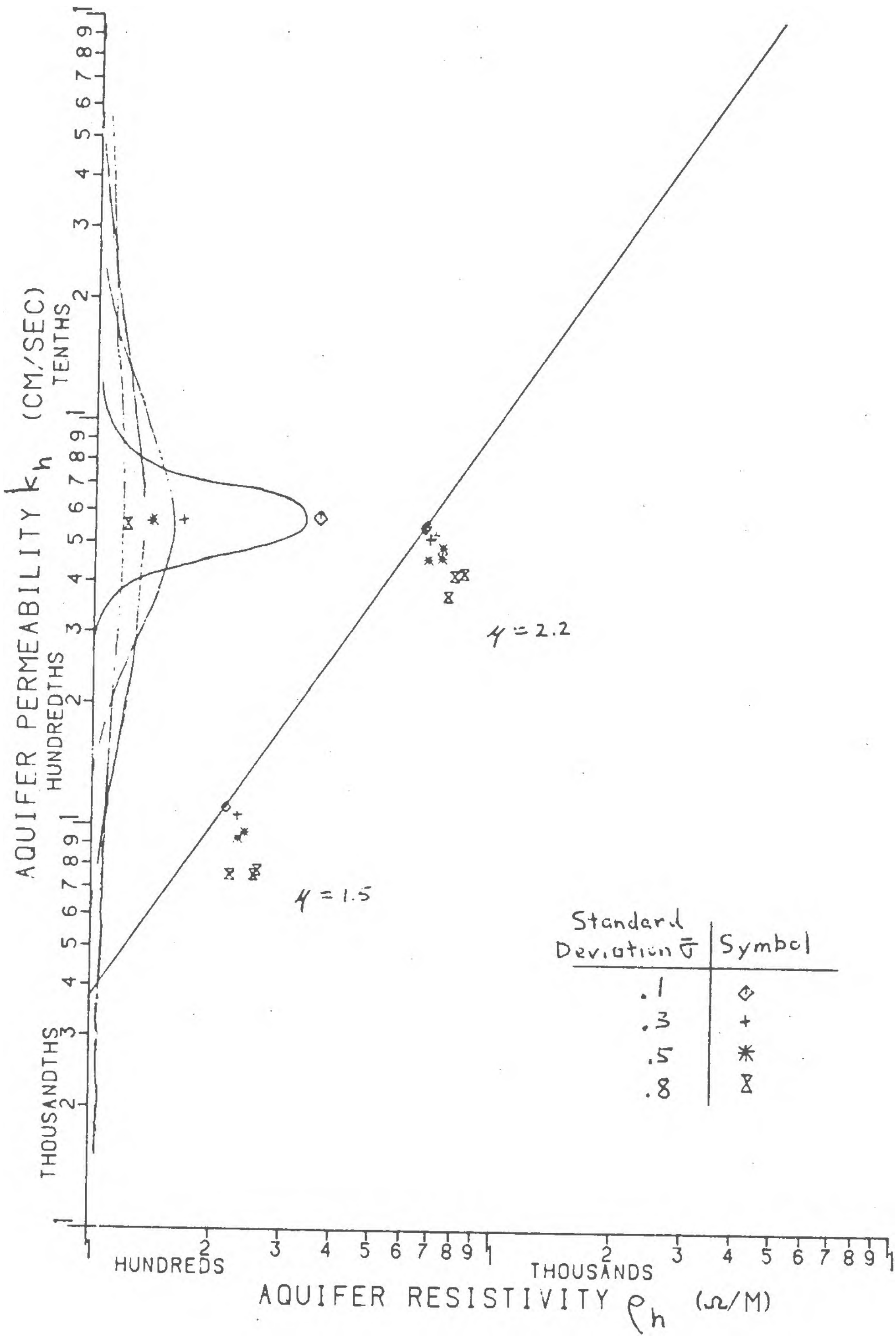

Figure 28. Aquifer permeability vs. aquifer resistivity points for the LOGNORMAL permeability (ft/d) distributions with means (ψ) of 1.5 and 2.2. A frequency diagram is shown for ψ = 2.2 with the indicated standard deviations (σ). The line is equation 3.

OBSERVATIONS: QUASI-LINEAR STOCHASTIC MODEL

The following observations are noted from the results of the stochastic quasi-linear flow models, where conditions included: reasonable isotropic nodal permeability limits applicable to Darcy's law, and a material level relationship similar to that of equation 3 (approximately equal in slope).

1. The ρ_h, k_h point always lies on or to the right of the material relationship line (Figs. 22 to 25, 27, 28).

2. Differences in ρ_h versus k_h plots between uniform and exponential permeability distributions, where both distributions have the same limit values, are due to the increasd weighting low values have in an exponential range compared to the same range being uniformly distributed.

3. Aquifers which are conventionally defined homogeneously heterogeneous (low scale of heterogeneity as defined by Warren and Price, 1961) will show less scatter in ρ_h versus k_h than ones which are more heterogeneous (higher scale of heterogeneity). See Figs. 23 and 24.

4. Distances from the material relationship line to the ρ_h, k_h point are indicative of the spread of the permeability distribution (standard deviation, for example), when the aquifer has a low scale of heterogeneity (Figs. 22, 24, 27, 28).

FLOW GEOMETRY STUDY

Field methods used to obtain aquifer permeabilities and aquifer resistivities do not use the same flow geometry as is assumed for equations 4 through 7 or that assumed for the computer model. The linear and quasi-linear flow geometries require the fluid to move through a constant cross sectional area in a straight (or approximately straight) line from the source to the sink. Aquifer permeabilities are usually determined by pump tests where flow is quasi-radial. In vertical electric sounding techniques, a direct current moves from one surface point to another (quasi-point to point). Both methods utilize potential theory to interpret field data. The prefix quasi is used to imply that transport properties are spacially mixed such that flow paths deviate slightly from idealized smooth lines. Sketches of the quasi-linear, quasi-radial, and quasi-point to point flow geometries are shown in Fig. 28a.

This section will examine two cases of current flow.

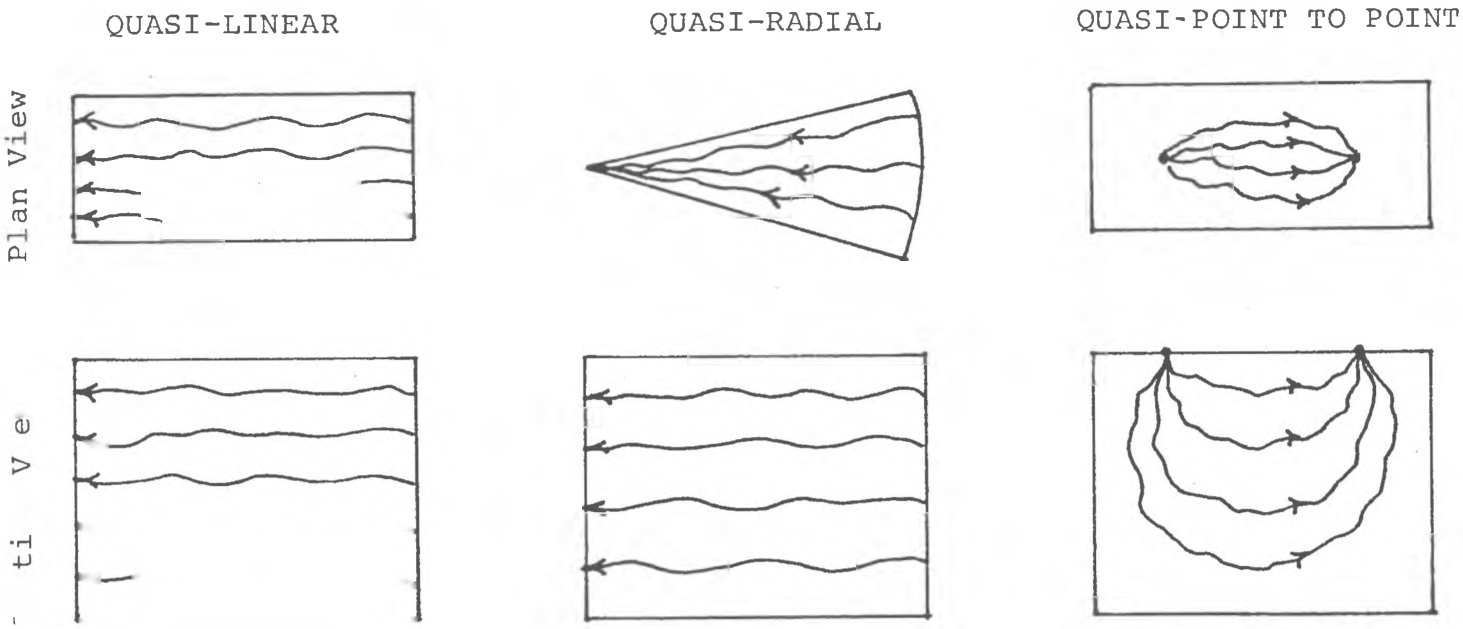

Figure 28a. Quasi-linear, quasi-radial and quasi-point to point flow geometries in a spacially mixed aquifer

1. Where the aquifer is considered "isolated" from surrounding formations. For this case, the current moves only through the aquifer and is not influenced (refracted) by materials above and below the aquifer. Flow geometry is quasi-point to point due to spacial mixing (Fig. 28a).

2. Where most of the current moves through the aquifer, yet is strongly influenced by materials overlying and underlying the aquifer. The idealized point to point flow pattern may be severely distorted due to refraction caused by resistivities of surrounding strata. This will be referred to as the "non-isolated" aquifer case.

For the first case, attempts will be made to provide quantitative information showing the significance of flow geometry in determining aquifer properties. The use of results in previous sections with simulated field-like aquifer resistivities at short electrode spacings will be evaluated. A comparison between aquifer permeabilities for linear and radial flow geometries will also be made. The second case will be examined in a more qualitative manner by citing from the literature some methods which may enable aquifer resistivities to be obtained from vertical electric sounding curve interpretations.

Warren and Price (1961) demonstrated how aquifer permeability could be determined numerically for the quasi-radial flow geometry of a confined aquifer in three dimensions. Their equation is derived for the case of 2-D confined steady state horizontal flow. Fig. 21 depicts the parameters used in this derivation. Total flow through the model is defined as:

$$Q = k_h \; I \; A \tag{15}$$

where

k_h = aquifer horizontal permeability

I = effective aquifer gradient = $\Delta H / \Delta L$

A = effective aquifer area

Since $$Q = \sum_{i=1}^{R} \bar{k}_{i,j} \; i \; a \tag{16}$$

where

R = number of model rows

$\bar{k}_{i,j}$ = connection permeability between $h_{i,j}$ and $h_{i,j+1}$ computed as in equation 13a

i = potential gradient

$= \dfrac{\Delta h_{i,j}}{\Delta l}$

where $\Delta h_{i,j} = h_{i,j} - h_{i,j+1}$

Δl = length between $h_{i,j}$ and $h_{i,j+1}$

a = nodal cross sectional area

i = row subscript

j = column subscript

then,
$$\sum_{i=1}^{R} \bar{k}_{i,j} \frac{\Delta h_{i,j}}{\Delta l} a = k_h I A \tag{17}$$

The ratio $a/\Delta l$ will be constant for every row, providing model rows are uniformly spaced.

hence
$$k_h = \sum_{i=1}^{R} \bar{k}_{i,j} \Delta h_{i,j} \frac{a}{\Delta l\, I\, A} \tag{18}$$

Let
$$S = \frac{a}{\Delta l\, I\, A} \tag{19}$$

then
$$k_h = S \sum_{i=1}^{R} \bar{k}_{i,j} \Delta h_{i,j} \tag{20}$$

where S is a shape factor.

For the conventionally defined uniform isotropic homogeneous case,

$$S = \frac{1}{\sum_{i=1}^{R} \overline{\Delta h}_{i,j}} \tag{21}$$

where

$\overline{\Delta h}_{i,j} = \Delta h_{i,j}$ for the uniform isotropic homogeneous case

In this study equation 20 will be used with the S value determined from equation 21, only when streamlines do not refract or where the refraction is expected to be small due to an isotropic homogeneously heterogeneous media (conventional definition). Under these conditions, equation 20 can be used for 2-D steady state flow, where the j and j+1 columns are confined at their bounds and serve to separate all inflow nodes from outflow nodes. It should be noted that equation 20 is the same as equation 13 for the quasi-linear case where I (equals $\Delta H/\Delta L$), A, and a are known. Furthermore, it can be shown that the k_h determined by equation 20 for linear flow with horizontal layering or vertical layering is exactly k_{hh} and k_{hv} from equations 4 and 6 respectively.

For radial flow with horizontal layering where vertical boundary heads are fully penetrating, equation 20 can be shown to be equivalent to equation 4, since the radial flow steady state hydraulic heads are the same for the isotropic uniform homogeneous case (see Fig. 20) and the horizontally layered case. Equation 20 is rewritten for the radial aquifer permeability (k_r) as

$$k_r = \frac{\sum_{i=1}^{R} \overline{k_{i,j}}\, \Delta h_{i,j}}{\sum_{i=1}^{R} \overline{\Delta h_{i,j}}} \qquad (22)$$

Since all $\overline{\Delta h_{i,j}} = \Delta h_{i,j}$

then $$k_r = \frac{\sum_{i=1}^{R} \overline{k_{i,j}}}{R} \tag{23}$$

Equation 23 represents the arithmetic mean for R equally spaced layers where flow is parallel to the layering and is therefore equivalent to equation 4.

Although Warren and Price (1961) did not apply equation 20 to a confined vertically layered model with radial flow, the equation should apply because:

1. The equivalency of equations 4 and 20 demonstrates the correct application of equation 20 to a fully penetrating well model using the radial flow geometry, where streamlines converge to a line.

2. The equation can be shown to give the correct value of k_{hv} (equation 6) for the vertically layered section with horizontal flow, demonstrating the correct use of equation 20 for vertically layered sections.

3. Streamlines through a section do not refract.

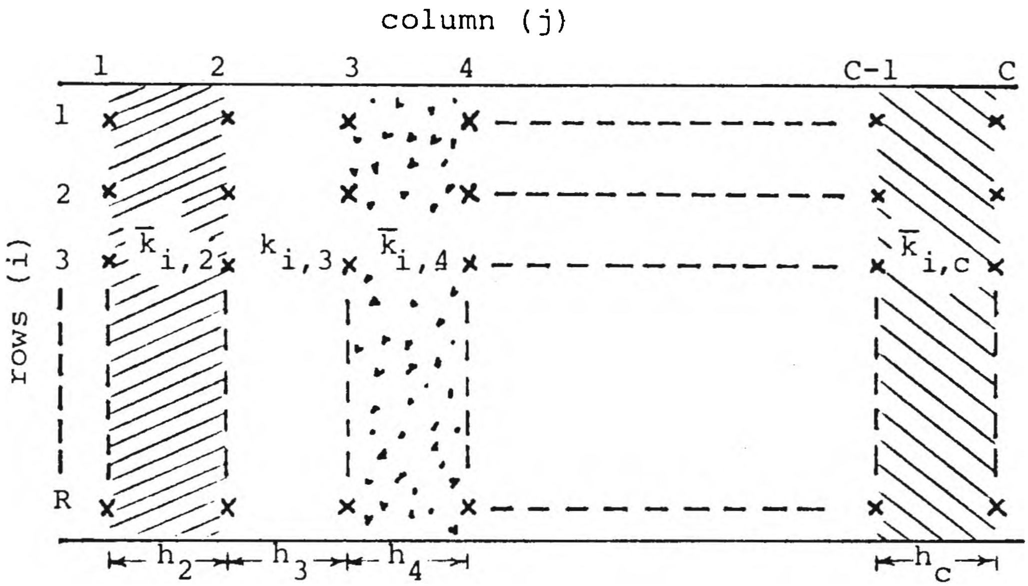

Fig. 28b. Idealized vertical layered model

The value of k_{hv} in equation 6 is shown to equal the aquifer permeability value computed by equation 20. Some terms used in the following derivation are shown in Fig. 28b. Rewriting equation 6 in discrete form, as it would be used to compute k_{hv} in the model,

$$k_{hv} = \frac{h_2 + h_3 \cdots\cdots + h_c}{\frac{h_2}{\bar{k}_{i,2}} + \frac{h_3}{\bar{k}_{i,3}} \cdots\cdots + \frac{h_c}{\bar{k}_{i,c}}}$$

where C = # of columns

$\bar{k}_{i,j}$ = connection permeability between columns j-1 and j

Let $h_2 = h_3 \ldots\ldots\ldots\ldots\ldots = h_c = b$

where b = constant

Then

$$k_{hv} = \frac{Cb}{\frac{b}{\bar{k}_{i,2}} + \frac{b}{\bar{k}_{i,3}} \cdots\cdots\cdots\cdots + \frac{b}{\bar{k}_{i,c}}} \qquad (24)$$

Multiplying both sides of equation 24 by Q/A gives

$$k_{hv} = \frac{Cb\frac{Q}{A}}{\left[\frac{b}{\bar{k}_{i,2}} + \frac{b}{\bar{k}_{i,3}} \cdots\cdots\cdots + \frac{b}{\bar{k}_{i,c}}\right]\frac{Q}{A}} \qquad (25)$$

Since $\Delta H = \left[\frac{b}{\bar{k}_{i,2}} + \frac{b}{\bar{k}_{i,3}} \cdots\cdots + \frac{b}{\bar{k}_{i,c}}\right]\frac{Q}{A}$ (Perloff & Baron, 1976) (26)

where ΔH = total dissipated head for horizontal flow through a model with C vertical layers of thickness b

$$A = \sum_{i=1}^{R} a = Ra \qquad (27)$$

R = # of rows

and total flow can be computed as

$$Q = \sum_{i=1}^{R} \bar{k}_{i,j} \frac{\Delta h_{i,j}}{\Delta l} a \qquad (28)$$

Then substituting equations 26, 27, and 28 into 25 gives

$$k_{hv} = \frac{C b \sum_{i=1}^{R} \bar{k}_{i,j} \frac{\Delta h_{i,j}}{\Delta l} a \frac{1}{Ra}}{\Delta H}$$

Since $\Delta H/C = \overline{\Delta h_{i,j}}$

where $\overline{\Delta h_{i,j}}$ = change in head between two columns for the uniform isotropic case with radial flow

and each layer is the distance between columns ($\Delta l = b$)

then,
$$k_{hv} = \frac{\sum_{i=1}^{R} \bar{k}_{i,j} \Delta h_{i,j}}{R \overline{\Delta h_{i,j}}}$$

but
$$R = \sum_{i=1}^{R} i$$

therefore
$$k_{hv} = \frac{\sum_{i=1}^{R} \bar{k}_{i,j} \Delta h_{i,j}}{\sum_{i=1}^{R} \overline{\Delta h_{i,j}}}$$

which is the same as equation 20 (using the S value of equation 21).

To use the Warren and Price technique for radial flow, the cartesian coordinate computer program had to be modified to handle radial symetric flow through a 2-D cross section where vertical boundary heads are fully penetrating. The governing differential equation for radial symetric flow in the steady state is;

$$\frac{1}{r}\,\frac{\partial\left(r k_r \frac{\partial h}{\partial r}\right)}{\partial r} + \frac{\partial\left(k_z \frac{\partial h}{\partial z}\right)}{\partial z} = 0 \qquad (29)$$

The discretized equation is formulated in appendix I, where the method of computing connection permeabilities is also shown. After appropriate modifications were made to the computer program, the Theim equation,

$$k_r = \frac{Q \ln(r_2/r_1)}{2\pi b(h_2-h_1)} \qquad \text{(Bouwer, 1978)} \qquad (30)$$

where Q = total flow

r_i = radius to h_i

h_i = head at point i

b = aquifer thickness

was used to check the radial model. For the uniform isotropic homogeneous case (see Fig. 20), the input permeability was within .1% of the value computed by equation 30. With data from the model, the value of S was determined by applying equation 21 to the middle column. Values of k_{rv}, the aquifer permeability due to radial flow with vertical layering, were then determined by applying equation 20 to steady state heads obtained by the radial model for different arrangements of six permeability values.

Results are shown in table 7, where the lowest value is approximately half of the k_{hv} value and the highest is close to double the linear flow value. Clearly demonstrating that the k_{rv} value is dependent upon the exact arrangement of the vertical layering and hence, the linear and radial flow geometries cannot be expected to yield the same aquifer parameters.

Well	Permeabilities (ft/d) in each vertical layer					Total Flow (cfd)	k_{rv} (ft/d)	$\frac{k_{rv}}{k_{hv}}$
	400	300	200	100	50	1418506	257	2.11
	50	100	200	300	400	347357	63	.52
	300	100	50	400	200	995309	180	1.48
	100	300	400	200	50	660701	120	.98
	50	300	100	400	200	357494	65	.53
	400	300	100	50	200	1300169	236	1.93

Table 7: Effect of vertical layering rearrangement on k when k_{hv} = 122 ft/d

Equation 20 was not applied to the layered cases where flow moved from a point source to a point sink. It appears equation 20 may only be applied to situations where flow is linear or quasi-linear and moves in the same direction as a principal permeability, or where the material is homogeneously heterogeneous and isotropic (conventional definition). Neither of these situations are met in the layered case of point to point flow, where streamlines move in many directions and refract at layer boundaries throughout a very heterogeneous material.

Further proof of the inapplicability of equation 20 for the layered point to point flow model may be found in examining the requirements for equivalent aquifer sections. According to Freeze (1975), aquifer sections will be equivalent when the total flow through the true section equals the total flow through the equivalent section. Table 8 shows the total flow through a layered model section under point to point flow depends on the exact arrangement of the layers for both horizontal and vertical layered cases. These flow rates are obtained by calculating total inflow based on numerically solved steady state heads, permeability in the upper layer, and nodal cross sectional areas. Thus, the equivalent section is not simply one with principal permeabilities having values of the arithmetic and harmonic means of the layered permeabilities; for this section would give one value of flow for the horizontal layered case, and one value for the vertical layered case. It was not within the scope of this study to devise a method which computes aquifer properties for the layered case with point to point flow. It may be impossible to produce an equivalent section under these conditions.

Permeabilities (ft/d) in each layer					Total flow through the model (cfd): vertical layering	horizontal layering
50	100	200	300	400	4027	3767
300	100	50	400	200	5981	19897
100	300	400	200	50	3744	7614
50	300	100	400	200	4255	3893
400	300	100	50	200	5674	27347

Table 8: Effect of layering rearrangement on total flow with the point to point flow regime

For the spacially mixed case, quasi-linear, quasi-radial, and quasi-point to point flow geometries were used to compute aquifer permeabilities and aquifer resistivities. Uniform, exponential and lognormal permeability distribtions were tested. The cartesian coordinate model was used for the quasi-linear and quasi-point to point flow geometries, and the radial program determined aquifer properties for quasi-radial flow. Equation 20 was used to calculate the aquifer properties, since the applied 900 node model with spacially mixed permeabilities was approximately isotropic and homogeneously heterogeneous (conventional definition). The value of S in equation 21 was determined for the quasi-radial and quasi-point to point geometries by numerically solving for the steady state heads in an isotropic section of constant permeability. The quasi-point to point numerical simulations assumed a line source electrode. According to Mufti (1978) results from a 2-D line source simulation are comparable to the 3-D point source case only when the results are used in the computation of resistivities. Also, the 2-D case assumes the current emitted per unit length of the line source is equal to the total current emitted by the point source.

Twelve models were formed for each distribution and flow regime. Values of k_h, k_r and k_ρ for the uniform distribution are compared in Table 9, where the mean $(\hat{k})$ and standard deviation $(\hat{\sigma})$ of each column is also shown. Warren and Price (1961) concluded that this standard deviation $(\hat{\sigma})$ is indicative of the scale of heterogeneity. Tables 10 and 11 show aquifer permeability data for the exponential and lognormal distributions. The expected or mean value (μ) of nodal permeability was 77.6 ft/d for all distributions, with the limits for the uniform and exponential cases set at 10 ft/d and 600 ft/d. The standard deviation $(\bar{\sigma})$ was .4 for the lognormal distribution (k in ft/d). Table 12 shows the aquifer resistivities for the lognormal distribution with quasi-linear (ρ_h) and point to point (ρ_p) flow geometries. Tables 9 to 12 also include the geometric mean of the aquifer parameters. Table 13 shows the ratio of $\hat{\sigma}/\hat{\rho}$ to be less than the $\hat{\sigma}/\hat{k}$ ratio for quasi-point to point and

#	k_h quasi-linear	k_r quasi-radial	k_p quasi-point-point	geometric mean
1	215.8	213.7	215.0	229.7
2	222.5	218.1	204.1	232.9
3	230.8	248.5	185.6	243.0
4	224.8	229.0	227.1	240.8
5	222.0	227.5	199.3	239.2
5	225.1	239.9	137.0	240.1
7	228.3	228.2	228.8	242.2
8	212.9	202.9	220.5	228.1
9	220.2	232.5	222.1	2r37.7
10	229.0	237.1	241.4	240.0
11	226.7	230.6	240.5	240.6
12	232.5	250.3	234.6	248.6
mean ($\hat{k}$)	224.2	229.9	213.0	238.6
s.dev. ($\hat{\sigma}$)	5.89	13.7	29.3	5.79

Table 9: Numerically computed aquifer permeabilities (ft/d) when nodal permeabilities have a uniform distribution with limits of 10 ft/d and 600 ft/d.

#	k_h quasi-linear	k_r quasi-radial	k_p quasi-point-point	geometric mean
1	62.60	67.17	52.82	80.68
2	66.64	70.12	54.90	75.95
3	65.60	70.12	80.00	80.88
4	65.05	69.97	76.50	74.63
5	65.08	70.65	56.97	79.68
6	65.47	75.34	73.78	79.15
7	64.11	55.29	60.49	77.48
8	66.51	74.79	59.37	75.41
9	58.59	60.96	50.20	79.76
10	69.48	77.40	61.44	79.61
11	61.97	66.02	55.15	81.04
12	65.25	72.02	55.43	75.48
mean ($\hat{k}$)	64.70	69.15	61.42	78.31
s.dev. ($\hat{\sigma}$)	2.72	6.21	9.85	2.38

Table 10: Numerically computed aquifer permeabilities (ft/d) when nodal permeabilities have a exponential distribution with limits of 10 ft/d and 600 ft/d.

#	k_h quasi-linear	k_r quasi-radial	k_p quasi-point-point	geometric mean
1	69.29	67.24	76.32	78.52
2	68.95	77.27	53.73	77.07
3	70.61	72.04	41.91	77.40
4	70.79	73.76	73.18	78.49
5	64.00	68.41	62.51	72.59
6	67.59	75.66	71.85	75.14
8	67.56	69.11	65.42	76.34
9	72.88	73.23	61.08	80.93
10	67.88	64.58	62.57	75.25
11	70.77	70.72	65.66	79.64
12	72.44	75.83	56.33	81.03
mean ($\hat{k}$)	69.77	71.94	63.57	78.03
s.dev. ($\hat{\sigma}$)	2.84	3.96	9.69	3.09

Table 11: Numerically computed aquifer (ft/d) permeabilities when nodal permeabilities have a lognormal distribution (μ = 1.89, $\bar{\sigma}$ = .4).

#	ρ_h quasi-linear	ρ_p point-point	geometric mean
1	442.1	514.5	409.8
2	433.8	408.0	404.6
3	431.9	366.8	405.8
4	434.8	509.2	409.7
5	413.1	421.4	387.9
6	463.5	459.3	429.5
7	422.1	451.3	397.4
8	428.2	427.2	401.9
9	444.4	450.3	418.6
10	422.9	394.9	397.8
11	443.5	423.3	413.9
12	442.2	416.7	419.0
mean ($\hat{\rho}$)	435.2	436.9	408.0
s.dev. ($\hat{\sigma}$)	13.2	43.3	11.3

Table 12: Numerically computed aquifer resistivities when converted (eq. 3) nodal permeabilities have a lognormal distribution (μ = 1.89, σ = .4)

quasi-linear flow with a lognormal permeability distribution. This can be attributed to the spread and magnitude of their nodal transport properties when the material relationship (eq. 3) converts permeabilities to resistivities.

	flow	
	quasi linear	quasi pt. to pt.
hydraulic $\hat{\sigma}/\hat{k}$	.041	.15
electric $\hat{\sigma}/\hat{\rho}$	.03	.1

Table 13: Comparison of $\hat{\sigma}/\hat{k}$ and $\hat{\sigma}/\hat{\rho}$ values for the hydraulic and electric case of lognormally distributed nodal values

	flow	
Distribution	quasi radial	quasi pt. to pt.
Uniform	+2.5%	-5.0%
Exponential	+6.9%	-5.0%
Lognormal	+3.1%	-8.9%

Table 14: Deviation of mean values ($\hat{k}$) from the mean value of quasi-linear hydraulic flow

A comparison of the mean values of quasi-radial computed aquifer permeability and quasi point to point aquifer permeability to the quasi-linear computed aquifer permeability is shown in table 14. The data indicates that flow geometry does not play a significant role in determining aquifer permeability when the nodal permeabilities are represented by a stochastic distribution and the scale of heterogeneity is low. This agrees with the Warren and Price results for the 3-D case.

Actually, the point to point flow is only used in the field for the electrical case. Data from table 12 shows the mean aquifer resistivity with quasi point to point flow is within .4% of the mean value with quasi-linear flow.

To examine the case where electrode spacings are large and the current is influenced (refracted) by materials above and below the aquifer (non-isolated aquifer), vertical electric sounding curve interpretation techniques can be used to obtain resistivities of layers in an assumed horizontally stratified formation. To make a vertical electric sounding, a current is introduced into the ground via two surface electrodes and the potential difference is measured between a second pair of electrodes. Apparent resistivities are calculated as a function of the current, potential difference and a geometric factor based on the exact electrode configuration.

Previous results from this study are comparable to the "isolated" aquifer case, where current moves only through the aquifer and is not refracted by surrounding strata. This situation exists when overlying materials are either not present or considered negligible and the electrode spacing is small (less than the aquifer thickness). The more common situation is when the aquifer thickness is unknown and a resistivity layer or layers overlie and underlie the aquifer. For this case, apparent resistivities are obtained as the current electrode spacing is expanded. These values are plotted against half the electrode spacing resulting in vertical electric sounding curve. Using interpretation techniques, it is possible to use this field curve to estimate the resistivity of the aquifer when materials of significantly different resistivity lie above and below the aquiter.

Interpretation procedures which combine curve matching methods with techniques that utilize the Dar Zarrouk parameters appear to be well suited for aquifer exploration (Kosinski, 1978). The Dar Zarrouk parameters longitudinal unit conductance (S) and transverse unit resistance (T) may sometimes be estimated from sounding curves. They are defined as

$$S = \sum \frac{h_i}{\rho_{\ell i}} \qquad \text{(Zohdy, Eaton \& Mabey, 1974)} \quad (31)$$

$$T = \sum \rho_{t_i} h_i \qquad \text{(Zohdy, Eaton \& Mabey, 1974)} \quad (32)$$

where i is a layer subscript and includes all resistivity layers in the formation, ρ_ℓ is the longitudinal or horizontal resistivity , ρ_t is the transverse or vertical resistivity and h is the layer thickness. The transverse unit resistance (T) is based on current flow perpendicular to the layering, whereas the longitudinal unit conductance (S) is based on current movement parallel to layering.

Surficial geologic formations in New England typically consist of an unsaturated zone, the aquifer and a resistive bedrock (igneous or metamorphic). To demonstrate the flow pattern associated with this case, the cartesian coordinate finite difference model was used to produce a flow net. Data for the model was obtained from the interpretation of electric sounding #36 in a thesis by Kosinski (1978). Four layers were used, with $\rho_1 = 1737\ \Omega$-m (unsaturated topsoil), $\rho_2 = 5334\ \Omega$-m (unsaturated sand and gravel), $\rho_3 = 468\ \Omega$-m (saturated aquifer) and $\rho_4 = 5.17 \times 10^6$ Ω-m (bedrock). Current electrodes are 384 feet apart, representing a relatively large spacing. The bedrock resistivity in the field is effectively infinite, with the value of 5.17×10^6 used to allow program convergence. Fig. 29 shows 97% of the flow moves through the saturated aquifer (layer 3), approximating horizontal linear flow. This model demonstrates why S is the important factor and that the resistivity of the aquifer will be the longitudinal or horizontal resistivity for the resistive bedrock case.

The layering arrangement of Fig. 29 would produce a minimum type sounding curve, since the resistivity of the aquifer is less than the resistivities of surrounding strata. For this case, the auxilary point method implies

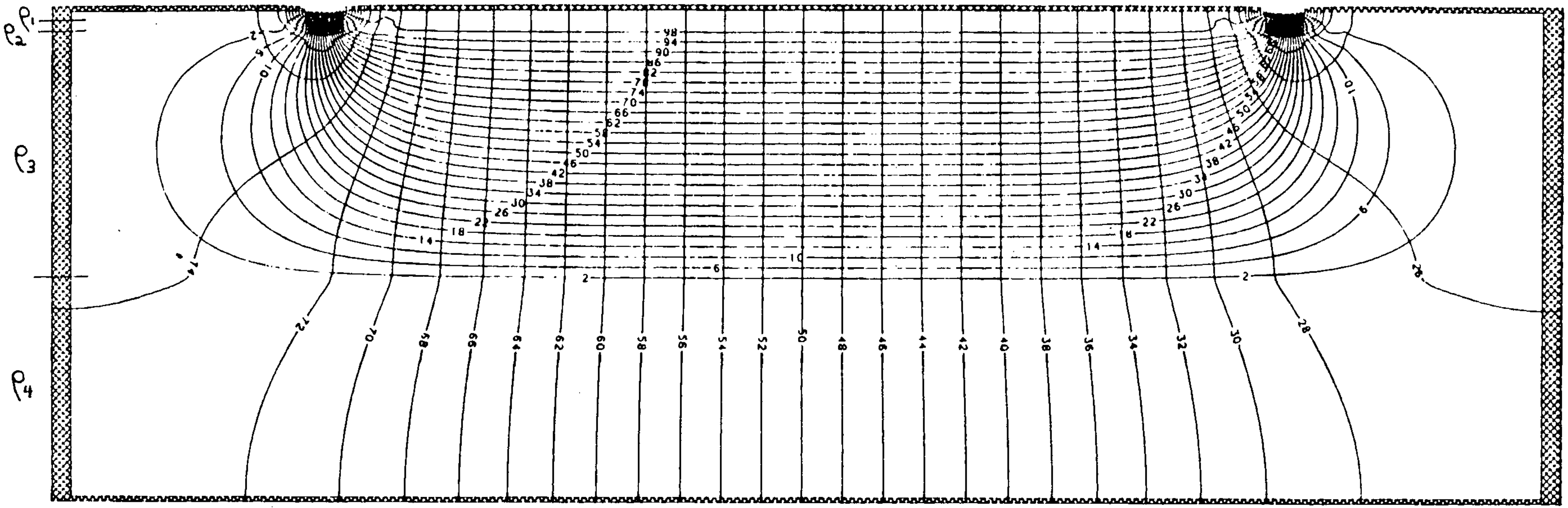

FLOW NET

1'' ≈ 64.4'

Figure 29. Flow net demonstrating the point to point electric current flow and scalar electrical potentials for a typical aquifer section where the bedrock has high resistivity. Layer resistivities are based on field data from Kosinski (1978), with $\rho_1 = 1737\ \Omega$-m (unsaturated topsoil), $\rho_2 = 5334\ \Omega$-m (unsaturated sand & gravel), $\rho_3 = 468\ \Omega$-m (saturated aquifer material) and $\rho_4 = 5.17 \times 10^6\ \Omega$-m (bedrock). Electrode spacing = 384'.

that layer resistivities obtained through curve matching will be longitudinal resistivities because S is the governing average parameter (Zohdy, 1965). This was demonstrated by Kosinski and Kelly (1981), who showed that when the aquifer is the middle layer of the minimum sounding curve, the single aquifer resistivity value calculated from the sounding curve is representative of the entire aquifer section in the horizontal direction. Zohdy, Eaton and Mabey (1974) discuss a technique capable of obtaining aquifer horizontal resistivity for minimum type sounding curves where the middle low resistivity layer (the aquifer) is at least three times the thickness of the upper layer. When the basement layer is very resistive causing the terminal branch of the sounding curve to rise at a 45 angle, the value of S for all layers above the basement may be estimated with a simple graphical method. For this case equation 31 can be used to estimate the horizontal aquifer resistivity provided reasonable estimates of parameters in the equation for layers above the aquifer (ρ_{ℓ_i} and h_i) and the aquifer thickness may be obtained by interpretation of the sounding curve, geophysical methods, borehole control or a combination of these.

Zohdy, Eaton and Mabey (1974) showed how the transverse unit resistance of two layers above the basement (T_{1+2}) may be estimated through graphical interpretation of a three layer maximum type sounding curve when the resistivity of the middle layer (ρ_2) is greater than the upper (ρ_1) and basement (ρ_3) layers ($\rho_1 < \rho_2 > \rho_3$). They also discuss a technique for determining the transverse unit resistance of the middle layer. Therefore, for the three layer case where a maximum sounding curve is obtained and the middle layer represents the aquifer, it is possible to estimate values for the vertical or transverse aquifer resistivity by incorporating curve matching and simple graphical techniques.

Fig. 30 shows the flow net obtained from the computer model for a horizontally layered formation where ρ_4 = 8.9 Ω-m represents a conductive basement layer. Other layer resistivity values and the current electrode separation are as in Fig. 29. Streamlines show current flow through the aquifer is approximately vertical. This approximation will improve as the thickness of the aquifer increases. It should be noted that this case will produce a double descending type sounding curve since $\rho_{1+2} > \rho_3 > \rho_4$. However, the top two layers (ρ_{1+2}) are very thin campared to the aquifer and therefore the flow pattern should not change significantly if these layers had a resistivity lower than the aquifer, as in the maximum sounding curve arrangement. It is primarily the low conductivity of the basement layer that causes current to move vertically through the aquifer section. This case will exist when the bedrock is shale, the situation reported by Duprat, Simler and Ungemach (1970), or where saline water occurs in the fissures and joints of the upper portion of the bedrock, as in some sections of northwestern Missouri (Frolich, 1974).

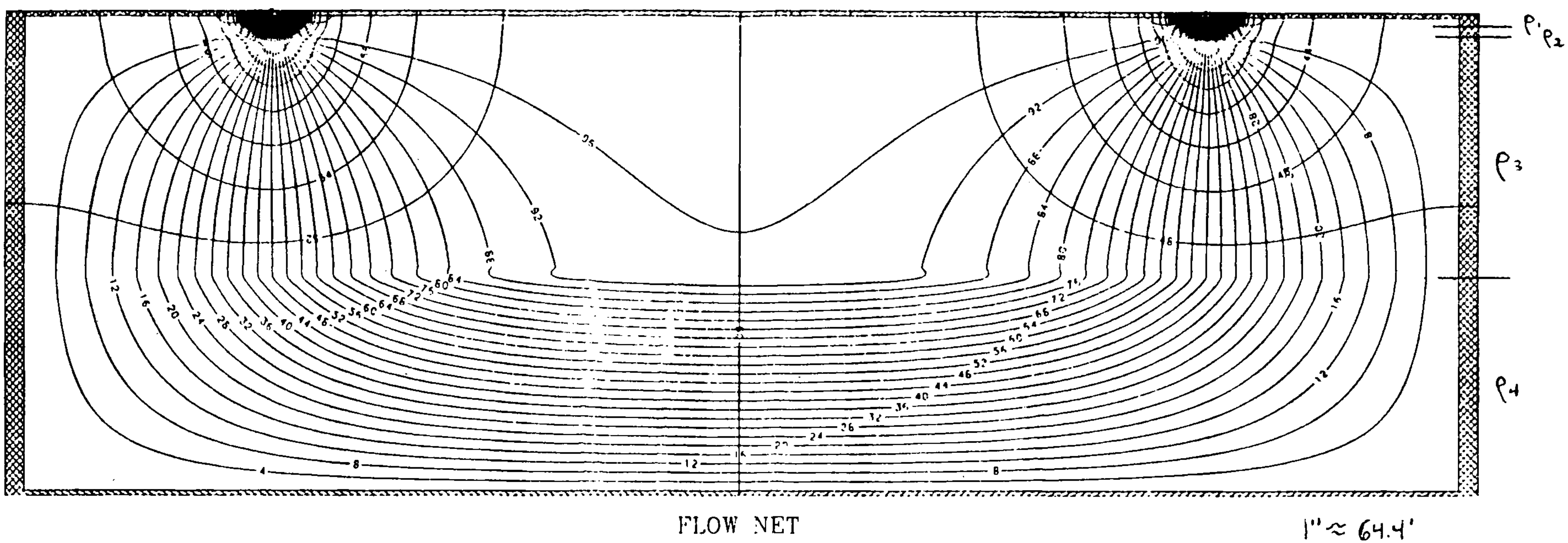

Figure 30. Flow net demonstrating the point to point electric current flow and scalar electrical potentials for a typical aquifer section where the base layer has high conductivity. Layer resistivities are the same as in Figure 29, except $\rho_4 = 8.9\ \Omega$-m. Electrode spacing = 384'.

OBSERVATIONS: FLOW GEOMETRY STUDY

The following observations are drawn from the flow geometry study:

1. When aquifer layering is horizontal, the aquifer permeability for horizontal flow k_h will equal the aquifer permeability for radial flow k_r.

2. For vertical layering, k_r will not equal k_h, since k_r depends on the exact arrangement of the layers (Table 7).

3. For horizontally or vertically layered aquifers in the isolated case, where current flows only through the aquifer and is not refracted by surrounding strata, the amount of current moving through the aquifer from point source to point sink will depend on the exact arrangement of the layers (Table 8).

4. In the isolated case, aquifers that are isotropic and homogeneously heterogeneous (conventional definition) will not depend significantly on flow geometry for determining aquifer properties (Tables 9 thru 12).

5. For the isolated aquifer case, the standard deviation of aquifer properties is effected by flow geometry. Tables 9 thru 11 demonstrate the increasing trend of standard deviation ($\hat{\sigma}$) from quasi-linear to quasi-radial to quasi-point to point cases.

6. For the non-isolated aquifer case, where current is refracted by surrounding strata, if electrode spacing is large (relative to the aquifer thickness) and the basement and upper layers are more resistive than the aquifer section, current flow will be approximately horizontal through the aquifer (Fig. 29).

7. For the non-isolated aquifer case, when current is introduced at large electrode spacings and the basement layer is very conductive compared to the aquifer and upper layers, current flow will be approximately vertical through the aquifer section (Fig. 30).

CONCLUSIONS

The following conclusions have been drawn from this study assuming that, at the material level, aquifer soils are isotropic and obey a relationship similar to equation 3 (approximately equal in slope), where pore water resistivity is constant and Darcy's law is valid.

1. For a horizontally layered aquifer, where electric current moves parallel to the layering, it is possible to estimate horizontal aquifer permeability when hydraulic or electric anisotropy and aquifer horizontal (longitudinal) resistivity values are known. The aquifer horizontal resistivity may be estimated for the non-isolated aquifer case using sounding curve interpretation techniques and graphical methods when formations are horizontally layered and the basement layer is very resistive compared to the aquifer (vertical electric sounding curves that end with a forty five degree incline). For a horizontally layered aquifer, the estimated horizontal aquifer resistivity (ρ_{hh}) could be used to estimate aquifer horizontal permeability (k_{hh}) when the hydraulic or electric anisotropy is known (Fig. 3).

2. For cases where electric current moves vertically through a horizontally layered aquifer, it is possible to estimate horizontal aquifer permeability using the aquifer vertical (transverse) resistivity. The aquifer vertical resistivity may be estimated for the non-isolated aquifer case using sounding curve interpretation techniques and graphical methods when formations are horizontally layered and the basement layer is very conductive compared to the aquifer (maximum or double descending type sounding curve). For a horizontally layered aquifer, the vertical aquifer resistivity (ρ_{vh}) could be used to estimate aquifer horizontal permeability (k_{hh}) (Fig. 11). Knowledge of the hydraulic or electric anisotropy would improve this estimate, but it is not necessary to obtain a reasonable value.

3. Since spacially mixed aquifers do not depend significantly on flow geometry it may be possible to estimate the aquifer permeability for the isolated and non-isolated aquifer cases. In the isolated case, where current moves in a quasi-point to point geometry, the apparent resistivity obtained from a vertical electric sounding will represent the aquifer resistivity. Quasi-point to point flow geometry will be maintained only if the electrode

spacing is less than the aquifer thickness.

In the non-isolated aquifer case it is possible to estimate the aquifer resistivity with vertical electric sounding interpretations. For this case, the current path through the aquifer need not be horizontal or vertical, so long as it is possible to estimate the aquifer resistivity by interpretation.

The known aquifer resistivity may be used with figures similar to Figs. 22, 27 or 28 to estimate the horizontal aquifer permeability when the type of distribution (uniform, exponential, lognormal, etc.) and the mean or standard deviation is known. Fig. 31 demonstrates the trend of Fig. 28 applied in an example. When the spacial permeability distribution is known to be lognormal with a standard deviation of .8 and the aquifer resistivity is determined to be 500 Ω-m, then the aquifer horizontal permeability would be estimated at about .022 cm/sec. Figs. 22 and 27 would be utilized in a similar manner.

4. It is possible to have a relation between aquifer resistivity and aquifer radial permeability with a positive or negative slope when aquifer resistivities are estimated from electric soundings and aquifer radial permeabilities are estimated from pump test data. Fig. 28 shows both conditions are

possible when the permeability distribution is lognormal. A negative slope could exist for a field situation where the mean permeability was constant with standard deviation varying at each location tested. Similarly, a positive trend could occur for a constant standard deviation with a mean permeability that was location dependent. For the layered case, Fig. 3 shows both a positive or negative slope could pass through the spread of points when layering is horizontal, the bedrock has a high resistivity and the anisotropy varies with location. From the results of Fig. 11, it can be seen that it would be difficult to get a negative sloped correlation between aquifer vertical (transverse) resistivity and aquifer radial permeability when the bedrock is very conductive and the aquifer is horizontally layered.

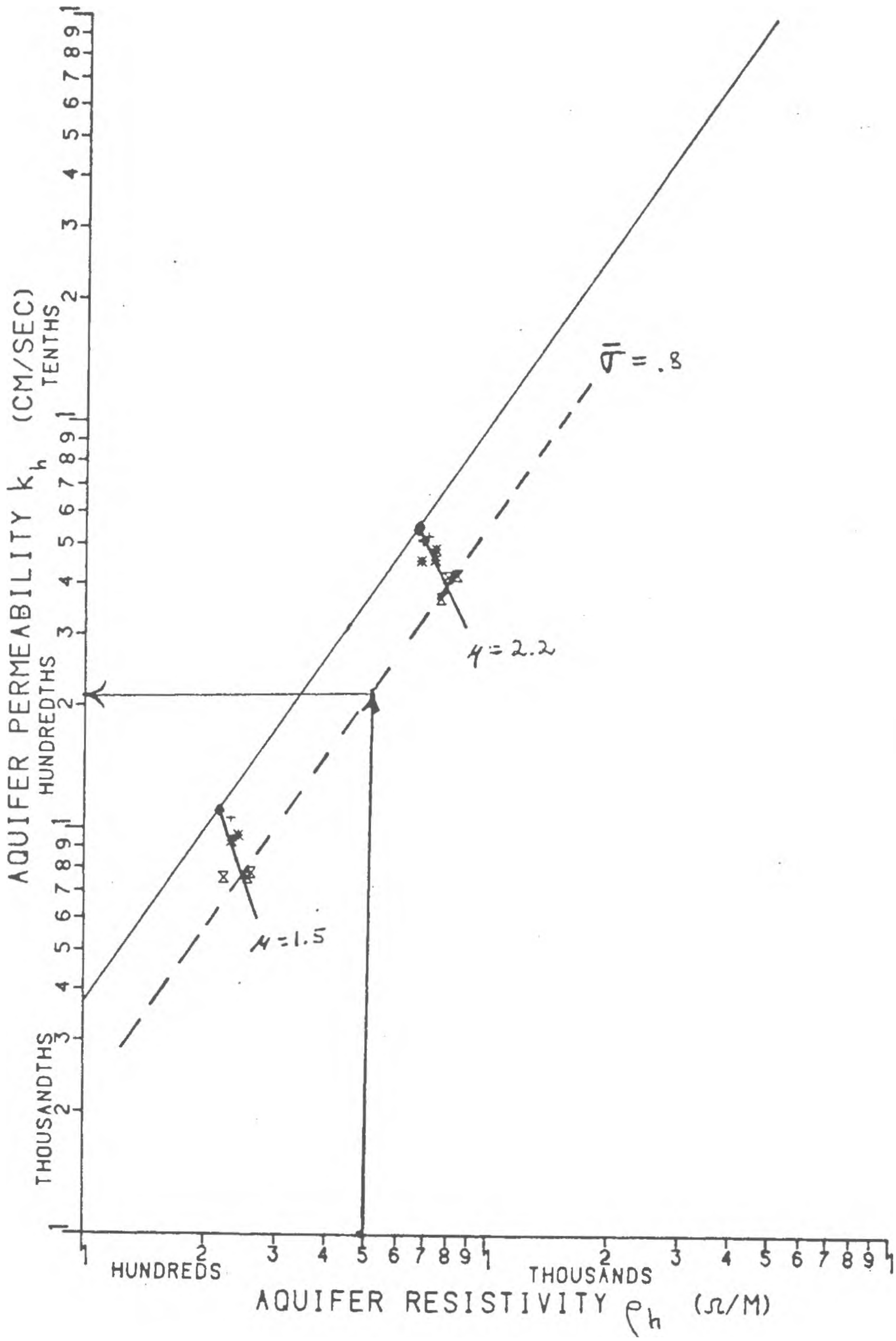

Figure 31. Aquifer permeability vs. aquifer resistivity showing broad trends based on the LOGNORMAL distribution results for aquifers with a low scale of heterogeneity

REFERENCES

Aiken, C.L., Hastings, D.A., and Sturgul, J.R., 1973, "Physical and Computer Modeling of Induced Polization", Geophysical Prospecting, Vol. 21, pp. 763-782.

Alger, R.P., 1966, "Interpretation of Electric Logs in Freshwater Wells in Unconsolidated Formations", Seventh Annual Logging Symposium Transactions, Sec. CC, pp. 1-25.

Allen, W.B., Hahn, G.W., and Tottle, C.R., 1963, Geohydrological Data for the Upper Pawcatuck River Basin, Rhode Island: Rhode Island Water Resources Coordinating Board Geol. Bull. 13, 68 p.

Archie, G.E., 1950, "Introduction to Petrophysics of Reservoir Rocks", Bull. of the Amer. Assoc. of Petroleum Geologists, Vol. 34, No. 5, pp. 943-961.

Bear, J., Dynamics of Fluids in Porous Media, American Elsevier Publishing Co., N.Y., 764 p.

Bouwer, H., 1969, "Planning and Interpreting Soil Permeability Measurements, J. Irrig. Drain. Div. Amer. Soc. Civil Eng., Vol. 95, pp. 391-402.

Bouwer, H., 1978, Groundwater Hydrology, McGraw-Hill Book Co., N.Y., 480 p.

Carothers, J.E., 1968, "A Statistical Study of the Formation Factor Relation", The Log Analyst, Sept.-Oct., pp. 13-20.

Clarke, R.T., 1973, "A Review of Some Mathematical Models used in Hydrology with Observations on their Calibration and Use," Journal of Hydrology, Vol. 19, pp. 1-20.

Dakhnov, V.N., 1962, "Geophysical Well Logging", Quarterly of the Colorado School of Mines, Vol. 57, No. 2.

Davis, S.N., and DeWiest, J.M., 1966, Hydrogeology, John Wiley & Sons, N.Y., 463 p.

Douglas, J., 1959, "Round-off Error in the Numerical Solution of the Heat Equation", J. Assoc. of Computing Mach., Vol. 6, pp. 48-58.

Duprat, A., Simler, L. and Ungemach, P., 1970, "Contribution de la Prospection Électrique a la Recherche Des Caractéristiques Hydrodynamiques D'un Milieu Aquifère", Terres et Eaux, Vol. XXIII, No. 62.

Fraser, H.J., 1935, "Experimental Study of the Porosity and Permeability of Clastic Sediments", J. of Geology, Vol. 43, No. 8, pp. 910-1010.

Freeze, R.A., 1975, "A Stochastic-Conceptual Analysis of One-Dimensional Groundwater Flow in Nonuniform Homogeneous Media", Water Resources Research, Vol. 11, No. 5, pp. 725-741.

Freeze, R.A., and Cherry, J.A., Groundwater, 1979, Prentice-Hall, Inc., Englewood Cliffs, N.J., 604 p.

Frohlich, R.K., 1974, "Combined Geoelectrical and Drill-Hole Investigations for Detecting Fresh-Water Aquifers in Northwestern Missouri", Geophysics, Vol. 39, No. 3, pp. 340-352.

Gonthier, J.B., H.E. Johnson, and G.T. Malinberg, 1974, "Availability of Ground Water in the Lower Pawcatuck River Basin, Rhode Island", Geological Water Supply Paper 2033.

Graton, L.C., and Fraser, H.J., 1935, "Systematic Packing of Spheres - With Particular Relation to Porosity and Permeability", J. of Geology, Vol. 43, No. 8, pp. 785-909.

Greenkorn, R.A., and Kessler, D.P., 1969, "Dispersion in Heterogeneous Nonuniform Anisotropic Porous Media", Ind. Eng. Chem., Vol. 61, No. 9, pp. 14-32.

Halliday, D., and Resnick, R., 1970, Fundamentals of Physics, John Wiley & Sons, N.Y., 837 p.

Heigold, P.C., Gilkeson, R.H., Cartwright, K., and Reed, P.C., 1979, "Aquifer Transmissivity from Surficial Electrical Methods", Groundwater, Vol. 17, No. 4, pp. 338-345.

Higdon, W.T., 1963, Discussion of "Variation of Electrical Resistivity of River Sands, Calcite, and Quartz Powders with Water Content" by V.J. Sarma and V.B. Rao, Geophysics, April, pp. 309-310.

Hill, H.J., and Milburn, J.D., 1956, "Effect of Clay and Water Salinity on Electrochemical Behavior of Reservoir Rocks", Petroleum Transactions, AIME, Vol. 207, pp. 65-72.

Jepsen, A.F., 1969, "Resistivity and Induced Polarization Modeling", Ph.D. dissertation, University of Calif., Berkeley.

Keller, G.V., and Frischknecht, F.C., 1966, Electrical Methods in Geophysical Prospecting, Pergamon Press, Oxford, 517 p.

Kelly, W.E., 1976, Estimating Aquifer Permeability by Surface Electrical Resistivity Measurements, Technical Report to the National Science Foundation, August.

Kelly, W.E., 1977, "Geoelectric Sounding for Estimating AquiferHydraulic Conductivity", Ground Water, Vol. 15, No. 6, pp. 420-425.

Kelly, W.E., Frohlich, R.K., 1978, Estimating Hydraulic Properties of Glacial Aquifers with Surface Geophysical Measurements; Research Proposal to the National Science Foundation, April 1.

Kelly, W.E., 1980, "Porosity-Permeability Relationship in Stratified Glacial Deposits", paper presented at American Geophysical Union Annual Meeting, Toronto, May 23.

Kezdi, A., 1974, Handbook of Soil Mechanics, Vol. 1 (Soil Physics), Elsevier Scientific Pub. Co., N.Y., p. 49.

Kosinski, W.K., 1978, "Geoelectric Studies for Predicting Aquifer Properties; M.S. Thesis, University of Rhode Island, Kingston, R.I.

Kosinski, W.K. and Kelly, W.E., 1981, "Geoelectric Soundings for Predicting Aquifer Properties", Ground Water, Vol. 19, No. 2, pp. 163-171.

Krumbien, W.C., and Monk, G.D., 1942, "Permeability as a Function of the Size Parameters of Unconsolidated Sand, Am. Inst. of Mining & Metal. Engrs., Vol. 151, pp. 153-163.

Law, J.A., 1944, "A Statistical Approach to the Interstitial Heterogeneity of Sand Reservoirs, Trans. of A.I.M.E., Vol. 155, pp. 202-222.

Lee, C. H., and Ellis, A. J., 1919, "Geology and Ground Waters of the Western Part of San Diego County, California", U.S.G.S. Water Supply Paper 446, pp. 121-123.

Loudon, A. G., 1952, "The Computation of Permeability from Simple Soil Tests", Geotechniques (British), Vol. 3, No. 2, pp. 165-183.

Masch, F. D., and Denny, K. J., 1966, "Grain Size Distribution and Its Effect on the Permeability of Unconsolidated Sands", Water Resources Research, Vol. 2, No. 4, pp. 665-677.

McMillan, W. D., 1966, "Theoretical Analysis of Groundwater Basin Operations", Water Resource Center Contrib. 114, 167 pp., University of California, Berkley.

Mufti, I. R., 1976, "Finite-Difference Resistivity Modeling for Arbitrarily Shaped Two-Dimensional Structures", Geophysics, Vol. 41, No. 1, pp. 62-78.

Mufti, I. R., 1978, "A Practical Approach to Finite Difference Resistivity Modeling", Geophysics, Vol. 43, No. 5, pp. 930-942.

Muscat, M., 1946, "The Flow of Homogeneous Fluids Through Porous Media, McGraw-Hill.

Patnode, H. W. and Wyllie, M. R. J., 1950, "The Presence of Conductive Solids in Reservoir Rocks as a Factor in Electric Log Interpretation", Pet. Trans., A.I.M.E., Vol. 189, pp. 47-52.

Peaceman, D. W., and Rachford, H. R., 1955, "The Numerical Solution of Parabolic and Elliptic Differential Equations", J. Soc. Indust. Appl. Math., Vol. 3, No. 1, pp. 28-41.

Perloff, W. H., and Baron, W., 1976, Soil Mechanics Principles and Applications, Ronald Press, N. Y., 745 p.

Prickett, T. A., and Lonnquist, C. G., 1971, Selected Digital Computer Techniques for Groundwater Resource Evaluation, Illinois State Water Survey, Bulletin 55.

Reiter, P. F., 1980, "A Computer Study of the Correlation Between Aquifer Hydraulic and Electric Properties", thesis presented to the University of Rhode Island in partial fulfillment of the requirements for the degree of Master of Science.

Remson, I., Hornberger, G.M., and Molz, F.J., 1971, Numerical Methods in Subsurface Hydrology, Wiley-Interscience, N.Y., 389 p.

Roach, P., 1972, Conceptual Fluid Dynamics, Hermosa Publishers, Alburquerque, N.M.

Rushton, K. R., and Redshaw, S. C., 1979, Seepage and Groundwater Flow, John Wiley & Sons, N. Y., 339 p.

Sarma, V. V. J., and Rao, V. B., 1962, "Variation of Electrical Resistivity of River Sands, Calcite and Quartz Powders with Water Content", Geophysics, Vol. 27, No. 4, pp. 470-479.

Terzaghi, C., 1925, Engineering News Record, Dec. 3, 1925, p. 914.

Trask, P.H., 1931, Amer. Assoc. Petrol. Geol. Bull., Vol. 15, p. 273.

Trescott, P.C., 1975, Documentation of Finite Difference Model for Simulation of Three Dimensional Groundwater Flow, U.S.G.S. Open File Report, 75-438, Sept.

Trescott, P.C., Pinder, G.F., and Larson, S.P., 1976, Techniques of Water-Resources Investigations of the U.S.G.S., Chapt. C1, Finite-Difference Model for Aquifer Simulation in Two-Dimensions with Results of Numerical Experiments, U.S. Gov. Printing Office.

Ungemach, P., Mostaghimi, F., and Duprat, A., 1969, "Essais de Determination Du Coefficient D'Emmagasinement en Nappe Libre Application of la Nappe Alluviale du Rhin", International Assoc. of Scientific Hydrology, Vol. 14, No. 2, pp. 169-190.

Urish, D.W., 1978, "A Study of the Theoretical and Practical Determination of Hydrogeological Parameters in Glacial Outwash Sands by Surface Geoelectrics", Ph.D. Dissertation, Univ. of Rhode Island, Kingston, RI.

Walton, W.C., 1970, Groundwater Resource Evaluation, McGraw-Hill Book Co., NY, p. 664.

Warren, J.E., and Price, H.S., 1961, "Flow in Heterogeneous Porous Media", Soc. of Petrol. Eng. J., Vol. 1, pp. pp. 153-169.

Willardson, L.S. and Hurst, R.L., 1965, "Sample Size Estimates in Permeability Studies", J. Irrig. Drain. Div. Amer. Soc. Civil Eng., Vol. 91 (IR1), pp. 1-9.

Winsauer, W.O. and McCardell, W.M., 1953, "Ionic Double-Layer Conductivity in Reservoir Rock", Petrol. Trans., A.I.M.E., Vol. 198, pp. 129-134.

Worthington, P.F., and Barker, R.D., 1972, "Methods for the Calculation of True Formation Factors in the Bunter Sandstone of Northwest England", Engineering Geology, Vol. 6, pp. 213-228.

Worthington, P.F., 1977, "Influence of Matrix Conduction Upon Hydrogeophysical Relationships in Arenaceous Aquifiers", Water Resources Research, Vol. 13(1), pp. 87-92.

Wyllie, M.R.J., and Gregory, A.R., 1953, "Formation Factors of Unconsolidated Porous Media: Influence of Particle Shape and Effect of Cementation", Petrol. Trans., A.I.M.E., Vol. 198, pp. 103-109.

Zohdy, A.A.R., 1965, "The Auxiliary Point Method of Electrical Sounding Interpretation, and Its Relationship to the Dar Zarrouk Parameters", Geophysics, Vol. 30, p. 644-660.

Zohdy, A.A.R., Eaton, G.P., and Mabey, D.R., 1974, "Application of Surface Geophysics to Groundwater Investigations", Techniques of Water Resources Investigations of the U.S.G.S., Chapt. D1, Book 2.

SECTION II

Appendix A

Material Level Relationships

Porosity and permeability are the hydrogeological properties that most researchers have attempted to correlate with electrical properties at the material level. Archie (1942) introduced the concept of formation factor in his study of brine saturated rocks. Formation factor is defined as

$$F = \frac{\rho_o}{\rho_w} \qquad (1)$$

where ρ_o = bulk resistivity of the brine saturated rock

and ρ_w = resistivity of the brine

According to Archie (1950) and Carothers (1968), formation factor (F) is inversely related to the porosity (ϕ) by,

$$F = a\phi^{-m} \text{ (Archies Law)} \qquad (2)$$

where a and m are constants relating to the rock type. Unconsolidated sands have also been shown to follow the trend of Archies Law (Wyllie and Gregory, 1953).

Patnode and Wyllie (1950), and Hill and Milburn (1956) found the formation factor to vary with porewater resistivity in argillaceous sandstones tested in the laboratory. Later, Worthington and Barker (1972) made similar observations of the argillaceous material of the Bunter Sandstone of Northwest England. Winsauer and McCardell (1953) attributed the abnormal effect to absorption on the clay surface, which varies with electrolyte concentration. Both Hill and Milburn (1956) and Worthington and Barker (1972) distinguish between this formation factor, which changes with pore water resistivities, and a formation factor dependent only on solid properties. The Worthington and Barker term of "apparent formation factor" (F_a) will be used for this quantity. Serious errors are shown to result if F_a values are used to determine porosities. According to Worthington and Barker, the F_a value can be less than half of the F value over the range of 1 - 40 Ω-m for porewater resistivity (ρ_w). The previously designated formation factor (F) shall henceforth be called the intrinsic or true formation factor (F_i).

Worthington (1977) reports good correlations between true formation factor and porosity for unsorted argillaceous samples of the Bunter Sandstone. The plot followed the trend of Archies Law. The true formation factors were determined by using an equation that expressed F_a in terms of ρ_w and F_i. This equation was of the form

$$\frac{1}{F_a} = \frac{1}{F_i} + \frac{\rho_w}{A} \qquad (3)$$

where A is a constant, related to the matrix and surface conductance of the sample. This model is similar to the parallel resistor model developed by Patnode and Wyllie (1950), where

$$\frac{1}{F_a} = \frac{1}{F_i} + \frac{\rho_w}{\rho_c} \qquad (4)$$

or

$$\frac{1}{\rho_o} = \frac{1}{\rho_t} + \frac{1}{\rho_c} \qquad (5)$$

since

$$F_i = \rho_t / \rho_w \qquad (6)$$

or

$$\frac{1}{\rho_o} = \frac{1}{F_i \rho_w} + \frac{1}{\rho_c} \qquad (7)$$

where
ρ_o = bulk resistivity
ρ_c = resistivity due to clay content
ρ_t = true resistivity (resistivity that would be measured if the soil matrix is a perfect insulator and there are no surface conductance effects)

This model was disputed by Winsauer and McCardell (1953) on the basis that it implied a constant contribution to the conduction by solid constituents (taken to include surface conduction), independent of porewater conductivity. This is illustrated in equation (3) where $1/\rho_c$ is a constant. Yet Worthington and Barker (1972) demonstrated the good fit of equation 3 to their empirical data. They extrapolated F_i from F_a vs. ρ_w data used in equation 3. True formation factor could be determined easier by saturating the sample with pore water of high conductance to surpress the effects of surface conduction.

The relationship between porosity and true formation factor appears to be very strong. Groundwater modeling, however, requires values for the hydraulic conductivity or permeability (k). The relationship of true formation factor to permeability is not as well understood, but tests indicate that true formation factor increases as permeability decreases with a broad trend on a log-log scatter diagram (Worthington). Inherent in this relationship is the direct correlation between permeability and porosity, which is demonstrated by Worthington's data for unsorted sandstones.

A demonstration of the effect of the ϕ:k relatiohship on the F_i:k relationship is shown in figure A1. Here two cases are illustrated. Case A shows a direct relationship between ϕ:k which yields the inverse relationship for F_i:k, assuming the validity of Archies Law. The Case B situation yields the direct relationship between F_i:k because an inverse relationship was used for ϕ:k.

Since F_i:k relationships seem to depend on the ϕ:k correlations, the latter relationship deserves some attention. The concepts of porosity

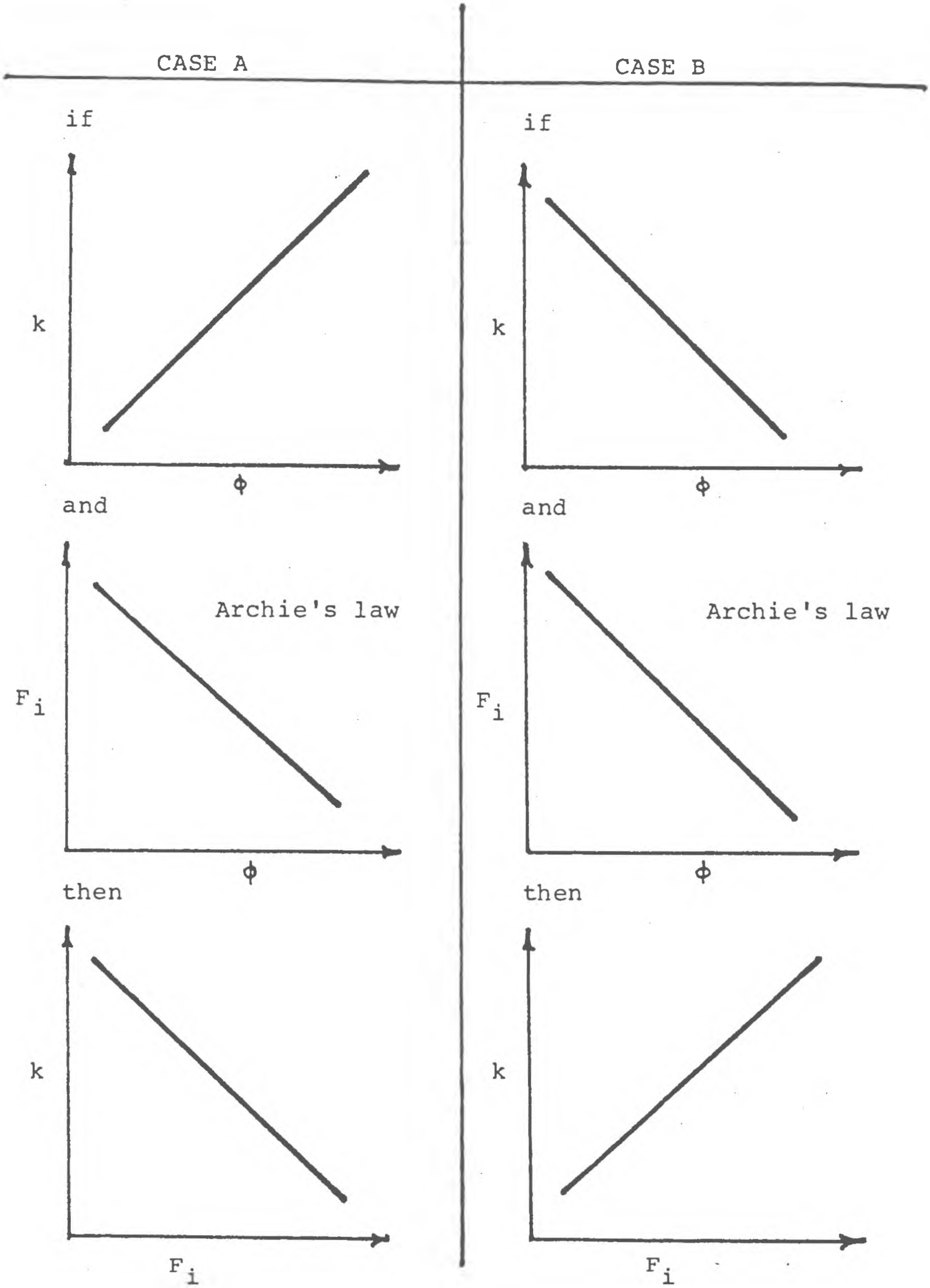

Figure A1 Cases of Permeability (k) Versus Intrinsic Formation Factor (F_i) as dependent on Porosity (ϕ) vs. Permeability and permeability are comprehensively explained in two articles by Graton and Fraser (1935). Their ideas are reviewed in appendix B. The dependence of the ϕ :k relationship upon average grain size and sorting is also reviewed. Essentially it appears that the ϕ :k relationship is not always well defined for unconsolidated sands on a sample to sample basis, most notably when there is a poor correlation between D_{50} and S_o. In sandstone S_o and D_{50} may be constant with only porosity varying; thus yielding a strong direct ϕ:k relationship.

It was noted before that apparent formation factor (F_a) changed as the pore water resistivity (ρ_w) changed for the argillaceous sandstones studied by Hill and Milburn (1956), Winsauer and McCardell (1953), Worthington and Barker (1972) and Worthington (1977). Some aquifers, like those in southern Rhode Island, are virtually clay free (clean) and are composed primarily of sand grains which are poor conductors.

The mechanisms causing greater surface conductance near clay particles are also present in clean sands. All fine grained minerals including quartz have a finite cation exchange capacity resulting from unsatisfied crystal bonds along the edges of grains; exchange capacity is larger for fine grained particles (Keller and Frischknecht, 1966). The magnitude of surface conductance is related to the ion concentration of the saturating solution. As the concentration decreases, the magnitude of surface conductance also decreases, but in the low conductivity environment of a fresh water sand, even this reduced surface conductance is most notably effected by the surface exposed to the saturating solution, with the larger the surface per unit volume exposed to the electrolyte, the larger is the total surface conductance (Alger, 1966). This is of major importance since permeability is also dependent upon surface area (specific total surface), which can be thought of as a parameter combining the effects due to absolute grain size and sorting (see appendix B).

Variations of formation factor with respect to the pore water resistivity for fresh water saturated unconsolidated samples are illustrated in lab tests by Sarma and Rao (1963), showing that "clean" (containing no clay) granular formations do not behave normally for water resistivities typical of good quality water. That is, the formation factor changes as pore water resistivity changes. This indicates that the following assertion by Winsauer and McCardell (1953) must be inaccurate: data from Patnode and Wyllie (1950) showed clean sandstones do not exhibit variations in formation factor with varying pore water concentrations. Examination of the Patnode and Wyllie data shows this conclusion must be based upon the alundum core tests, which used only very low pore water resistivities (.119 and 8.29 Ω-m).

Since the formation factor data from Sarma and Rao varies with pore water resistivity, it must be considered as an apparent formation factor. They measure bulk resistivities (ρ_o) for washed and graded river sand samples, which are considered clean. This assumption is supported by Higdon (1963) who says, "--the sands should have been washed free of clay in the process of deposition, and/or panning---" in a discussion of the Sarma and Rao paper. The range of pore water resistivities tested was about .2 Ω-m to 45 Ω-m with one very dilute solution (ρ_w = 2176 Ω-m) tested for two samples. The data show differences between F_a and F_i are more pronounced in samples with high pore water resistivity. Alger (1966) points out that the Sarma and Rao data indicate a relationship between grain size and F_a for fresh waters. The data show F_a increases with increasing grain size, indicating that F_a may correlate well with permeability.

Laboratory data from Jones and Buford (1951) were used by Alger (1966) and Croft (1971) to develop a relationship between apparent formation factor and permeability. The Jones and Buford samples were graded with relatively constant porosities, ranging from .40 to .45, and the pore water resisitivity was 35 Ω-m. Kelly (1976) measured permeability and apparent formation factor concurrently, using a permeameter with electrodes embedded in the cell to enable the measurement of conductance (inverse of resistivity). His samples were clean, of constant porosity (.415) and ρ_w was approximately 10 Ω-m. Points from the Jones and Buford, and Kelly (1976) data are shown in figure A2. Both are in good agreement.

Worthington (1977) claims the Jones and Buford samples may have contained some clay and he points out that it is the argillaceous nature of the samples which calls for the use of apparent formation factor. He claims that the finer graded samples contain more clay and this changing clay content is what brings about the good F_a:k relationship. Evidence from Kelly (1976) indicates the F_a:k correlation is strong in graded samples of fairly constant porosity that did not contain clay. It appears Worthington's conclusion would serve to enhance the F_a:k relationship in graded argillaceous sand deposits.

Currently there is no laboratory data of F_a vs. k for ungraded clean samples where the porosity may vary. The behavior of such a sample to sample relationship was postulated in a dissertation by Urish (1978). His theoretical model used an equation developed by Pfannkuch (1969) for

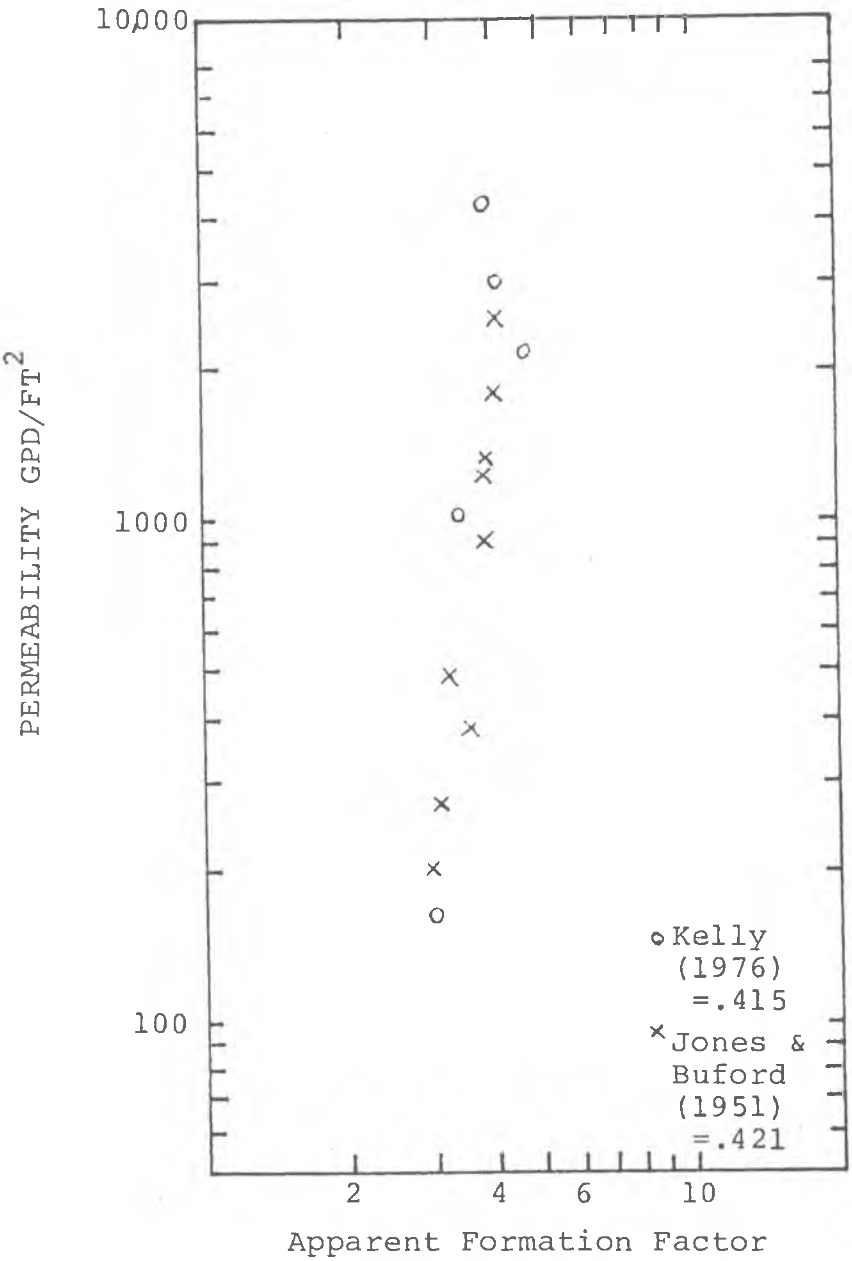

Figure A2. Laboratory Relation of Permeability to Apparent Formation Factor (from Kelly, 1976) apparent formation factor and the Kozeny-Carmen equation for permeability.The Pfankuch model was selected because of its comprehensive treatment of the role surface conductivity plays in the electrical transport process, even in clean sands. This model is expressed as;

$$\frac{1}{R_o} = \frac{1}{R_f} + \frac{1}{R_d} + \frac{1}{R_s} \qquad (8)$$

or in conductance terms

$$K_o = K_f + K_d + K_s \qquad (9)$$

where

$K_o = \frac{1}{R_o}$ conductance of the combined or bulk phase

$K_f = \frac{1}{R_f}$ conductance of the pore water phase

$K_d = \frac{1}{R_d}$ conductance of the dispersed or soil matrix phase

$K_s = \frac{1}{R_s}$ surface conductance

and the subscripted R values denote the resistance for each phase. When this model is expressed in terms of the geometry of the matrix system, incorporating the concept of tortuosity and assuming there is no conduction through the soil matrix or dispersed phase, the resulting expression for the apparent formation factor (F_a) is:

$$F_a = \frac{F_i}{1 + \frac{k_s}{k_f} S_p} \qquad \text{(Urish, 1978)} \quad (10)$$

where F_i = intrinsic or true formation factor = f (ϕ) Archies Law

k_s = specific surface conductivity (mho)

k_f = conductivity of the porewater phase (mho-cm^{-1})

S_p = specific internal pore surface (cm^{-1})

$= S_T \frac{1 - \phi}{\phi} = \frac{\text{surface area}}{\text{void volume}}$

where S_T = total specific surface, ϕ = porosity

F_i may be considered as a function of porosity (ϕ) and tortuosity. Since tortuosity is difficult to express numerically, most researchers show true formation factor to be a function only of porosity. Typical is the one by Dakhnov (1962), expressed as

$$F_i = \frac{1 + .25(1-\phi)^{.33}}{1-(1-\phi)^{.67}} \quad \text{(Urish, 1978)} \qquad (11)$$

Loudon (1952), as a result of laboratory investigations, concluded that the Kozeny-Carmen equation agreed better with observed permeability then any other published theoretical equation. This equation is expressed as,

$$k = \frac{g}{c\eta S_T^2} \cdot \frac{\phi^3}{(1-\phi)^2} \quad \text{cm/sec (Loudon, 1952)} \qquad (12)$$

where: ϕ = porosity

g = 7489.16 cm^{-1} sec^{-1} at 10 °C

c = 5 (for spherical particles)

S_T = total specific surface $= \frac{\text{total surface area}}{\text{volume of grains}}$

$= a\,(X_1S_1 + X_2S_2 \ldots\ldots + X_nS_n)\ cm^{-1}$

where: a = angularity with a range from 1.1 for rounded sands to 1.4 for angular sand

X = fractions of the total sample by grain size

$S = \frac{6}{D}$ = specific surface of equivalent diameter sphere in each grain size fraction, where D = equivalent diameter

Examination of these theoretical equations for F_a and k, show that both are very dependent upon surface area, with internal specific surface (S_p) found in the denominator of the Pfannkuch expression and total specific surface (S_T) found in the denominator of the Kozeny-Carmen equation. Thus changes in surface area will effect F_a and k in the same manner.

The other common parameter in equations 10 and 12 is the porosity, which when increased, will serve to decrease F_a and increase k. When the porosity is fairly constant, the F_a:k relationship proves to be one that is strong and direct on a theoretical basis, since the surface area parameters control. This is the case most researchers have shown empirically (Sarma & Rao, Alger, Croft, Kelly, Worthington), where graded samples of relatively constant porosity exhibit increasing S_T and S_P as the average grain size (D_{50}) decreases. It should also be noted that if the sorting coefficient (S_o) increases as D_{50} decreases, the surface area parameters will increase at an even greater rate, and very strong F_a:k correlations might be expected. However, the D_{50}:S_o inverse relationship does not appear to occur in granular outwash deposits (see appendix B). This relationship does not appear to be of significance in establishing the direct F_a:k relationship since samples with small D_{50} values exhibiting small sorting coefficients (S_o), will still show larger S_T and S_P values then samples containing large D_{50} values and large S_o values. Furthermore, the porosity fluctuations from sample to sample should not provide significant influence to alter the direct relationship for F_a:k, since the magnitude of porosities must be from 0.0 to 1.0 (and practically from .2 to .7), which cannot control over the S_T and S_P values that are always at least one order of magnitude higher.

These observations are shown by Urish (1978), where the direct F_a:k relationship results when the Pfankuch and Kozeny-Carmen expressions are utilized. The porosities he uses in equations 10, 11, and 12 are based on wet packing tests for natural outwash samples. These were obtained for both the loosest (Φ_{MAX}) and densest (Φ_{MIN}) states. Figure A3 shows the hypothesized in-situ behavior of F_a vs. k for Φ_{MAX} and ϕ_{MIN} as grain size changes. Also shown is the effect of changing pore water resistivity for one group of points. Inherent in this plot is an inverse trend between uniformity and porosity. The probably average curve shows theoretical in-situ behavior when an inverse trend exists for porosity vs. permeability. Validity of the Urish model is demonstrated when the resulting F_a vs. k plot for spherical particles of constant porosity equal to .4 correlated well with the Jones and Buford data (figure A4), which was for an average porosity of .42 (minimum was .40, maximum was .45) and samples were well sorted. Examination of Urish's input data for ungraded in-situ samples shows an inherent inverse relationship between porosity (ϕ) and permeability (k) and a poor correlation between average grain size (D_{50}) and uniformity coefficient (U_o).

Data from Worthington (1977) (illustrated in figure A5) for unsorted argillaceous sands shows an F_a:k inverse relationship. This situation agrees with the case A trend of figure 1. The inverse relationship appears to reverse as the pore water resistivity increases and the formation factor departs from the true value. This reversing trend may have been seen clearer if tests for pore water resistivities higher than 25 Ω-m were run. Since Worthington claims that matrix conducting properties of unsorted sands will vary unsystematically owing to different concentrations and arrangements of the conducting minerals it must be the surface area parameters (S_T and S_P)that are responsible for converting the inverse F_i:k trend into a direct F_a:k relationship.

From empirical and theoretical studies, both F_i:k and the F_a:k

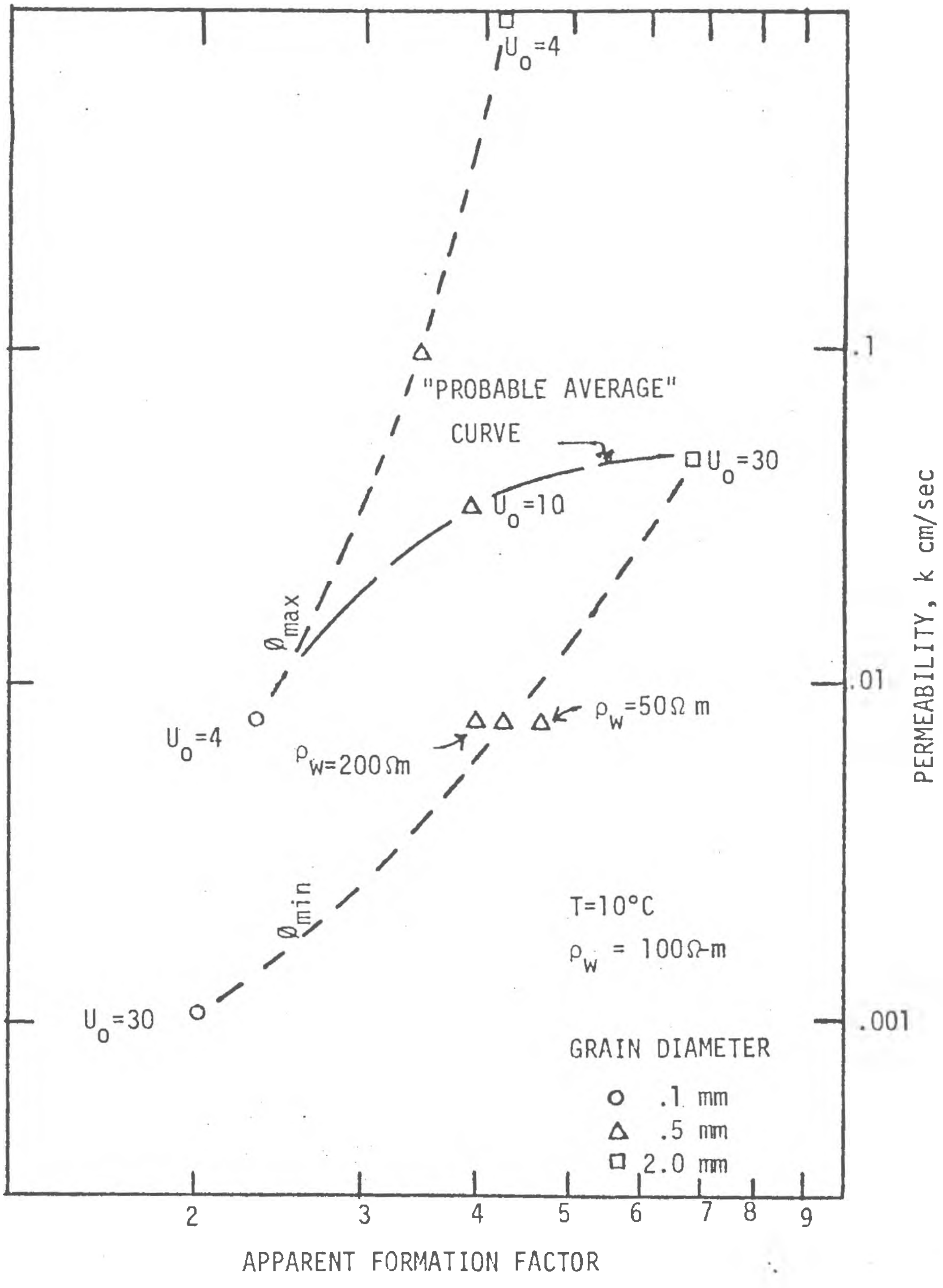

Fig. A3. Range limits for variation of apparent formation factor versus permeability under in-situ condition (from Urish, 1978)

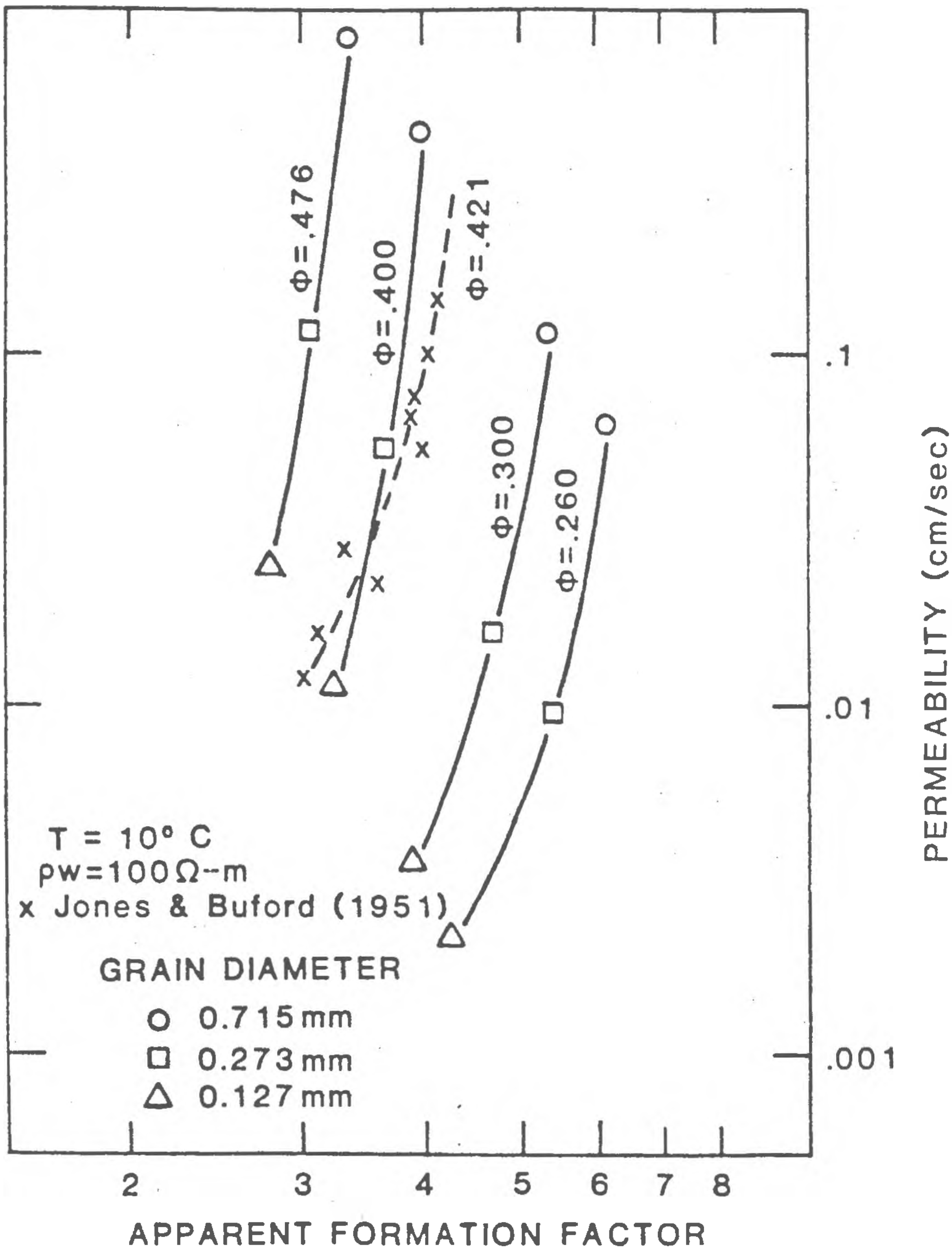

Figure A4. Variation of Apparent Formation Factor Versus Permeability for Spherical Particles (from Urish, 1978)

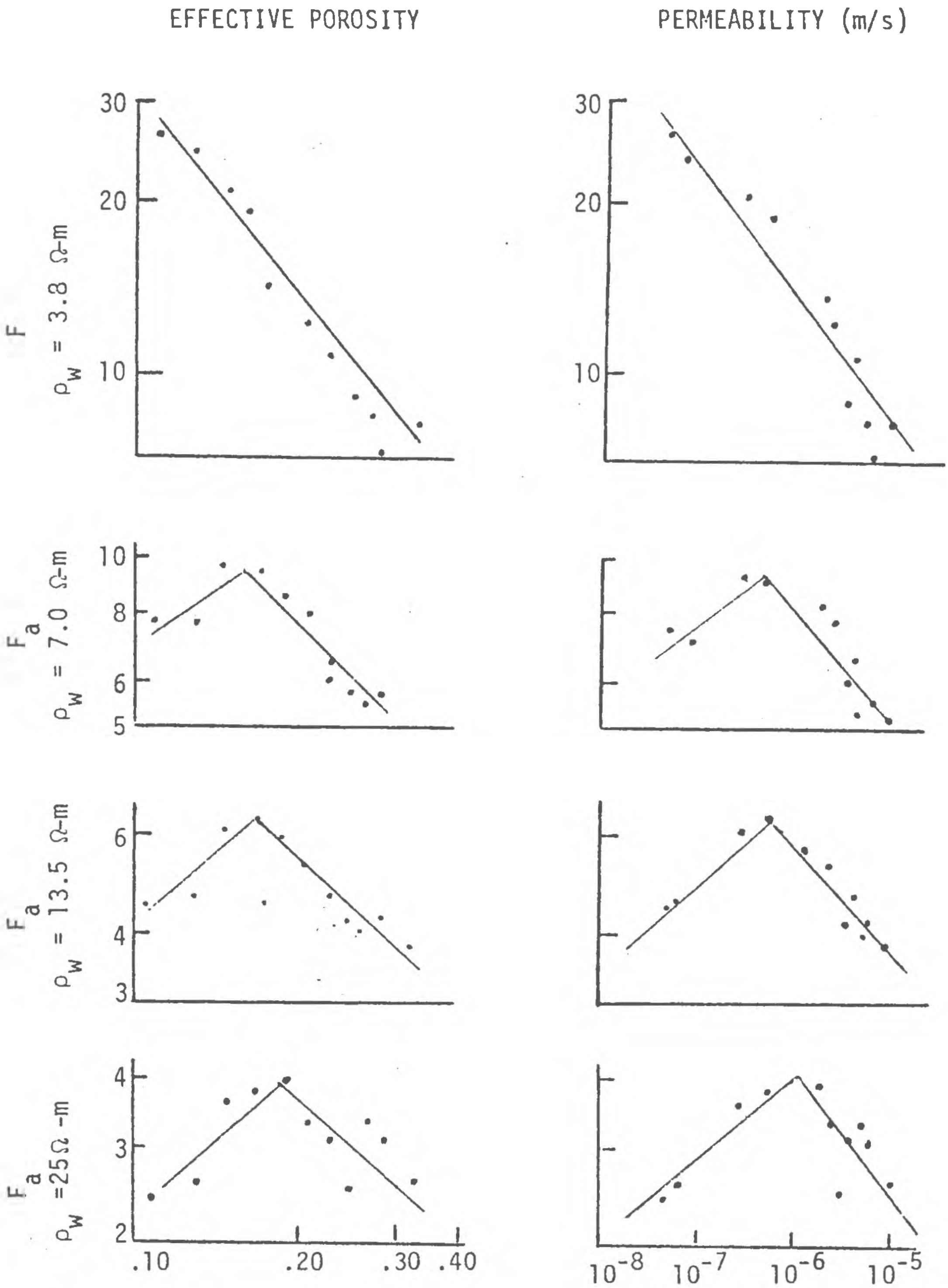

Figure A5. Formation factor - porosity - permeability generalized relationship for unsorted sands (Worthington, 1977).

relationships may be useful for estimating permeabilities in fresh water aquifers. The F :k relationship will depend on the ϕ :k correlation, which must be sloped (not vertical or horizontal). If this relationship is successfully obtained, the technique would then require some kind of in-situ determination of true formation factor. Samples would have to be saturated with a saline solution (water or drilling mud) of known conductivity. Downhole measurements of resistivities in existing wells would be prevented by metal casings, which are found in all wells through unconsolidated soils. However, when water wells are drilled, downhole techniques similar to those employed in the oil industry might be developed to obtain true formation factors. Some background is reviewed from Schlumberger Documentation Number Eight, concerning such methodology.

The drilling mud in a borehole is usually conditioned so that the hydrostatic pressure it exerts on the hole wall exceeds the natural pressure of the formations. Under these conditions mud filters into the permeable beds. In doing so, the solid particles associated with the infiltrating liquid settle on the exposed face of the permeable bed, forming a mud cake. Behind and close to the wall of the hole, the displacement of the formation water by mud filtrate is practically complete. This region, usually referred to as the "flushed zone", generally extends over a distance of at least 3 inches from the hole wall. The Micro-latero log is a micro device involving a focusing system, whereby the effect of the mud cake on the measurement is reduced, and even rendered negligible if the mud cake thickness is small. In fact, it seems that the mud cakes are soft and are reduced to a very thin film by the pressure of the device against the borehole wall. Thus, for thin mud cakes the resistivity of the flushed zone is obtainable and since the resistivity of the invading mud filtrate is known, the true formation factor can be determined. This technique would have to be restricted to drill holes which maintained relatively smooth walls, a situation which rarely exists in unconsolidated sands.

The determination of permeabilities from F_a :k correlations may prove more effective than a down hole method as described above. First, the method appears not to depend on other relationships as the F_i :k relationship depends upon ϕ :k. Also, the apparent resistivities would be determined by surficial array techniques such as the Schlumberger or Wenner configurations. Thus giving apparent resistivity data for very large volumes of subsurface material. This macroscopic value may be more representative of an aquifers performance, as opposed to the discrete sampling by costly boreholes. A problem with the method is the accurate determination of porewater resistivity with depth. If the resistivity of the water (ρ_w) were constant with depth, the F_a :k relationship could be converted to a ρ_a :k relationship; where ρ_a is the apparent resistivity.

Appendix B

Porosity and Permeability

Since intrinsic formation factor vs. permeability relationships appear to depend on the form of the porosity vs. permeability correlations, the latter relationship deserves some examination. According to Graton and Fraser (1935), who examined the concepts of porosity and permeability for spheres, if the diameter of the particle spheres is kept constant, the porosity will depend only on the packing. Furthermore, if the packing is the same, porosity will remain constant, regardless of the particle sphere size. Permeability also depends on packing, however, this is not the whole of the story. If the absolute size of the spherical particles in a given packing arrangement is increased; the permeability will increase.

The in-situ case is not one of uniformly sized particles. Fraser examines the following factors, which he believes affect the in-situ porosity of natural clastic deposits:

1. absolute grain size
2. non-uniformity in the size of the grain
3. proportions of various sizes of grain
4. shape of grain (angularity)

plus the following more general factors

5. method of deposition
6. compaction during and following deposition

As has already been stated, the actual size of the particle has no influence on the porosity of uniform spheres. According to Fraser this is not true for natural sediments, since as the grain size decreases, friction, adhesion and bridging become of increasing importance, because of the higher ratio of surface area to volume and mass; therefore the smaller the grain size, the greater is porosity. This trend of increasing porosity with decreasing grain size (all other factors held constant) for in-situ materials has been observed by Lee (1919), Terzaghi (1925), and Trask (1931) and is illustrated in figure B1 from Davis and DeWeist (1966).

Sorting, or uniformity of grain size is of fundamental importance for determining porosity. Higher porosities are invariably obtained in mixtures where one size predominates; and as the mixture becomes less uniform, the porosity tends to decrease. Since many mixtures can yield the same porosity, Fraser noted the probable extreme complexity of deriving a mathematical expression relating size distribution and porosity. In general, the more uniform the grain size distribution, i.e., the lower the uniformity or sorting coefficients, the greater is porosity (Kezdi, 1974).

Angularity was found to be of minor importance as compared to other factors. Tests showed increases in angularity caused porosity to either increase or decrease; most often increasing (Fraser).

Mode of packing was shown to be of major importance in controlling porosities of uniform spheres (Graton and Fraser). For the in-situ case, the greater the size of grain (up to a certain limit), the greater is its downward component of velocity at the time of deposition. Therefore larger grains have a greater chance of coming to rest in a relatively stable position and should deposit at lower porosities (Fraser).

Compaction after deposition is relatively unimportant except in cases where large pressures were applied, or when the soil matrix has low

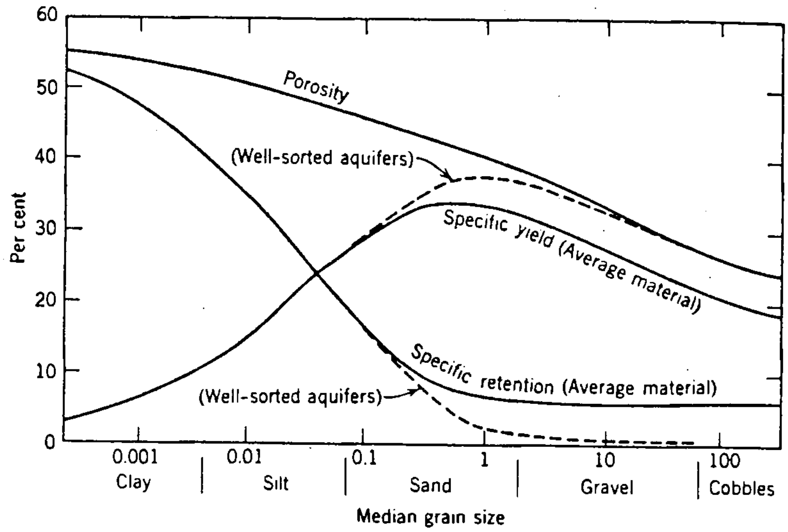

Figure B1. Relation between Median Grain Size and Water Storage Properties of Alluvium from Large Valleys (from Davis & DeWiest, 1966)

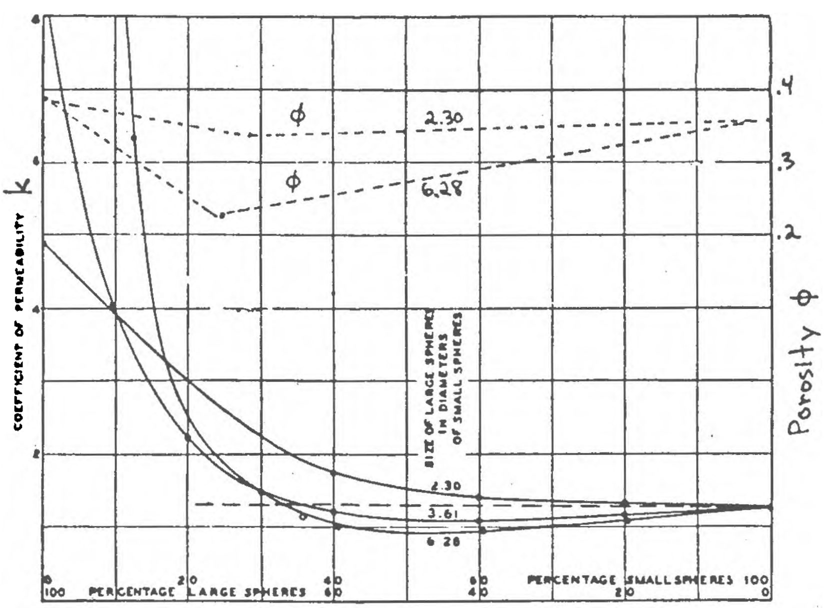

Figure B2. Relation between Proportion of Two Constituents with Permeability and Porosity rigidity.

The permeability of natural deposits is also effected by the uniformity of the mixture. Fraser claims permeability is lowered, within certain limits, when material of a different grain size is added to an existing mixture. These limits are the added materials ability to either fill in existing voids, or to create a net increase in voids. Fraser shows that as two constituents come closer to the point where each make up 50% of the volume of solids, the permeability decreases when the small spheres are added to the large ones, but when the larger spheres are added to the small ones, the permeability decreases only if the ratio of the size of the large particle to the size of the small particle exceeds some limit. This trend is illustrated in figure B2. The plot also shows porosity changes for two of the binary mixtures; and the possibility of increasing permeability with decreasing porosity. This occurs at the right side of the curve for the ratio of 2.3, and from the 50/50 to the 25/75 percentage ratios of small spheres to large spheres for the 6.28 diameter ratio. When many constituents make up the soil mixture, the problem becomes even more complicated. Fraser notes that adding particles to the mixture, which are of intermediate size between two others and keeping the proportions to the volume of solids equal for each constituent, increases permeability. However, when these proportions are not equal, as is often the case for natural deposits, the permeability trend of multi-component systems becomes difficult to assess.

The common increase in permeability with increase in porosity applies within any one sample, (when all other factors controlling permeability are constant). That is, as the sample becomes more compacted, the porosity and permeability both decrease. Graton and Fraser report that while porosity and permeability commonly vary in the same direction, there is extremely elastic variation between the two properties, so that, under certain conditions, low porosity may be associated with high permeability; and very often indeed, material of high porosity has very low permeability. Here they are implying these associations of low porosity with high permeability are possible on a sample to sample basis. This in-situ condition can be explained due to the different depositional environments of coarse and fine sediments. Silts and clays are deposited mainly by slow settling from slack water, whereas coarse gravels are deposited in a high energy environment with much less uniformity in texture and more lateral variation than sands (Fraser, 1935). This suggests that for an alluvial deposited soil mass, the finer the average soil particle is, the lower was its depositional energy and the more uniformity it will possess.

From the articles by Graton and Fraser (1935) and Fraser (1935) then, it would seem logical that porosity would correlate with average grain size and uniformity, where average grain size would tend to indicate the type of packing. Permeability might also be expected to correlate well with average grain size and uniformity coefficient, where the average grain size would indicate the absolute size scale as well as the depositional packing energy.

The importance of grain size and degree of sorting relative to in-situ porosity is reasonably well established. Urish (1978) shows good correlations between dependent variable, porosity (ϕ) and independent variables, average grain size (D_{50}) and uniformity coefficient (U_o) ($U_o = D_{90}/D_{10}$). When his average porosities for twenty two wet packing tests are correlated to D_{50} and S_o, the following equation

$$\phi = .4\, D_{50}^{-.115}\, S_o^{-.119} \qquad (13)$$

was formed which gave a correlation coefficient of .742. Equation 13 is plotted in figure B3.

Kelly (1980) presented results of 116 density tests taken at five sites in ice contact deposits in southern Rhode Island. Resulting wet densities and water contents were converted to dry densities, which were regressed with laboratory determined values of D_{50} and S_o for 96 of the tested samples. The equation is;

$$\gamma_d = 5.3\, D_{50} + 4.2\, S_o + 90.4 \tag{14}$$

The correlation coefficient was .688.

Since

$$\phi = 1 - \frac{\gamma_d}{G_s \gamma_w}$$

where

ϕ = porosity

γ_d = dry density

γ_w = unit weight of water

= 62.4 $\mathrm{lb/ft^3}$

G_s = specific gravity of solids

= 2.65

then

$$\phi = 1 - \frac{5.3\, D_{50} + 4.2\, S_o + 90.4}{2.65\,(62.4)} \tag{15}$$

$$\phi = 1 - (.032\, D_{50} + .025\, S_o + .55) \tag{16}$$

The equation is plotted in figure B4 and shows a trend similar to the expression developed in equation 13.

In 1943 Krumbien and Monk recognized the potential for correlating permeability with average grain size and degree of sorting. They used

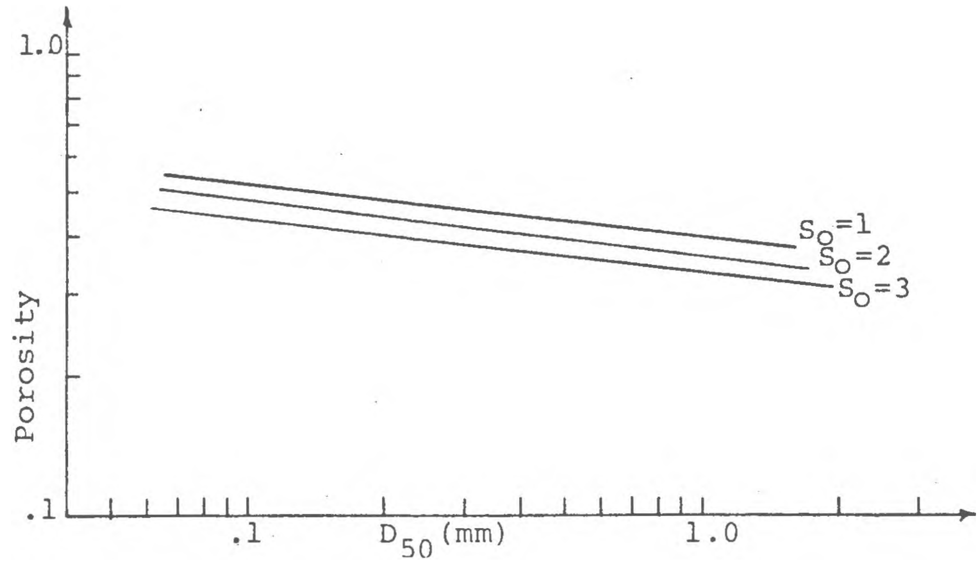

Figure B3. Porosity (ϕ) vs. median grain diameter (D_{50}) and sorting coefficient (S_o), where $\phi = .4\ D_{50}^{-.115} S_o^{-.119}$ as modified from Urish, 1978.

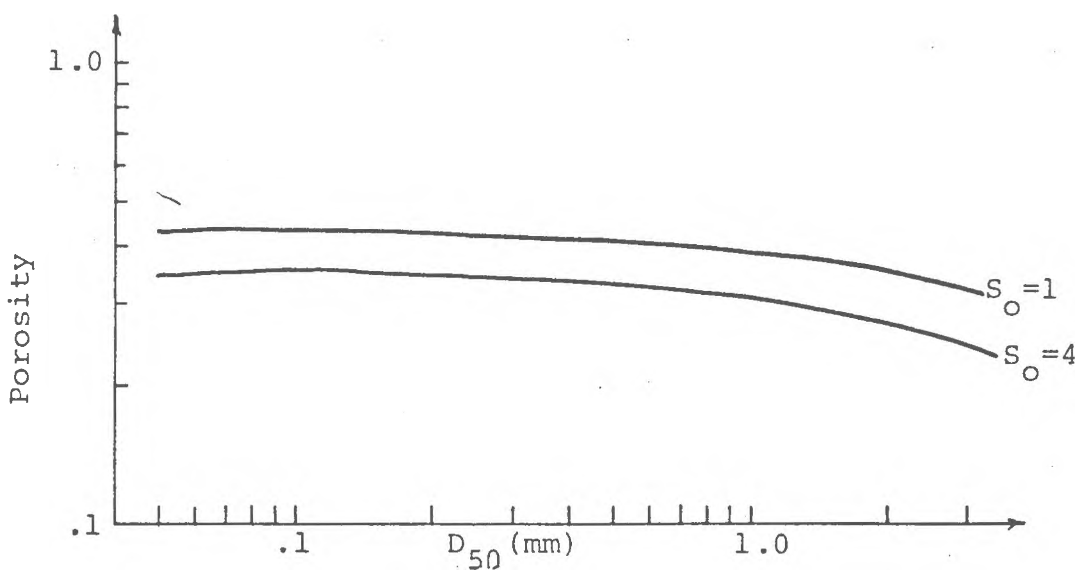

Figure B4. Porosity (ϕ) vs. median grain diameter (D_{50}) and sorting coefficient (S_o), where $\phi = -.032\ D_{50} - .025 S_o + .45$ as developed by Kelly, 1980.

the geometric mean diameter as the average grain size and the phi standard deviation as a sorting indicator. Only these sizing parameters were varied, with other factors such as packing and shape kept as constant as possible during their experiments. Porosities were kept at 40% and the temperature was 68°F. Furthermore, each sizing distribution of glacial outwash (Wisconsin age) was represented as a straight line on phi probability paper and is therefore a log normal distribution by weight. The laboratory tests best fit the following expression;

$$k = 760\, D_G^2\, e^{-1.31\sigma_\phi} \text{ darcies} \qquad (17)$$

where σ_ϕ = phi standard deviation

D_G = geometric mean diameter

When the phi standard deviation (σ_ϕ) was converted to sorting coefficient (S_o) and the average grain size (D_{50}) is used interchangeably with the geometric mean diameter (D_G), the expression becomes

$$k = .731\, D_{50}^2\, e^{-1.31\left(\frac{S_o - 1}{1.67}\right)^{.8}} \text{ cm/sec} \qquad (18)$$

Equation 18 is plotted in figure B5.

A similar experiment was carried out by Masch and Denny (1966). They used washed Colorado River sand and sythesized samples for various values of average grain size (D_{50}) and inclusive standard deviation. Temperatures were constant at 60° F but they do not specify porosities as constant. Distributions were linear plots on semilogarithmic probability paper, where grain sizes were in phi units and cumulative percent courser values were evenly spaced. Their distributions were close to log normal but lacked the characteristic tails when plotted on a frequency diagram.

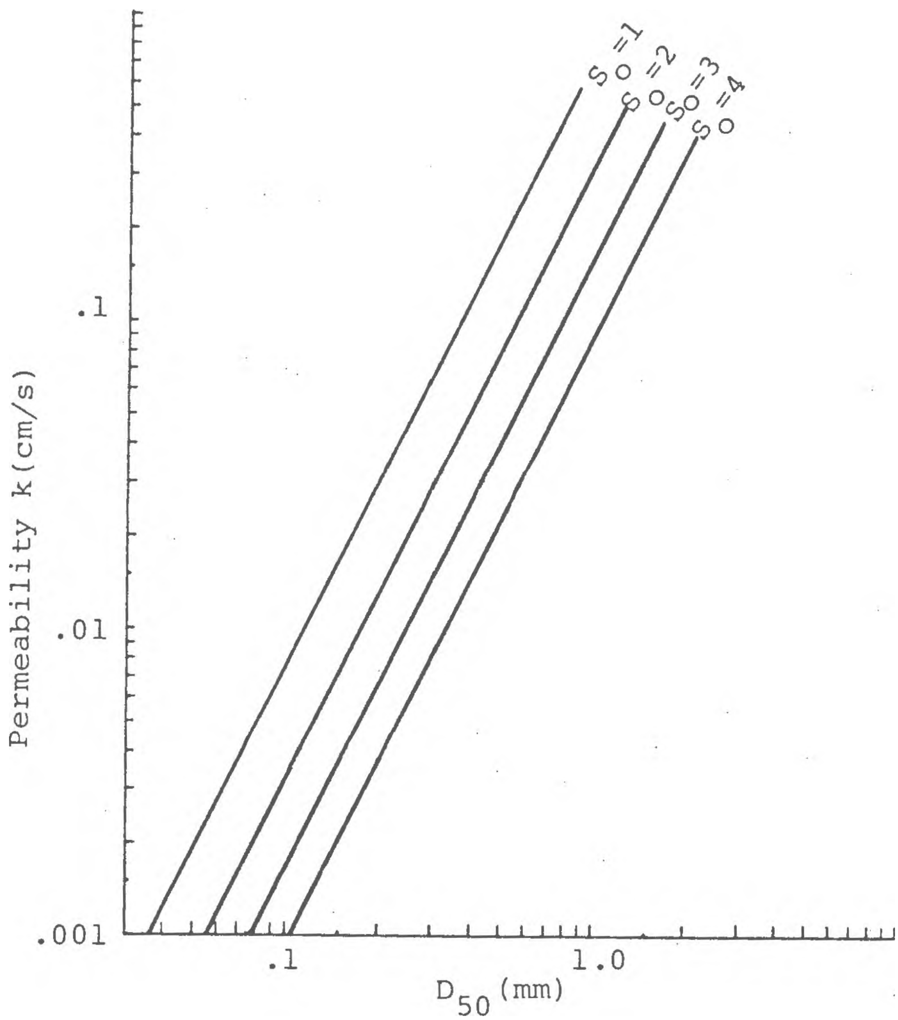

Figure B5. Permeability vs. D_{50} and S_o, where

$$k = .731 D_{50}^2 e^{-1.31 \frac{S_o - 1}{1.67}}$$

as modified from Krumbien & Monk, 1943.

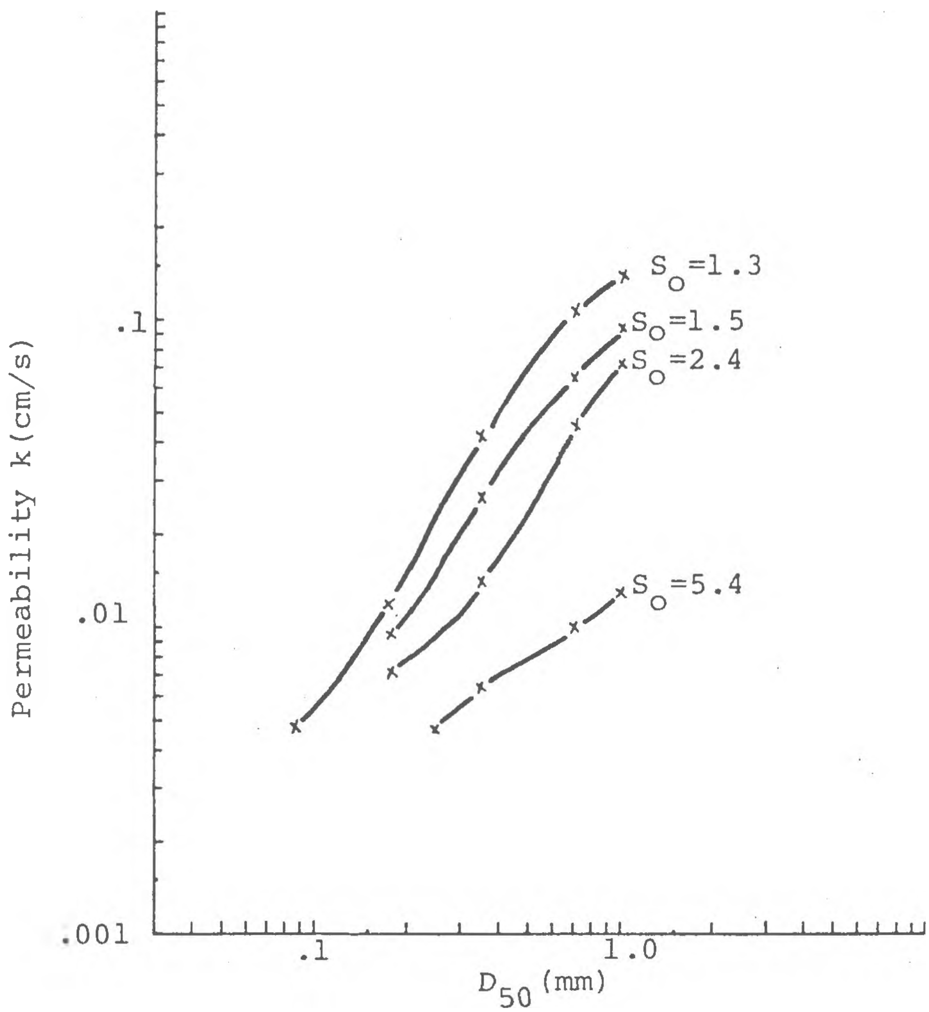

Figure B6. Permeability vs. D_{50} and and S_o from Masch and Denny, 1966

The results are plotted in figure B6, which demonstrates the added influence on permeability of high S_o values (greater than 3) as grain size increases.

Differences between the results of Krumbien and Monk (figure B10) and those of Masch and Denny (figure B11) may be due in part to variable porosities since Masch and Denny do not explicitly state their porosities. The porosities may be important because of their ability to indicate packing. The assumption of D_{50} being an indicator of packing may be poor. Both plots do however, show similar trends (i.e., increases in k with increasing D_{50} and constant S_o --- decreases in k with increasing S_o and constant D_{50}). A set of curves more characteristic of a particular region may be obtained by sample testing. Such a relationship should still follow the general trends exhibited by these researchers, with deviations due to different depositional features (alluvial, ice contact, glacial outwash, etc.).

Regression analysis of permeability (k), average grain size (D_{50}) and sorting coefficient (S_o) from 38 samples of the Pawcatuck River Basin in Rhode Island (Allen et al.) gave the relationships shown in the following equations.

$$k = .13\, D_{50}^{1.54}\, S_o^{-2.53} \qquad \text{m.c.} = .71 \qquad (19)$$

$$k = .17\, D_{50}^{1.51}\, e^{-1.01 S_o} \qquad \text{m.c.} = .72 \qquad (20)$$

$$k = .19\, D_{50}^{3.3/S_o}\, S_o^{-2.74} \qquad \text{m.c.} = .66 \qquad (21)$$

$$k = .22\, D_{50}^{3.2/S_o}\, e^{-1.04 S_o} \qquad \text{m.c.} = .65 \qquad (22)$$

Multiple correlation coefficients (m.c.) are indicated and graphs of these expressions are shown in figures B7 thru B10. Equations 19 and 20

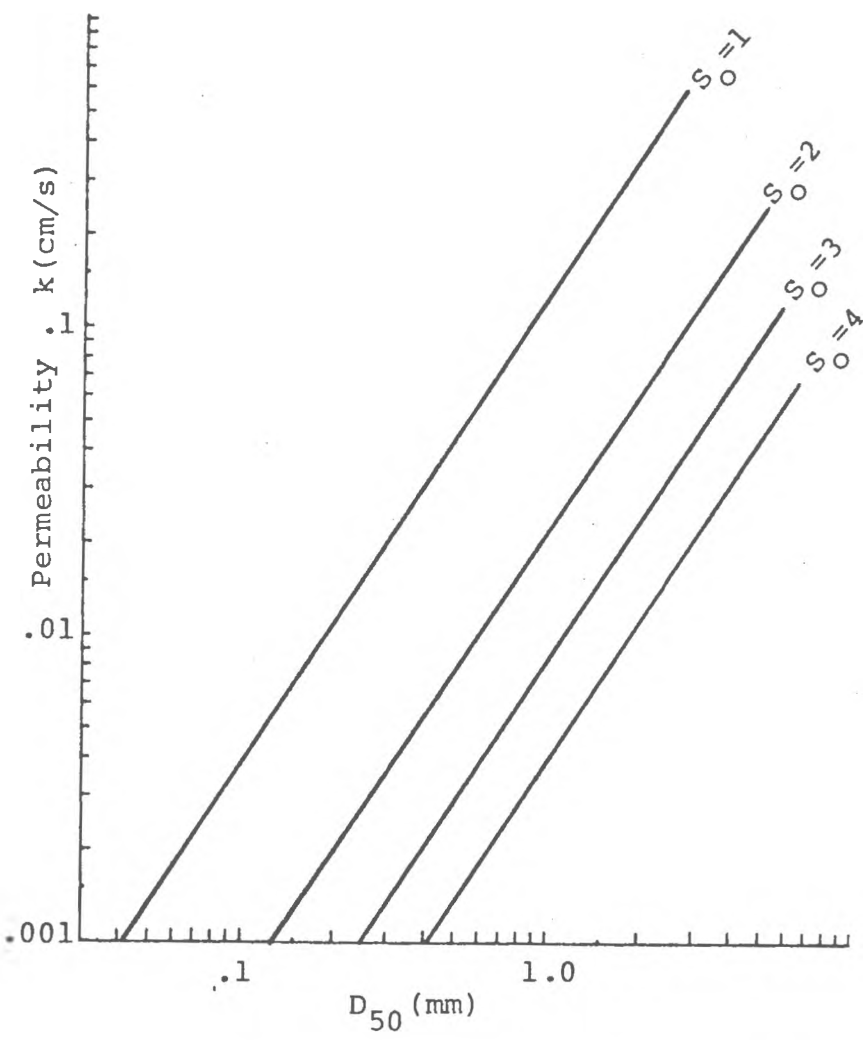

Figure B7. Permeability vs. D_{50} and S_o from Regression Equation

$k = .13D_{50}^{1.5}S_o^{-2.53}$ as fit

to the Allen et al. data

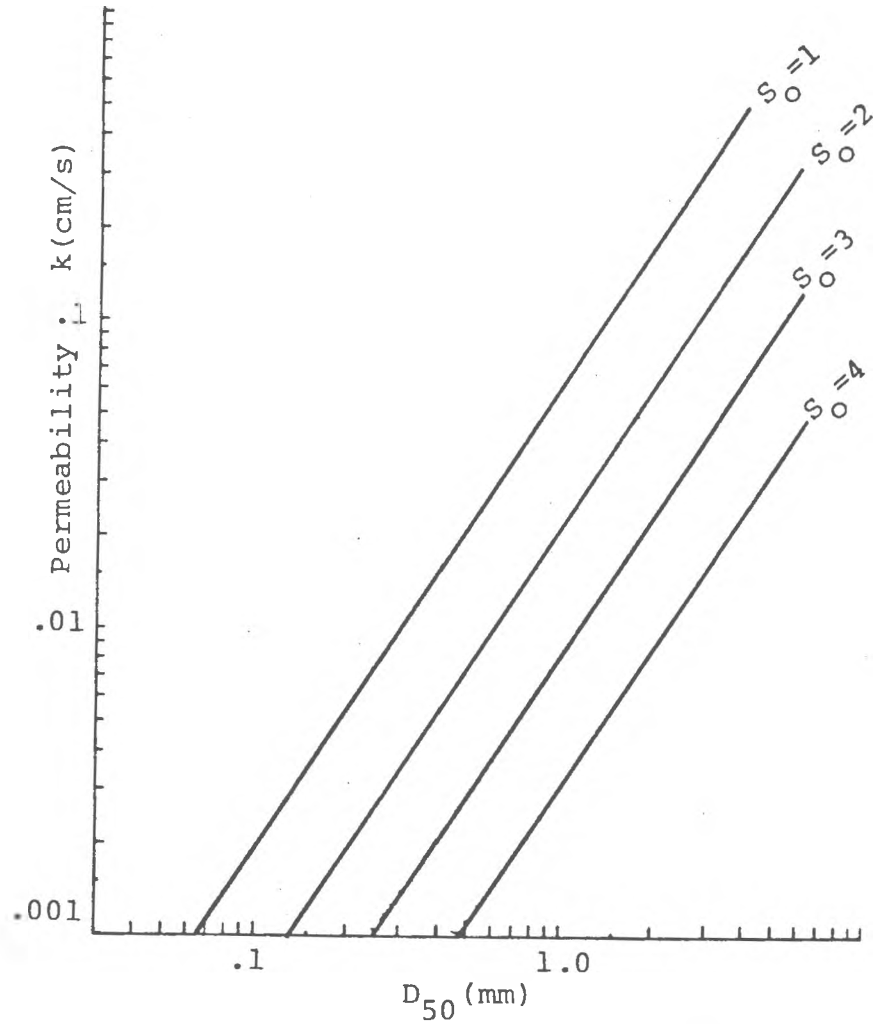

Figure B8. Permeability vs. D_{50} and S_o from Regression Equation $k = .17D_{50}^{1.5}\, e^{-1.01S_o}$ as

fit to the Allen et al. data

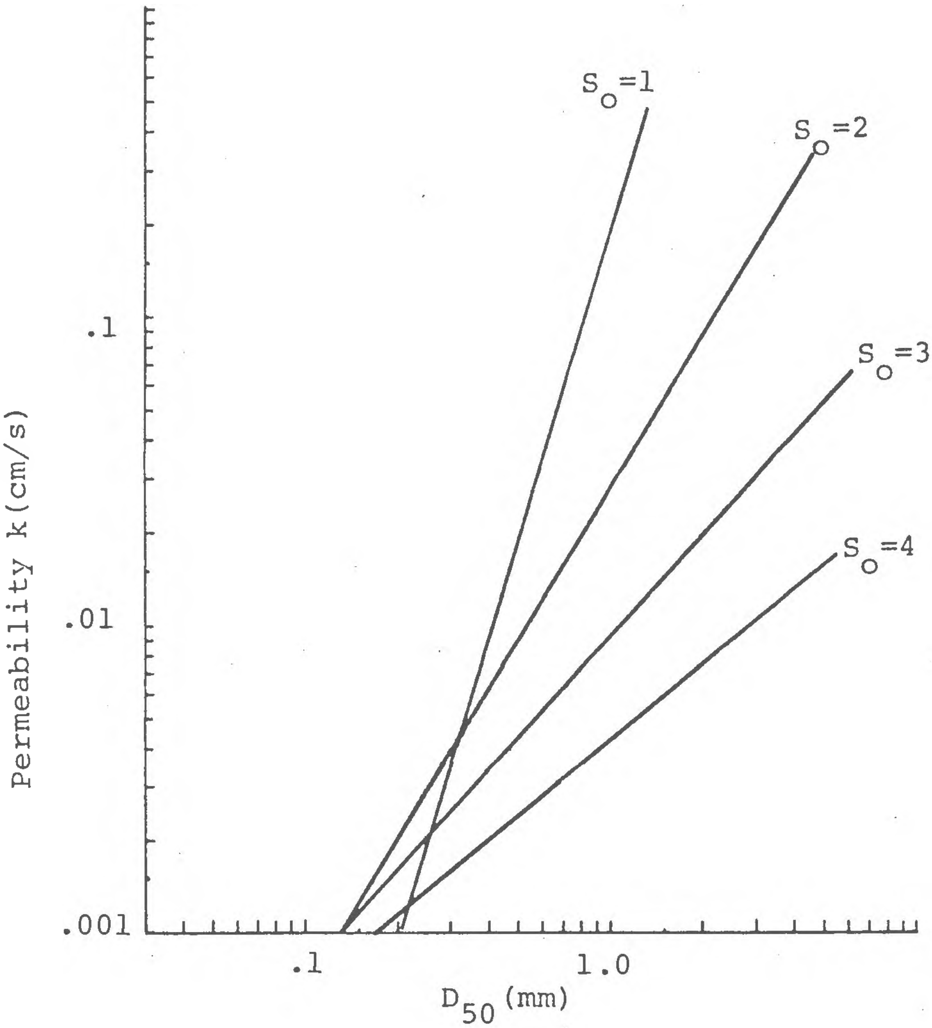

Figure B9. Permeability vs. D_{50} and S_o from Regression Equation

$k = .19D_{50}^{3.3/S_o} S_o^{-2.74}$ as fit to the Allen et al. data

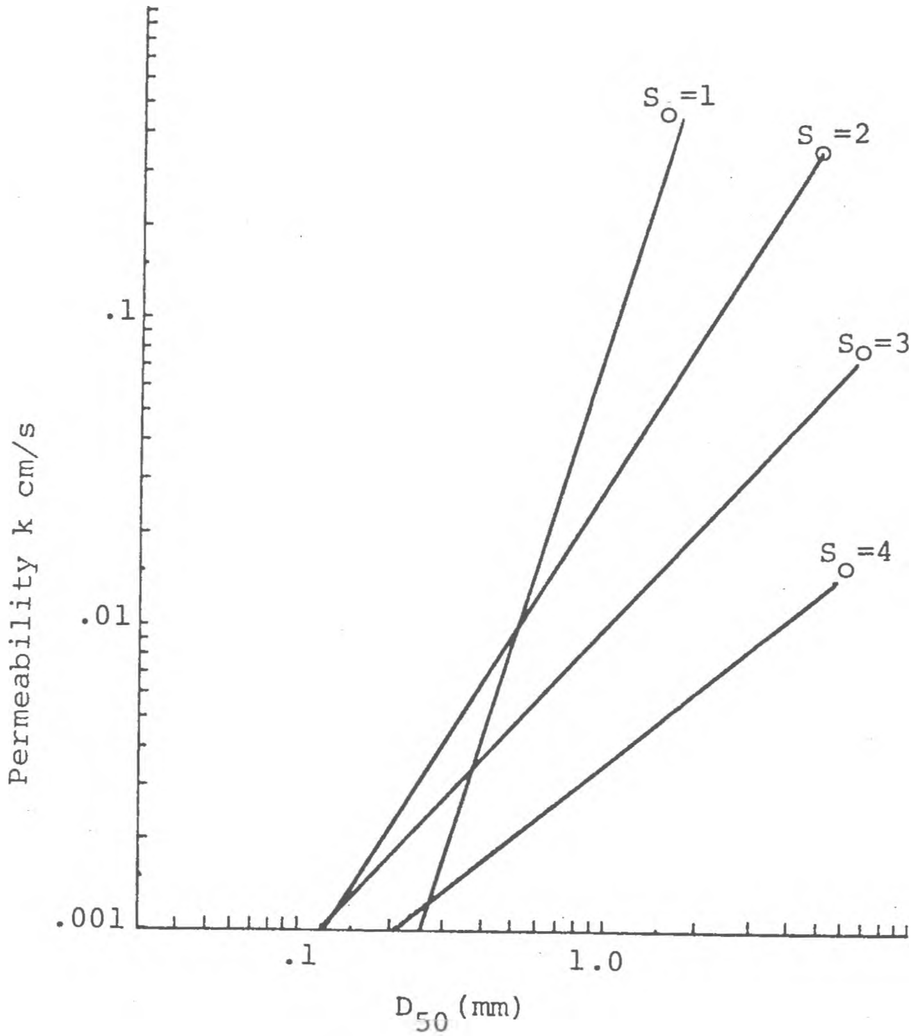

Figure B10. Permeability vs. D_{50} and S_o from Regression Equation $k = .22 D_{50}^{3.18/S_o} e^{-1.04 S_o}$ as fit to the Allen et al. data are similar to the expression developed by Krumbien and Monk in the sense that parallel lines result; however, for a given D_{50} and S_o the value of k is considerably less than the value from the Krumbien and Monk plot. Equations 21 and 22 are similar to the trend appearing in the Masch and Denny plot; decreasing slope of the k vs. D_{50} line as S_o increases. Here again, the permeability values obtained from equations 9 and 10 are lower than those from the Masch and Denny plot in the range of average grain size from .2 to 1.0.

The differences between the plots in figures B7 and B10 and those of Krumbien & Monk, and Masch & Denny may be due to unknown varying porosities in the Allen data.

To demonstrate the probable ϕ versus k trend in southern Rhode Island, it is first necessary to relate D_{50} to S_o. This relation can then be substituted into equations 16 and 19 and k's and ϕ's computed as a function of the same properties (either D_{50} or S_o). When D_{50} and S_o data obtained from 96 tests at 4 ice contact deposits in southern Rhode Island was regressed, the correlation coefficient was .533 and the equation was

$$S_o = 1.12\ D_{50}^{\ .41} + 1 \qquad (23)$$

Pairs of D_{50} and S_o satisfying equation 23 are plotted on the graph of figure B11. A line through these points shows how permeability (k) varies with average grain size (D_{50}). The direct relationship is apparent. When the relationship between S_o and D_{50} is incorporated into equation 16, the predicted trend of in-situ porosity (ϕ) with D_{50} is shown in figure B12. Since the direct D_{50} : S_o relationship yields a direct D_{50} : k relationship (figure B11) and an inverse D_{50} : ϕ (figure B12), the sample to sample ϕ :k relationship for southern Rhode Island

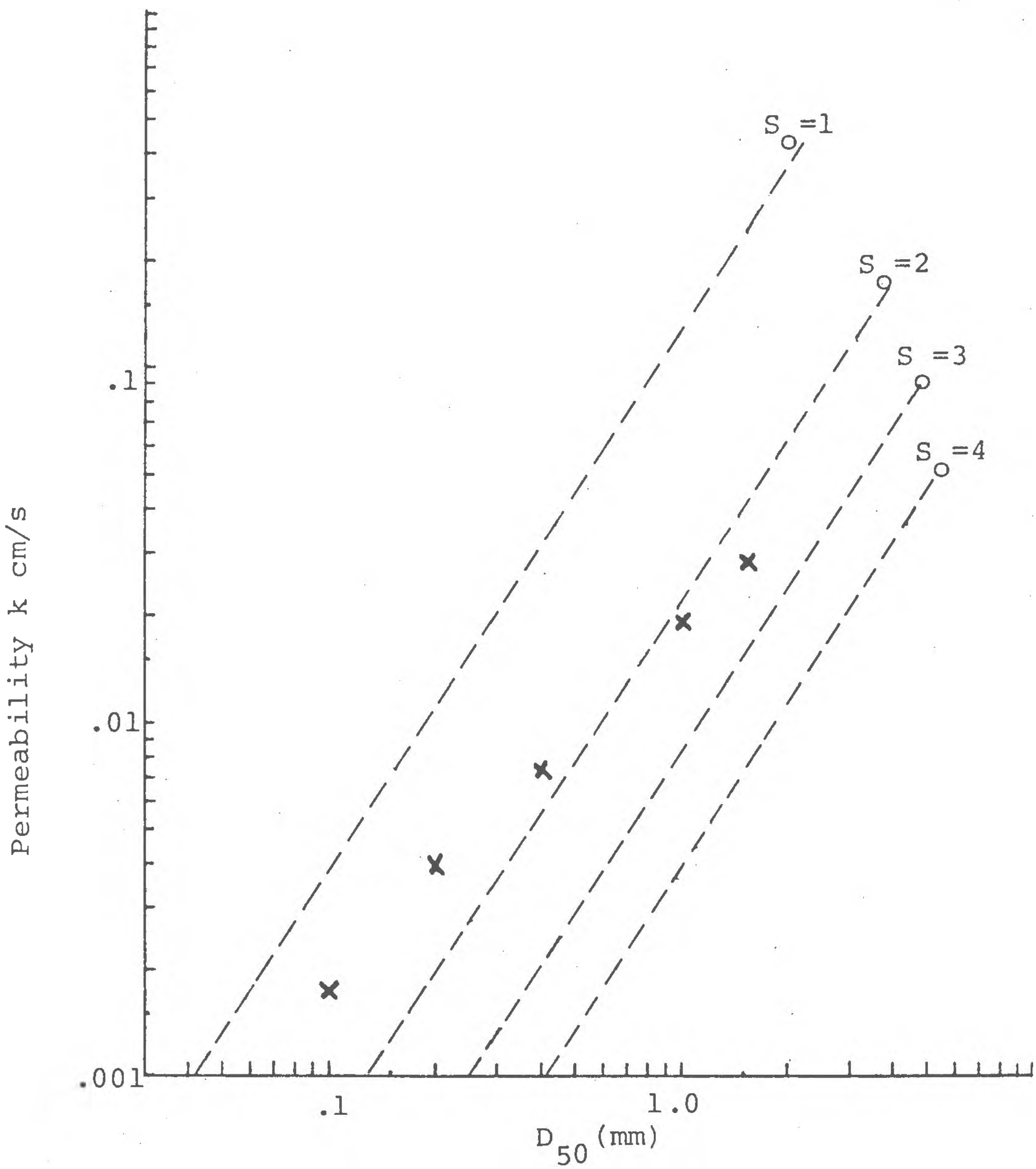

Figure B11. Permeability vs. D_{50} Trend in Southern Rhode Island (points), with Dashed Lines Representing the Regression Equation of Figure B7

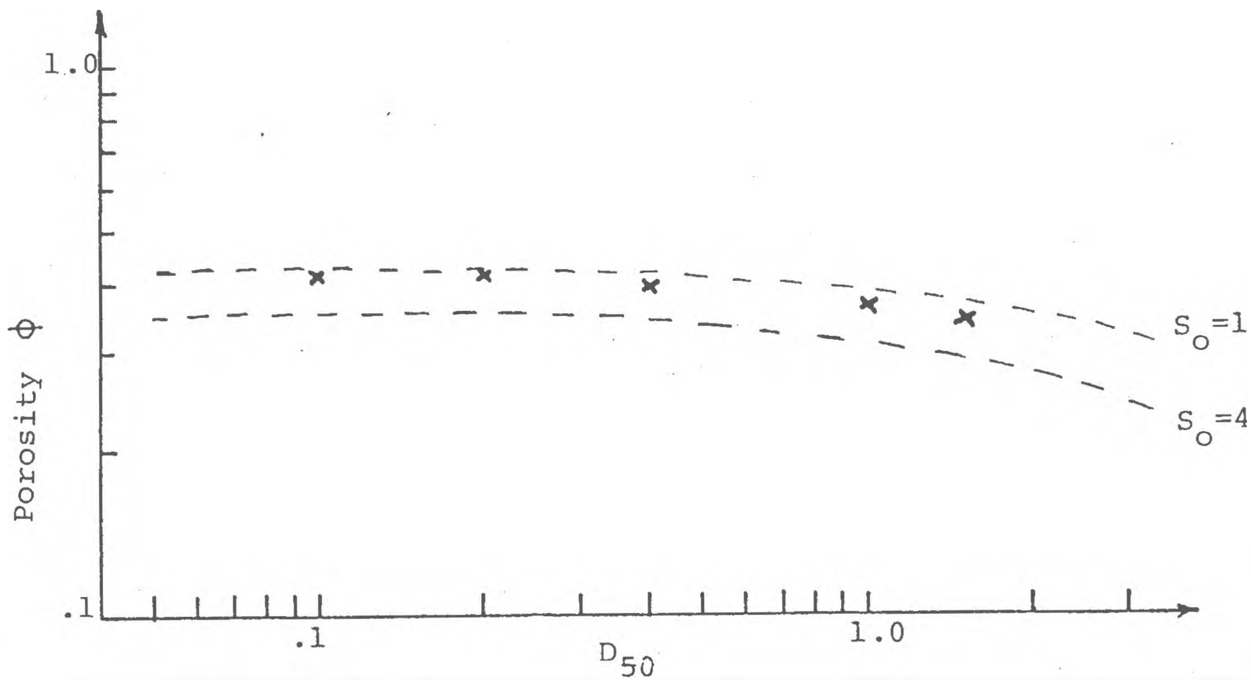

Figure B12. Porosity vs. D_{50} Trend in Southern Rhode Island (points), with Dashed lines Representing the Regression Equation in Figure B4 must be inverse.

This demonstration shows the importance of the D_{50} : S_o trend in determining the ϕ : k trend, with the best correlations occuring in the ϕ: k when good correlations exist between k : D_{50} , S_o ; ϕ: D_{50}, S_o and D_{50} : S_o.

Appendix C

Previous Work: Field Scale

There are numerous reports showing the use of electrical resistivity in hydrogeologic investigations, but only a few have attempted to relate these measurements to the hydraulic properties of aquifers. Ungemach (1969) demonstrated a direct relationship between transmissivity (T) and transverse resistance (T_a) using 6 data points, with transmissivities obtained from pump test data and resistances taken from sounding curves obtained using the Schlumberger sounding technique. Field data collected at three sites in southern Rhode Island by Kelly (1977), Kosinski (1978) and Urish (1978) is best summarized in the dissertation by Urish (1978). Electrical and hydraulic properties were obtained in the same manner as the Ungemach data. Water resistivities measured at 25 C were converted to actual in-situ temperatures.

Plots of F_a vs. k and T_a vs. T for the Rhode Island data are shown in figures C1 and C2 respectively. Regression lines are shown for all 19 points as well as the 13 (Chipuxet and Beaver sites) which were considered better defined by field test results and appeared to conform more closely to theory. Correlation coefficient values were .629 for all values and .800 for the Chipuxet and Beaver sites in figure C1 (F_a vs. k). The best correlation coefficient for the T_a vs. T plot (figure C2) was .488, using only the Chipuxet and Beaver sites.

A field study in central Illinois by Heigold et al. (1979) shows an inverse relationship between field measured values of apparent resistivity ( ) and permeability (k). This relationship was developed with only

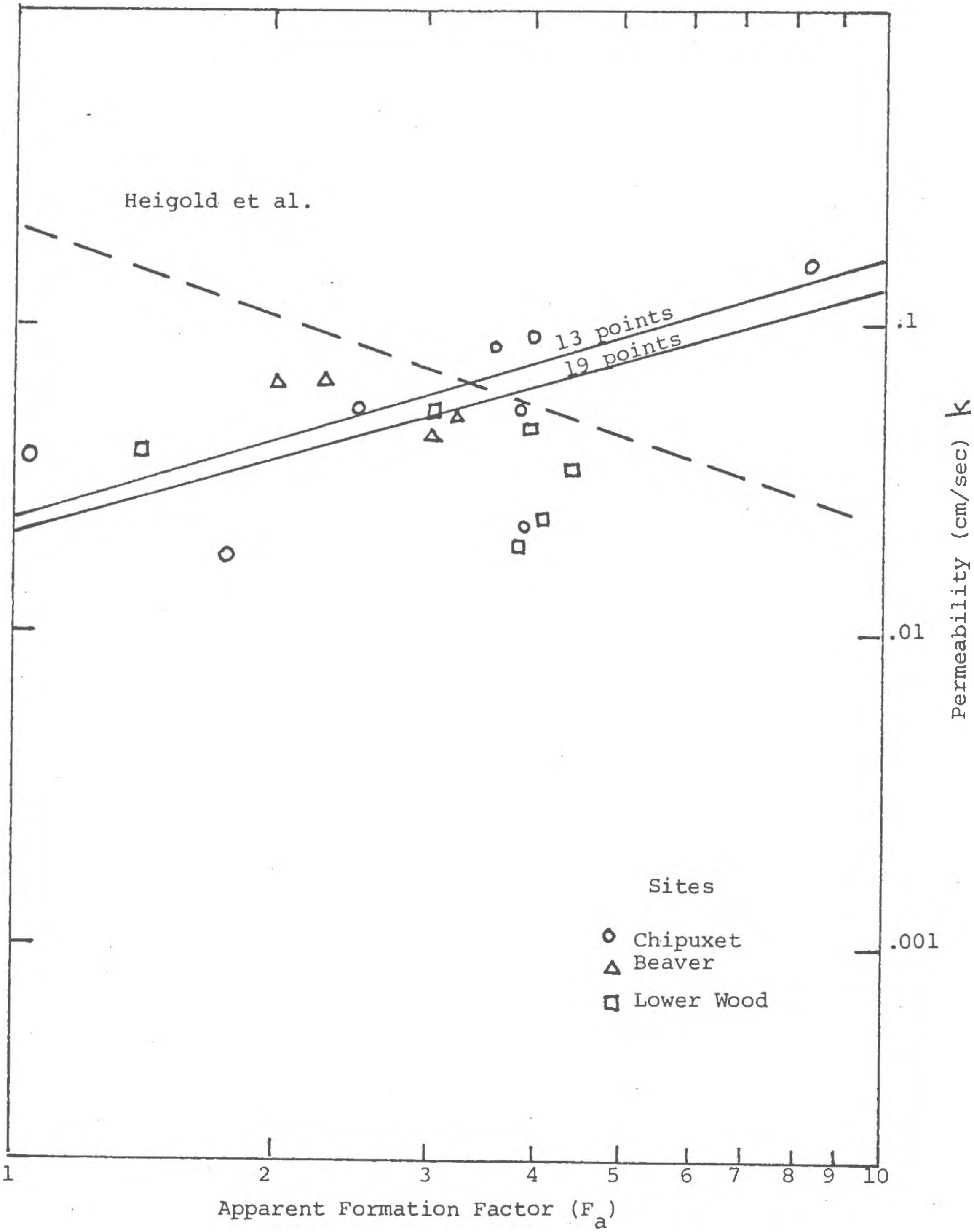

Figure C1. Field Data of Apparent Formation Factor (F_a) vs. Permeability (k) (from Urish, 1978)

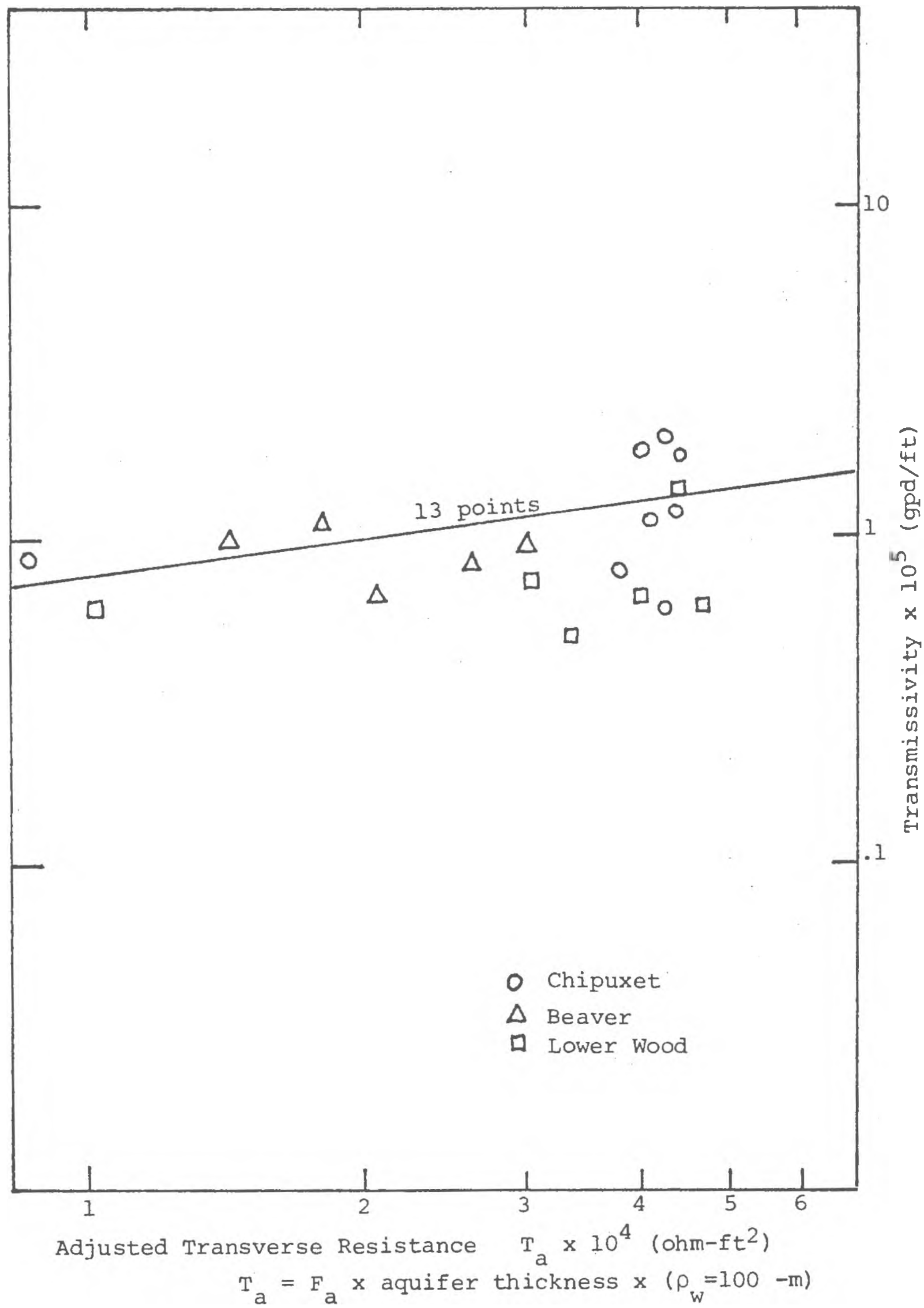

Figure C2. Field Data of Adjusted Transverse Resistance (T_a) vs. Transmisivity (T) (from Urish, 1978) data points for pump test permeabilities and apparent formation factors were obtained from the Wenner electrode configuration. Bore hole samples showed the clay fraction was less than 4%. The regression they obtained was

$$k = 386.4\ \rho_a^{-.933} \qquad (24)$$

and since $F_a = \rho_a / \rho_w$

$$k = .213\ F_a^{-.933} \qquad (25)$$

when the mean value of water resistivity ($\rho_w = 1818\ \Omega\text{-cm}$) is incorporated. Equation 25 is plotted on figure C1.

Only one researcher has done theoretical work with field scale correlations between hydraulic and electrical transmitting properties. Urish (1978) investigated the effect of layering by considering the calculation of "aquifer permeability" and "aquifer resistivity" for layered aquifer models. He assumed in-situ permeabilities of sands (constant within each layer) and then determined the layer resistivities from the "probably average" curve of figure A3, with pore water resistivity equal to 100 Ω-m. When both the layering and the flow were horizontal, the aquifer permeability (k_{hh}) and the aquifer resistivity (ρ_{hh}) were calculated by the following equations:

$$k_{hh} = \frac{\sum_{i=1}^{n} h_i k_i}{\sum_{i=1}^{n} h_i} \qquad \text{(Perloff \& Baron, 1976)} \qquad (26)$$

$$\rho_{hh} = \frac{\sum_{i=1}^{n} h_i}{\sum_{i=1}^{n} h_i / \rho_i} \qquad \text{(Zohdy et al., 1974)} \qquad (27)$$

where

k_{xy} = aquifer permeability with

$\begin{bmatrix} x = h = \text{horizontal} \\ x = v = \text{vertical} \end{bmatrix}$ flow and

$\begin{bmatrix} y = h = \text{horizontal} \\ y = v = \text{vertical} \end{bmatrix}$ layering

ρ_{xy} = aquifer resistivity (x and y same as in k_{xy})

k_i = permeability in layer i

ρ_i = resistivity in layer i

h_i = thickness in layer i

The results showed a significant difference between the predicted horizontal permeability (based on the theoretical homogeneous material) and the calculated horizontal permeability, thus indicating the influence of the averaging process. When aquifer resistivity vs. aquifer permeability was plotted, the approximate regression line was shown to be flatter than the slope of the "probable average curve", which represents an isotropic aquifer of constant permeability. Since only four models were tested and only horizontal layered models were considered, these results may not adequately define the general field case, where layering may be vertical or spacially mixed.

Differences between laboratory and field results based on empirical studies are undoubtedly influenced by measurement errors, inaccurate aquifer porewater resistivities, inaccurate estimates of thicknesses due to poorly defined lower boundaries or lower boundaries effectively different for electrical and hydrological purposes, and field scale averaging of permeabilities and resistivities.

Appendix D

Numerical Modeling of Resistivity

The state-of-the-art of digital resistivity modeling is not as well developed as its hydraulic counterpart. Aiken et al. (1973) developed a finite difference algorithm for two-dimensional problems, which must be sent up with square grids. They note that the model developed by Jepsen (1969) was only a special case of theirs. Mufti (1976) shows that finite difference modeling is a very powerful tool capable of yielding accurate results for a variety of two dimensional geologic structures. He uses the simple arithmetic mean for the connection conductivity values, contrary to the practice of using the harmonic mean in hydraulic models.

Consider

$$k_{hv} = \frac{\sum_{i=1}^{n} h_i}{\sum_{i=1}^{n} \frac{h_i}{k_i}} \qquad \text{Perloff \& Baron (1976)} \qquad (28)$$

$$\sigma_{hv} = \frac{\sum_{i=1}^{n} h_i}{\sum_{i=1}^{n} \frac{h_i}{\sigma_i}} \qquad \text{Zohdy et al. (1974)} \qquad (29)$$

where k_{hv} is the aquifer permeability when horizontal flow and vertical layering occur, and σ_{hv} is the aquifer conductivity with the same flow and layering conditions. The connection value between adjacent nodes in the hydraulic model is the two layer case of equation 28, therefore equation 29 should be used as the connection value of conductivity, since the hydraulic and electrical cases are completely analagous potential problems.

Appendix E

Log - Normal Permeability Distribution

There is general agreement that field permeabilities follow a log normal distribution. The first to propose this distribution was Law (1944), who analyzed cores from a carbonate oil reservoir. Examination of frequency plots for permeabilities in oil sands by Musket (1946) demonstrates the log normal trend. These findings were further supported by Warren et al. (1961), who showed permeabilities from build up tests in oil reservoirs yield log normal distributions. Willardson and Hurst (1965) found log normal distribution for soils from Australia and California; and McMillan (1966) presented additional evidence that permeabilities and transmissivities are log normally distributed.

Freeze (1975) cites indirect evidence supporting a log normal frequency distribution for permeability. Log normal distributions of specific capacity, which is related to transmissivity; normal distributions for porosity, which when used in an exponential function correlates well with permeability; and the fact that the geometric mean provides the best estimate of aquifer permeability in spacially mixed (permeability) media, all support a log normal permeability distribution.

Appendix F

Potential Flow Theory: Cartesian Coordinates

The partial differential equation governing 2-D steady flow through porous media in cartesian coordinates is derived and discretized for numerical modeling in the following procedure.

Figure F1 represents a typical 2-D node in cartesian coordinates, where h_o is the total hydraulic head at the node center and A, B, C and D represent surfaces on the node boundaries. By continuity, the flow into the node (Q_{in}) must equal the outflow (Q_{out}).

$$Q_{in} + Q_{out} = 0$$

since $Q = k\ i\ A$ (Darcy's Law) (30)

where k = permeability

i = total hydraulic head gradient

A = cross sectional area

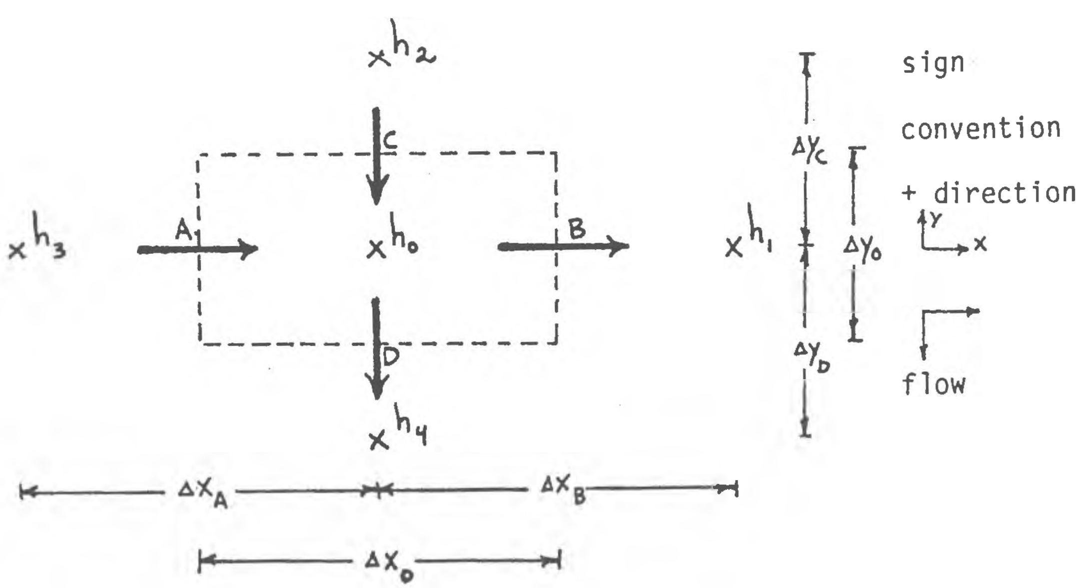

Figure F1

Figure F1. 2-D Node in Cartesian Coordinates let Q_A = flow across surface A

Q_B = flow across surface B

etc.

then $Q_A - Q_B + Q_C - Q_D = 0$ (31)

substituting Darcy's law at each node boundary surface, equation 31 becomes

$$k_A i_A A_A - k_B i_B A_B + k_C i_C A_C - k_D i_D A_D = 0 \quad (32)$$

since for the general case,

k_S = connection value of permeability at S

= a weighted harmonic mean of the nodal permeabilities on each side of S (see Trescott, 1975)

e.g.

$$k_A = \frac{\Delta x_3 + \Delta x_0}{\frac{\Delta x_3}{k_3} + \frac{\Delta x_0}{k_0}} \quad \text{in the x-direction} \quad (33)$$

$$k_C = \frac{\Delta y_2 + \Delta y_0}{\frac{\Delta y_2}{k_2} + \frac{\Delta y_0}{k_0}} \quad \text{in the y-direction} \quad (34)$$

$$i = \frac{\text{change in head across surface S in the direction orthogonal to S}}{\text{length between head values}}$$

A = cross sectional area of S

numerical approximations become

$$k_A i_A A_A = k_A \frac{h_3 - h_0}{\Delta x_A} \Delta y_0$$

$$k_B i_B A_B = k_B \frac{h_0 - h_1}{\Delta x_B} \Delta y_0$$

$$k_C i_C A_C = k_C \left(\frac{h_2 - h_0}{\Delta y_C}\right) \Delta x_0$$

$$k_D i_D A_D = k_D \left(\frac{h_0 - h_4}{\Delta y_D}\right) \Delta x_0$$

substituting into 32 yields

$$k_A\left(\frac{h_3 - h_0}{\Delta x_A}\right)\Delta y_0 - k_B\left(\frac{h_0 - h_1}{\Delta x_B}\right)\Delta y_0 + k_C\left(\frac{h_2 - h_0}{\Delta y_C}\right)\Delta x_0 - k_D\left(\frac{h_0 - h_4}{\Delta y_D}\right)\Delta x_0 = 0 \quad (35)$$

dividing by $\Delta y_0 \Delta x_0$ and rearranging gives

$$\frac{k_A\left(\frac{h_3 - h_0}{\Delta x_A}\right) - k_B\left(\frac{h_0 - h_1}{\Delta x_B}\right)}{\Delta x_0} + \frac{k_C\left(\frac{h_2 - h_0}{\Delta y_C}\right) - k_D\left(\frac{h_0 - h_4}{\Delta y_D}\right)}{\Delta y_0} = 0 \quad (36)$$

when the following conditions are applied to equation 36

$$h_c = h$$

$$\text{Lim} \left.\begin{array}{l} \Delta x_P \to 0 \\ \Delta y_P \to 0 \\ h_P \to h \end{array}\right\} \text{ for all points or surfaces P}$$

a partial differential equation (PDE) is obtained

$$\frac{\partial\left(k_x \frac{\partial h}{\partial x}\right)}{\partial x} + \frac{\partial\left(k_y \frac{\partial h}{\partial y}\right)}{\partial y} = 0 \quad (37)$$

where k_x = permeability in the x-direction

k_y = permeability in the y-direction

Equation 37 is the PDE governing the steady state flow through porous media, which may be anisotropic and with spacially mixed permeabilities.

To derive the discretized basic equation, expression 35 is solved for

h_o giving

$$h_o = \frac{\left(\frac{k_A \Delta y_0}{\Delta x_A}\right) h_3 + \left(\frac{k_B \Delta y_0}{\Delta x_B}\right) h_1 + \left(\frac{k_C \Delta x_0}{\Delta y_C}\right) h_2 + \left(\frac{k_D \Delta x_0}{\Delta y_D}\right) h_4}{\frac{k_A \Delta y_0}{\Delta x_A} + \frac{k_B \Delta y_0}{\Delta x_B} + \frac{k_C \Delta x_0}{\Delta y_C} + \frac{k_D \Delta x_0}{\Delta y_D}}$$

The basic discretized equation becomes

$$h_o = \frac{a h_3 + b h_1 + c h_2 + d h_4}{a + b + c + d} \tag{38}$$

where

$$a = \frac{k_A \Delta y_0}{\Delta x_A}$$

$$b = \frac{k_B \Delta y_0}{\Delta x_B}$$

$$c = \frac{k_C \Delta x_0}{\Delta y_C}$$

$$d = \frac{k_D \Delta x_0}{\Delta y_D}$$

Equation 38 is effective at every node in the cartesian coordinate system.

For the electrical case, the hydraulic head values are replaced by the scalar electrical potential v. The equivalent to Darcy's law is

$$I = \sigma \frac{dv}{dx} A \qquad \text{(Halliday \& Resnick, 1970)} \tag{39}$$

where

I = electrical charge flux (current)

σ = conductivity

$\frac{dv}{dx}$ = electrical potential gradient

A = cross sectional area

Applied to soils, σ becomes the conductivity of the bulk soil (grains, water and air). The PDE may be obtained by using these electrical quantities in place of their analogous hydraulic counterparts of the previous derivation. The PDE is

$$\frac{\partial\left(\sigma_x \frac{\partial v}{\partial x}\right)}{\partial x} + \frac{\partial\left(\sigma_y \frac{\partial v}{\partial y}\right)}{\partial y} = 0 \qquad (40)$$

where σ_x = bulk soil conductivity in the x-direction

σ_y = bulk soil conductivity in the y-direction

The discretized basic equation will be

$$V_0 = \frac{a V_3 + b V_1 + c V_2 + d V_4}{a + b + c + d} \qquad (41)$$

where

$$a = \frac{\sigma_A \Delta y_0}{\Delta x_A}$$

$$b = \frac{\sigma_B \Delta y_0}{\Delta x_B}$$

$$c = \frac{\sigma_C \Delta x_0}{\Delta y_C}$$

$$d = \frac{\sigma_D \Delta x_0}{\Delta y_D}$$

Appendix G

Potential Flow Theory: Radial Coordinates

The partial differential equation for 2-D radial symetric steady flow through porous media in r, z coordinates is derived by physics and discretized for numerical modeling in the following procedure.

Figure G1 represents a typical 2-D model node, where h is the total hydraulic head at the node center and A, B, C and D represent surfaces on the node boundaries. By continuity the flow into the model (Q_{in}) must equal the outflow (Q_{out}).

$$Q_{in} + Q_{out} = 0$$

since Q = k i A Darcy's Law

where k = permeability
i = total hydraulic head gradient
A = cross sectional area

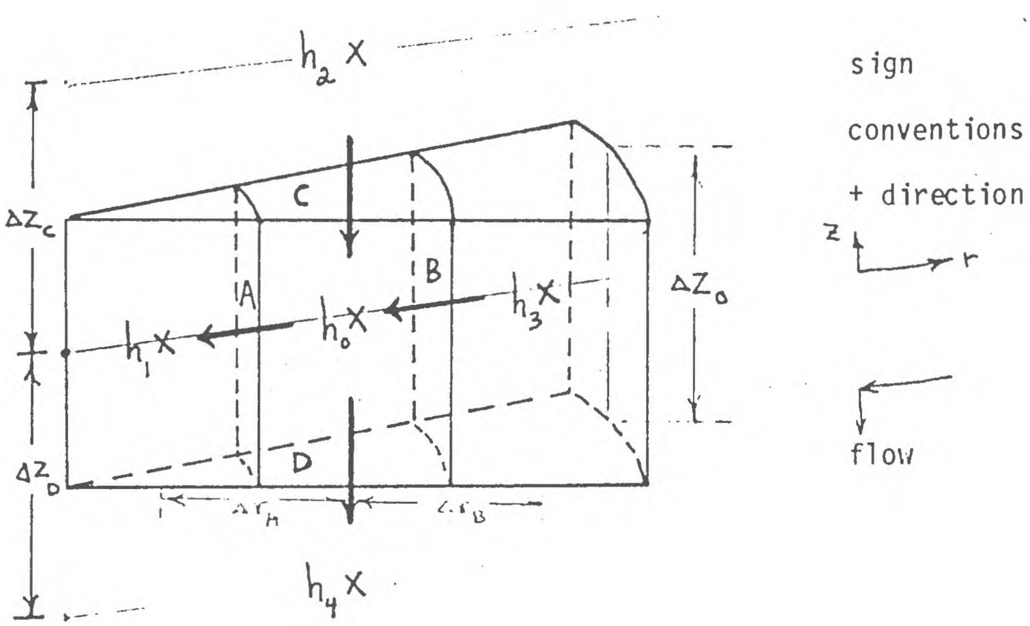

Figure G1. 2-D Node in Radial Coordinates

Let Q_A = flow across surface A

Q_B = flow across surface B

etc.

then $Q_B - Q_A + Q_C - Q_D = 0$ (42)

substituting Darcy's Law at each node boundary surface, equation 42 becomes

$$k_B i_B A_B - k_A i_A A_A + k_c i_c A_c - k_D i_D A_D = 0 \qquad (43)$$

where k_C and k_D are computed as in the cartesian coordiante model of appendix F

k_A and k_B will require special equations which are developed later in this section

Recalling definitions for numerical approximations of gradients (i_s) and cross sectional areas (A_s) in Appendix F, the numerical forms become

$$k_B i_B A_B = k_B \left(\frac{h_3 - h_0}{\Delta r_B}\right) r_B \,\Delta\theta \,\Delta z_0 \qquad (44)$$

$$k_A i_H A_A = k_A \left(\frac{h_0 - h_1}{\Delta r_A}\right) r_B \,\Delta\theta \,\Delta z_0 \qquad (45)$$

$$k_c i_c A_c = k_c \left(\frac{h_2 - h_c}{\Delta z_D}\right)\left[\left(r_0 + \frac{\Delta r_0}{2}\right)^2 - \left(r_0 - \frac{\Delta r_c}{2}\right)^2\right]\frac{\Delta\theta}{2}$$

$$= k_c \left(\frac{h_2 - h_0}{\Delta z_D}\right) r_0 \,\Delta r_0 \,\Delta\theta \qquad (46)$$

$$k_D i_D A_D = k_D \left(\frac{h_0 - h_4}{\Delta z_c}\right) r_c \,\Delta r_c \,\Delta\theta \qquad (47)$$

where, for the general case, r_p = radius to P

with other quantities indicated on figure G1

substituting 44 to 47 into 43 and dividing by $\Delta\theta$ yields

$$k_B\left(\frac{h_3-h_0}{\Delta r_B}\right)r_B\Delta z_0 - k_H\left(\frac{h_0-h_1}{\Delta r_H}\right)r_A\Delta z_0 + k_c\left(\frac{h_2-h_0}{\Delta z_c}\right)r_0\Delta r_0$$

$$-k_D\frac{h_0-h_4}{\Delta z_D}r_0\Delta r_0 = 0 \qquad (48)$$

dividing 48 by $r_0\Delta r_0\Delta z_0$ yields

$$\frac{1}{r_0}\left[\frac{r_B k_B\dfrac{h_3-h_0}{\Delta r_B} - r_A k_H\dfrac{h_0-h_1}{\Delta r_H}}{\Delta r_0}\right]$$

$$+\left[\frac{k_c\left(\dfrac{h_2-h_0}{\Delta z_c}\right) - k_D\left(\dfrac{h_0-h_4}{\Delta z_D}\right)}{\Delta z_0}\right] = 0 \qquad (49)$$

when the following conditions are applied to equation 49

$h_0 = h$

$r_0 = r$

$$\text{Lim}\left.\begin{array}{l} r_p \to r \\ \Delta r_p \to 0 \\ \Delta z_p \to 0 \\ h_p \to h \end{array}\right\} \quad \text{for all points or surfaces } P$$

a partial differential equation (PDE) is obtained

$$\frac{1}{r}\,\frac{\partial\left(r k_r \frac{\partial h}{\partial r}\right)}{\partial r} + \frac{\partial\left(k_z \frac{\partial h}{\partial z}\right)}{\partial z} = 0 \qquad (50)$$

where k_r = permeability in the r-direction

k_z = permeability in the z-direction

Equation 50 is the PDE governing radial symetric steady state flow through porous media, which may be anisotropic and contain spacially mixed permeabilities.

To derive the discretized basic equation, expression 48 is solved for h_0 giving

$$h_0 = \frac{\left(\frac{k_A r_A \Delta z_0}{\Delta r_A}\right)h_1 + \left(\frac{k_B r_B \Delta z_0}{\Delta r_B}\right)h_3 + \left(\frac{k_C r_0 \Delta r_0}{\Delta z_C}\right)h_2 + \left(\frac{k_D r_0 \Delta r_0}{\Delta z_D}\right)h_4}{\frac{k_A r_A \Delta z_0}{\Delta r_A} + \frac{k_B r_B \Delta z_0}{\Delta r_B} + \frac{k_C r_0 \Delta r_0}{\Delta z_C} + \frac{k_D r_0 \Delta r_0}{\Delta z_D}}$$

The basic discretized equation becomes

$$h_0 = \frac{a h_1 + b h_3 + c h_2 + d h_4}{a + b + c + d} \qquad (51)$$

where

$$a = \frac{k_A r_A \Delta z_c}{\Delta r_A}$$

$$b = \frac{k_B r_B \Delta z_c}{\Delta r_B}$$

$$c = \frac{k_c r_0 \Delta r_0}{\Delta z_c}$$

$$d = \frac{k_D r_0 \Delta r_c}{\Delta z_D}$$

For the electrical case, the PDE can be derived by using quantities v and σ (as defined in Appendix F) in place of their analogous hydraulic counterparts h and k of the previous derivation. The PDE becomes

$$\frac{1}{r}\frac{\partial\left(r\,\sigma_r \frac{\partial v}{\partial r}\right)}{\partial r} + \frac{\partial\left(\sigma_z \frac{\partial v}{\partial z}\right)}{\partial z} = 0 \qquad (52)$$

where σ_r = bulk soil conductivity in the r-direction

σ_z = bulk soil conductivity in the z-direction

The discretized basic equation form of the PDE (equation 52) is

$$V_c = \frac{a V_1 + b V_3 + c V_2 + d V_4}{a + b + c + d} \qquad (53)$$

where

$$a = \frac{\sigma_A r_A \Delta z_c}{\Delta r_A}$$

$$b = \frac{\sigma_B r_B \Delta z_c}{\Delta r_B}$$

$$c = \frac{\sigma_c r_c \Delta r_c}{\Delta z_c} \qquad d = \frac{\sigma_D r_0 \Delta r_0}{\Delta z_D}$$

The basic equations 51 or 53 will not apply to the nodes where r = 0, therefore an expression will be derived for this location.

By continuity the flow into the node (Q_{in}) must equal the outflow (Q_{out})

$$Q_{in} + Q_{out} = 0$$

Let Q_B = flow across B

etc.

Equation 42 is rewritten assuming flow vectors across node boundaries shown in Figure G2

$$Q_B + Q_C - Q_D = 0$$

substituting equation 30 (Darcy's Law) for flow across each surface yields

$$k_B i_B A_B + k_C i_C A_C - k_D i_D A_D = 0 \qquad (54)$$

where $$k_B i_B A_B = k_B \frac{h_3 - h_c}{c r_B} r_B \Delta\theta \Delta z_o$$

$$k_C i_C A_C = k_C \frac{h_2 - h_o}{\Delta z_C} \left(\frac{r_B}{2}\right)^2 \frac{\Delta\theta}{2}$$

$$k_D i_D A_D = k_D \frac{h_c - h_4}{\Delta z_D} \left(\frac{r_B}{2}\right)^2 \frac{\Delta\theta}{2}$$

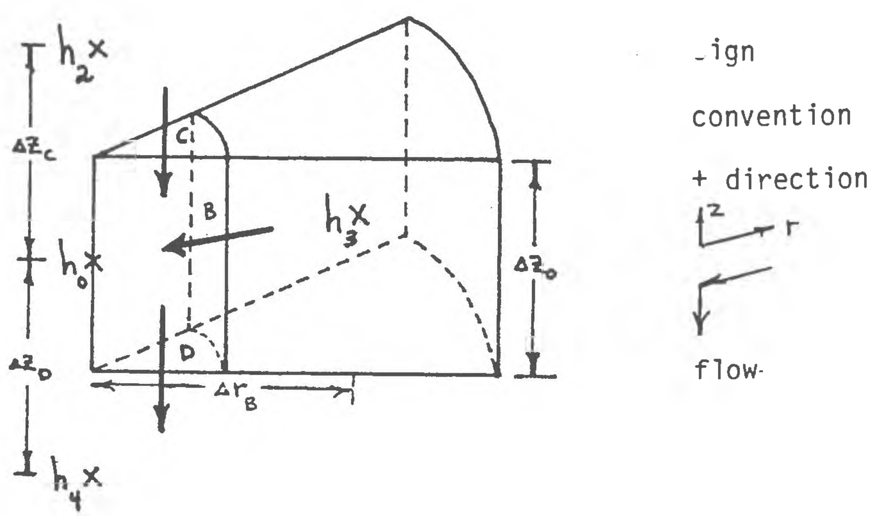

Figure G2. 2-D Node in Radial Coordinates at the Well (r = 0) substituting into 54 and dividing by $\Delta\theta$ yields

$$k_B\left(\frac{h_3-h_0}{\Delta r_B}\right) r_B \Delta z_0 + \frac{k_c}{2}\left(\frac{h_2-h_0}{\Delta z_c}\right)\left(\frac{r_B}{2}\right)^2 - \frac{k_D}{2}\,\frac{h_0-h_4}{\Delta z_D}\left(\frac{r_B}{2}\right)^2 = 0$$

rearranging gives

$$\left(\frac{k_B r_B \Delta z_0}{\Delta r_B}\right) h_3 + \left[\frac{k_c}{2\Delta z_c}\left(\frac{r_B}{2}\right)^2\right] h_2 + \left[\frac{k_D}{2\Delta z_D}\left(\frac{r_B}{2}\right)^2\right] h_4 =$$

$$\left(\frac{k_B r_B \Delta z_0}{\Delta r_B} + \frac{k_c}{2\Delta z_c}\left(\frac{r_B}{2}\right)^2 + \frac{k_D}{2\Delta z_D}\left(\frac{r_B}{2}\right)^2\right) h_0$$

The basic equation becomes

$$h_0 = \frac{b h_3 + c h_2 + d h_4}{b+c+d} \qquad (55)$$

where

$$b = \frac{k_B r_B \Delta t_0}{\Delta r_B} \qquad c = \frac{k_c}{2\Delta t_c}\left(\frac{r_B}{2}\right)^2 \qquad d = \frac{k_D}{2\Delta z_D}\left(\frac{r_B}{2}\right)^2$$

Equation 55 is the correct form to be applied to nodes at r = 0. This form is also suitable for partially penetrating well problems.

The electrical case of equation 55 would be

$$V_0 = \frac{b V_3 + c V_2 + d V_4}{b+c+d} \qquad (56)$$

where $b = \dfrac{\sigma_B r_B \Delta z_0}{\Delta r_B}$

$c = \dfrac{\sigma_c}{2\Delta z_c}\left(\dfrac{r_B}{2}\right)^2$

$$d = \frac{\sigma_D}{2 \Delta z_D} \left(\frac{r_B}{2}\right)^2$$

In the z-direction, the connection permeabilities for a 2-D radial symetric flow model will be the same as those computed for the cartesian coordiante case in the y-direction. The weighted harmonic mean becomes the connection value.

$$k_c = \frac{\Delta z_1 + \Delta z_2}{\frac{\Delta z_1}{k_1} + \frac{\Delta z_2}{k_2}} \tag{56a}$$

where k_1 and k_2 are nodal permeabilities

Δz_1, and Δz_2 are shown in Figure G3

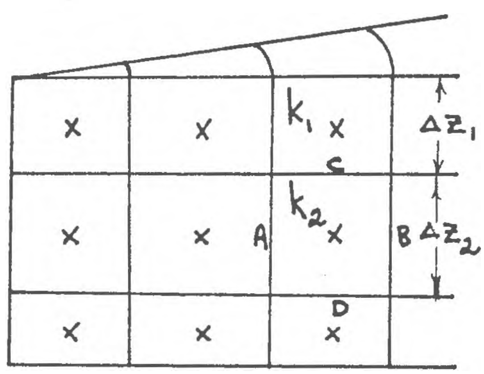

Figure G3. Location of Typical Nodal Permeabilities used to Compute k_c

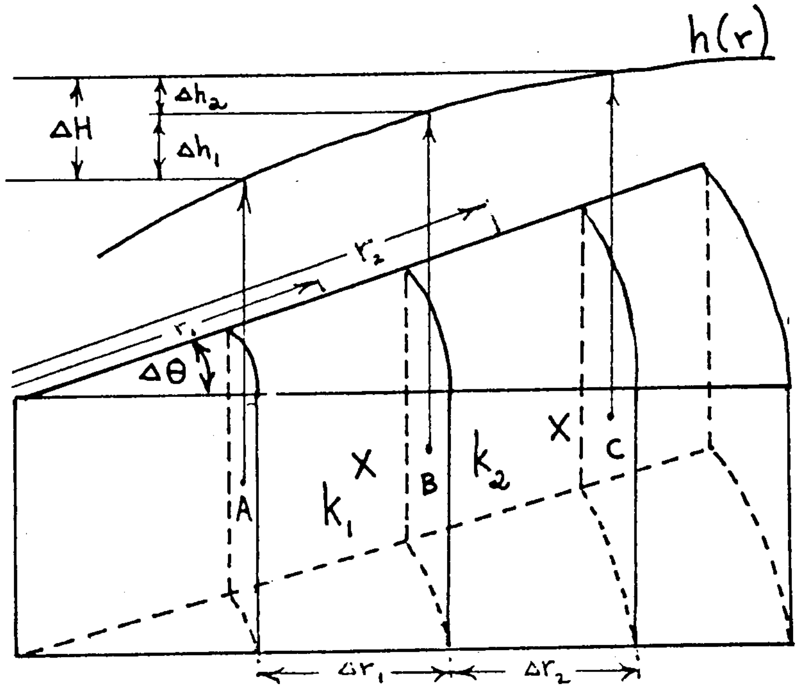

Figure G4. Radial Secion with Total Head Distribution

The connection permeability in the r-direction is computed using potential theory. Figure G4 provides a sketch with labeled quantities. Nodal permeabilities, k_1 and k_2 are shown in Figure G4 where k_1 extends between surfaces A and B, and k_2 extends between B and C. As water moves radially toward the well, the head loss through k_1 is Δh_1, and through k_2, Δh_2. The combined head loss through both nodes is ΔH.

Then

$$\Delta H = \Delta h_1 + \Delta h_2 \tag{57}$$

The flow through the section may be written;

$$Q = k_1 \frac{\Delta h_1}{\Delta r_1} r_1 \Delta\theta = k_2 \frac{\Delta h_2}{\Delta r_2} r_2 \Delta\theta \tag{58}$$

where r_1 = radius to point 1

r_2 = radius to point 2

rearranging 58 gives

$$\Delta h_1 = \frac{Q \Delta r_1}{k_1 r_1 \Delta\theta} \qquad \Delta h_2 = \frac{Q \Delta r_2}{k_2 r_2 \Delta\theta}$$

substituting into 57 yields

$$\Delta H = \frac{Q \Delta r_1}{k_1 r_1 \Delta\theta} + \frac{Q \Delta r_2}{k_2 r_2 \Delta\theta}$$

factoring gives

$$\Delta H = \frac{Q}{\Delta\theta}\left[\frac{\Delta r_1}{k_1 r_1} + \frac{\Delta r_2}{k_2 r_2}\right] \tag{59}$$

since the flow through the cross section may also be computed as

$$Q = k_B \frac{\Delta H}{\Delta R} r_B \Delta\theta \tag{60}$$

where k_B = connection permeability effective at B

r_B = radius to surface B

rearranging 60 gives

$$\Delta H = \frac{Q \Delta R}{k_B r_B \Delta\theta} \tag{61}$$

equating 61 to 59

$$\frac{Q \Delta R}{k_B r_B \Delta\theta} = \frac{Q}{\Delta\theta}\left[\frac{\Delta r_1}{k_1 r_1} + \frac{\Delta r_2}{k_2 r_2}\right]$$

factoring out $\frac{Q}{\Delta\theta}$ and rearranging yields

$$k_B = \frac{\Delta R}{\left[\frac{\Delta r_1}{k_1 r_1} + \frac{\Delta r_2}{k_2 r_2}\right] r_B} \qquad (62)$$

rearranging gives

$$k_B = \frac{\Delta R\, k_1 r_1 k_2 r_2}{(\Delta r_1 k_2 r_2 + \Delta r_2 k_1 r_1) r_B}$$

Connection permeabilities are computed at all nodes in the radial program in the same manner as equation 62.

Appendix H

The IADI Procedure and the Thomas Algorithm

For a steady state 2-D model in the hydraulic or electrical case and for radial or cartesian coordinates, the general form of equations 38, 41, 51, and 53 may be written;

$$(a_{i,j} + b_{i,j} + c_{i,j} + d_{i,j})\,\phi_{i,j} = a_{i,j}\,\phi_{i,j-1} + b_{i,j}\,\phi_{i,j+1} + c_{i,j}\,\phi_{i-1,j} + d_{i,j}\,\phi_{i+1,j} \quad (63)$$

where i = model row

j = model column

$\phi_{i,j}$ = scalar potential at row i and column j

Equation 63 will apply at every node in the model. Thus there are as many equations as there are nodes.

The iterative alternating direction implicit procedure for steady state problems first involves reducing the large set of simultaneous equations to a number of small sets. This is done by taking each row as an individual set of simultaneous equations, with hydraulic heads in adjacent rows held constant. According to Peaceman and Rachford (1955), the set of row equations is then implicit in the direction along the row and explicit in the direction orthogonal to the row. The set of row equations forms a tridiagonal matrix and is solved readily by the Thomas algorithm.

After all sets of row equations have been processed row by row, attention is focused on solving the node equations again using the Thomas algorithm for an individual column while all terms related to adjacent columns are held constant. Finally, after all equations have been solved column by column, an "iteration" is completed. The above process continues until the change in hydraulic head at any point between successive iterations is within a specified error criteria value.

As first applied to the row equations, the basic equation becomes

$$(a_{i,j}+b_{i,j})\phi_{i,j}+(c_{i,j}+d_{i,j})\phi_{i,j}^{n-1}=a_{i,j}\phi_{i,j-1}^{n}+b_{i,j}\phi_{i,j+1}^{n}+c_{i,j}\phi_{i-1,j}^{n-1}+d_{i,j}\phi_{i+1,j}^{n-1} \quad (64)$$

where n = iteration index

It was necessary to separate $\phi_{i,j}$ into $\phi_{i,j}^{n}$ and $\phi_{i,j}^{n-1}$ to utilize the correct spacial derivative terms. That is, for example, the $\frac{\partial(k_x \frac{\partial h}{\partial x})}{\partial x}$ term in equation 37 is computed for the n th iteration and $\frac{\partial(k_y \frac{\partial h}{\partial y})}{\partial y}$ is computed for the n-1 iteration.

To accelerate convergence, iteration parameters are applied to equation 64. The use and computation of iteration parameters is explained by Trescott et al. (1976). Equation 64 becomes

$$(a_{i,j}+b_{i,j}+I_p)\phi_{i,j}^{n}+(c_{i,j}+d_{i,j}-I_p)\phi_{i,j}^{n-1}=a_{i,j}\phi_{i,j-1}^{n}+b_{i,j}\phi_{i,j+1}^{n}+c_{i,j}\phi_{i-1,j}^{n-1}+d_{i,j}\phi_{i+1,j}^{n-1} \quad (65)$$

Since the ϕ's at the n-1 iteration are known in equation 65, the coefficient matrix of the nodal simultaneous equations of each row will be tridiagonal. Solution of this tridiagonal problem will be achieved using the algorithm generally attributed to Thomas. Douglas (1959) showed the scheme to be extremely stable with respect to round off errors.

The form of equation 65 used with the implicit column equations would be

$$(a_{i,j}+b_{i,j}-I_p)\phi_{i,j}^{n-1}+(c_{i,j}+d_{i,j}+I_p)\phi_{i,j}^{n}=a_{i,j}\phi_{i,j-1}^{n-1}+b_{i,j}\phi_{i,j+1}^{n-1}+c_{i,j}\phi_{i-1,j}^{n}+d_{i,j}\phi_{i+1,j}^{n} \quad (66)$$

Sets of simultaneous equations for each column also form tridiagonal coefficient matrices and are solved by the Thomas algorithm.

The steps toward the solution of a 7 X 7 problem will be demonstrated. Figure H1 shows a typical row with impermeable boundaries and the location of factors a, b, c,and d at a typical node. The model will always maintain perimeter nodes with permeabilities of zero. All sources and discharges are located at interior nodes of constant potential.

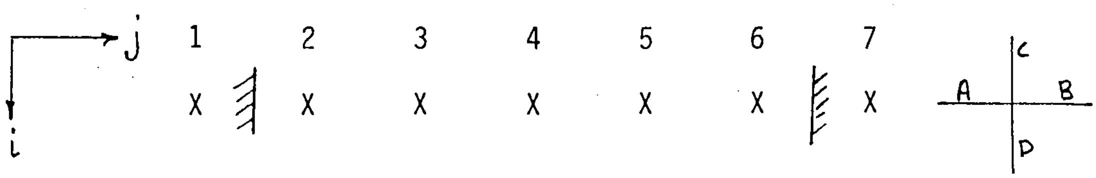

Figure H1, Typical Row with Impermeable Boundaries

Applying equation 65 at column 2,

$$\phi_2^n = \frac{a_2\phi_1^n + b_2\phi_3^n + c_2\phi_{i-1}^{n-1} + d_2\phi_{i+1,2}^{n-1} - (c_2 + d_2 - I_p)\phi_2^{n-1}}{a_2 + b_2 + I_p} \qquad (67)$$

where unlabeled row subscripts imply the i'th row.

Equation 67 can be formlulated into a known part (G) plus a factor (F) multiplied by an unknown potential value.

$$\phi_2 = G_2 + F_2\phi_3^n \qquad (68)$$

where

$$G_2 = \frac{a_2\phi_1^n + c_2\phi_{i-1,2}^{n-1} + d\,\phi_{i+1,2}^{n-1} - (c_2 + d_2 - I_p)\phi_2^{n-1}}{a_2 + b_2 + I_p}$$

$$F_2 = \frac{b_2}{a_2 + b_2 + I_p}$$

let $RKNOWN_j = c_j\phi_{i+1}^{n-1} + d_j\phi_{i+1,j}^{n-1} - (c_j + d_j - I_p)\phi_{i,j}^{n-1}$

$$E_j = a_j + b_j + I_p$$

then $$G_2 = \frac{a_2 \phi_1^n + RKNOWN_2}{E_2}$$

since $$a_2 = 0$$

$$G_2 = \frac{RKNOWN_2}{E_2}$$

$$F_2 = \frac{B_2}{E_2}$$

for column 3

$$\phi_3^n = \frac{a_3 \phi_2^n + b_3 \phi_4^n + c_3 \phi_{i-1,3}^{n-1} + d_3 \phi_{i+1,3}^{n-1} - (c_3 + d_3 - I_P)\phi_3^{n-1}}{a_3 + b_3 + I_P}$$

substituting equation 68 for ϕ_2^n and E_3 for the denominator.

$$\phi_3^n = \frac{a_3\left[G_2 + F_2 \phi_3^n\right] + b_3 \phi_4^n + RKNOWN_3}{E_3}$$

rearranging

$$\phi_3^n = \frac{a_3 G_2 + b_3 \phi_4^n + RKNOWN_3}{E_3 - a_3 F_2}$$

formulating into G and F parts

$$\phi_3^n = G_3 + F_3 \phi_4 \qquad (69)$$

where $$G_3 = \frac{a_3 G_2 + RKNOWN_3}{E_3 - a_3 F_2}$$

$$F_3 = \frac{b_3}{E_3 - a_3 F_2}$$

similarly

$$\phi_4 = G_4 + F_4 \phi_5^n \tag{70}$$

where
$$G_4 = \frac{a_4 G_3 + RKNOWN_4}{E_4 - a_4 F_3}$$

$$F_4 = \frac{b_4}{E_4 - a_4 F_3}$$

$$\phi_5 = G_5 + F_5 \phi_6^n \tag{71}$$

where
$$G_5 = \frac{a_5 G_4 + RKNOWN_5}{E_5 - a_5 F_4}$$

$$F_5 = \frac{b_5}{E_5 - a_5 F_4}$$

$$\phi_6 = G_6 + F_6 \phi_7^n$$

where
$$G_6 = \frac{a_6 G_5 + RKNOWN_6}{E_6 - a_6 F_5}$$

$$F_6 = \frac{b_6}{E_6 - a_6 F_5}$$

since $B_6 = 0.0$, $F_6 = 0.0$

and $\phi_6^n = G_6$

Other potentials in the row are solved by back substituting into equations 71, 70, 69, and 68 respectively.

If constant potentials appear in the row, the algorithm changes. The case of constant potential boundaries is shown in Figure H2.

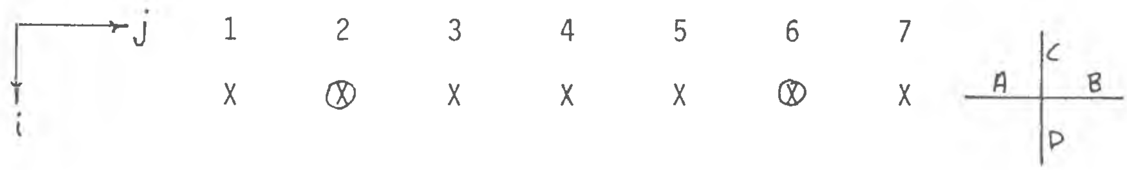

⊗ = constant potential node

Figure H2. Typical Row with Constant Head Boundaries

For this case

$$\phi_2^n = c_2$$

where c_2 = constant

$$\phi_3^n = \frac{a_3 c_2 + b_3 \phi_4^n + RKNOWN_3}{E_3}$$

$$\phi_3^n = G_3 + F_3 \phi_4^n \qquad (72)$$

where

$$G_3 = \frac{a_3 c_2 + RKNOWN_3}{E_3}$$

$$F_3 = \frac{B_3}{E_3}$$

as before

$$\phi_4^n = G_4 + F_4 \phi_5^n \qquad (73)$$

where

$$G_4 = \frac{a_4 G_3 + RKNOWN_4}{E_4 - a_4 F_3}$$

$$F_4 = \frac{b_4}{E_4 - a_4 F_3}$$

and $\qquad \phi_5^n = G_5 + F_5 \phi_6^n$

where $\qquad G_5 = \dfrac{a_5 G_4 + RKNOWN_5}{E_5 - a_5 F_4}$

$$F_5 = \frac{b_5}{E_5 - a_5 F_4}$$

but $\qquad \phi_6^n = c_6$

Back substituting into respective equations 74, 73, and 72 solves for all potentials in the row. This method will apply to constant head nodes located anywhere in the row, providing

$\phi_j^n = c_j$ where c_j = constant

then $\qquad G_{j+1} = \dfrac{a_{j+1}\, c_j + RKNOWN_{j+1}}{E_{j+1}}$

and $\qquad F_{j+1} = \dfrac{b_{j+1}}{E_{j+1}}$

Next, each set of column equations is solved using the Thomos algorithm by applying equation 66 to a column of the 7 X 7 grid, where boundaries are impermeable as shown in Figure H3.

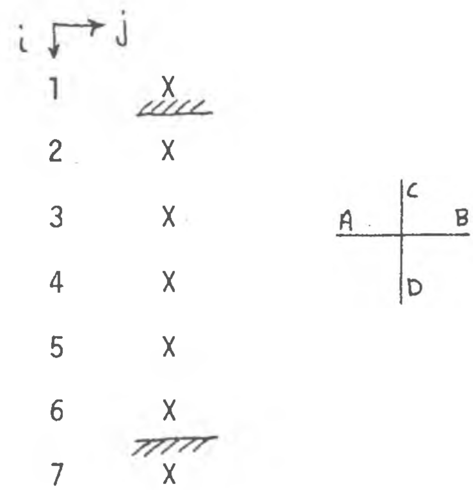

Figure H3. Typical Column with Impermeable Boundaries

Starting at i = 2

$$\phi_2^{\,n} = \frac{c_2\phi_1^{\,n} + d_2\phi_3^{\,n} + a_2\phi_{2,j}^{\,n-1} + b_2\phi_{2,j+1}^{\,n-1} - (a+b+I_p)\,\phi_2^{\,n-1}}{c_2 + d_2 + I_p}$$

where unlabeled j subscripts imply the j'th row

Let $\quad E_i = (c_i + d_i + I_p)$

and $\quad CKNOWN_i = a_i\,\phi_{i,j-1}^{\,n-1} + b_i\,\phi_{i,j+1}^{\,n-1} - (a_i + b_i - I_p)\,\phi_{i,j}^{\,n-1}$

substituting gives

$$\phi_2^{\,n} = \frac{c_2\phi_1^{\,n} + d_2\phi_3^{\,n} + CKNOWN_i}{E_2}$$

Formulating into G and F parts yields

$$\phi_2^{\,n} = G_2 + F_2\,\phi_3^{\,n} \qquad (75)$$

where

$$G_2 = \frac{c_2\phi_1^{\,n} + CKNOWN_2}{E_2}$$

$$F_2 = \frac{d_2}{E_2}$$

since $\quad c_2 = 0.0$

$$G_2 = \frac{CKNOWN_2}{E_2}$$

similarly

$$\phi_3^{\,n} = G_3\ F_3\ \phi_4^{\,n} \qquad (76)$$

where

$$G_3 = \frac{c_3 G_2 + CKNOWN_3}{E_3 - c_3 F_2}$$

$$F_3 = \frac{d_3}{E_3 - c_3 F_2}$$

$$\phi_4^n = G_4 + F_4 \phi_5^n \tag{77}$$

where
$$G_4 = \frac{c_4 G_3 + CKNOWN_4}{E_4 - c_4 F_3}$$

$$F_4 = \frac{d_4}{E_4 - c_4 F_3}$$

$$\phi_5^n = G_5 + F_5 \phi_6^n \tag{78}$$

where
$$G_5 = \frac{c_5 G_4 + CKNOWN_5}{E_5 - c_5 F_4}$$

$$F_5 = \frac{d_5}{E_5 - c_5 F_4}$$

$$\phi_6^n = G_6 + F_6 \phi_7^n$$

where
$$G_6 = \frac{c_6 G_5 + CKNOWN_6}{E_6 - c_6 F_5}$$

$$F_6 = 0 \quad \text{since } d_6 = 0$$

$$\phi_6^n = G_6 \tag{79}$$

Back substituting into respective equations 78, 77, 76, and 75 solves for potentials in the column.

For unknown potentials in a column where there are constant potential nodes, the equations 75 to 79 will apply except where

$$\phi_i = c_i$$

or $\phi_i = c_i$ and ϕ_{i+1} is not constant

Pages 176 and 177 are not missing from the Reiter thesis, the text is numbered incorrectly.

then

$$G_{i+1} = \frac{c_i \phi^{h}_{i-1} + CKNOWN_{i+1}}{E_i}$$

$$F_{i+1} = \frac{d_{i+1}}{E_{i+1}}$$

Appendix I

Number Generators

The methods used in the computer models for obtaining uniform, exponential, and log normal distributions are developed in this section.

Random Deviate

The algorithms used to compute the uniform and exponential distributions, first require a random deviate between zero and one. This was achieved by using the International Mathematics and Statistical Libraries (IMSL) routine called GGUBFS (IMSL, Inc., 1979), which used the following algorithm:

1) an integer seed value (S_o) is picked between 4 and 2147483647
2) compute $S = 7^5\, S_o$ modulo $(2^{31} - 1)$
3) compute the random deviate between zero and one (R)

   $$R = 2^{-31} \times S$$

4) let $S = S_o$ for the next random deviate generated

Uniform Distribution

The uniform distribution was generated between limits A and B by the following procedure:

1) a random deviate (R) is generated between zero and one
2) compute $NUM = R \cdot 10^n$
   where n = smallest integer such that

   $$10^n \geq B$$

3) if NUM is less than A, return to step 1;
   if NUM is greater than B, return to step 1;
   otherwise proceed to the next step

4) NUM = nodal permeability

5) go to step 1 until all nodal permeability values are determined

Exponential Distribution

The exponential or log uniform distribution had limits of A and B, where the lowest value of A was one, and the frequency scale was log k (k in ft/d). The distribution was generated as follows:

1) a random deviate (R) is generated between zero and one

2) compute $NUM = R \cdot 10^n$ (integer)
where n = smallest integer such that
$n \geq B$

3) if NUM is less than $A \cdot 10^{n-1}$ (integer), then go to step 1;
if NUM is greater than $B \cdot 10^{n-1}$ (integer), then go to step 1;
otherwise proceed to the next step

4) compute $XNUM = NUM/10^{n-1}$ (real)

5) compute $k(i,j) = 10^{XNUM}$ (real)
where k (i,j) = nodal permeability at row i, colunn j

6) go to step 1 until all nodal permeabilities are computed

Normal Deviate

The algorithm used to compute the log normal distribution, first required a normal deviate with a mean of zero and a standard deviation of one $N[0, 1]$. This was achieved using the IMSL routine called GGNQF (IMSL, Inc., 1979).

Log Normal Distribution

The log normal distribution $LN[\mu_Y, \sigma_Y]$ distribution with mean (μ_Y) and standard deviation (σ_Y) was generated by the following procedure:

1) generate a normal deviate $N[0, 1]$
where $\mu = 0$ and $\sigma = 1$

2) convert N $[0,1]$ to LN $[\mu_y, \sigma_y]$

LN $[\mu_y, \sigma_y] = \sigma_y \, N\,[0,1] + \mu_y$

3) compute k (i, j) = $10^{N[\mu_y, \sigma_y]}$

4) go to step 4 until all the nodal k (i, j) values are computed.

Appendix J

Stream Function

Stream functions are of great importance for understanding groundwater flow (Rushton and Redshaw, 1979). A comprehensive derivation and discussion of the stream function was given by Bear, 1972. He states;

> In practical terms, it is impossible to label a single fluid particle (say in an experiment of flow through porous media) and observe its motion. Instead we label a group of particles occupying a small neighborhood, or we continuously inject a tracer into a point in a steadily moving fluid. In laminar flow, in spite of hydrodynamic dispersion, and in the case of a continuous injection, in spite of the lateral dispersion, it is possible to define the average path of the particles and to use it in defining the flow.

Accoring to Bear at any instant of time there is at every point in the flow domain a velocity (from Darcy's law) vector with a definite direction. The instantaneous curves that are at every point tangent to the direction of velocity at that point are called streamlines of the flow. Assuming the existence of streamlines in a steady state situation, a stream function may be derived. The derivation by Bear (1972) is demonstrated here for the 2-D case.

Figure J1 shows a streamline with tangential velocity (V) at dr, an element of arc along the streamline. Since by the definition of a streamline, V and dr must have the same direction, then

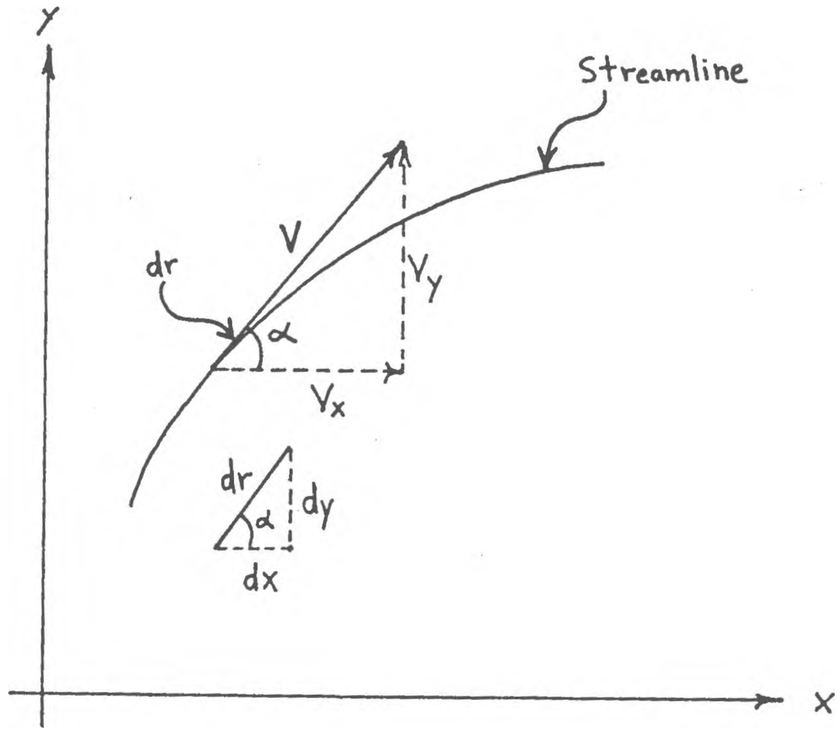

Figure J1. Streamline and Velocity Vector in 2-D Steady Flow

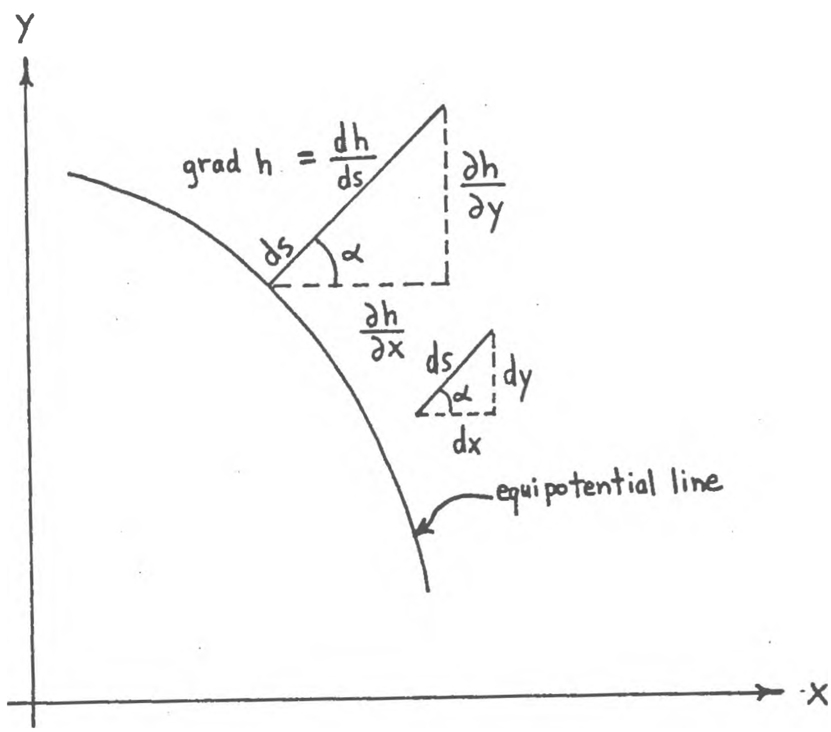

Figure J2. Equipotential Line and Gradient of Total Head Vector in 2-D Steady Flow

$V \times dr = 0$

where $V = V_s$

= average velocity vector Darcy's equation

V_s = seepage velocity (see Lombe & Whitman, 1969)

= porosity

dr = element of arc along a streamline (vector)

Figure J1 shows similar triangles V, V_x, V_y and dr, dx, dy; hence

$$\frac{dx}{V_x} = \frac{dy}{V_y} \tag{80}$$

According to Bear, equation 80 is valid for both isotropic and anisotropic media. For a flow described by Darcy's law, where x and y are the principal directions of permeability, equation 80 becomes

$$\frac{dx}{k_x \frac{\partial h}{\partial x}} = \frac{dy}{k_y \frac{\partial h}{\partial y}} \tag{81}$$

Consider the equipotential surface and an elementary displacement ds normal to this surface, as shown in Figure J2. Then the maximum hydraulic gradient (grad h), will always occur along the normal or ds direction. Therefore

grad $h \times ds = 0$

Grad h is represented vectorially in Figure J2, which also shows similar triangles dh/ds, $\partial h/\partial x$, $\partial h/\partial y$ and ds, dx, dy. Hence

$$\frac{dx}{\frac{\partial h}{\partial x}} = \frac{dy}{\frac{\partial h}{\partial y}} \tag{82}$$

which defines curves in space normal to the equipotential surfaces. These are the streamlines. When equation 81 is written for an isotropic media and multiplied by k, equation 82 is obtained. Thus, in an isotropic medium, streamlines are perpendicular to the equipotential surfaces. Furthermore, since the differential equations (81) define what happens at a point, we may have k = k(x, y), i.e., a non homogeneous medium (Bear, 1972).

Rearranging equation 80 gives

$$V_x\,dx - V_y\,dy = 0 \qquad (83)$$

The solution of 83 is

$$\Psi = \Psi(x,\ y) = \text{constant} \qquad (84)$$

The condition for equation 83 to be an exact differential of same function $\Psi = \Psi(x, y)$ is

$$\frac{\partial V_x}{\partial x} + \frac{\partial V_y}{\partial y} = 0 \qquad \text{(Bear, 1972)}$$

which is the continuity equation. Since the continuity expression describes flow of an incompressible fluid in a nondeformable medium, the stream function (Ψ) as defined here is valid only for such a case. When equation 83 is rewritten as

$$\frac{dy}{dx} = \frac{V_y}{V_x} = f(x,y)$$

it follows that this expression defines for any point in the xy plane an angle,

$$\alpha = \tan^{-1} f(x,y)$$

which the tangent to equation 84 makes with the +x axis. Equation 84 actually describes a family of curves for various values of the constant.

Since Ψ is an exact differential, then along any streamline,

$$d\Psi = \frac{\partial \Psi}{\partial x}\,dx + \frac{\partial \Psi}{\partial y}\,dy = V_y\,dx - V_x\,dy = 0$$

from which can be obtained the expressions

$$V_x = -\frac{\partial \Psi}{\partial y} \qquad (85)$$

$$V_y = \frac{\partial \Psi}{\partial x} \qquad (86)$$

The function $\Psi = \Psi(x,y)$, which is constant along streamlines (or $d\Psi = 0$), is called the stream function of two-dimensional flow. An impervious boundary of a flow domain, with the flow always tangential to it, invariably coincides with a streamline.

Since the quasi-linear flow model assumes positive flow from left to right and top to bottem (unlike Bear's notation of Figure J1), equations 85 and 86 become

$$\partial \Psi = V_x \, \partial y \qquad (87)$$

$$\partial \Psi = V_y \, \partial x \qquad (88)$$

Integrating equation 87 between y limits of i and l and equation 88 between x limits of j and m

$$\Psi_l - \Psi_i = \int_i^l V_x \, \partial y$$

$$\Psi_m - \Psi_j = \int_j^m V_y \, \partial x$$

The numerical approximation to equations 87 and 88 becomes

$$\Psi_l - \Psi_i = \sum_i^l V_x \Delta y \qquad (89)$$

along the y - direction

where i = row i

l = row l

and $$\Psi_m - \Psi_j = \sum_j^m V_y \Delta x \qquad (90)$$

along the x - direction

where j = column j

m = column m

Numerical approximations to the components of velocity as defined in Darcy's equation are

$$V_x = k_x \frac{\Delta h}{\Delta x} \qquad (91)$$

$$V_y = k_y \frac{\Delta h}{\Delta y} \qquad (92)$$

where h = steady state total head

Substituting equations 91 and 92 into rearranged equations 89 and 90 respectively yields

$$\Psi_l = \Psi_i + \sum_i^l k_x \frac{\Delta h}{\Delta x} \Delta y \qquad (93)$$

along the y - direction

$$\Psi_m = \Psi_j + \sum_j^m k_y \frac{\Delta h}{\Delta y} \Delta x \qquad (94)$$

along the x - direction

Equations 93 and 94 can also be written

$$\Psi_l = \Psi_i + \sum_i^l q_x \qquad (95)$$

along the y - direction

$$\Psi_m = \Psi_j + \sum_j^m q_y \qquad (96)$$

along the x - direction

where q_x = x - direction component of flow

q_y = y - direction component of flow

The discrete values of stream function (Ψ) are computed at nodal boundary intersections. Figure J3 shows the node center locations and the discretized stream function locations ($\Psi_{i,j}$). A dashed arrow from the node center location (3, 4) points to the stream function location (3, 4). In this manner, row and column subscripts (i, j) serve to identify $\Psi_{i,j}$.

Figure J3 actually represents horizontal flow through a section of confined aquifer, where constant head nodes along the left vertical boundary all have the same high total head value and constant head nodes at the right vertical boundary have a common low total head value. All steady state total values and nodel permeabilities are assumed to be known.

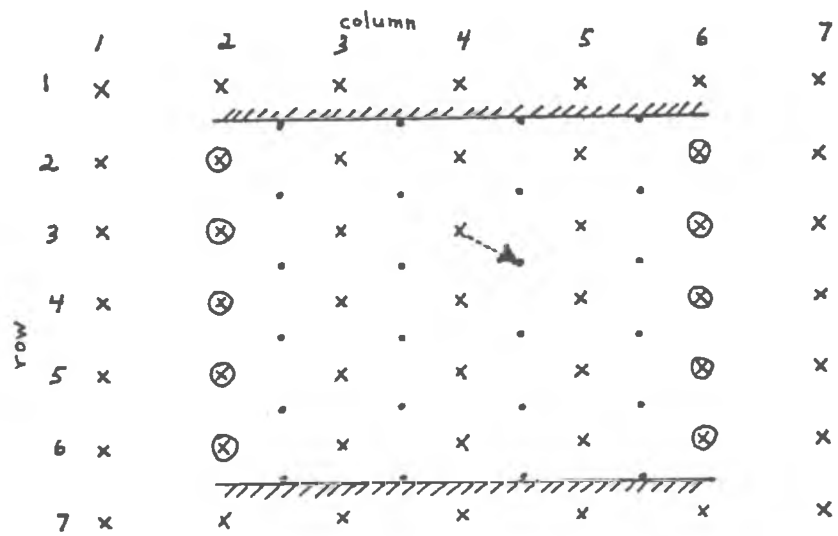

Figure J3. Location of Stream Function Values

x = node center
⊗ = constant head node
- - - -► points to (3, 4) location from (3, 4) nodal location
• = $\Psi_{i,j}$ location

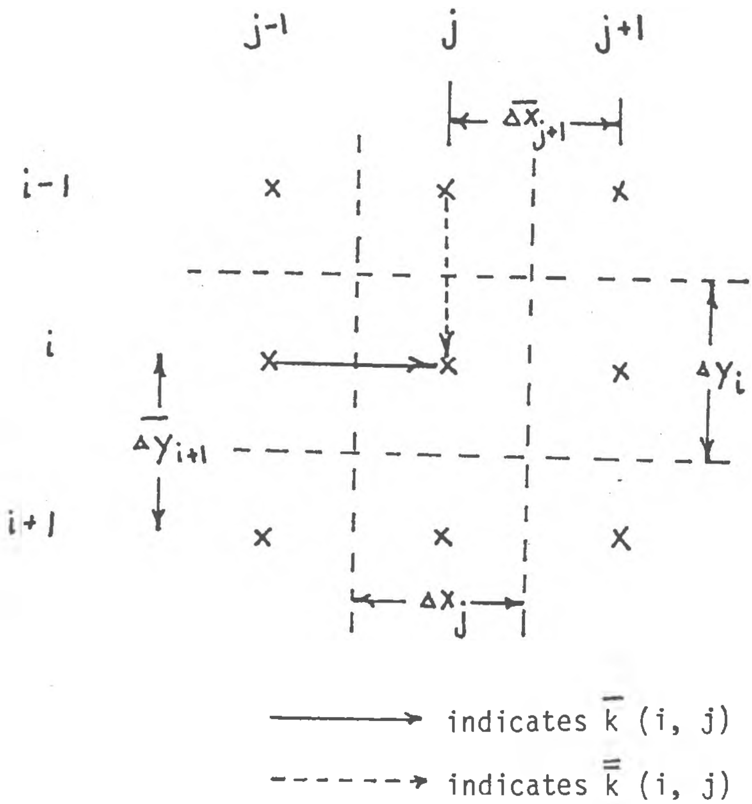

Figure J4. Permeabilities and Distances used in the Stream Function Algorithm

To compute the $\Psi_{i,j}$ values for the 2-D section in cartesian coordinates of figure J3, as the computer program of appendix K does, first the values along the bottom boundary are assumed to have a value of zero.

$$\Psi(5,2) = \Psi(5,3) = \Psi(5,4) = \Psi(5,5) = 0$$

where subscripts (i, j) indicate (row, column)

Stream function values are then computed along the left side based on equation 93. Numerical integration proceeds between columns 2 and 3 from the bottom impermeable boundary, where $\Psi(6,2)$ = 0, to the top impermeable boundary. Hence the algorithm is

$$\Psi(4,2) = \Psi(5,2) + \bar{k}(5,3)\left[\frac{h(5,2) - h(5,3)}{\overline{\Delta x}(3)}\right]\Delta y(5)$$

$$\Psi(3,2) = \Psi(4,2) + \bar{k}(4,3)\left[\frac{h(4,2) - h(4,3)}{\Delta x(3)}\right]\Delta y(4)$$

$$\Psi(2,2) = \Psi(3,2) + \bar{k}(3,3)\left[\frac{h(3,2) - h(3,3)}{\Delta \bar{x}(3)}\right]\Delta y(3)$$

$$\Psi(1,2) = \Psi(2,2) + \bar{k}(2,3)\left[\frac{h(2,2) - h(2,3)}{\Delta \bar{x}(3)}\right]\Delta y(2)$$

where $\bar{k}$ (i,j+1) = connection value of permeability in the x - direction between nodes i, j and i, j + 1. (see Figure J4)

$\Delta \bar{X}$ = (j+1) = distance between node centers i, j and i, j + 1. (see Figure J4)

In similar fashion, the Ψ (i, 5) values are computed along with right boundary for i = 4, 3, 2, and 1.

The rest of the values of Ψ (i, j) can be computed using either equation 93 or 94. The general form of equation 93 as applied to the cartesian coordiate model becomes

$$\Psi(i,j) = \Psi(i+1,j) + \bar{k}(i+1,j+1)\left[\frac{h(i+1,j) - h(i+1,j+1)}{\Delta \bar{x}(j+1)}\right]\Delta y(i+1) \qquad (97)$$

along any j column

and equation 94 becomes

$$\Psi(i,j) = \Psi(i,j+1) + \bar{\bar{k}}(i+1,j+1)\left[\frac{h(i,j+1) - h(i+1,j+1)}{\Delta \bar{y}(i+1)}\right]\Delta x(j+1) \qquad (98)$$

along any i row

where $\bar{\bar{k}}$ (i+1,j+1) = connection value of permeability in the y - direction between nodes (i,j+1) and (i+1,j) (see Figure J4)

$\overline{\Delta y}$ = distance between node centers (i,j) and (i+1,j) (see Figure J4)

The radial flow program of appendix L uses the same technique just outlined, with $\overline{\Delta r}$ replacing $\overline{\Delta x}$ and $\overline{\Delta z}$ replacing $\overline{\Delta y}$. Also, the proper cross sectional area terms and connection permeabilities (eqs. 56a and 62) must be applied.

It is convenient to nondimensionalize the stream function by dividing all values by the total flow through the model. This total flow may be determined for the horizontal flow case of figure J3 by computing the total inflow as

$$Q = \sum_{i=2}^{6} \bar{k}(i,3)\left[\frac{h(i,2) - h(i,3)}{\overline{\Delta x}(2)}\right] \Delta y(i)$$

All stream function values in the computer programs of appendices K and L are divided by total inflow and multiplied by 100, hence nondimensionalizing the $\Psi(i,j)$ values in the range of 0 to 100. The $\Psi(1,j)$ values of Figure J3 are actually known to equal 100, since this is an impermeable boundary.

Figure J5 shows an exaggerated picture of horizontal quasi-linear flow. Flow vectors (q) cross every nodal boundary, where inflow must equal outflow. These vectors are the q values of equations 95 and 96, which are used to compute the Ψ values. The dashed line represents a possible path of integration, where equation 95 is used when moving in the y direction and equation 96 when moving in the x direction. values of Figure J5 are not nondimensionalized.

The algorithm used in the computer program of appendix K for point to point flow first computes total inflow at the high constant potential node, which is used to nondimensionalize other Ψ values. Boundary conditions are known to be the maximum or minimum Ψ value. Interior values are then computed using equation 97 or 98. The computer program uses equation 97. Figure J6 provides nodal flow vectors (q) and values for an exaggerated point to point flow regime. Flow continuity is preserved at every node. The Ψ values are not nondimensionalized and boundary conditions are the maximum (40) and minimum (0) streamlines. Interior Ψ values are computed based on equation 97 or 98.

When total head values are contoured over a streamline plot, a flow net results. Figure J7 shows the computer drawn flow net for a section with a low permeability center. To see if the stream function algorithm gave reasonable results when refraction occurs, a section with a wedge shaped interface was run. Figure J8 shows the flow net for this section, where flow appears to remain orthogonal to the total head contours. The technique was also applied to an isotropic section with point to point flow (figure J9), and the same section with anisotrophy of 10 to 1 (figure J10). Both show reasonable results.

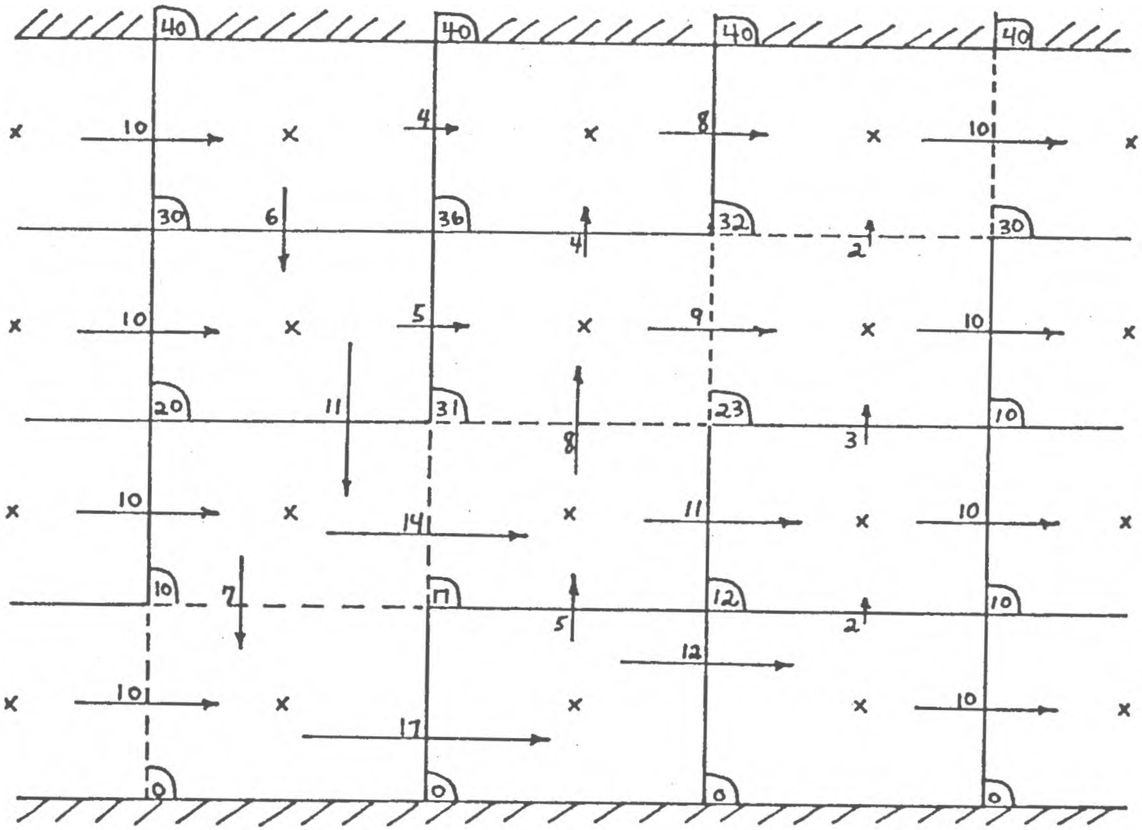

Figure J5. Flow Vectors and Stream Function Values for Exaggerated Quasi-Linear Horizontal Flow

10 = stream function value

9 = flow across node boundary

X = node center

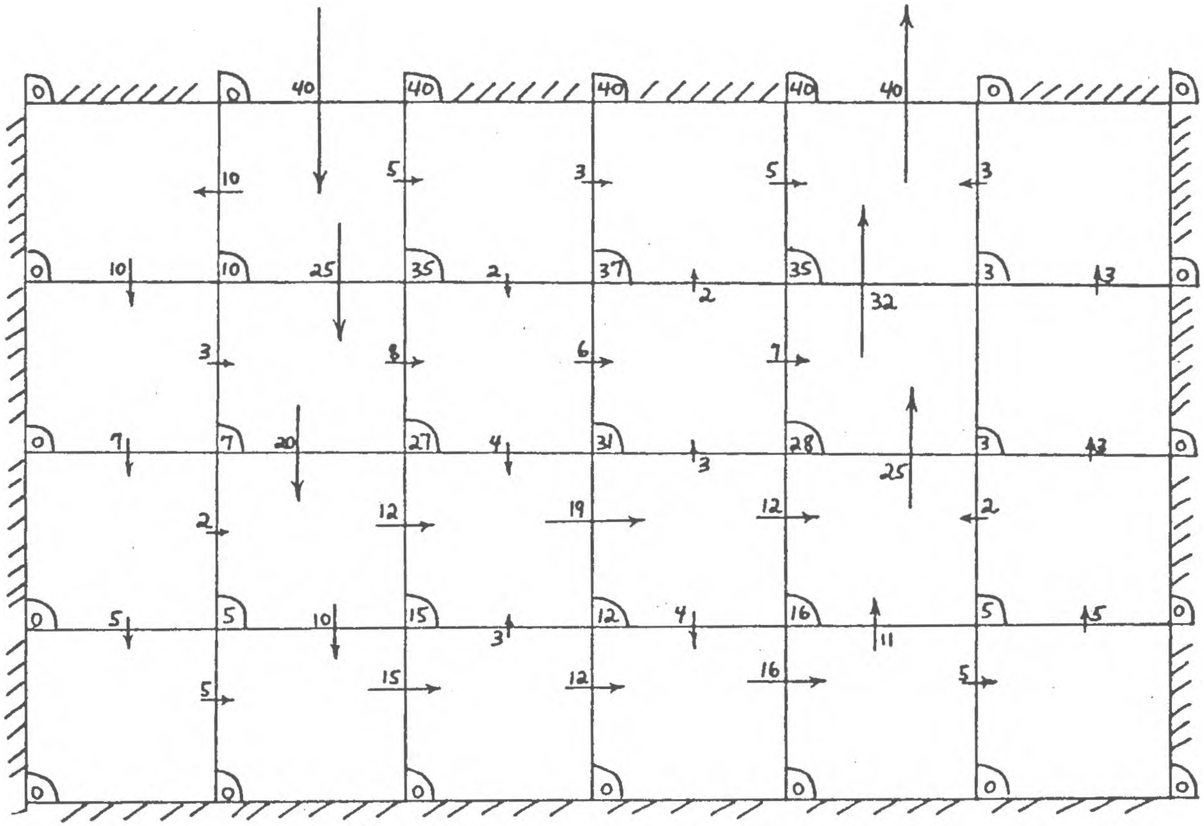

Figure J6. Flow Vectors and Stream Function Values for Exaggerated Quasi-Point to Point Flow

5 = stream function value

20 = flow across node boundary

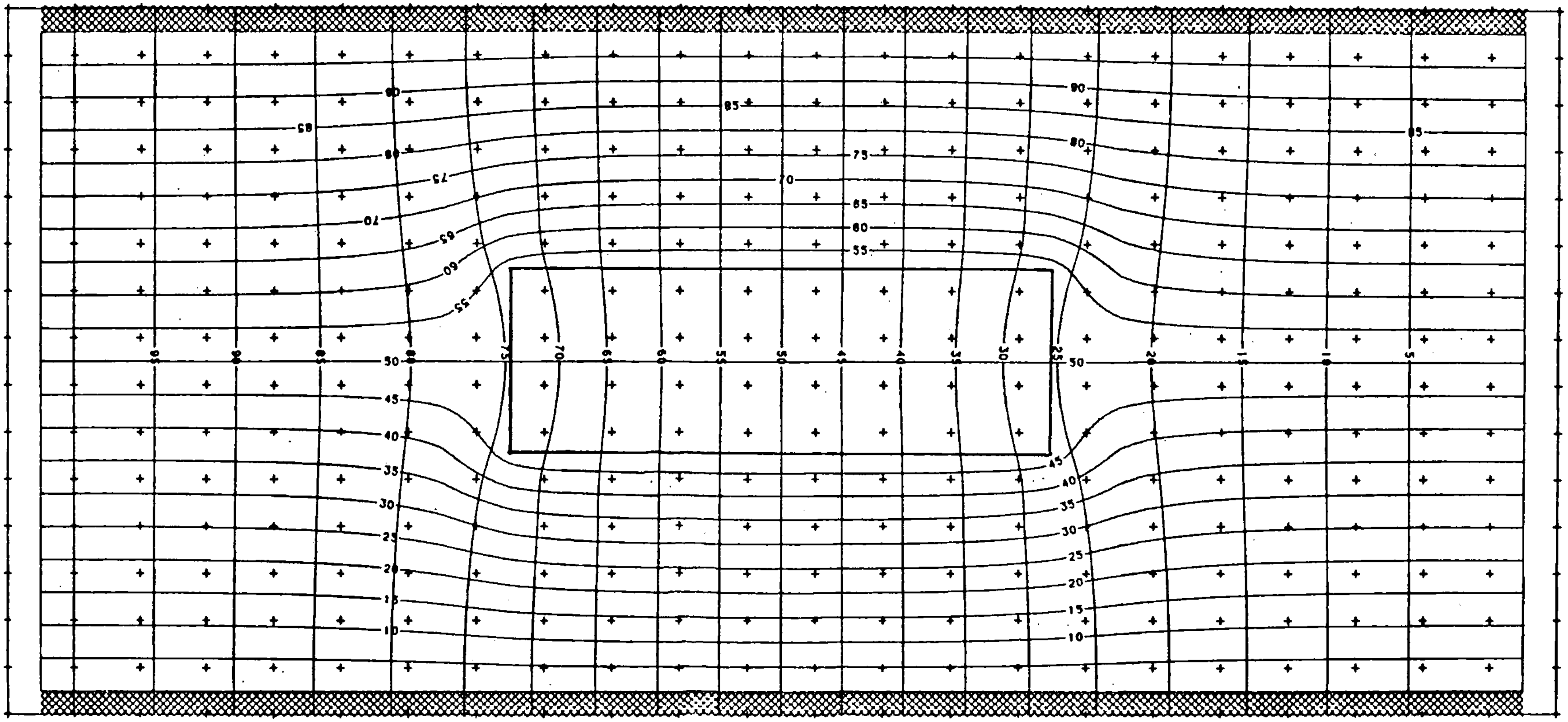

FLOW NET

Figure J7. Flow net for linear flow through a section where the center permeability is 1/10 the value at other nodes. Flow moves from left to right. Shaded boundaries are impermeable.

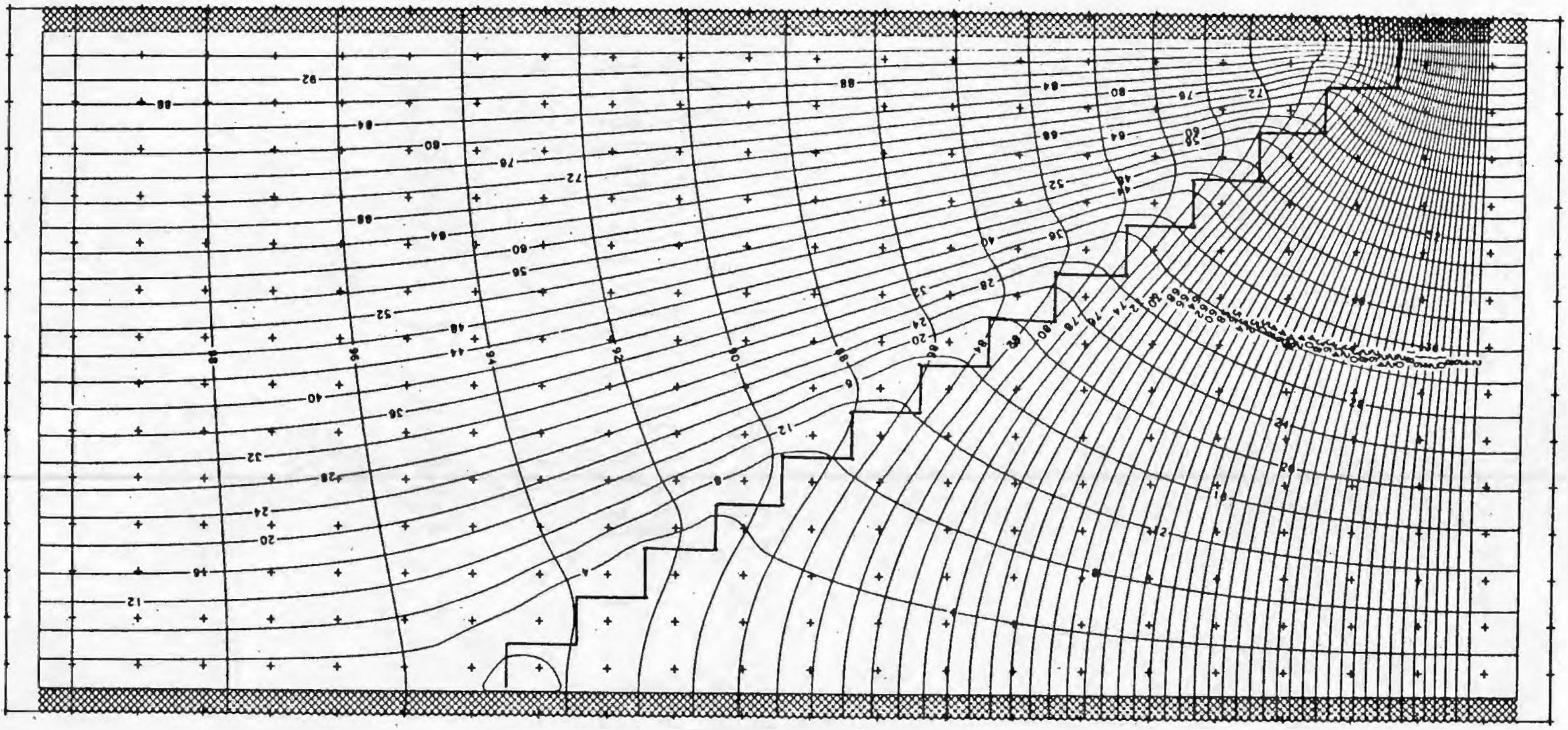

FLOW NET

Figure J8. Flow net for linear flow through a wedge shaped inface between two permeabilities, with the value to the right of the interface twenty times less than the left side value. Shaded boundaries are impermeable. Flow moves from left to right.

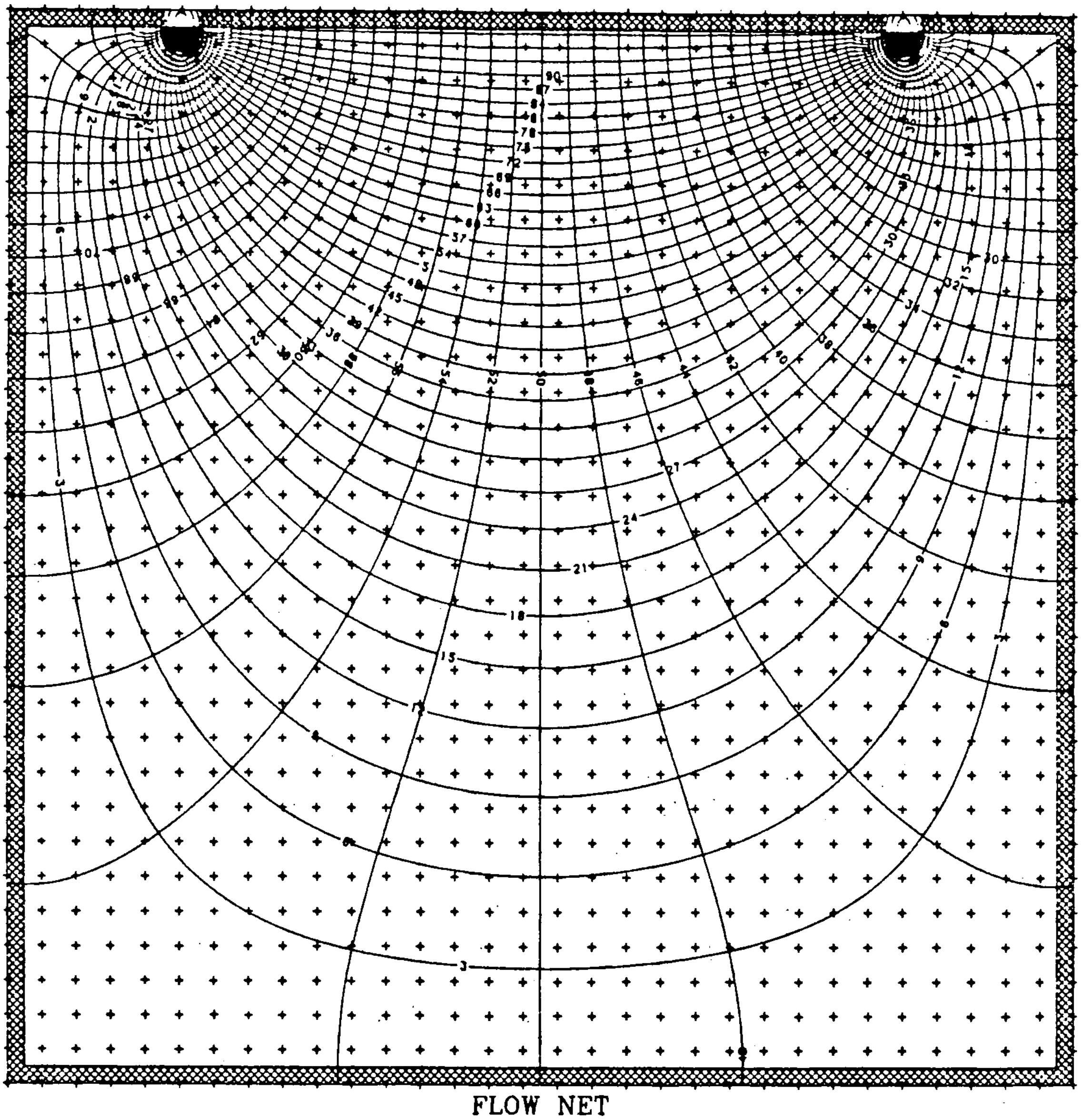

Figure J9. Flow net for point to point flow in an isotropic section with constant permeability. Shaded boundaries are impermeable.

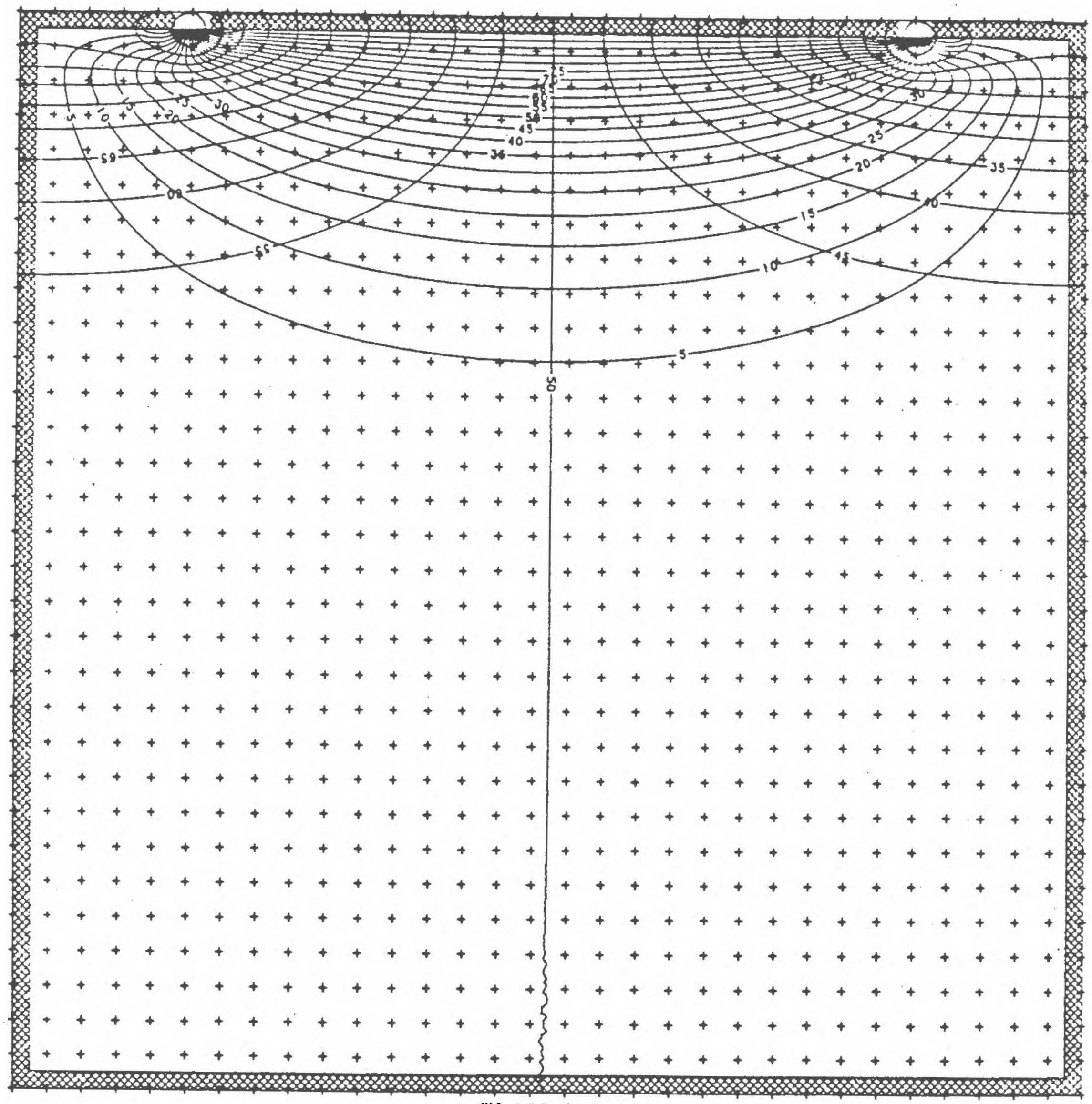

Figure J10. Flow net for point to point flow in a section with anisotropy of 10 to 1 and constant permeability. Shaded boundaries are impermeable.

Appendix K

2-D Cartesian Coordinate Program

The 2 D quasi-linear flow program performs the following tasks:

1. Nodal permeabilities are assigned
2. If the electrical case is specified in the options, nodal permeabilities are converted to apparent electrical conductivities by

$$\sigma_a = 1 \Big/ \left(\frac{k}{5.13 \times 10^{-6}}\right)^{.7}$$

   which is an approximation to the "probably average" curve of Figure 1, developed by Urish, 1978.
3. Solves for the steady state potentials using the iterative alternating direction implicit (IADI) procedure. Zero values of permeability are placed around the perimeter of the model, hence the no flow boundary is at the nodal boundary between the perimeter node and the adjacent interior node. Constant potential boundaries are located at the node center.
4. Aquifer permeability and aquifer resistivity are computed based on potential theory.
5. If specified in the options, stream function values are computed.
6. If specified in the options, stream function values and/or potential quantities are written onto a data set, where they may later be read by the Cal Comp contouring program to produce a flow net.

The program will solve for steady state potentials when constant head values are located anywhere in the 2-D section. However, the stream function and aquifer property determining algorithms are suitable only for boundary conditions which produce linear, quasi-linear or surficial point to point flow. Stream function algorithms may be developed for other cases where constant head nodes appear only on the model perimeter.

User instructions and a listing of the cartesian coordiate program follow.

DATA DECK PREPARATION

CARD(CD) CARD SETS(CS)	COLUMNS	FORMAT	VARIABLE	DESCRIPTION
CD 1	1 - 80	20A4	HEADIN	Any title the user wishes to print on one line at the start of output
CD 2	1 - 10	I10	NROW	Number of model rows
	11 - 20	I10	NCOL	Number of model columns
	21 - 30	F105	EC	Error criteria for closure at the steady state
	31 - 40	I10	ISO	Code for type of permeability distribution 0 = deterministically layered 1 = all the same 2 = uniformly distributed 3 = lognormally distributed 4 = exponentially distributed 5 = values are read in at each node
	41 - 50	F10.5	PERM	permeability value all the k(i,j)'s are to assume if ISO = 1
CD 3	1 - 5	A4, 1X	CONH	punch CONH to write the total head values onto disk
	6 - 10	A4, 1X	CONK	punch CONK to write permeability values onto disk
	11 - 15	A4, 1X	ELEC	punch ELEC to convert permeabilities to electrical conductivities
	16 - 20	A4, 1X	MINI	punch MINI to read in the minimum iteration value
	21 - 25	A4, 1X	STRF	punch STRF to compute and write onto disk, the stream function values
	26 - 30	A4, 1X	FLOW	punch VERT for the vertical quasi-linear flow case punch HORI for the horizontal quasi-linear flow case punch PTPT for the point source to point sink flow case
	31 - 35	A4, 1X	SKIP	punch SKIP to truncate output
	36 - 40	A4, 1X	WARP	punch WARP to use the Warren and Price technique (equation 20 in section I) to compute aquifer properties
CD 4	1 - 10	I10	LSTRM	Column (when FLOW = HORI), or row (when FLOW = VERT), or column of leftmost constant head node (when FLOW = PTPT), where total flow is computed for nondimensionalizing the stream function
	11 - 20	I10	LEQUIV	Column (when FLOW = HORI), or row (when FLOW = VERT) where the total flow is computed to be used in determining the aquifer properties. Not used when FLOW = PTPT

CARD(CD) CARD SET(CS)	COLUMNS	FORMAT	VARIABLE	DESCRIPTION
	21 - 30	F10.5	DHEAD	Total dissipated head through the model. Not used when FLOW = PTPT
CD 5	1 - 10	F10.1	WPFACT	Shape function S computed by equation 21 (section I). Used when FLOW = PTPT or WARP is specified in CD 3
CD 6	1 - 10	I10	ITMAX	Maximum number of iterations
	11 - 20	I10	NUMPAR	Number of iteration parameters
	21 - 30	F10.5	HMAX	Maximum iteration value
	31 - 40	F10.5	HMIN	Minimum iteration parameter (used only if MINI was specified in CD 3
CARD SET				
CS 1	1 - 80	8F10.1	XD(J)	Nodal spacing in the x - direction
CS 2	1 - 80	8F10.1	YD(J)	Nodal spacing in the y - direction

IF ISO = 0 (permeabilities are layered and deterministic)

CD 7	1 - 5	A4, 1X	LAYTY	Type of layering punch H for horizontal layering, punch V for vertical layering
	1 - 10	I10	LAYERS	Number of layers

Go to CS 4

IF 1SO = 2 (permeabilities are uniformly distributed)

CD 7	1 - 10	I10	LAYERS	Number of layers
CS 3	1 - 10	I10	UNILO	Lower limit of the uniform permeability distribution (ft/d)
	11 - 20	I10	UNIHI	Upper limit of the uniform permeability distribution (ft/d)
	21 - 30	I10	LAYLO	First row where UNILO and UNIHI apply
	31 - 40	I10	LAYHI	Last row where UNILO and UNIHI apply

IF ISO = 3 (permeabilities have a log normal distribution)

CD 7	1 - 10	F10.1	MEAN	Mean value of the log normal permeability (ft/d) distribution
	11 - 20	F10.1	SDEV	Standard deviation of the log normal permeability (ft/d) distribution

60 to CS 4

IF ISO = CS4 (permeabilities have an exponential distribution)

CD 7	1 - 10	I10	EXLO	Lower limit of the exponential permeability (ft/d) distribution
	11 - 20	I10	EXHI	Upper limit of the exponential permeability (ft/d) distribution

GO to CS 4

DATA DECK PREPARATION

CARD(CD) CARD SET(CS)	COLUMNS	FORMAT	VARIABLE	DESCRIPTION
IF ISO = 5 (permeabilities are read in)				
CS 3	1 - 80	8F10.1	K(I, J)	Permeabilities (ft/d)
CS 4	1 - 80	8F10.1	ANISO (I)	Anisotropy ratios for each layer
CS 5	1 - 80	16I5	IC (2, J)	Constant head node indicator for row 2 where J = 2 to NCOLM1 (IC = -1 at a constant head node, otherwise IC = 0)
	1 - 80	16I5	IC(NROWMI,J)	Constant head node indicator for row NROWM1 where J = 2 to NCOLM1
	1 - 80	16I5	IC (I, 2)	Constant head node indicator for column 2, where I = 2 to NROWM1
	1 - 80	16I5	IC(I,NCOLM1)	Constant head node indicator for column NCOLM1, where I = 2 to NROWM1
CS 6	1 - 80	8D10.3	H (2, J)	Starting head values along row 2, where J = 2 to NCOLM1
CS 6	1 - 80	8D10.3	H(NROWM1, J)	Starting head values along row NROWM1, where J = 2 to NCOLM1.
	1 - 80	8D10.3	H (I, 2)	Starting head values along column 2, where I = 2 to NROWM1.
	1 - 80	8D10.3	H(I, NCOLM1)	Starting head values along column NCOLM1, where I = 2, NROWM1

Linear Program (cartesian coordinates)

```
C  2-D STEADY, HETEROGENEOUS, ANISOTROPIC FLOW THROUGH POROUS MEDIA
C USING FINITE DIFFERENCE WITH VARIABLE GRID SPACINGS
C AND THE ITERATIVE ALTERNATING DIRECTION IMPLICIT PROCEDURE
C
C SPECIFICATIONS
      INTEGER CHECK,CONH,CONK,ELEC,MINI,STRF,FLOW,SKIP,UNILO,UNIHI
      INTEGER EXLO,EXHI,WARP,PTPT
      REAL K,KHARM,LENGTH,KHEQFD,KVEQFD,KVEQCS,KHEQCS,HARMK,MEAN,KLOG
      REAL KY
      DOUBLE PRECISION H,HNEW,A,B,C,D,E,F,G,QPARM,QKNOWN,DABS,HOLD
      DOUBLE PRECISION ITPARM
      REAL*8 DSEED/992299.D0/
      DIMENSION KHARM(52,52,2),H(52,52),K(52,52),XD(52),YD(52),AX(52),
     $AY(52),HEADIN(20),ANISO(52),CHECK(10),X(52,52),Y(52,52),ERR(300)
      DIMENSION G(52),F(52),IC(52,52),HNEW(52),ITPARM(52),HOLD(52,52),
     $STRFUN(52,52),HSTRAT(52,52),KY(52,52)
      DATA CHECK/'CONK','CONH','ELEC','MINI','STRF','VERT','SKIP',
     1'V','WARP','PTPT'/
      READ(5,10) HEADIN
   10 FORMAT (20A4)
      WRITE(6,20) HEADIN
      WRITE(6,25) DSEED
   25 FORMAT ('0',/,5X,'DSEED=',F12.0)
   20 FORMAT ('1',20X,20A4)
C
C INPUT PARAMETERS
C NOTE**** ALL INPUT PARAMETERS ARE NODAL VALUES****
C
      READ(5,30) NROW,NCOL,EC,ISO,PERM
      READ(5,35) CONH,CONK,ELEC,MINI,STRF,FLOW,SKIP,WARP
      READ(5,30) LSTRM,LEQUIV,DHEAD
C LSTRM IS THE COLUMN (FOR THE HORIZONTAL FLOW CASE, FLOW=HORI)
C         OR THE    ROW (FOR THE VERTICAL FLOW CASE, FLOW=VERT)
C         OR THE COLUMN OF THE CONSTANT HEAD POINT ON THE
C         LEFT SIDE OF THE UPPER BOUNDARY
C WHERE THE TOTAL FLOW IS COMPUTED FOR THE USE OF NONDIMENSIONALIZING
C THE STREAM FUNCTION *** IT IS USED ONLY WHEN CHECK(5)=STRF
C
C LEQUIV IS THE COLUMN (FOR THE HORIZONTAL FLOW CASE, FLOW=HORI)
C          OR THE    ROW (FOR THE VERTICAL FLOW CASE, FLOW=VERT)
C WHERE THE TOTAL FLOW IS COMPUTED TO BE USED IN SOLVING
C FOR THE EQUIVALENT PERMEABILITY (RESISTIVITY) OR WHERE THE
C WARREN AND PRICE TECHNIQUE IS APPLIED
      READ(5,40) WPFACT
      NROWM1=NROW-1
      NCOLM1=NCOL-1
      NROWM2=NROW-2
      NCOLM2=NCOL-2
C NOTE **** THE VALUE READ IN FOR HMIN IS THE LOWEST ITERATION
C PARAMETER AND IS USED ONLY IF MINI WAS SPECIFIED IN THE OPTIONS
      READ(5,32) ITMAX,NUMPAR,HMAX,HMIN
   30 FORMAT (2I10,1F10.5,I10,F10.5)
   32 FORMAT (2I10,2F10.5)
```

```
   33 FORMAT (3I10,1F10.5)
   35 FORMAT(16(A4,1X))
      READ(5,40)  (XD(J),J=1,NCOL)
   40 FORMAT (8F10.1)
      READ(5,40)  (YD(I),I=1,NROW)
C COMPUTE AX AND AY
C AX= X-DISTANCE FROM ONE NODE CENTER TO THE NEXT
C AY= Y-DISTANCE FROM ONE NODE CENTER TO THE NEXT
C
      DO 42 J=2,NCOL
   42 AX(J)= (XD(J)+XD(J-1))/2.0
      DO  44 I=2,NROW
   44 AY(I)=(YD(I)+YD(I-1))/2.0
C
      IF(ISO.EQ.1) GO TO 80
      IF(ISO.EQ.2) GO TO 91
      IF(ISO.EQ.3) GO TO 50
      IF(ISO.EQ.4) GO TO 84
      IF(ISO.EQ.5) GO TO 60
C OTHERWISE
C  READ VALUES FOR A LAYERED DETERMINISTIC MODEL
C
      READ(5,35) LAYTY
      READ(5,96) LAYERS
      IF(LAYTY.EQ.CHECK(8)) GO TO 78
C OTHERWISE THE MODEL IS HORIZONTALLY LAYERED
      DO 76 IL=1,LAYERS
      READ(5,73) LAYLO,LAYHI,PERM
   73 FORMAT(2I10,F10.2)
      DO 76 I=LAYLO,LAYHI
      DO 76 J=2,NCOLM1
      K(I,J)=PERM
   76 CONTINUE
      GO TO 95
C
C THE MODEL IS VERTICALLY LAYERED
   78 DO 79 IL=1,LAYERS
      READ(5,73) LAYLO,LAYHI,PERM
      DO 79 I=2,NROWM1
      DO 79 J=LAYLO,LAYHI
      K(I,J)=PERM
   79 CONTINUE
      GO TO 95
C
C PERMEABILITY VALUES HAVE A LOG NORMAL DISTRIBUTION
C OVER THE ENTIRE REGION
   50 READ(5,40) MEAN,SDEV
      WRITE(6,51) MEAN,SDEV
   51 FORMAT ('0',/,5X,'PERMEABILITIES ARE LOG NORMALLY DISTRIBUTED',
     $' OVER THE ENTIRE REGION',/,75X,'MEAN=',F10.5,
     $/,75X,'STNDRD. DEV. =',F10.5)
      DO 54 I=2,NROWM1
      DO 54 J=2,NCOLM1
C FIRST PICK A NORMAL DEVIATE
   52 YFL=GGNQF(DSEED)
C THEN CONVERT N 0,1  DEVIATE TO N MEAN,SDEV  DEVIATE
      KLOG=SDEV*YFL+MEAN
C VALUE KLOG= LOG OF K
```

```
      K(I,J)=10**KLOG
   54 CONTINUE
      GO TO 95
C
C PERMEABILITIES ARE READ IN AT EACH NODE
   60 READ(5,40) ((K(I,J),J=1,NCOL),I=1,NROW)
      GO TO 95
C
C PERMEABILITY  VALUES ARE ALL THE SAME
   80 DO 82 I=1,NROW
      DO 82 J=1,NCOL
   82 K(I,J)= PERM
      GO TO 95
C
C PERMEABILITY VALUES HAVE AN EXPONENTIAL DISTRIBUTION
C OVER THE ENTIRE REGION
C EXLO= MINIMUM LOG OF K VALUE *100
C EXHI= MAXIMUM LOG OF K VALUE *100
C        THE HIGHEST VALUE FOR EXHI IS 300
   84 READ(5,96) EXLO,EXHI
      DO 88 I=1,NROW
      DO 88 J=1,NCOL
   86 YFL=GGUBFS(DSEED)
      NUM=INT(YFL*1000.)
      IF(NUM.LT.EXLO) GO TO 86
      IF(NUM.GT.EXHI) GO TO 86
      XNUM=FLOAT(NUM)/100.
      K(I,J)=10**XNUM
   88 CONTINUE
      GO TO 95
C
C THE PERMEABILITY VALUES ARE UNIFORMLY DISTRIBUTED
C WITH A DIFFERENT DISTRIBUTION WITHIN EACH OF THE LAYERS
   91 READ(5,96) LAYERS
      DO 93 IL=1,LAYERS
      READ(5,96) UNILO,UNIHI,LAYLO,LAYHI
      WRITE(6,94) UNILO,UNIHI,LAYLO,LAYHI
      XER=1000.
      IF(UNIHI.LE.100) XER=100.
      DO 93 I=LAYLO,LAYHI
      DO 93 J=2,NCOLM1
   92 YFL=GGUBFS(DSEED)
      NUM=INT(YFL*XER)
      IF(NUM.LT.UNILO) GO TO 92
      IF(NUM.GT.UNIHI) GO TO 92
      K(I,J)=FLOAT(NUM)
   93 CONTINUE
   94 FORMAT ('0',/,5X,'PERMEABILITY RANGE FOR UNIFORM DISTRIBUTION=',
     1I6,2X,'TO',I6,1X,'FT/D',1X,'FOR LAYERS',1X,I2,1X,'TO',1X,I2)
   96 FORMAT (4I10)
C
C
   95 DO 100 I=1,NROW
      K(I,1)=0.0
  100 K(I,NCOL)=0.0
      DO 110 J=1,NCOL
      K(1,J)=0.0
  110 K(NROW,J)=0.0
```

```
      C
      C
      C READ ANISOTROPY AT EACH ROW
      C  VALUE IS THE RATIO OF KH/KV
        120 READ(5,40)  (ANISO(I),I=1,NROW)
      C
      C
      C COMPUTE KY(I,J) VALUES
      C THESE ARE THE NODAL VALUES TO BE USED IN COMPUTING
      C KHARM(I,J,2) --THE CONNECTION VALUE IN THE Y-DIRECTION
            DO 112 I=2,NROWM1
            DO 112 J=2,NCOLM1
        112 KY(I,J)=K(I,J)/ANISO(I)
      C CONVERT HYDRAULIC CONDUCTIVITIES TO ELECTRICAL CONDUCTIVITIES IF SPECIFIED
            IF(ELEC.NE.CHECK(3))GO TO 117
            DO 115 I=2,NROWM1
            DO 115 J=2,NCOLM1
            KY(I,J)=1/(((KY(I,J)*.0003528)/5.13E-06)**.7)
        115 K(I,J)=1/(((K(I,J)*.0003528)/5.13E-06)**.7)
      C
      C COMPUTE THE ARITHMATIC,HARMONIC AND GEOMETRIC MEANS OF THE
      C PERMEABILITY(CONDUCTIVITY) DISTRIBUTION
      C
        117 SUMK=0.0
            RECIPK=0.0
            PRODK=0.0
            DO 119 I=2,NROWM1
            DO 119 J=2,NCOLM1
            SUMK=SUMK+K(I,J)
            RECIPK=RECIPK+(1./K(I,J))
            PRODK=PRODK+ALOG10(K(I,J))
        119 CONTINUE
            XROWM2=FLOAT(NROWM2)
            XCOLM2=FLOAT(NCOLM2)
            ARITHK=SUMK/(XROWM2*XCOLM2)
            HARMK=(XROWM2*XCOLM2)/RECIPK
            GEOMK=10**(PRODK/(XROWM2*XCOLM2))
      C
      C PERMEABILITY(CONDUCTIVITY) VALUES ARE WRITTEN ONTO A DISK DATA SET
      C                 TO BE USED WITH PLOTTING
            IF(CONK.NE.CHECK(1)) GO TO 130
            DO 105 I=2,NROWM1
            DO 105 J=2,NCOLM1
            WRITE(10,2110) K(I,J)
        105 CONTINUE
      C
      C ECHO CHECK OF INPUT PARAMETERS
      C
        130 WRITE(6,140) NROW,NCOL,EC,ITMAX
        140 FORMAT ('0',4X,'# OF ROWS =',T25,I5,/,5X,'# OF COLUMNS =',T25,I5,/
           $///,5X,'CLOSURE ERROR CRITERIA=',  E16.5   ,5X,'MAXIMUM ITERATIONS
           $=',I5)
            WRITE(6,148) CONH,CONK,ELEC,MINI,STRF,FLOW,SKIP,WARP
        148 FORMAT ('0',/,5X,'PROBLEM OPTIONS SPECIFIED:',2X,10A8)
            IF(SKIP.EQ.CHECK(7)) GO TO 175
            WRITE(6,150)
            WRITE(6,160)  (XD(J),J=1,NCOL)
        150 FORMAT ('0',/,5X,'DELTAX NODAL VALUES')
```

```
  160 FORMAT ('0',4X,10F12.1/(5X,10F12.1))
      WRITE(6,170)
      WRITE(6,160) (YD(I),I=1,NROW)
  170 FORMAT ('0',5X,'DELTAY NODAL VALUES')
  175 WRITE(6,180)
  180 FORMAT ('1',5X,'HORIZONTAL PERMEABILITY VALUES AT NODE CENTER')
      DO 190 I=1,NROW
  190 WRITE(6,200) I,(K(I,J),J=1,NCOL)
  200 FORMAT ('0',I2,2X,10F12.6/(5X,10F12.6))
  210 FORMAT ('0',I2,2X,10I10/(5X,10I10))
      WRITE(6,220)
  220 FORMAT ('0',5X,'ANISOTROPY RATIO KH/KV')
      WRITE(6,160) (ANISO(I),I=1,NROW)
C
C WRITE AX AND AY
C
      IF(SKIP.EQ.CHECK(7)) GO TO 262
      WRITE(6,250)
  250 FORMAT('0',5X,'AX VALUES')
      WRITE(6,160)  (AX(J),J=2,NCOL)
      WRITE(6,260)
  260 FORMAT ('0',5X,'AY VALUES')
      WRITE(6,160) (AY(I),I=2,NROW)
C
C COMPUTE KHARM(I,J,1) AND KHARM(I,J,2)
C KHARM(I,J,1)= HARMONIC MEAN OF THE PERMEABILITIES AT ADJACENT NODES
C IN THE X DIRECTION
C KHARM(I,J,2)= HARMONIC MEAN OF THE PERMEABILITIES AT ADJACENT NODES
C IN THE Y DIRECTION
C
  262 DO 270 I=2,NROWM1
      DO 270 J=2,NCOL
  270 KHARM(I,J,1)=((XD(J-1)+XD(J))*K(I,J-1)*K(I,J))/(K(I,J)*XD(J-1)+
     $K(I,J-1)*XD(J))
      DO 280 I=2,NROW
      DO 280 J=2,NCOLM1
  280 KHARM(I,J,2)=((YD(I+1)+YD(I))*KY(I-1,J)*KY(I,J))
     $/(KY(I,J)*YD(I-1)+KY(I-1,J)*YD(I))
C
C WRITE VALUES OF KHARM
C
      IF(SKIP.EQ.CHECK(7)) GO TO 325
      WRITE(6,290)
  290 FORMAT ('1',//,5X,'VALUES OF KHARM I,J,1')
      DO 300 I=2,NROWM1
  300 WRITE(6,200) I,(KHARM(I,J,1),J=2,NCOL)
      WRITE(6,310)
  310 FORMAT ('1',//,5X,'VALUES OF KHARM I,J,2')
      DO 320 I=2,NROW
  320 WRITE(6,200) I,(KHARM(I,J,2),J=2,NCOLM1)
C
C
C SET BOUNDARY CONDITIONS
C NOTE *** PERIMETER BOUNDARY POINTS CAN BE EITHER CONSTANT HEAD OR IMPERMEABLE
C NOTE *** FLOW SHOULD BE FROM RIGHT TO LEFT OR TOP TO BOTTOM
C I.E.  HIGH HEADS SHOULD BE LOCATED AT THE TOP OR LEFT SIDE
C
C SET ALL HEADS EQUAL TO SOME INITIAL VALUE
```

```
C AND ALL IC(I,J) VALUES TO ZERO
  325 DO 330 I=1,NROW
      DO 330 J=1,NCOL
      IC(I,J)=0
  330 H(I,J)= 50.0
C
C READ LOCATIONS OF CONSTANT HEAD NODES
C ALONG THE PERIMETER
C NOTE: THE PERIMETER IS THE ONLY LOCATION FOR A SOURCE OR A SINK
C THAT IS -- A HIGH CONSTANT HEAD OR A LOW CONSTANT HEAD
C
C READ THE TOP ROW
      READ(5,336) (IC(2,J),J=2,NCOLM1)
  336 FORMAT (16I5)
C READ THE BOTTOM ROW
      READ(5,336) (IC(NROWM1,J),J=2,NCOLM1)
C READ THE LEFT SIDE
      READ(5,336) (IC(I,2),I=3,NROWM2)
C READ THE RIGHT SIDE
      READ(5,336) (IC(I,NCOLM1),I=3,NROWM2)
C
C READ HEAD VALUES ALONG THE PERIMETER
C READ TOP ROW
      READ(5,350) (H(2,J),J=2,NCOLM1)
C READ THE BOTTOM ROW
      READ(5,350) (H(NROWM1,J),J=2,NCOLM1)
C READ THE LEFT SIDE
      READ(5,350) (H(I,2),I=3,NROWM2)
C READ THE RIGHT SIDE
      READ(5,350) (H(I,NCOLM1),I=3,NROWM2)
  350 FORMAT (8D10.3)
C
C WRITE STARTING HEAD MATRIX
      IF(SKIP.EQ.CHECK(7)) GO TO 392
      WRITE(6,360)
  360 FORMAT('1',//,5X,'STARTING HEAD MATRIX')
      DO 370 I=1,NROW
  370 WRITE(6,200) I,(H(I,J),J=1,NCOL)
      WRITE(6,380)
  380 FORMAT('1',//,5X,'CONSTANT HEAD NODES')
      DO 390 I=1,NROW
  390 WRITE(6,210) I,(IC(I,J),J=1,NCOL)
C
  392 IF(MINI.EQ.CHECK(4)) GO TO 396
      HMIN=2.
      XVAL=3.1415**2/(2.*NCOL**2)
      YVAL=3.1415**2/(2.*NROW**2)
      DO 395 I=2,NROW
      DO 395 J=2,NCOL
      IF(K(I,J).EQ.0.0) GO TO 395
      XPART=XVAL*(1/(1+XD(J)**2/YD(I)**2*ANISO(I)))
      YPART=YVAL*(1/(1+YD(I)**2*ANISO(I)/XD(J)**2))
      HMIN=AMIN1(HMIN,XPART,YPART)
  395 CONTINUE
  396 ALPHA=EXP(ALOG(HMAX/HMIN)/(NUMPAR-1))
      ITPARM(1)=HMIN
      DO 397 NTIME=2,NUMPAR
  397 ITPARM(NTIME)=ITPARM(NTIME-1)*ALPHA
```

```
      WRITE(6,398) NUMPAR,(ITPARM(J),J=1,NUMPAR)
  398 FORMAT ('0',3X,I5,2X,'ITERATION PARAMETERS:',6D12.3,//,6X,10D12.3)
      IF(MINI.EQ.CHECK(4)) WRITE(6,399)
  399 FORMAT ('0',2X,'NOTE--MINIMUM ITERATION PARAMETER WAS SET')
C
      IER=0
  400 CONTINUE
C SOLUTION ALGORITHM USING THE ITERATIVE ALTERNATING DIRECTION IMPLICIT PROC.
      DO 500 I=1,NROW
      DO 500 J=1,NCOL
  500 HOLD(I,J)=H(I,J)
      DO 510 L=2,NCOLM1
  510 HNEW(L)=H(1,L)
      IF (MOD(IER,NUMPAR))520,520,530
  520 NTH=0
  530 NTH=NTH+1
      PARM=ITPARM(NTH)
C
      IER=IER+1
      ERR(IER)=0.0
C
C    ROW CALCULATIONS
C
      DO 700 KK=2,NROW
      I=KK
      DO 620 J=2,NCOLM1
      IF(K(I,J))605,620,605
  605 A=(KHARM(I,J,1)*YD(I))/AX(J)
      B=(KHARM(I,J+1,1)*YD(I))/AX(J+1)
      C=(KHARM(I,J,2)*XD(J))/AY(I)
      D=(KHARM(I+1,J,2)*XD(J))/AY(I+1)
      QPARM=(A+B+C+D)*PARM
      E=A+B+QPARM
      QKNOWN=C*H(I-1,J)+D*H(I+1,J)-(C+D-QPARM)*H(I,J)
      IF(J.EQ.2) GO TO 615
      IF(IC(I,J-1).EQ.-1) GO TO 610
      G(J)=(A*G(J-1)+QKNOWN)/(E-A*F(J-1))
      F(J)=B/(E-A*F(J-1))
      GO TO 620
  610 G(J)=(A*H(I,J-1)+QKNOWN)/E
      F(J)=B/E
      GO TO 620
  615 G(2)=QKNOWN/E
      F(2)=B/E
  620 CONTINUE
C CALCULATE HEADS BY BACK SUBSTITUTION
      N=NCOLM1
      H(I-1,N)=HNEW(N)
      IF(IC(I,NCOLM1).EQ.-1) GO TO 640
      HNEW(N)=G(N)
      GO TO 655
  640 HNEW(N)=H(I,N)
      GO TO 655
  650 HNEW(N)= G(N)+F(N)*HNEW(N+1)
  655 N=N-1
      IF(N.EQ.1) GO TO 700
      H(I-1,N)=HNEW(N)
      IF(IC(I,N).NE.-1) GO TO 650
```

```
      GO TO 640
  700 CONTINUE
C
C    COLUMN CALCULATIONS
C
      DO 703 L=2,NROWM1
  703 HNEW(L)=H(L,1)
      DO 800 KK=2,NCOL
      J=KK
      DO 720 I=2,NROWM1
      IF(K(I,J)) 705,720,705
  705 A=(KHARM(I,J,1)*YD(I))/AX(J)
      B=(KHARM(I,J+1,1)*YD(I))/AX(J+1)
      C=(KHARM(I,J,2)*XD(J))/AY(I)
      D=(KHARM(I+1,J,2)*XD(J))/AY(I+1)
      QPARM=(A+B+C+D)*PARM
      E=(C+D+QPARM)
      QKNOWN=A*H(I,J-1)+B*H(I,J+1)-(A+B-QPARM)*H(I,J)
      IF(I.EQ.2) GO TO 715
      IF(IC(I-1,J).EQ.-1) GO TO 710
      G(I)=(C*G(I-1)+QKNOWN)/(E-C*F(I-1))
      F(I)=D/(E-C*F(I-1))
      GO TO 720
  710 G(I)=(C*H(I-1,J)+QKNOWN)/E
      F(I)=D/E
      GO TO 720
  715 G(2)=QKNOWN/E
      F(2)=D/E
  720 CONTINUE
C CALCULATE HEADS BY BACK SUBSTITUTION
      N=NROWM1
      H(N,J-1)=HNEW(N)
      IF(IC(NROWM1,J).EQ.-1) GO TO 740
      HNEW(N)=G(N)
      GO TO 755
  740 HNEW(N)=H(N,J)
      GO TO 755
  750 HNEW(N)=G(N)+F(N)*HNEW(N+1)
  755 N=N-1
      IF(N.EQ.1) GO TO 757
      H(N,J-1)=HNEW(N)
      IF(IC(N,J).NE.-1) GO TO 750
      GO TO 740
  757 IF(J.EQ.NCOL) GO TO 800
      DO 770 I=2,NROWM1
      ET=DABS(HNEW(I)-HOLD(I,J))
      IF(ET.GT.ERR(IER)) GO TO 760
      GO TO 770
  760 ERR(IER)=ET
      IET=I
      JET=J
  770 CONTINUE
  800 CONTINUE
C
C CHECK CLOSURE CRITERIA FOR STEADY STATE
 1000 IF(IER.GE.ITMAX) GO TO 1045
      IF(ERR(IER).GT.EC) GO TO 400
C OTHERWISE  THE STEADY STATE HEADS HAVE BEEN COMPUTED
```

```
C
C COMPUTE HEADS AROUND THE PERIMETER OF THE MODEL
C THIS IS DONE TO GIVE A BETTER PLOT EFFECT
C
C ALONG TOP ROW
      DO 950 J=1,NCOL
  950 H(1,J)=H(2,J)
C
C ALONG BOTTOM ROW
      DO 960 J=1,NCOL
  960 H(NROW,J)=H(NROWM1,J)
C
C ALONG LEFT VERTICAL BOUNDARY
      DO 970 I=1,NROW
  970 H(I,1)=H(I,2)
C
C ALONG RIGHT VERTICAL BOUNDARY
      DO 980 I=1,NROW
  980 H(I,NCOL)=H(I,NCOLM1)
C
      WRITE(6,1005) (ERR(I),I=1,IER)
 1005 FORMAT('1',5X,'HEAD DIFFERENCE FOR EACH ITERATION',//,
     $(/,3X,10F12.5))
 1010 WRITE(6,1020) IER,ERR(IER),IET,JET
 1020 FORMAT('1',//,10X,'STEADY STATE HEAD MATRIX AFTER',I4,2X,'ITERATIO
     $NS',//,10X,'LARGEST HEAD DIFFERENCE =',E12.3,2X,'AT POINT',2X,'ROW
     $',I3,2X,'COLUMN',I3)
 1030 DO 1040 I=1,NROW
 1040 WRITE(6,200) I,(H(I,J),J=1,NCOL)
      IF(CONH.NE.CHECK(2)) GO TO 1100
      DO 1042 I=1,NROW
      DO 1042 J=1,NCOL
 1042 WRITE(11,2110) H(I,J)
      WRITE(6,1043)
 1043 FORMAT('0',4X,'***** HEADS WRITTEN ONTO DSN *****')
      GO TO 1100
C
 1045 WRITE(6,1055)
      WRITE(6,1005) (ERR(I),I=1,IER)
 1050 WRITE(6,1060) IER,ERR(IER),IET,JET
 1055 FORMAT('1','*********** ITERATIONS EXCEEDED *************')
 1060 FORMAT ('1',//,10X,'HEAD MATRIX AFTER',I4,2X,'ITERATIONS',//,10X,'
     $LARGEST HEAD DIFFERENCE =',E12.3,2X,'AT POINT',2X,'ROW',I3,2X,
     $'COLUMN',I3)
      DO 1070 I=1,NROW
 1070 WRITE(6,200) I,(H(I,J),J=1,NCOL)
      GO TO 3000
C
 1100 IF(ELEC.EQ.CHECK(3)) GO TO 1120
C OTHERWISE CONVERT PERMEABILITIES FROM FT/D TO CM/SEC
      CARITH=ARITHK*.0003528
      CHARM=HARMK*.0003528
      CGEOM=GEOMK*.0003528
C
      WRITE(6,1110) ARITHK,CARITH,GEOMK,CGEOM,HARMK,CHARM
 1110 FORMAT ('1',5X,'STATISTICAL MEANS OF THE PERMEABILITY',
     1' DISTRIBUTION',//,8X,'ARITHMATIC MEAN=',F10.4,1X,'FT/D',1X,
     2'=',1X,F10.6,1X,'CM/SEC',//,8X,'GEOMETRIC  MEAN=',F10.4,1X,'FT/D',
```

```
      31X,'=',1X,F10.6,,1X,'CM/SEC',//,8X,'HARMONIC   MEAN=',F10.4,1X,
      4'FT/D',1X,'=',1X,F10.6,1X,'CM/SEC')
       GO TO 1140
C
C CONVERT CONDUCTIVITIES TO RESISTIVITIES
 1120 ARITHK=1./HARMK
       GEOMK=1./GEOMK
       HARMK=1./ARITHK
       WRITE(6,1130) ARITHK,GEOMK,HARMK
 1130 FORMAT ('1',5X,'STATISTICAL MEANS OF THE RESISTIVITY ',
      1'DISTRIBUTION',//,8X,'ARITHMATIC MEAN=',F10.4,1X,'OHM-METERS',
      2//,8X,'GEOMETRIC  MEAN=',F10.4,1X,'OHM-METERS',//,8X,
      3'HARMONIC   MEAN=',F10.4,1X,'OHM-METERS')
C
 1140 IF(FLOW.EQ.CHECK(6)) GO TO 1300
       IF(WARP.EQ.CHECK(9).OR.FLOW.EQ.CHECK(10)) GO TO 1293
C
C
C
C OTHERWISE THE PREDOMINANT FLOW MUST BE HORIZONTAL
C COMPUTE THE EQUIVALENT HORIZONTAL PERMEABILITY
C
C
       Q=0.0
       AREA=0.0
C AREA= TOTAL CROSS SECTIONAL AREA THAT THE FLOW PASSES THROUGH
C
       DO 1200 I=2,NROWM1
       AREA=AREA+YD(I)
       Q=Q+(KHARM(I,LEQUIV,1)*((H(I,LEQUIV-1)-H(I,LEQUIV))/AX(LEQUIV))
      1*YD(I))
 1200 CONTINUE
C LENGTH=MACROSCOPIC LENGTH OVER WHICH THE TOTAL HEAD DIFFERENCE
C (DHEAD) IS DISSIPATED
C
       LENGTH=0.0
       DO 1250 J=3,NCOLM1
       LENGTH=LENGTH+AX(J)
 1250 CONTINUE
C
C KHEQFD=EQUIVALENT HORIZONTAL PERMEABILITY IN UNITS OF FT./DAY
       KHEQFD=(Q*LENGTH)/(DHEAD*AREA)
C KHEQCS=EQUIVALENT HORIZONTAL PERMEABILITY IN UNITS OF CM./SEC.
       KHEQCS=KHEQFD*.0003528
       IF(ELEC.EQ.CHECK(3)) GO TO 1290
C
C OTHERWISE WE HAVE THE HYDRAULIC CASE
       WRITE(6,1280)KHEQFD,KHEQCS,Q,LENGTH,AREA,DHEAD
 1280 FORMAT('0',/////,5X,'MACROSCOPIC PARAMETERS',//,8X,'EQUIVALENT ',
      1'HORIZONTAL PERMEABILITY=',F10.4,1X,'FT/D',1X,'=',F10.6,1X,
      2'CM/SEC',//,8X,'TOTAL FLOW=',F10.1,1X,'CFD',//,8X,'LENGTH=',F10.4,
      31X,'FT',//,8X,'AREA=',F10.4,1X,'SQ.FT.',//,8X,
      4'TOTAL DISSIPATED HEAD=',F10.4,1X,'FT.')
       GO TO 1400
 1290 KHEQFD=1/KHEQFD
C THE EQUIVALENT ELECTRICAL HORIZONTAL CONDUCTIVITY WAS CONVERTED TO
C  AN EQIVALENT HORIZONTAL ELECTRICAL RESISTIVITY
C CONVERT CURRENT FLOW TO AMPERES
```

```
      Q=Q/3.281
      WRITE(6,1292) KHEQFD,Q,LENGTH,AREA,DHEAD
 1292 FORMAT('0',/////,5X,'MACROSCOPIC PARAMETERS',//,8X,'EQUIVALENT',
     1' HORIZONTAL ELECTRICAL RESISTIVITY=',F10.4,1X,'OHM-METERS',//,8X,
     2'TOTAL CURRENT FLOW=',F10.6,1X,'AMPERES',//,8X,'LENGTH=',F10.3,1X,
     3'FT.',//,8X,'AREA=',F10.3,1X,'SQ.FT.',//,8X,'TOTAL VOLTAGE DROP=',
     4F10.4,1X,'VOLTS')
      GO TO 1400
C
C COMPUTE THE AQUIFER PERMEABILITY FOR POINT TO POINT FLOW USING
C THE METHOD SHOWN BY WARREN AND PRICE
C
 1293 FKI=0.0
      DO 1294 I=2,NROWM1
      FKI=FKI+KHARM(I,LEQUIV,1)*(H(I,LEQUIV-1)-H(I,LEQUIV))
 1294 CONTINUE
      KHEQFD=FKI/WPFACT
      WRITE(6,1298)
      IF(ELEC.EQ.CHECK(3)) GO TO 1296
      WRITE(6,1295) FKI,KHEQFD
      GO TO 1400
 1295 FORMAT ('0',5X,'FKI=',1X,F10.2,1X,'FT**2/D',///,5X,
     1'AQUIFER PERMEABILITY=',1X,F10.3,1X,'FT/D')
C
 1296 KHEQFD=1./KHEQFD
      WRITE(6,1297) FKI,KHEQFD
 1297 FORMAT ('0',///,5X,'FKI=',1X,F10.6,1X,'VOLT/OHM-M',///,5X,
     1'AQUIFER RESISTIVITY=',1X,F10.2)
 1298 FORMAT ('0',/////,5X,'MACROSCOPIC TRANSPORT PROPERTIES',
     1' WERE COMPUTED BY THE WARREN & PRICE TECHNIQUE')
C
      GO TO 1400
C
C HERE THE PREDOMINANT FLOW IS VERTICAL
C COMPUTE THE EQUIVALENT VERTICAL PERMEABILITY
C
 1300 IF(WARP.EQ.CHECK(9)) GO TO 1393
      Q=0.0
      AREA=0.0
      DO 1350 J=2,NCOLM1
      AREA=AREA+XD(J)
      Q=Q+(KHARM(LEQUIV,J,2)*((H(LEQUIV-1,J)-H(LEQUIV,J))/AY(LEQUIV))
     1*XD(J))
 1350 CONTINUE
C
C LENGTH= MACROSCOPIC LENGTH OVER WHICH THE TOTAL HEAD DIFFERENCE
C (DHEAD) IS DISSIPATED
C COMPUTE LENGTH
      LENGTH=0.0
      DO 1370 I=3,NROWM1
      LENGTH=LENGTH+AY(I)
 1370 CONTINUE
C
C  KVEQFD= EQUIVALENT VERTICAL PERMEABILITY IN UNITS OF FT./DAY
      KVEQFD=(Q*LENGTH)/(DHEAD*AREA)
C KVEQCS= EQUIVALENT VERTICAL PERMEABILITY IN UNITS OF CM./SEC.
      KVEQCS=KVEQFD*.0003528
      IF(ELEC.EQ.CHECK(3)) GO TO 1390
```

```
      WRITE(6,1380) KVEQFD,KVEQCS,Q,LENGTH,AREA,DHEAD
 1380 FORMAT('0',/////,5X,'MACROSCOPIC PARAMETERS',//,8X,'EQUIVALENT ',
     1'VERTICAL PERMEABILITY=',F10.4,1X,'FT/D',1X,'=',F10.6,1X,
     2'CM/SEC',//,8X,'TOTAL FLOW=',F10.1,1X,'CFD',//,8X,'LENGTH=',F10.4,
     31X,'FT',//,8X,'AREA=',F10.4,1X,'SQ.FT.',//,8X,
     4'TOTAL DISSIPATED HEAD=',F10.4,1X,'FT.')
C
      GO TO 1400
C
C THE EQUIVALENT VERTICAL ELECTRICAL CONDUCTIVITY IS CONVERTED TO
C THE EQUIVALENT VERTICAL ELECTRICAL RESISTIVITY
 1390 KVEQFD=1/KVEQFD
C
C CONVERT CURRENT FLOW TO AMPERES
      Q=Q/3.281
      WRITE(6,1392) KVEQFD,Q,LENGTH,AREA,DHEAD
 1392 FORMAT('0',/////,5X,'MACROSCOPIC PARAMETERS',//,8X,'EQUIVALENT',
     1' VERTICAL ELECTRICAL RESISTIVITY=',F10.4,1X,'OHM-METERS',//,8X,
     2'TOTAL CURRENT FLOW=',F10.6,1X,'AMPERES',//,8X,'LENGTH=',F10.3,1X,
     3'FT.',//,8X,'AREA=',F10.3,1X,'SQ.FT.',//,8X,'TOTAL VOLTAGE DROP=',
     4F10.4,1X,'VOLTS')
      GO TO 1400
C
C COMPUTE THE AQUIFER PERMEABILITY FOR VERT. FLOW USING
C THE METHOD SHOWN BY WARREN AND PRICE
 1393 FKI=0.0
      DO 1394 J=2,NCOLM1
      FKI=FKI+KHARM(LEQUIV,J,2)*(H(LEQUIV-1,J)-H(LEQUIV,J))
 1394 CONTINUE
      KVEQFD=FKI/WPFACT
      WRITE(6,1398)
      IF(ELEC.EQ.CHECK(3)) GO TO 1396
      WRITE(6,1395) FKI,KVEQFD
      GO TO 1400
 1395 FORMAT ('0',5X,'FKI=',1X,F10.2,1X,'FT**2/D',///,5X,
     1'AQUIFER PERMEABILITY=',1X,F10.3,1X,'FT/D')
C
 1396 KVEQFD=1./KVEQFD
      WRITE(6,1397) FKI,KVEQFD
 1397 FORMAT ('0',///,5X,'FKI=',1X,F10.6,1X,'VOLT/OHM-M',///,5X,
     1'AQUIFER RESISTIVITY=',1X,F10.2)
 1398 FORMAT ('0',/////,5X,'MACROSCOPIC TRANSPORT PROPERTIES',
     1' WERE COMPUTED BY THE WARREN & PRICE TECHNIQUE')
C
 1400 IF(STRF.NE.CHECK(5)) GO TO 3000
C OTHERWISE COMPUTE THE STREAM FUNCTION FROM THE
C STEADY STATE HEADS
C
C BRANCH TO THE APPROPRIATE LOCATION TO COMPUTE THE STREAM FUNCTION
C DEPENDING ON THE FLOW TYPE (HORIZONTAL,VERTICAL OR POINT TO POINT).
C
      IF(FLOW.EQ.CHECK(6)) GO TO 2500
      IF(FLOW.EQ.CHECK(10)) GO TO 2560
C
C OTHERWISE THE FLOW IS PREDOMINATELY HORIZONTAL
C SET BOTTOM ROW STREAM FUNCTION VALUES TO ZERO
      DO 1500 J=1,NCOLM1
 1500 STRFUN(NROWM1,J)=0.0
```

```
C
C
C COMPUTE INTERIOR VALUES OF THE STREAM FUNCTION MOVING ALONG
C SUCCESSIVE COLUMNS FROM THE BOTTOM STREAMLINE
C
      DO 1800 J=2,NCOLM2
      DO 1800 I=2,NROWM1
      II=NROW-I
      STRFUN(II,J)=STRFUN(II+1,J)+(KHARM(II+1,J+1,1)*((H(II+1,J)-
     $H(II+1,J+1))/AX(J+1))*YD(II+1))
 1800 CONTINUE
C
C SET THE VALUES OF STRFUN(I,1) AND STRFUN(I,NCOLM1) TO
C PRODUCE A BETTER PLOT EFFECT
C
      DO 1850 I=1,NROWM1
      STRFUN(I,1)=STRFUN(I,2)
 1850 STRFUN(I,NCOLM1)=STRFUN(I,NCOLM2)
C
C NONDIMENSIONALIZE THE STREAM FUNCTION
C
      STRNOR=STRFUN(1,LSTRM)
      DO 1900 I=1,NROWM1
      DO 1900 J=1,NCOLM1
 1900 STRFUN(I,J)=(STRFUN(I,J)/STRNOR)*100.
C
C WRITE OUT THE VALUES OF THE NONDIMENSIONALIZED STREAM FUNCTION
C
      WRITE(6,2100)
 2100 FORMAT('1',5X,'STREAM FUNCTION VALUES')
      DO 2000 I=1,NROWM1
 2000 WRITE(6,2640) I,(STRFUN(I,J),J=1,NCOLM1)
C
C WRITE STREAM FUNCTION VALUES ONTO DSN
      DO 2200 I=1,NROWM1
      DO 2200 J=1,NCOLM1
 2200 WRITE(13,2110) STRFUN(I,J)
 2110 FORMAT(30X,F10.5)
      WRITE(6,2300)
 2300 FORMAT ('0','*** STREAM FUNCTION VALUES WRITTEN ONTO DSN ***')
C
      GO TO 3000
C
C
C COMPUTE STREAM FUNCTION FOR VERTICAL FLOW
C SET RIGHT SIDE STREAM FUNCTION VALUES TO ZERO
C
 2500 DO 2510 I=1,NROWM1
 2510 STRFUN(I,NCOLM1)=0.0
C
C COMPUTE INTERIOR VALUES OF THE STREAM FUNCTION MOVING ALONG
C SUCCESSIVE ROWS FROM THE RIGHT SIDE STREAM LINE
C WHERE THE STREAM FUNCTION IS EQUAL TO ZERO
C
C
      DO 2520 I=2,NROWM2
      DO 2520 J=2,NCOLM1
      JJ=NCOL-J
```

```
      STRFUN(I,JJ)=STRFUN(I,JJ+1)+(KHARM(I+1,JJ+1,2)*((H(I,JJ+1)-
     1H(I+1,JJ+1))/AY(I+1))*XD(JJ+1))
 2520 CONTINUE
C
C SET THE VALUES OF STRFUN(1,J) AND STRFUN(NROWM1,J) TO
C PRODUCE A BETTER PLOT EFFECT
      DO 2525 J=1,NCOLM1
      STRFUN(1,J)=STRFUN(2,J)
 2525 STRFUN(NROWM1,J)=STRFUN(NROWM2,J)
C
C NONDIMENSIONALIZE THE STREAM FUNCTION
C
      STRNOR=STRFUN(LSTRM,1)
      DO 2530 I=1,NROWM1
      DO 2530 J=1,NCOLM1
 2530 STRFUN(I,J)=(STRFUN(I,J)/STRNOR)*100.
C
C WRITE THE VALUES OF THE NONDIMENSIONALIZED STREAM FUNCTION
C
      WRITE(6,2100)
      DO 2540 I=1,NROWM1
 2540 WRITE(6,200) I,(STRFUN(I,J),J=1,NCOLM1)
C
C WRITE STREAM FUNCTION VALUES ONTO DATA SET
C
      DO 2550 I=1,NROWM1
      DO 2550 J=1,NCOLM1
 2550 WRITE(13,2110) STRFUN(I,J)
      WRITE(6,2300)
C
      GO TO 3000
C
C
C COMPUTE STREAM FUNCTION FOR POINT TO POINT FLOW
C SET RIGHT SIDE STREAM FUNCTION VALUES TO ZERO
C
 2560 DO 2570 I=2,NROWM2
      STRFUN(I,1)=0.0
 2570 STRFUN(I,NCOLM1)=0.0
C
C COMPUTE INTERIOR VALUES OF THE STREAM FUNCTION MOVING ALONG
C SUCCESSIVE ROWS FROM THE RIGHT SIDE STREAM LINE
C WHERE THE STREAM FUNCTION IS EQUAL TO ZERO
C
C
      DO 2600 I=2,NROWM2
      DO 2600 J=2,NCOLM2
      JJ=NCOL-J
      Q1=KHARM(I+1,JJ+1,2)*((H(I+1,JJ+1)-H(I,JJ+1))
     1/AY(I+1))*XD(JJ+1)
 2600 STRFUN(I,JJ)=STRFUN(I,JJ+1)+Q1
C
C COMPUTE TOTAL INFLOW AND OUTFLOW AT THE
C CONSTANT HEAD NODES IN ROW 2
C
      QIN=0.0
      QOUT=0.0
      DO 2606 J=2,NCOLM1
```

```
      IF(IC(2,J).GE.0) GO TO 2606
C OTHERWISE COMPUTE FLOW THROUGH THE LEFT(QL), RIGHT(QR)
C AND BOTTOM(QB) FACES OF THE CONSTANT HEAD NODE
      QL=KHARM(2,J,1)*(H(2,J)-H(2,J-1))/AX(J)*YD(2)
      QR=KHARM(2,J+1,1)*(H(2,J)-H(2,J+1))/AX(J+1)*YD(2)
      QB=KHARM(3,J,2)*(H(2,J)-H(3,J))/AY(3)*XD(J)
      QNODE=QL+QR+QB
      IF(QNODE.LT.0.0) GO TO 2604
C OTHERWISE INFLOW OCCURS AT THE NODE
      QIN=QIN+QNODE
      GO TO 2606
C OUTFLOW OCCURS AT THE NODE
 2604 QOUT=QOUT+QNODE
 2606 CONTINUE
C
C SET STREAM FUNCTION VALUES OF ROW 1
C THIS IS VALID ONLY WHEN ALL INFLOW IS FROM ONE NODE
C AND ALL OUTFLOW LEAVES AT ONE NODE
      LSTRM1=LSTRM-1
      DO 2608 J=1,LSTRM1
      JJ=NCOL-J
      STRFUN(1,J)=0.0
 2608 STRFUN(I,JJ)=0.0
      J1=LSTRM
      J2=NCOL-J1
      DO 2609 J=J1,J2
 2609 STRFUN(1,J)=QIN
C
C MAKE THE BOTTOM ROW OF THE STREAM FUNCTION= 0.0
C
      DO 2610 J=1,NCOLM1
 2610 STRFUN(NROWM1,J)=0.0
C
C NONDIMENSIONALIZE THE STREAM FUNCTION
C AS BASED ON THE TOTAL INFLOW
      DO 2620 I=1,NROWM1
      DO 2620 J=1,NCOLM1
 2620 STRFUN(I,J)=(STRFUN(I,J)/QIN)*100.
C
C WRITE THE VALUES OF THE NONDIMENSIONALIZED STREAM FUNCTION
C
      WRITE(6,2100)
      DO 2630 I=1,NROWM1
 2630 WRITE(6,2640) I,(STRFUN(I,J),J=1,NCOLM1)
 2640 FORMAT ('0',I2,2X,10F12.3/(5X,10F12.3))
C
      WRITE(6,2650) QIN,QOUT
 2650 FORMAT ('0',3X,'FLOW INTO THE MODEL=',F12.2,//,
     13X,'FLOW OUT OF THE MODEL=',F12.3)
C
C WRITE STREAM FUNCTION VALUES ONTO DATA SET
C
      DO 2660 I=1,NROWM1
      DO 2660 J=1,NCOLM1
 2660 WRITE(13,2670) STRFUN(I,J)
 2670 FORMAT (30X,F10.4)
      WRITE(6,2300)
C

 3000 STOP
      END
```

Appendix L

2-D Radial Flow Program

To convert the 2-D cartesian coordinate program into a 2-D radial symetric flow program in (r, z) coordinates the following modifications were made.

1) The expressions for a, b, c and d in the basic equation are changed to those used in equations 51 or 53.

2) Provisions are made to use equations 55 or 56 when at a well node.

3) Connection permeabilities in the r-direction are computed by the appropriate form of equation 62.

The program will solve for steady state potentials when constant potentials are located anywhere in the 2-D section; however, the stream function and aquifer permeability algorithm apply only when radial (or quasi-radial) flow occurs. Partial penetration problems should also work by these algorithms.

Modification to the users guide of appendix K and a listing of the radial flow program follow.

DATA DECK PREPARATION

The data deck instructions for the radial flow program are the same as the linear flow program instructions in appendix K, with the exception of the following:

CARD	COLUMNS	FORMAT	VARIABLE	DESCRIPTION
CD 3	1 - 5	A4, 1X	CONH	punch CONH to write total head values onto disk
	6 - 10	A4, 1X	CONK	punch CONK to write permeability values onto disk
	11 - 15	A4, 1X	ELEC	punch, ELEC to convert permeabilities to electrical conductivities
	16 - 20	A4, 1X	MINI	punch MINI to read in the minimum iteration value
	21 - 25	A4, 1X	STRF	punch STRF to compute and write onto disk, the streamfunction values
	26 - 30	A4, 1X	SKIP	punch SKIP to truncate output
CARD SET				
CS 1	1 - 80	8F10.1	RD (J)	nodal spacing in the r - direction
CS 2	1 - 80	8F10.1	2D (I)	nodal spacing in the z - direction

Radial Program (r,z) coordinates

```
C  2-D STEADY, HETEROGENEOUS, ANISOTROPIC FLOW THROUGH POROUS MEDIA
C USING FINITE DIFFERENCE WITH VARIABLE GRID SPACINGS
C AND THE ITERATIVE ALTERNATING DIRECTION IMPLICIT PROCEDURE
C
C SPECIFICATIONS
      INTEGER CHECK,CONH,CONK,ELEC,MINI,STRF,SKIP,UNILO,UNIHI
      INTEGER EXLO,EXHI
      REAL K,KCONN,LENGTH,KHEQFD,KVEQFD,KVEQCS,KHEQCS,HARMK,MEAN,KLOG
      REAL KY
      DOUBLE PRECISION H,HNEW,A,B,C,D,E,F,G,QPARM,QKNOWN,DABS,HOLD
      DOUBLE PRECISION ITPARM
      REAL*8 DSEED/992299.D0/
      DIMENSION KCONN(50,50,2),H(50,50),K(50,50),RD(50),ZD(50),AR(50),
     $AZ(50),HEADIN(20),ANISO(50),CHECK(7),ERR(300)
      DIMENSION G(50),F(50),IC(50,50),HNEW(50),ITPARM(50),HOLD(50,50),
     $STRFUN(50,50),HSTRAT(50,50),KY(50,50),R(50)
      DATA CHECK/'CONK','CONH','ELEC','MINI','STRF','SKIP','V'/
      READ(5,10) HEADIN
   10 FORMAT (20A4)
      WRITE(6,20) HEADIN
      WRITE(6,25) DSEED
   25 FORMAT ('0',/,5X,'DSEED=',F12.0)
   20 FORMAT ('1',20X,20A4)
C
C INPUT PARAMETERS
C NOTE**** ALL INPUT PARAMETERS ARE NODAL VALUES****
C
      READ(5,30) NROW,NCOL,EC,ISO,PERM
      READ(5,35) CONH,CONK,ELEC,MINI,STRF,SKIP
      READ(5,30) LSTRM,LEQUIV,DHEAD
C WPFACT IS THE FACTOR WARREN & PRICE USE TO COMPUTE THE
C EQUIVALENT PERMEABILITY- IT IS THE SUM OF THE CHANGES IN HEAD
C THROUGH A COLUMN OF THE STEADY HEAD MATRIX FOR THE ISOTROPIC
C AND CONSTANT PERMEABILITY THROUGHOUT - CONDITIONS
      READ(5,40) WPFACT
C LSTRM IS THE COLUMN
C WHERE THE TOTAL FLOW IS COMPUTED FOR THE USE OF NONDIMENSIONALIZING
C THE STREAM FUNCTION *** IT IS USED ONLY WHEN CHECK(5)=STRF
C
C LEQUIV IS THE COLUMN
C WHERE THE TOTAL FLOW IS COMPUTED TO BE USED IN SOLVING
C FOR THE EQUIVALENT PERMEABILITY (RESISTIVITY).
      NROWM1=NROW-1
      NCOLM1=NCOL-1
      NROWM2=NROW-2
      NCOLM2=NCOL-2
C NOTE **** THE VALUE READ IN FOR HMIN IS THE LOWEST ITERATION
C PARAMETER AND IS USED ONLY IF MINI WAS SPECIFIED IN THE OPTIONS
      READ(5,32) ITMAX,NUMPAR,HMAX,HMIN
   30 FORMAT (2I10,1F10.5,I10,F10.5)
   32 FORMAT (2I10,2F10.5)
   33 FORMAT (3I10,1F10.5)
   35 FORMAT(16(A4,1X))
```

```
      READ(5,40)  (RD(J),J=1,NCOL)
   40 FORMAT (8F10.1)
      READ(5,40)  (ZD(I),I=1,NROW)
C COMPUTE AR AND AZ
C AR= R-DISTANCE FROM ONE NODE CENTER TO THE NEXT
C AZ= Z-DISTANCE FROM ONE NODE CENTER TO THE NEXT
C
      DO 42 J=2,NCOL
   42 AR(J)= (RD(J)+RD(J-1))/2.0
      DO   44 I=2,NROW
   44 AZ(I)=(ZD(I)+ZD(I-1))/2.0
C
C COMPUTE R(J) VALUES
C R(J) IS THE RADIUS TO THE J'TH NODE CENTER
      R(1)=-AR(2)
      R(2)=0.0
      DO 46 J=3,NCOL
   46 R(J)=R(J-1)+AR(J)
C
      IF(ISO.EQ.1) GO TO 80
      IF(ISO.EQ.2) GO TO 91
      IF(ISO.EQ.3) GO TO 50
      IF(ISO.EQ.4) GO TO 84
      IF(ISO.EQ.5) GO TO 60
C OTHERWISE
C  READ VALUES FOR A LAYERED DETERMINISTIC MODEL
C
      READ(5,35) LAYTY
      READ(5,96) LAYERS
      IF(LAYTY.EQ.CHECK(7)) GO TO 78
C OTHERWISE THE MODEL IS HORIZONTALLY LAYERED
      DO 76 IL=1,LAYERS
      READ(5,73) LAYLO,LAYHI,PERM
   73 FORMAT(2I10,F10.2)
      DO 76 I=LAYLO,LAYHI
      DO 76 J=2,NCOLM1
      K(I,J)=PERM
   76 CONTINUE
      GO TO 95
C
C THE MODEL IS VERTICALLY LAYERED
   78 DO 79 IL=1,LAYERS
      READ(5,73) LAYLO,LAYHI,PERM
      DO 79 I=2,NROWM1
      DO 79 J=LAYLO,LAYHI
      K(I,J)=PERM
   79 CONTINUE
      GO TO 95
C
C
C PERMEABILITY VALUES HAVE A LOG NORMAL DISTRIBUTION
C OVER THE ENTIRE REGION
   50 READ(5,40) MEAN,SDEV
      WRITE(6,51) MEAN,SDEV
   51 FORMAT ('0',/,5X,'PERMEABILITIES ARE LOG NORMALLY DISTRIBUTED',
     $' OVER THE ENTIRE REGION',/,75X,'MEAN=',F10.5,
     $/,75X,'STNDRD. DEV. =',F10.5)
      DO 54 I=2,NROWM1
```

```
      DO 54 J=2,NCOLM1
C FIRST PICK A NORMAL DEVIATE
   52 YFL=GGNQF(DSEED)
C THEN CONVERT N 0,1  DEVIATE TO N MEAN,SDEV  DEVIATE
      KLOG=SDEV*YFL+MEAN
C VALUE KLOG= LOG OF K
      K(I,J)=10**KLOG
   54 CONTINUE
      GO TO 95
C
C
C PERMEABILITIES ARE READ IN AT EACH NODE
   60 READ(5,40)  ((K(I,J),J=1,NCOL),I=1,NROW)
      GO TO 95
C
C PERMEABILITY  VALUES ARE ALL THE SAME
   80 DO 82 I=1,NROW
      DO 82 J=1,NCOL
   82 K(I,J)= PERM
      GO TO 95
C
C PERMEABILITY VALUES HAVE AN EXPONENTIAL DISTRIBUTION
C OVER THE ENTIRE REGION
C EXLO= MINIMUM LOG OF K VALUE *100
C EXHI= MAXIMUM LOG OF K VALUE *100
C        THE HIGHEST VALUE FOR EXHI IS 300
   84 READ(5,96) EXLO,EXHI
      DO 88 I=1,NROW
      DO 88 J=1,NCOL
   86 YFL=GGUBFS(DSEED)
      NUM=INT(YFL*1000.)
      IF(NUM.LT.EXLO) GO TO 86
      IF(NUM.GT.EXHI) GO TO 86
      XNUM=FLOAT(NUM)/100.
      K(I,J)=10**XNUM
   88 CONTINUE
      GO TO 95
C
C THE PERMEABILITY VALUES ARE UNIFORMLY DISTRIBUTED
C WITH A DIFFERENT DISTRIBUTION WITHIN EACH OF THE LAYERS
   91 READ(5,96) LAYERS
      DO 93 IL=1,LAYERS
      READ(5,96)UNILO,UNIHI,LAYLO,LAYHI
      WRITE(6,94) UNILO,UNIHI,LAYLO,LAYHI
      XER=1000.
      IF(UNIHI.LE.100) XER=100.
      DO 93 I=LAYLO,LAYHI
      DO 93 J=2,NCOLM1
   92 YFL=GGUBFS(DSEED)
      NUM=INT(YFL*XER)
      IF(NUM.LT.UNILO) GO TO 92
      IF(NUM.GT.UNIHI) GO TO 92
      K(I,J)=FLOAT(NUM)
   93 CONTINUE
   94 FORMAT ('0',/,5X,'PERMEABILITY RANGE FOR UNIFORM DISTRIBUTION=',
     1I6,2X,'TO',I6,1X,'FT/D',1X,'FOR LAYERS',1X,I2,1X,'TO',1X,I2)
   96 FORMAT (4I10)
C
```

```
C
   95 DO 100 I=1,NROW
      K(I,1)=0.0
  100 K(I,NCOL)=0.0
      DO 110 J=1,NCOL
      K(1,J)=0.0
  110 K(NROW,J)=0.0
C
C
C READ ANISOTROPY AT EACH ROW
C  VALUE IS THE RATIO OF KH/KV
  120 READ(5,40)  (ANISO(I),I=1,NROW)
C
C
C COMPUTE KY(I,J) VALUES
C THESE ARE THE NODAL VALUES TO BE USED IN COMPUTING
C KCONN(I,J,2) --THE CONNECTION VALUE IN THE Z-DIRECTION
      DO 112 I=2,NROWM1
      DO 112 J=2,NCOLM1
  112 KY(I,J)=K(I,J)/ANISO(I)
C CONVERT HYDRAULIC CONDUCTIVITIES TO ELECTRICAL CONDUCTIVITIES IF SPECIFIED
      IF(ELEC.NE.CHECK(3))GO TO 117
      DO 115 I=2,NROWM1
      DO 115 J=2,NCOLM1
      KY(I,J)=1/(((KY(I,J)*.0003528)/5.13E-06)**.7)
  115 K(I,J)=1/(((K(I,J)*.0003528)/5.13E-06)**.7)
C
C COMPUTE THE ARITHMATIC,HARMONIC AND GEOMETRIC MEANS OF THE
C PERMEABILITY(CONDUCTIVITY) DISTRIBUTION
C
  117 SUMK=0.0
      RECIPK=0.0
      PRODK=0.0
      DO 119 I=2,NROWM1
      DO 119 J=2,NCOLM1
      SUMK=SUMK+K(I,J)
      RECIPK=RECIPK+(1./K(I,J))
      PRODK=PRODK+ALOG10(K(I,J))
  119 CONTINUE
      XROWM2=FLOAT(NROWM2)
      XCOLM2=FLOAT(NCOLM2)
      ARITHK=SUMK/(XROWM2*XCOLM2)
      HARMK=(XROWM2*XCOLM2)/RECIPK
      GEOMK=10**(PRODK/(XROWM2*XCOLM2))
C
C PERMEABILITY(CONDUCTIVITY) VALUES ARE WRITTEN ONTO A DISK DATA SET
C              TO BE USED WITH PLOTTING
      IF(CONK.NE.CHECK(1)) GO TO 130
      DO 105 I=2,NROWM1
      DO 105 J=2,NCOLM1
      WRITE(10,2110) K(I,J)
  105 CCNTINUE
C
C ECHO CHECK OF INPUT PARAMETERS
C
  130 WRITE(6,140) NROW,NCOL,EC,ITMAX
  140 FORMAT ('0',4X,'# OF ROWS =',T25,I5,/,5X,'# OF CCLUMNS =',T25,I5,/
     $///,5X,'CLOSURE ERROR CRITERIA=',  E16.5   ,5X,'MAXIMUM ITERATIONS
```

```
     $=',I5)
      WRITE(6,148) CONH,CONK,ELEC,MINI,STRP,SKIP
  148 FORMAT ('0',/,5X,'PROBLEM OPTIONS SPECIFIED:',2X,10A8)
      IF(SKIP.EQ.CHECK(6)) GO TO 175
      WRITE(6,150)
      WRITE(6,160)  (RD(J),J=1,NCOL)
  150 FORMAT ('0',/,5X,'DELTA-R (DR) NODAL VALUES')
  160 FORMAT ('0',4X,10F12.1/(5X,10F12.1))
      WRITE(6,170)
      WRITE(6,160) (ZD(I),I=1,NROW)
  170 FORMAT ('0',5X,'DELTA-Z (DZ) NODAL VALUES')
  175 WRITE(6,180)
  180 FORMAT ('1',5X,'HORIZONTAL PERMEABILITY VALUES AT NODE CENTER')
      DO 190 I=1,NROW
  190 WRITE(6,200) I,(K(I,J),J=1,NCOL)
  200 FORMAT ('0',I2,2X,10F12.6/(5X,10F12.6))
  210 FORMAT ('0',I2,2X,10I10/(5X,10I10))
      WRITE(6,220)
  220 FORMAT ('0',5X,'ANISOTROPY RATIO KH/KV')
      WRITE(6,160) (ANISO(I),I=1,NROW)
C
C WRITE AR AND AZ
C
      IF(SKIP.EQ.CHECK(6)) GO TO 261
      WRITE(6,250)
  250 FORMAT('0',5X,'AR VALUES')
      WRITE(6,160)  (AR(J),J=2,NCOL)
      WRITE(6,260)
  260 FORMAT ('0',5X,'AZ VALUES')
      WRITE(6,160) (AZ(I),I=2,NROW)
C
C WRITE R VALUES
C
  261 IF(SKIP.EQ.CHECK(6)) GO TO 262
      WRITE(6,265)
  265 FORMAT ('0',5X,'R VALUES')
      WRITE(6,160)  (R(J),J=1,NCOL)
C
C COMPUTE KCONN(I,J,1) AND KCONN(I,J,2)
C KCONN(I,J,1)= CONNECTION VALUE OF THE PERMEABILITIES AT ADJACENT NODES
C IN THE R DIRECTION
C KCONN(I,J,2)= CONNECTION VALUE OF THE PERMEABILITIES AT ADJACENT NODES
C IN THE Z DIRECTION
C
  262 DO 270 I=2,NROWM1
      KCONN(I,2,1)=0.0
      KCONN(I,NCOL,1)=0.0
      KCONN(I,3,1)=((R(3)+RD(3)/2.)*K(I,2)*K(I,3)*(RD(2)/4.)
     1*R(3))/(((RD(2)/2.)*K(I,3)*R(3)+RD(3)*K(I,2)*(RD(2)/4.
     2))*RD(2)/2.)
      DO 270 J=4,NCOLM1
C NOTE ***  (R(J-1)+RD(J-1)/2.) IS THE RADIUS WHERE THE
C            CONNECTION PERMEABILITY IS COMPUTED
  270 KCONN(I,J,1)=(((R(J)+RD(J)/2.)-(R(J-1)-RD(J-1)/2.))*K(I,J-1)*
     1K(I,J)*R(J-1)*R(J))/((RD(J-1)*K(I,J)*R(J)+RD(J)*K(I,J-1)*R(J-1)
     2)*(R(J-1)+RD(J-1)/2.))
      DO 280 I=2,NROW
      DO 280 J=2,NCOLM1
```

```
  280 KCONN(I,J,2)=((ZD(I+1)+ZD(I))*KY(I-1,J)*KY(I,J))
     $/(KY(I,J)*ZD(I-1)+KY(I-1,J)*ZD(I))
C
C WRITE VALUES OF KCONN
C
      IF(SKIP.EQ.CHECK(6)) GO TO 325
      WRITE(6,290)
  290 FORMAT ('1',//,5X,'VALUES OF KCONN I,J,1')
      DO 300 I=2,NROWM1
  300 WRITE(6,200) I,(KCONN(I,J,1),J=2,NCOL)
      WRITE(6,310)
  310 FORMAT ('1',//,5X,'VALUES OF KCONN I,J,2')
      DO 320 I=2,NROW
  320 WRITE(6,200) I,(KCONN(I,J,2),J=2,NCOLM1)
C
C
C SET BOUNDARY CONDITIONS
C NOTE *** PERIMETER BOUNDARY POINTS CAN BE EITHER CONSTANT HEAD OR IMPERMEABLE
C NOTE *** FLOW MUST BE FROM RIGHT TO LEFT
C I.E.  HIGH HEADS SHOULD BE LOCATED ON THE LEFT SIDE
C
C SET ALL HEADS EQUAL TO SOME INITIAL VALUE
C AND ALL IC(I,J) VALUES TO ZERO
  325 DO 330 I=1,NROW
      DO 330 J=1,NCOL
      IC(I,J)=0
  330 H(I,J)= 50.0
C
C READ LOCATIONS OF CONSTANT HEAD NODES
C ALONG THE PERIMETER
C NOTE: THE PERIMETER IS THE ONLY LOCATION FOR A SOURCE OR A SINK
C THAT IS -- A HIGH CONSTANT HEAD OR A LOW CONSTANT HEAD
C
C READ THE TOP ROW
      READ(5,336)  (IC(2,J),J=2,NCOLM1)
  336 FORMAT (16I5)
C READ THE BOTTOM ROW
      READ(5,336)  (IC(NROWM1,J),J=2,NCOLM1)
C READ THE LEFT SIDE
      READ(5,336)  (IC(I,2),I=3,NROWM2)
C READ THE RIGHT SIDE
      READ(5,336)  (IC(I,NCOLM1),I=3,NROWM2)
C
C READ HEAD VALUES ALONG THE PERIMETER
C READ TOP ROW
      READ(5,350)  (H(2,J),J=2,NCOLM1)
C READ THE BOTTOM ROW
      READ(5,350)  (H(NROWM1,J),J=2,NCOLM1)
C READ THE LEFT SIDE
      READ(5,350)  (H(I,2),I=3,NROWM2)
C READ THE RIGHT SIDE
      READ(5,350)  (H(I,NCOLM1),I=3,NROWM2)
  350 FORMAT (8D10.3)
C
C WRITE STARTING HEAD MATRIX
      IF(SKIP.EQ.CHECK(6)) GO TO 392
      WRITE(6,360)
  360 FORMAT('1',//,5X,'STARTING HEAD MATRIX')
```

```
      DO 370 I=1,NROW
  370 WRITE(6,200) I,(H(I,J),J=1,NCOL)
      WRITE(6,380)
  380 FORMAT('1',//,5X,'CONSTANT HEAD NODES')
      DO 390 I=1,NROW
  390 WRITE(6,210) I,(IC(I,J),J=1,NCOL)
C
  392 IF(MINI.EQ.CHECK(4)) GO TO 396
      HMIN=2.
      XVAL=3.1415**2/(2.*NCOL**2)
      YVAL=3.1415**2/(2.*NROW**2)
      DO 395 I=2,NROW
      DO 395 J=2,NCOL
      IF(K(I,J).EQ.0.0) GO TO 395
      XPART=XVAL*(1/(1+RD(J)**2/ZD(I)**2*ANISO(I)))
      YPART=YVAL*(1/(1+ZD(I)**2*ANISO(I)/RD(J)**2))
      HMIN=AMIN1(HMIN,XPART,YPART)
  395 CONTINUE
  396 ALPHA=EXP(ALOG(HMAX/HMIN)/(NUMPAR-1))
      ITPARM(1)=HMIN
      DO 397 NTIME=2,NUMPAR
  397 ITPARM(NTIME)=ITPARM(NTIME-1)*ALPHA
      WRITE(6,398) NUMPAR,(ITPARM(J),J=1,NUMPAR)
  398 FORMAT ('0',3X,I5,2X,'ITERATION PARAMETERS:',6D12.3,//,6X,10D12.3)
      IF(MINI.EQ.CHECK(4)) WRITE(6,399)
  399 FORMAT ('0',2X,'NOTE--MINIMUM ITERATION PARAMETER WAS SET')
C
      IER=0
  400 CONTINUE
C SOLUTION ALGORITHM USING THE ITERATIVE ALTERNATING DIRECTION IMPLICIT PROC.
      DO 500 I=1,NROW
      DO 500 J=1,NCOL
  500 HOLD(I,J)=H(I,J)
      DO 510 L=2,NCOLM1
  510 HNEW(L)=H(1,L)
      IF (MOD(IER,NUMPAR))520,520,530
  520 NTH=0
  530 NTH=NTH+1
      PARM=ITPARM(NTH)
C
      IER=IER+1
      ERR(IER)=0.0
C
C     ROW CALCULATIONS
C
      DO 700 I=2,NROW
      DO 620 J=2,NCOLM1
      IF(K(I,J).EQ.0..OR.IC(I,J).EQ.-1) GO TO 620
  605 IF(J.NE.2) GO TO 606
      A=0.0
      B=(KCONN(I,3,1)*(RD(2)/2.)*ZD(I))/AR(3)
      C=(KCONN(I,2,2)*((RD(J)/2.)**2)/2.)/AZ(I)
      D=(KCONN(I+1,2,2)*((RD(J)/2.)**2)/2.)/AZ(I+1)
      GO TO 608
  606 A=(KCONN(I,J,1)*(R(J-1)+RD(J-1)/2.)*ZD(I))/AR(J)
      B=(KCONN(I,J+1,1)*(R(J)+RD(J)/2.)*ZD(I))/AR(J+1)
      C=(KCONN(I,J,2)*R(J)*RD(J))/AZ(I)
      D=(KCONN(I+1,J,2)*R(J)*RD(J))/AZ(I+1)
```

```
  608 QPARM=(A+B+C+D)*PARM
      E=A+B+QPARM
      QKNOWN=C*H(I-1,J)+D*H(I+1,J)-(C+D-QPARM)*H(I,J)
      IF(J.EQ.2) GO TO 615
      IF(IC(I,J-1).EQ.-1) GO TO 610
      G(J)=(A*G(J-1)+QKNOWN)/(E-A*F(J-1))
      F(J)=B/(E-A*F(J-1))
      GO TO 620
  610 G(J)=(A*H(I,J-1)+QKNOWN)/E
      F(J)=B/E
      GO TO 620
  615 G(2)=QKNOWN/E
      F(2)=B/E
  620 CONTINUE
C CALCULATE HEADS BY BACK SUBSTITUTION
      N=NCOLM1
      H(I-1,N)=HNEW(N)
      IF(IC(I,NCOLM1).EQ.-1) GO TO 640
      HNEW(N)=G(N)
      GO TO 655
  640 HNEW(N)=H(I,N)
      GO TO 655
  650 HNEW(N)= G(N)+F(N)*HNEW(N+1)
  655 N=N-1
      IF(N.EQ.1) GO TO 657
      H(I-1,N)=HNEW(N)
      IF(IC(I,N).NE.-1) GO TO 650
      GO TO 640
  657 CONTINUE
  700 CONTINUE
C
C    COLUMN CALCULATIONS
C
      DO 703 L=2,NROWM1
  703 HNEW(L)=H(L,1)
C
      DO 800 J=2,NCOL
      DO 720 I=2,NROWM1
      IF(K(I,J).EQ.0..OR.IC(I,J).EQ.-1) GO TO 720
      IF(J.NE.2) GO TO 706
      A=0.0
      B=(KCONN(I,3,1)*(RD(2)/2.)*ZD(I))/AR(3)
      C=(KCONN(I,2,2)*((RD(J)/2.)**2)/2.)/AZ(I)
      D=(KCONN(I+1,2,2)*((RD(J)/2.)**2)/2.)/AZ(I+1)
      GO TO 708
  706 A=(KCONN(I,J,1)*(R(J-1)+RD(J-1)/2.)*ZD(I))/AR(J)
      B=(KCONN(I,J+1,1)*(R(J)+RD(J)/2.)*ZD(I))/AR(J+1)
      C=(KCONN(I,J,2)*R(J)*RD(J))/AZ(I)
      D=(KCONN(I+1,J,2)*R(J)*RD(J))/AZ(I+1)
  708 QPARM=(A+B+C+D)*PARM
      E=(C+D+QPARM)
      QKNOWN=A*H(I,J-1)+B*H(I,J+1)-(A+B-QPARM)*H(I,J)
      IF(I.EQ.2) GO TO 715
      IF(IC(I-1,J).EQ.-1) GO TO 710
      G(I)=(C*G(I-1)+QKNOWN)/(E-C*F(I-1))
      F(I)=D/(E-C*F(I-1))
      GO TO 720
  710 G(I)=(C*H(I-1,J)+QKNOWN)/E
```

```
      F(I)=D/E
      GO TO 720
  715 G(2)=QKNOWN/E
      F(2)=D/E
  720 CONTINUE
C CALCULATE HEADS BY BACK SUBSTITUTION
      N=NROWM1
      H(N,J-1)=HNEW(N)
      IF(IC(NROWM1,J).EQ.-1) GO TO 740
      HNEW(N)=G(N)
      GO TO 755
  740 HNEW(N)=H(N,J)
      GO TO 755
  750 HNEW(N)=G(N)+F(N)*HNEW(N+1)
  755 N=N-1
      IF(N.EQ.1) GO TO 757
      H(N,J-1)=HNEW(N)
      IF(IC(N,J).NE.-1) GO TO 750
      GO TO 740
  757 CONTINUE
      IF(J.EQ.NCOL) GO TO 800
      DO 770 I=2,NROWM1
      ET=DABS(HNEW(I)-HOLD(I,J))
      IF(ET.GT.ERR(IER)) GO TO 760
      GO TO 770
  760 ERR(IER)=ET
      IET=I
      JET=J
  770 CONTINUE
  800 CONTINUE
C
C CHECK CLOSURE CRITERIA FOR STEADY STATE
 1000 IF(IER.GE.ITMAX) GO TO 1045
      IF(ERR(IER).GT.EC) GO TO 400
C OTHERWISE  THE STEADY STATE HEADS HAVE BEEN COMPUTED
C
C COMPUTE HEADS AROUND THE PERIMETER OF THE MODEL
C THIS IS DONE TO GIVE A BETTER PLOT EFFECT
C
C ALONG TOP ROW
      DO 950 J=1,NCOL
  950 H(1,J)=H(2,J)
C
C ALONG BOTTOM ROW
      DO 960 J=1,NCOL
  960 H(NROW,J)=H(NROWM1,J)
C
C ALONG LEFT VERTICAL BOUNDARY
      DO 970 I=1,NROW
  970 H(I,1)=H(I,2)
C
C ALONG RIGHT VERTICAL BOUNDARY
      DO 980 I=1,NROW
  980 H(I,NCOL)=H(I,NCOLM1)
C
      WRITE(6,1005) (ERR(I),I=1,IER)
 1005 FORMAT('1',5X,'HEAD DIFFERENCE FOR EACH ITERATION',//,
     $(/,3X,10F12.5))
```

```
 1010 WRITE(6,1020) IER,ERR(IER),IET,JET
 1020 FORMAT('1',//,10X,'STEADY STATE HEAD MATRIX AFTER',I4,2X,'ITERATIO
     $NS',//,10X,'LARGEST HEAD DIFFERENCE =',E12.3,2X,'AT POINT',2X,'ROW
     $',I3,2X,'COLUMN',I3)
 1030 DO 1040 I=1,NROW
 1040 WRITE(6,200) I,(H(I,J),J=1,NCOL)
      IF(CONH.NE.CHECK(2)) GO TO 1100
      DO 1042 I=1,NROW
      DO 1042 J=1,NCOL
 1042 WRITE(11,2110) H(I,J)
      WRITE(6,1043)
 1043 FORMAT('0',4X,'***** HEADS WRITTEN ONTO DSN *****')
      GO TO 1100
C
 1045 WRITE(6,1055)
      WRITE(6,1005) (ERR(I),I=1,IER)
 1050 WRITE(6,1060) IER,ERR(IER),IET,JET
 1055 FORMAT('1','*********** ITERATIONS EXCEEDED *************')
 1060 FORMAT ('1',//,10X,'HEAD MATRIX AFTER',I4,2X,'ITERATIONS',//,10X,'
     $LARGEST HEAD DIFFERENCE =',E12.3,2X,'AT POINT',2X,'ROW',I3,2X,
     $'COLUMN',I3)
      DO 1070 I=1,NROW
 1070 WRITE(6,200) I,(H(I,J),J=1,NCOL)
      GO TO 3000
C
 1100 IF(ELEC.EQ.CHECK(3)) GO TO 1120
C OTHERWISE CONVERT PERMEABILITIES FROM FT/D TO CM/SEC
      CARITH=ARITHK*.0003528
      CHARM=HARMK*.0003528
      CGEOM=GEOMK*.0003528
C
      WRITE(6,1110) ARITHK,CARITH,GEOMK,CGEOM,HARMK,CHARM
 1110 FORMAT ('1',5X,'STATISTICAL MEANS OF THE PERMEABILITY',
     1' DISTRIBUTION',//,8X,'ARITHMATIC MEAN=',F10.4,1X,'FT/D',1X,
     2'=',1X,F10.6,1X,'CM/SEC',//,8X,'GEOMETRIC  MEAN=',F10.4,1X,'FT/D',
     31X,'=',1X,F10.6,,1X,'CM/SEC',//,8X,'HARMONIC   MEAN=',F10.4,1X,
     4'FT/D',1X,'=',1X,F10.6,1X,'CM/SEC')
      GO TO 1140
C
C CONVERT CONDUCTIVITIES TO RESISTIVITIES
 1120 ARITHK=1./HARMK
      GEOMK=1./GEOMK
      HARMK=1./ARITHK
      WRITE(6,1130) ARITHK,GEOMK,HARMK
 1130 FORMAT ('1',5X,'STATISTICAL MEANS OF THE RESISTIVITY ',
     1'DISTRIBUTION',//,8X,'ARITHMATIC MEAN=',F10.4,1X,'OHM-METERS',
     2//,8X,'GEOMETRIC  MEAN=',F10.4,1X,'OHM-METERS',//,8X,
     3'HARMONIC   MEAN=',F10.4,1X,'OHM-METERS')
C
C
C
C
C COMPUTE THE FLOW THROUGH THE SECTION (THETA=1 RADIAN)
C
 1140 Q=0.0
C
      DO 1200 I=2,NROWM1
      Q=Q+(KCONN(I,LEQUIV,1)*((H(I,LEQUIV)-H(I,LEQUIV-1))/AR(LEQUIV))
```

```
     1*(ZD(I)*(R(LEQUIV-1)+RD(LEQUIV-1)/2.)))
 1200 CONTINUE
C
C COMPUTE THE AQUIFER PERMEABILITY USING THE METHOD
C USED BY WARREN & PRICE
      FKI=0.0
      DO 1220 I=2,NROWM1
      FKI=FKI+KCONN(I,LEQUIV,1)*(H(I,LEQUIV)-H(I,LEQUIV-1))
 1220 CONTINUE
      KHEQFD=FKI/WPFACT
      WRITE(6,1230) FKI,KHEQFD
 1230 FORMAT ('0',5X,'FKI=',1X,F10.2,////,5X,'AQUIFER PERM.=',
     11X,F10.3,1X,'FT/D')
      IF(ELEC.EQ.CHECK(3)) GO TO 1290
C
C OTHERWISE WE HAVE THE HYDRAULIC CASE
      WRITE(6,1280) Q,DHEAD
 1280 FORMAT ('0',////,5X,'FLOW THROUGH THE SECTION (THETA=1 RADIAN)=',
     1F12.1,1X,'CFD',//,5X,'TOTAL HEAD DISSIPATED=',F10.4,1X,'FT')
      GO TO 1400
 1290 KHEQFD=1/KHEQFD
C THE EQUIVALENT ELECTRICAL HORIZONTAL CONDUCTIVITY WAS CONVERTED TO
C  AN EQIVALENT HORIZONTAL ELECTRICAL RESISTIVITY
C CONVERT CURRENT FLOW TO AMPERES
      Q=Q/3.281
      WRITE(6,1295) KHEQFD,Q,LENGTH,AREA,DHEAD
 1295 FORMAT('0',/////,5X,'MACROSCOPIC PARAMETERS',//,8X,'EQUIVALENT',
     1' HORIZONTAL ELECTRICAL RESISTIVITY=',F10.4,1X,'OHM-METERS',//,8X,
     2'TOTAL CURRENT FLOW=',F10.6,1X,'AMPERES',//,8X,'LENGTH=',F10.3,1X,
     3'FT.',//,8X,'AREA=',F10.3,1X,'SQ.FT.',//,8X,'TOTAL VOLTAGE DROP=',
     4F10.4,1X,'VOLTS')
C
C
 1400 IF(STRF.NE.CHECK(5)) GO TO 3000
C
C OTHERWISE COMPUTE THE STREAM FUNCTION FROM THE
C STEADY STATE HEADS
C
C
C SET BOTTOM ROW STREAM FUNCTION VALUES TO ZERO
      DO 1500 J=1,NCOLM1
 1500 STRFUN(NROWM1,J)=0.0
C
C
C COMPUTE INTERIOR VALUES OF THE STREAM FUNCTION MOVING ALONG
C SUCCESSIVE COLUMNS FROM THE BOTTOM STREAMLINE
C
      DO 1800 J=2,NCOLM2
      DO 1800 I=2,NROWM1
      II=NROW-I
      STRFUN(II,J)=STRFUN(II+1,J)+(KCONN(II+1,J+1,1)*((H(II+1,J+1)-
     $H(II+1,J))/AR(J+1))*(ZD(II+1)*(R(J)+RD(J)/2.)))
 1800 CONTINUE
C
C SET THE VALUES OF THE STRFUN(I,1) AND STRFUN(I,NCOLM1) TO
C PRODUCE A BETTER PLOT EFFECT
C
      DO 1850 I=1,NROWM1
```

```
      STRFUN(I,1)=STRFUN(I,2)
 1850 STRFUN(I,NCOLM1)=STRFUN(I,NCOLM2)
C
C NONDIMENSIONALIZE THE STREAM FUNCTION
C
      STRNOR=STRFUN(1,LSTRM)
      DO 1900 I=1,NROWM1
      DO 1900 J=1,NCOLM1
 1900 STRFUN(I,J)=STRFUN(I,J)/STRNOR
C
C WRITE OUT THE VALUES OF THE NONDIMENSIONALIZED STREAM FUNCTION
C
      WRITE(6,2100)
 2100 FORMAT('1',5X,'STREAM FUNCTION VALUES')
      DO 2000 I=1,NROWM1
 2000 WRITE(6,200) I,(STRFUN(I,J),J=1,NCOLM1)
C
C WRITE STREAM FUNCTION VALUES ONTO DSN
      DO 2200 I=1,NROWM1
      DO 2200 J=1,NCOLM1
 2200 WRITE(13,2110) STRFUN(I,J)
 2110 FORMAT(30X,F10.4)
      WRITE(6,2300)
 2300 FORMAT ('0','*** STREAM FUNCTION VALUES WRITTEN ONTO DSN ***')
C
 3000 STOP
      END
```

REFERENCES

Aiken, C.L., Hastings, D.A., and Sturgul, J.R., 1973, "Physical and Computer Modeling of Induced Polization", Geophysical Prospecting, Vol. 21, pp. 763-782.

Alger, R.P., 1966, "Interpretation of Electric Logs in Freshwater Wells in Unconsolidated Formations", Seventh Annual Logging Symposium Transactions, Sec. CC, pp. 1-25.

Allen, W.B., Hahn, G.W., and Tottle, C.R., 1963, Geohydrological Data for the Upper Pawcatuck River Basin, Rhode Island: Rhode Island Water Resources Coordinating Board Geol. Bull. 13, 68 p.

Archie, G.E., 1950, "Introduction to Petrophysics of Reservoir Rocks", Bull. of the Amer. Assoc. of Petroleum Geologists, Vol. 34, No. 5, pp. 943-961.

Bear, J., Dynamics of Fluids in Porous Media, American Elsevier Publishing Co., N.Y., 764 p.

Bouwer, H., 1969, "Planning and Interpreting Soil Permeability Measurements, J. Irrig. Drain. Div. Amer. Soc. Civil Eng., Vol. 95, pp. 391-402.

Bouwer, H., 1978, Groundwater Hydrology, McGraw-Hill Book Co., N.Y., 480 p.

Carothers, J.E., 1968, "A Statistical Study of the Formation Factor Relation", The Log Analyst, Sept.-Oct., pp. 13-20.

Clarke, R.T., 1973, "A Review of Some Mathematical Models used in Hydrology with Observations on their Calibration and Use," Journal of Hydrology, Vol. 19, pp. 1-20.

Dakhnov, V.N., 1962, "Geophysical Well Logging", Quarterly of the Colorado School of Mines, Vol. 57, No. 2.

Davis, S.N., and DeWiest, J.M., 1966, Hydrogeology, John Wiley & Sons, N.Y., 463 p.

Douglas, J., 1959, "Round-off Error in the Numerical Solution of the Heat Equation", J. Assoc. of Computing Mach., Vol. 6, pp. 48-58.

Duprat, A., Simler, L. and Ungemach, P., 1970, "Contribution de la Prospection Électrique a la Recherche Des Caractéristiques Hydrodynamiques D'un Milieu Aquifère", Terres et Eaux, Vol. XXIII, No. 62.

Fraser, H.J., 1935, "Experimental Study of the Porosity and Permeability of Clastic Sediments", J. of Geology, Vol. 43, No. 8, pp. 910-1010.

Freeze, R.A., 1975, "A Stochastic-Conceptual Analysis of One-Dimensional Groundwater Flow in Nonuniform Homogeneous Media", Water Resources Research, Vol. 11, No. 5, pp. 725-741.

Freeze, R.A., and Cherry, J.A., Groundwater, 1979, Prentice-Hall, Inc., Englewood Cliffs, N.J., 604 p.

Frohlich, R.K., 1974, "Combined Geoelectrical and Drill-Hole Investigations for Detecting Fresh-Water Aquifers in Northwestern Missouri", Geophysics, Vol. 39, No. 3, pp. 340-352.

Gonthier, J.B., H.E. Johnson, and G.T. Malinberg, 1974, "Availability of Ground Water in the Lower Pawcatuck River Basin, Rhode Island", Geological Water Supply Paper 2033.

Graton, L.C., and Fraser, H.J., 1935, "Systematic Packing of Spheres - With Particular Relation to Porosity and Permeability", J. of Geology, Vol. 43, No. 8, pp. 785-909.

Greenkorn, R.A., and Kessler, D.P., 1969, "Dispersion in Heterogeneous Nonuniform Anisotropic Porous Media", Ind. Eng. Chem., Vol. 61, No. 9, pp. 14-32.

Halliday, D., and Resnick, R., 1970, Fundamentals of Physics, John Wiley & Sons, N.Y., 837 p.

Heigold, P.C., Gilkeson, R.H., Cartwright, K., and Reed, P.C., 1979, "Aquifer Transmissivity from Surficial Electrical Methods", Groundwater, Vol. 17, No. 4, pp. 338-345.

Higdon, W.T., 1963, Discussion of "Variation of Electrical Resistivity of River Sands, Calcite, and Quartz Powders with Water Content" by V.J. Sarma and V.B. Rao, Geophysics, April, pp. 309-310.

Hill, H.J., and Milburn, J.D., 1956, "Effect of Clay and Water Salinity on Electrochemical Behavior of Reservoir Rocks", Petroleum Transactions, AIME, Vol. 207, pp. 65-72.

Jepsen, A.F., 1969, "Resistivity and Induced Polarization Modeling", Ph.D. dissertation, University of Calif., Berkeley.

Keller, G.V., and Frischknecht, F.C., 1966, Electrical Methods in Geophysical Prospecting, Pergamon Press, Oxford, 517 p.

Kelly, W.E., 1976, Estimating Aquifer Permeability by Surface Electrical Resistivity Measurements, Technical Report to the National Science Foundation, August.

Kelly, W.E., 1977, "Geoelectric Sounding for Estimating AquiferHydraulic Conductivity", Ground Water, Vol. 15, No. 6, pp. 420-425.

Kelly, W.E., Frohlich, R.K., 1978, Estimating Hydraulic Properties of Glacial Aquifers with Surface Geophysical Measurements; Research Proposal to the National Science Foundation, April 1.

Kelly, W.E., 1980, "Porosity-Permeability Relationship in Stratified Glacial Deposits", paper presented at American Geophysical Union Annual Meeting, Toronto, May 23.

Kezdi, A., 1974, Handbook of Soil Mechanics, Vol. 1 (Soil Physics), Elsevier Scientific Pub. Co., N.Y., p. 49.

Kosinski, W.K., 1978, "Geoelectric Studies for Predicting Aquifer Properties; M.S. Thesis, University of Rhode Island, Kingston, R.I.

Kosinski, W.K. and Kelly, W.E., 1981, "Geoelectric Soundings for Predicting Aquifer Properties", Ground Water, Vol. 19, No. 2, pp. 163-171.

Krumbien, W.C., and Monk, G.D., 1942, "Permeability as a Function of the Size Parameters of Unconsolidated Sand, Am. Inst. of Mining & Metal. Engrs., Vol. 151, pp. 153-163.

Law, J.A., 1944, "A Statistical Approach to the Interstitial Heterogeneity of Sand Reservoirs, Trans. of A.I.M.E., Vol. 155, pp. 202-222.

Lee, C. H., and Ellis, A. J., 1919, "Geology and Ground Waters of the Western Part of San Diego County, California", U.S.G.S. Water Supply Paper 446, pp. 121-123.

Loudon, A. G., 1952, "The Computation of Permeability from Simple Soil Tests", Geotechniques (British), Vol. 3, No. 2, pp. 165-183.

Masch, F. D., and Denny, K. J., 1966, "Grain Size Distribution and Its Effect on the Permeability of Unconsolidated Sands", Water Resources Research, Vol. 2, No. 4, pp. 665-677.

McMillan, W. D., 1966, "Theoretical Analysis of Groundwater Basin Operations", Water Resource Center Contrib. 114, 167 pp., University of California, Berkley.

Mufti, I. R., 1976, "Finite-Difference Resistivity Modeling for Arbitrarily Shaped Two-Dimensional Structures", Geophysics, Vol. 41, No. 1, pp. 62-78.

Mufti, I. R., 1978, "A Practical Approach to Finite Difference Resistivity Modeling", Geophysics, Vol. 43, No. 5, pp. 930-942.

Muscat, M., 1946, "<u>The Flow of Homogeneous Fluids Through Porous Media</u>, McGraw-Hill.

Patnode, H. W. and Wyllie, M. R. J., 1950, "The Presence of Conductive Solids in Reservoir Rocks as a Factor in Electric Log Interpretation", Pet. Trans., A.I.M.E., Vol. 189, pp. 47-52.

Peaceman, D. W., and Rachford, H. R., 1955, "The Numerical Solution of Parabolic and Elliptic Differential Equations", J. Soc. Indust. Appl. Math., Vol. 3, No. 1, pp. 28-41.

Perloff, W. H., and Baron, W., 1976, <u>Soil Mechanics Principles and Applications</u>, Ronald Press, N. Y., 745 p.

Prickett, T. A., and Lonnquist, C. G., 1971, Selected Digital Computer Techniques for Groundwater Resource Evaluation, Illinois State Water Survey, Bulletin 55.

Reiter, P. F., 1980, "A Computer Study of the Correlation Between Aquifer Hydraulic and Electric Properties", thesis presented to the University of Rhode Island in partial fulfillment of the requirements for the degree of Master of Science.

Remson, I., Hornberger, G.M., and Molz, F.J., 1971, Numerical Methods in Subsurface Hydrology, Wiley-Interscience, N.Y., 389 p.

Roach, P., 1972, Conceptual Fluid Dynamics, Hermosa Publishers, Alburquerque, N.M.

Rushton, K. R., and Redshaw, S. C., 1979, Seepage and Groundwater Flow, John Wiley & Sons, N. Y., 339 p.

Sarma, V. V. J., and Rao, V. B., 1962, "Variation of Electrical Resistivity of River Sands, Calcite and Quartz Powders with Water Content", Geophysics, Vol. 27, No. 4, pp. 470-479.

Terzaghi, C., 1925, Engineering News Record, Dec. 3, 1925, p. 914.

Trask, P.H., 1931, Amer. Assoc. Petrol. Geol. Bull., Vol. 15, p. 273.

Trescott, P.C., 1975, Documentation of Finite Difference Model for Simulation of Three Dimensional Groundwater Flow, U.S.G.S. Open File Report, 75-438, Sept.

Trescott, P.C., Pinder, G.F., and Larson, S.P., 1976, Techniques of Water-Resources Investigations of the U.S.G.S., Chapt. C1, Finite-Difference Model for Aquifer Simulation in Two-Dimensions with Results of Numerical Experiments, U.S. Gov. Printing Office.

Ungemach, P., Mostaghimi, F., and Duprat, A., 1969, "Essais de Determination Du Coefficient D'Emmagasinement en Nappe Libre Application of la Nappe Alluviale du Rhin", International Assoc. of Scientific Hydrology, Vol. 14, No. 2, pp. 169-190.

Urish, D.W., 1978, "A Study of the Theoretical and Practical Determination of Hydrogeological Parameters in Glacial Outwash Sands by Surface Geoelectrics", Ph.D. Dissertation, Univ. of Rhode Island, Kingston, RI.

Walton, W.C., 1970, Groundwater Resource Evaluation, McGraw-Hill Book Co., NY, p. 664.

Warren, J.E., and Price, H.S., 1961, "Flow in Heterogeneous Porous Media", Soc. of Petrol. Eng. J., Vol. 1, pp. pp. 153-169.

Willardson, L.S. and Hurst, R.L., 1965, "Sample Size Estimates in Permeability Studies", J. Irrig. Drain. Div. Amer. Soc. Civil Eng., Vol. 91 (IR1), pp. 1-9.

Winsauer, W.O. and McCardell, W.M., 1953, "Ionic Double-Layer Conductivity in Reservoir Rock", Petrol. Trans., A.I.M.E., Vol. 198, pp. 129-134.

Worthington, P.F., and Barker, R.D., 1972, "Methods for the Calculation of True Formation Factors in the Bunter Sandstone of Northwest England", Engineering Geology, Vol. 6, pp. 213-228.

Worthington, P.F., 1977, "Influence of Matrix Conduction Upon Hydrogeophysical Relationships in Arenaceous Aquifiers", Water Resources Research, Vol. 13(1), pp. 87-92.

Wyllie, M.R.J., and Gregory, A.R., 1953, "Formation Factors of Unconsolidated Porous Media: Influence of Particle Shape and Effect of Cementation", Petrol. Trans., A.I.M.E., Vol. 198, pp. 103-109.

Zohdy, A.A.R., 1965, "The Auxiliary Point Method of Electrical Sounding Interpretation, and Its Relationship to the Dar Zarrouk Parameters", Geophysics, Vol. 30, p. 644-660.

Zohdy, A.A.R., Eaton, G.P., and Mabey, D.R., 1974, "Application of Surface Geophysics to Groundwater Investigations", Techniques of Water Resources Investigations of the U.S.G.S., Chapt. D1, Book 2.